



HAL
open science

New Insights in Asymmetric Au(I) Catalysis with Chiral Phosphate Counterions

Zhenhao Zhang

► **To cite this version:**

Zhenhao Zhang. New Insights in Asymmetric Au(I) Catalysis with Chiral Phosphate Counterions. Other. Institut Polytechnique de Paris, 2021. English. NNT : 2021IPPAX067 . tel-04224302

HAL Id: tel-04224302

<https://theses.hal.science/tel-04224302v1>

Submitted on 2 Oct 2023

HAL is a multi-disciplinary open access archive for the deposit and dissemination of scientific research documents, whether they are published or not. The documents may come from teaching and research institutions in France or abroad, or from public or private research centers.

L'archive ouverte pluridisciplinaire **HAL**, est destinée au dépôt et à la diffusion de documents scientifiques de niveau recherche, publiés ou non, émanant des établissements d'enseignement et de recherche français ou étrangers, des laboratoires publics ou privés.



New Insights in Asymmetric Au(I) Catalysis with Chiral Phosphates Counterions

Thèse de doctorat de l'Institut Polytechnique de Paris
préparée à l'École polytechnique

École doctorale n°626
Ecole Doctorale de l'Institut Polytechnique de Paris (ED IP Paris)
Spécialité de doctorat: Chimie

Thèse présentée et soutenue à Gif-sur-Yvette le 17/09/2021, par

Zhenhao ZHANG

Composition du Jury:

Véronique Michelet

Professeure des universités, Université Cote d'Azur (UMR7272)

Présidente

Marion Barbazanges

Maitre de Conférences, Sorbonne Université (IPCM)

Rapporteuse

Sandrine Py

Directrice de Recherche, Université Grenoble Alpes (DCM)

Rapporteuse

Philippe Belmont

Professeur des universités, Université de Paris (Faculté de Pharmacie)

Examinateur

Gilles Frison

Chargé de Recherche, CNRS (LSO, Ecole Polytechnique)

Directeur de thèse

Xavier Guinchard

Chargé de Recherche, CNRS (ICSN)

Co-Directeur de thèse

Acknowledgements

This thesis was completed under the guidance of Dr Xavier Guinchard, Dr Angela Marinetti and Dr Gilles Frison.

First of all, I would like to thank Dr Xavier Guinchard for helping me in my work or in my life during my PhD. Thank you very much Xavier. Dr Guinchard has given me great help when I was studying in France. Thanks to his attention and patience, I was able to successfully complete my studies. It's my greatest fortune to be able to work under his supervision, my abilities have been comprehensively improved during the four years of working with him. Thank you again Xavier.

I also want to thank Dr Angela Marinetti for helping me in my work and in my life. I am very grateful for her help in my PhD projects and the care she has given me in life. Thank you very much Angela.

I thank Dr Gilles Frison, for his kind help during the last four years. Moreover, I would also like to thank him for his great contribution to the DFT calculation parts of my projects. Thank you very much Gilles.

Dr Arnaud Voituriez and Dr Jean-François Betzer in our group often gave me some suggestions and help during my PhD, thank you very much.

Special thanks to Vitalii Smal for his contribution in the preliminary work, which made me avoid many detours in the process of synthesizing the catalyst. Also, many thanks to the other members of our team for their help. Thanks to Nicolas Glinsky-Olivier, Nazarii Sabat, Pierre Milcendeau, Yunliang Yu, Weiping Zhu, Charlotte Lorton, Julie Febvay, Youssef Sanogo, Fabrizio Medici, Thomas Castanheiro, Sebastien Thueillon, Vincent Delattre, Nawel Goual and Romain Losa.

I want to thank warmly the chiral HPLC responsables, Nathalie Hue and Vincent Steinmetz for their help and advice for chiral HPLC analyses (over 1114 injections!). I acknowledge Pascal Retailleau for the X-ray structures determinations, and the NMR responsables, Jean-François Gallard, François Giraud and Ewen Lescop for all the NMR analyses and DOSY analyses. Thank you to MS responsible Elie Nicolas for HRMS analyses, and all the technical staff for IR, polarimeter, IT, shop stuffs and other members in ICSN. Thank you for your support and help during my PhD.

I also want to thank my parents and my friends. Thanks to their support and help all the time, I was able to go to the present and successfully complete my PhD.

Finally, I would like to thank CSC for the financial support, which enabled me to successfully complete my PhD.

Foreword

This manuscript is the result of four years of work performed at the Institut de Chimie des Substances Naturelles in Gif sur Yvette, in the Phosphorus Chemistry and Catalysis group. This PhD project is a collaborative work between my supervisors Xavier Guinchard and Angela Marinetti (ICSN) and Gilles Frison (LCM, Ecole polytechnique).

This project is directed at the study of a novel approach in enantioselective Au(I) catalysis. An accurate analysis of the field indeed shows that the Asymmetric Counteranion-Directed Catalysis (ACDC) strategy, applied to enantioselective Au(I) catalysis, has not been used as much as expected. This analysis led us to envision a variant of this approach. We designed new chiral catalysts with a tether between the metal center and the chiral anion and we have named this concept “Tethered Counterion-Directed Catalysis” approach (TCDC). This manuscript summarizes the main results that provide a proof-of-concept to this approach.

This manuscript is divided in the following sections.

A brief general **Introduction** will summarize the main approaches in enantioselective catalysis, with a particular focus on the catalysts used.

Chapter 1 deals with the synthesis of different series of chiral bifunctional Au(I) complexes and their activation with silver salts.

Chapter 2 describes the main results obtained in the use of the Au(I) complexes in enantioselective catalysis. This chapter is largely focused on the Au(I)-catalyzed cycloisomerization of 2-alkynyl enones, followed by either a nucleophilic addition or a [3+2] cycloaddition of a nitron, for the synthesis of chiral furan derivatives.

Chapter 3 reports preliminary results in the application of the TCDC strategy to other catalytic reactions, with a focus on the activation of substrates that are chemically very different from those of Chapter 2.

A final **Conclusion** establishes a critical overview of the work performed as well as on future directions.

Nouvelles perspectives en catalyse énantiosélective par les complexes d'Au(I) à contre-ions phosphates

La catalyse à l'Au(I) représente aujourd'hui un outil de choix pour la synthèse de molécules complexes, à haute valeur ajoutée en raison de ses propriétés de π -acidité de Lewis. Cependant, la catalyse énantiosélective est confrontée à de nombreux défis en raison de la géométrie linéaire de l'or et du mécanisme par sphère externe, ce qui place la poche chirale à l'opposé du substrat. Aussi, au cours des dernières décennies, des stratégies efficaces ont été définies pour rendre énantiosélectives les réactions promues par l'Au(I), en s'appuyant sur des ligands chiraux, comme les diphosphines chirales, ou des ligands monodentés comme les phosphoramidites chirales. Une autre stratégie, développée par Dean Toste à partir de 2007, fait appel à des complexes d'Au(I) achiraux avec des contre-ions chiraux (ACDC = Asymmetric Counteranion Directed Catalysis). Cette approche, basée sur l'emploi de phosphates chiraux d'Au(I), a montré d'excellentes performances catalytiques dans certaines réactions, en particulier dans les réactions intramoléculaires d'hydrofonctionnalisation d'allènes ou d'alcynes. Cependant, cette approche ne s'est avérée réellement efficace que dans cette classe de réaction, constituant ainsi une limitation importante en termes d'étendue. Dans ce contexte et avec l'objectif de dépasser ces limitations, ces travaux de thèse ont porté sur un nouveau design de complexes d'Au(I), que nous avons nommés CPAPHosAuCl, dans lesquels le contre-ion phosphate serait relié au métal par un lien covalent. Selon l'hypothèse de travail initiale, le lien entre le ligand de l'Au(I) et son propre contre-ion doit réduire la flexibilité conformationnelle et augmenter les contraintes stériques des intermédiaires clés des cycles catalytiques, favorisant ainsi l'énantiosélectivité. Ces nouveaux complexes ont été caractérisés par RMN, HRMS et calculs DFT. Cette stratégie a été nommée "Tethered Counterion Directed Catalysis" (TCDC).

Nous avons donc conçu et synthétisé une série de six complexes d'Au(I) portant des ligands bifonctionnels phosphine-acide phosphorique, avec différentes chaînes entre les deux groupes. La fonction phosphine coordonne le métal tandis que la fonction acide phosphorique, dérivée des diols chiraux (*S*)-BINOL ou (*R*)-SPINOL, engendre un contre-ion phosphate dans un environnement chiral. L'efficacité de ces nouveaux complexes a été démontrée notamment dans des réactions tandem de cyclisation/addition nucléophile. Ces réactions permettent de convertir des α -éthynyl-énones cycliques en furanes bicycliques, fonctionnalisés par le nucléophile entrant (indoles, amines, phénols, etc...). Le nouveau catalyseur a également été utilisé dans une réaction multicomposant impliquant des cétones insaturées, des hydroxylamines et des aldéhydes, pour produire des composés tricycliques. Dans cette stratégie, une nitroène est formée in situ et réagit comme nucléophile et électrophile successivement. A notre connaissance, ceci constitue le premier exemple de réaction multicomposant énantiosélective catalysée par un complexe d'or. Des niveaux inédits d'activité catalytique et de stéréosélectivité ont pu être atteints grâce aux nouveaux catalyseurs : les réactions se déroulent le plus souvent avec une très faible charge catalytique (jusqu'à 0.2 mol%) et conduisent à des excès énantiomériques supérieurs à 90% dans de nombreux cas. De plus, l'activation du complexe par addition de sels d'argent n'est pas toujours nécessaire, ce qui représente une avancée majeure en catalyse à l'Au(I).

La stratégie TCDC peut également être appliquée à d'autres métaux. Notre groupe a préparé avec succès les complexes d'Ir et de Rh correspondants et les applications en catalyse asymétrique sont étudiées.

Dans l'ensemble, ces résultats valident l'hypothèse de travail initiale, repoussent certaines limites de la catalyse énantiosélective à l'Au(I) et ouvrent d'excellentes perspectives en synthèse asymétrique.

Abbreviations commonly used in this manuscript

(S)-BINOL	(S)-[1,1'-binaphalene]-2,2'-diol
ACDC	Asymmetric Counteranion Directed Catalysis
AIBN	Azobisisobutyronitrile
BINAP	2,2'-Bis(diphenylphosphino)-1,1'-binaphthyl
Bpin	4,4,5,5-tetramethyl-1,3,2-dioxaborolane
CPA	Chiral phosphoric acid
DABCO	1,4-diazabicyclo[2.2.2]octane
DMS	Dimethylsulfide
DOSY	Diffusion-ordered NMR spectroscopy
dpp	Diphenylphosphoric acid
dppf	1,1'-Bis(diphenylphosphino)ferrocene
dppm	Bis(diphenylphosphino)methane
dppp	1,3-Bis(diphenylphosphino)propane
dr	Diastereomeric ratio
DTBM	2,5-Di- <i>tert</i> butyl-4-methoxyphenyl
ECC	External calibration curves
ee	Enantiomeric excess
IPrAuCl	1,3-bis(diisopropylphenyl)imidazol-2-ylidene gold chloride
MOMCl	Chloro(methoxy)methane
MSA	Methanesulfonic acid
NBS	<i>N</i> -Bromosuccinimide
ND	Not detected
NHC	<i>N</i> -heterocyclic carbene
NR	No reaction
PPA	Polyphosphoric acid
r.t.	Room temperature
SPhos	2-Dicyclohexylphosphino-2',6'-dimethoxybiphenyl
SPINOL	2,2',3,3'-tetrahydro-1,1'-spirobi[indene]-7,7'-diol
TCDC	Tethered Counterion Directed Catalysis
TRIP	3,3'-Bis(2,4,6-triisopropylphenyl)-1,1'-binaphthyl-2,2'-diyl hydrogenphosphate

Contents

Introduction.....	1
1. Au(I) catalysis: general information	1
2. Enantioselective Au(I) catalysis	3
2.1. Au(I) complexes featuring chiral bidentate or monodentate phosphorus ligands.....	4
2.2. Au(I) complexes of bifunctional chiral ligands	6
3. The chiral-counterion strategy: Asymmetric Counteranion-Directed Catalysis (ACDC)	7
3.1. General information on this strategy	7
3.2. Selected examples of ACDC in transition metal catalysis.....	7
3.3. Application of the ACDC strategy in enantioselective Au(I) catalysis	9
4. The Tethered Counterion Directed Catalysis (TCDC): PhD project.....	15
Chapter 1: Synthesis of bifunctional chiral phosphine-phosphate Au(I) complexes	17
1. Synthesis and characterization of the BINOL-derived phosphine-phosphate Au(I) complex CPAPhos ^A AuCl	17
1.1. Synthesis of the gold complex CPAPhos ^A AuCl 1a.....	17
1.2. Silver-mediated activation of the chiral Au(I) catalyst 1a to 22a	24
1.3. Diffusion-ordered NMR spectroscopy (DOSY) analysis	26
1.4. Conclusions.....	30
2. Synthesis of phosphine-phosphoric acid Au(I) complexes CPAPhos ^{B-F} AuCl.....	31
2.1. Synthesis of the gold(I) complex CPAPhos ^B AuCl 1b	32
2.2. Synthesis of the gold(I) complex CPAPhos ^C AuCl 1c.....	33
2.3. Synthesis of the gold(I) complex CPAPhos ^D AuCl 1d	35
2.4. Synthesis of the gold(I) complex CPAPhos ^E AuCl 1e.....	36
2.5. Synthesis of the gold(I) complex CPAPhos ^F AuCl 1f	38
3. Conclusion	42
Chapter 2: Application of the TCDC strategy in enantioselective catalysis involving α -alkynyl-ketones	44
1. Metal promoted tandem cyclization-nucleophilic additions on α -alkynylketones: literature overview.	45
2. Application of the TCDC strategy in the cyclization/nucleophilic addition reactions on α -alkynylketones	49
2.1. Screening of catalysts and reaction conditions.....	49
2.2. DFT Calculations and mechanistic studies.....	54
2.3. Scope of the reaction	57
2.4. Silver-free reactions	61
2.5. Extension of the cyclization/nucleophilic addition reaction to other nucleophiles.....	64
2.6. Application of the cyclization/addition method in reactions involving naphthols	67
2.7. Application of the cyclization/nucleophilic addition reactions to conjugated oximes	71
3. The TCDC strategy in the cyclization/formal cycloaddition reactions involving nitrones	72
3.1. Optimization of the reaction of 2-alkynylketones with nitrones	74
3.2. Scope of the reaction	77

3.3. Application to a reaction variant: Reaction of oxime and nitron	83
4. Conclusion	84
Chapter 3: Application of the TCDC strategy in reactions involving other scaffolds	85
1. Cyclizations of imines combined with nucleophilic trapping	85
1.1. Bibliographic precedents	86
1.2. Results and discussion	87
2. Activation of allenamides combined with naphthol dearomatization	90
2.1. Bibliographic precedents in Au(I) catalysis	91
2.2. Main results obtained	92
3. The TCDC strategy in (<i>iso</i>)-Pictet-Spengler reactions	93
4. Conclusion	96
General Conclusion and Perspectives	97
Experimental section	100
General methods	100
Chapter 1. Synthesis of bifunctional chiral phosphine-phosphate Au(I) complexes	100
1. Synthesis and Characterization of 1a	100
2. Synthesis and Characterization of 1b	109
3. Synthesis and Characterization of 1c	112
4. Synthesis and Characterization of 1d	115
5. Synthesis and Characterization of 1e	118
6. Synthesis and Characterization of 1f	123
Chapter 2. Application of the TCDC strategy in enantioselective catalysis involving 2-alkynyl-ketones	126
Part 1. Application of the TCDC strategy in cyclization/nucleophilic addition reaction sequences	126
Part 2. Enantioselective Au(I)-catalyzed multicomponent reactions of ketones 71 (or oximes 96), hydroxylamines 101 and aldehydes 102	148
Chapter 3. Application of the TCDC strategy in reactions involving other scaffolds	171
Part 1. Cyclizations of imines combined with nucleophilic trapping	171
Part 2. Activation of allenamides combined with naphthol dearomatization	173
Part 3. The TCDC strategy in (<i>iso</i>)-Pictet-Spengler reactions	174
Bibliographic section	175

Introduction

1. Au(I) catalysis: general information

Gold(I) catalysis did not attract much attention until the early 21st century, due to the supposed inertness of gold complexes, despite some pioneering studies that opened the way soon to enantioselective catalytic processes.¹ During the last decades however, gold catalysis has bloomed and currently plays a major role in synthetic chemistry. This renewed attention is mainly related to the π -Lewis acidity of Au(I) complexes, which results in the coordination of unsaturated bonds triggering nucleophilic additions.²

Au(I) complexes mostly feature the general structure LAuX, where the L notably represents a phosphorus ligand or an NHC and X is an X-type ligand or a weakly coordinated counteranion (**Figure 1**). Different combinations of L/X pairs modulate the properties of Au(I) complexes in terms of electrophilicity and coordination properties.³

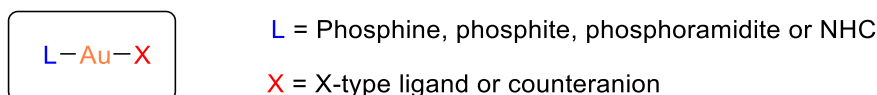
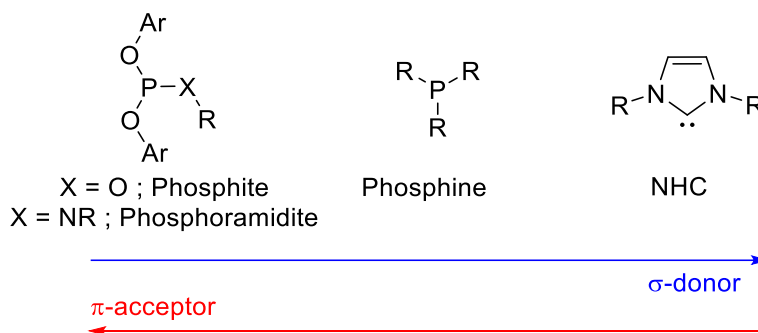


Figure 1. General Structure of Au(I) Complexes

More specifically, phosphites and phosphoramidites have a strong π -acceptor character, but a weak σ -donor character (Scheme 1). NHC, on the contrary, have a weak π -acceptor and a strong σ -donor character. Phosphines possess intermediate properties, in addition of being highly modular, and are hence among the most used ligands in Au(I) catalysis.

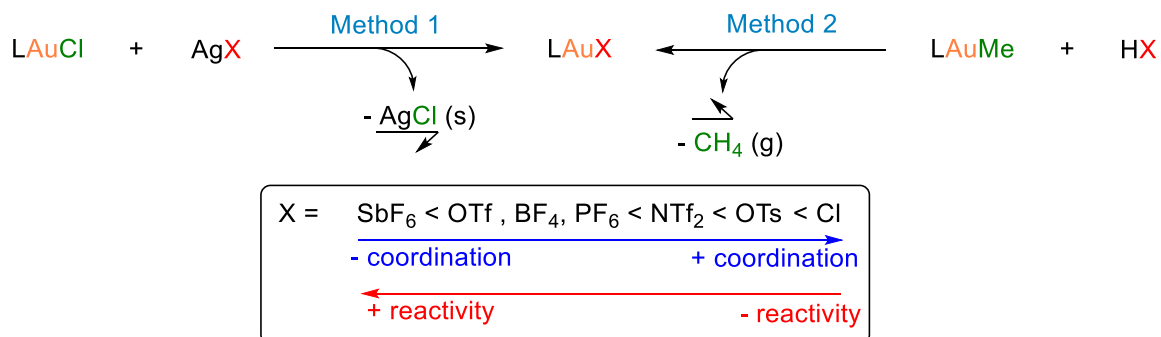


Scheme 1

The nature of the X ligand is also of crucial importance.⁴ For X = Cl, the complexes are not catalytically active, because of the strength of the Au-Cl bond that possesses an almost covalent character. These complexes are often qualified as precatalysts, as far as it is necessary to replace chloride with a less coordinating counterion, in order to get a catalytically active Au(I) complex. Most often, the chloride will be abstracted via anion metathesis, by means of a metallic salt, mostly a silver salt, displaying a weakly coordinating anion, such as OTf⁽⁻⁾, NTf₂⁽⁻⁾, SbF₆⁽⁻⁾, BF₄⁽⁻⁾ or PF₆⁽⁻⁾ (Method 1, Scheme 2). The reaction leads to precipitation of AgCl, which is usually considered a driving force. The role of the silver salt is however rarely

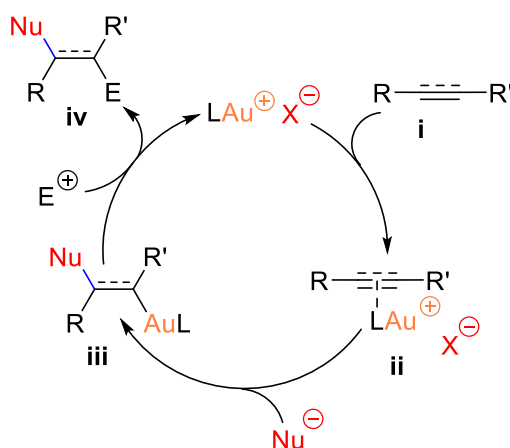
innocent, since silver can form catalytically active species, as shown by numerous groups.⁵ These phenomena will be discussed further in this manuscript.

Alternatively, catalytically active gold complexes can be generated from LAuMe precatalyst (X = Me), that form methane and cationic Au(I) complexes, under protonation with strong acids. This method concerns however a limited variety of easily available precatalysts (Method 2, Scheme 2).⁶



Scheme 2

The general mechanistic pathway for the gold catalyzed reactions can be typified by the addition of nucleophiles to unsaturated compounds shown in Scheme 3. The unsaturated substrate **i** coordinates to the gold cation LAu⁽⁺⁾, leading to the intermediate π -complex **ii**, in which the unsaturated substrate becomes highly electrophilic. This allows the addition of a nucleophile (Nu⁽⁻⁾) to form the vinyl-gold intermediate **iii**, forming meanwhile a new C-C or C-heteroatom bond. The catalytic species then reacts with an electrophile E⁽⁺⁾, most often a proton (then this step is called protodeauration), regenerating the catalyst and releasing the addition product **iv**.



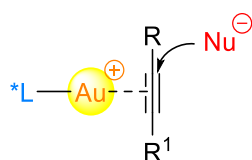
Scheme 3. Mechanistic Pathway for the Gold Catalyzed Addition of Nucleophiles to Unsaturated Compounds

In this process, if the substrate is prochiral, a stereogenic center may be formed on the backbone, thereby obtaining chiral compounds. It is then natural that the chemists decided to develop tools for enantioselective gold catalysis.

2. Enantioselective Au(I) catalysis

Chirality exists widely in nature and plays an important role in living organisms. The synthesis of chiral compounds is hence of crucial importance. In this context, asymmetric synthesis⁷ refers to a reaction that produces an optically active product with control of its absolute configuration. In the general pathway shown in Scheme 3, the probability for a nucleophile to add to the prochiral substrate from both faces is the same, resulting in a racemic mixture. However, if the reaction takes place in a chiral environment, created by either a chiral catalyst or a chiral auxiliary, this can result in the unequal production of the two enantiomers, leading to enantiomerically (or diastereomerically) enriched products. Asymmetric synthesis currently plays an important role notably in pharmaceutical industry and, mostly at the academic level, in the total synthesis of natural products. Strategies using the chiral pool substances,⁸ synthetic chiral auxiliaries⁹ or chiral stoichiometric reagents are efficient but suffer most often from a lack of atom and/or step economy and are not anymore among the privileged approaches. On the contrary, enantioselective organo- and organometallic catalysis, that involves catalytic amounts of chiral species to produce enantiomerically enriched compounds, often represents the method of choice due to its obvious advantages.

Among chiral catalysts, transition metal complexes have demonstrated not only high efficiency and enantioselectivity, but also a unique variety of catalytic applications, due to the large number of metals, each of them having specific properties and catalytic behavior. Nevertheless, despite the huge number of remarkable advances, there are still fascinating challenges to be tackled in asymmetric catalysis. One of them relates to Au(I) catalysts. Au(I) complexes feature a linear geometry, which places the substrate on a site opposite to the chiral ligand, far away from the ligand. This makes it difficult to exert stereochemical control in addition reactions where the nucleophile adds to the substrate directly, without previous coordination to the metal (outer sphere mechanism). This constitutes the greatest challenge in enantioselective gold(I) catalysis (Scheme 4).¹⁰



Scheme 4

A general strategy to achieve enantioselective gold catalysis is to use sterically hindered ligands providing an extended chiral pocket around the metal center. By following this approach, two main strategies were successfully applied to catalysts based on phosphorus auxiliaries: the use of bimetallic gold complexes of chiral diphosphines and the design of extremely bulky monodentate ligands, including phosphines and phosphoramidites. A second approach involves the use of phosphorus ligands displaying functional groups that give non-covalent bonds with the substrates. These weak interactions contribute efficiently to the stereochemical control of the catalytic reactions. Finally, an alternative recent approach makes use of chiral counterions (phosphates) combined with achiral phosphorus ligands. All these approaches (Figure 2) will be illustrated shortly in the next paragraphs.

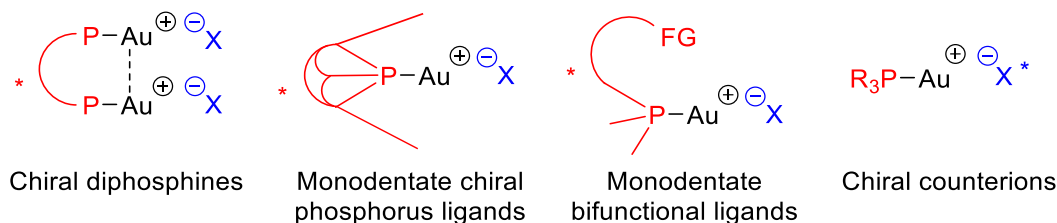


Figure 2. Main Series of Chiral Au(I) Complexes

2.1. Au(I) complexes featuring chiral bidentate or monodentate phosphorus ligands

Concerning chiral diphosphines for gold catalysis, most of them are based on the BINAP,¹¹ SEGPHOS¹² or MeO-BIPHEP¹³ scaffolds (Figure 3). These phosphines form bimetallic complexes in which, depending on the nature of the biaryl scaffold and its substitution patterns, aurophilic interactions are possible.¹⁴ These Au-Au interactions contribute to the stereochemical control, as far as they control the geometry and shape of the bimetallic complex, which might impact both the catalytic activity and enantioselectivity.¹⁵ In addition, starting from bis-gold chloride complexes, the chloride abstraction can be controlled in order to get either mono- or dicationic species, both having different catalytic activities. This strategy has been extensively applied to enantioselective Au(I) catalysis.¹⁶

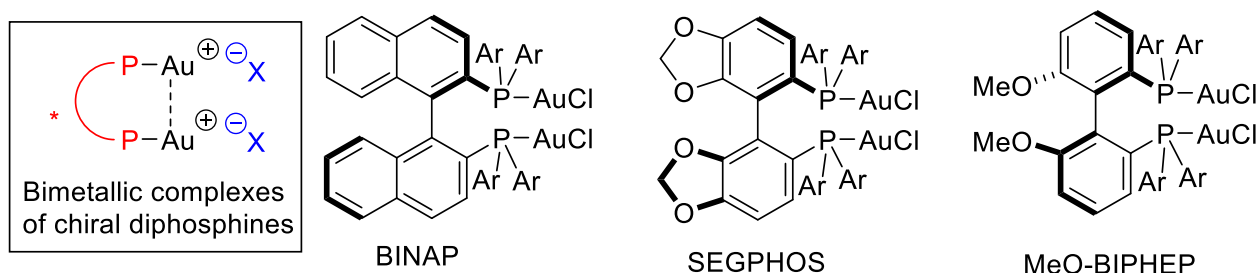


Figure 3. Bimetallic Gold Complexes

Studies on monometallic Au(I) complexes^{10b} have been focused mainly on the use of chiral phosphoramidites¹⁷ derived from BINOL or TADDOL,¹⁸ and chiral NHCs¹⁹ (Figure 4). These ligands benefit from the major advantage of being easily available and easily tunable, so as to adapt and optimize their structural features to each single catalytic reaction. In the phosphoramidite series, extended, bulky ligands can be created by modifying the substituents on the carbon backbone as well as on the amino group. Simple bulky monodentate phosphines are less common in the field of enantioselective catalysis. Nevertheless, in 2014, Dr A. Voituriez and Dr A. Marinetti in our group have demonstrated that helically chiral phosphines can provide a suitable chiral pocket around gold and control the enantioselectivity in many gold-catalyzed processes.²⁰ The HelPhos ligands (Figure 4) have been used successfully, leading to good catalytic activity and high enantioselectivity in the cycloisomerization of enynes, allen-yne and other rearrangement reactions.

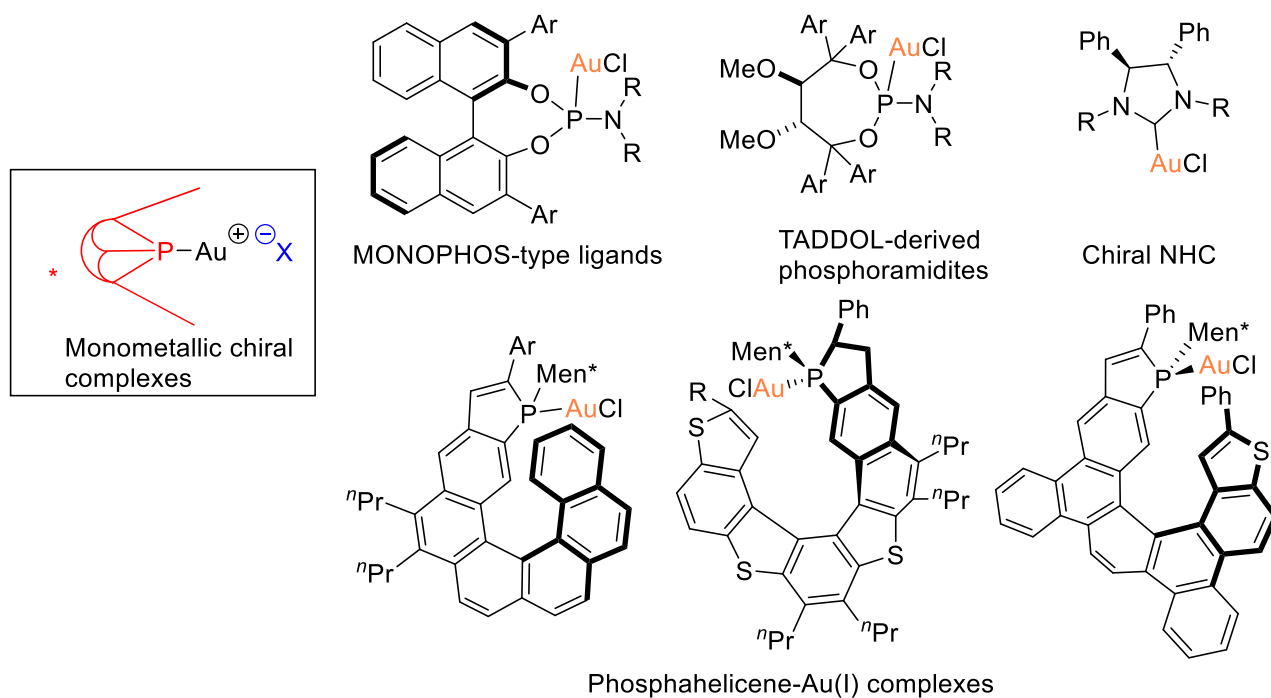
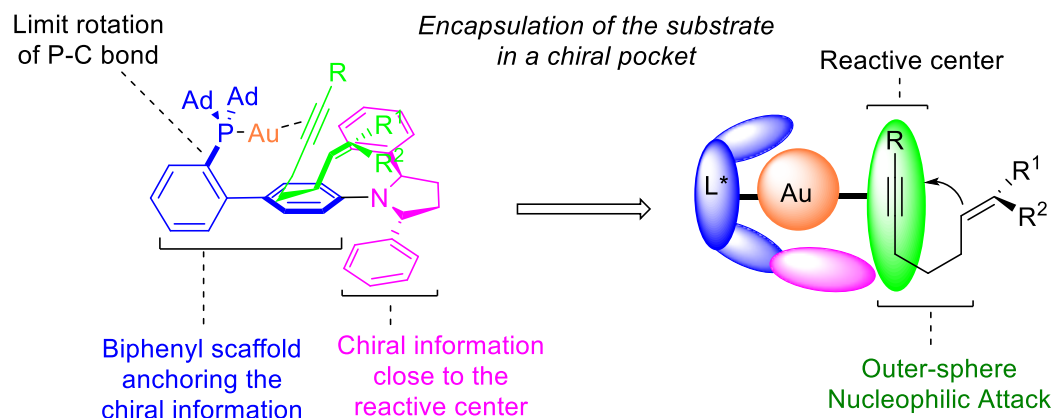


Figure 4. Monometallic Gold Complexes with Axial, Central and Helical Chirality

In 2019, Echavarren and co-workers developed another type of chiral gold catalysts inspired by the achiral JohnPhos ligand (JohnPhos = (2-biphenyl)di-*tert*-butylphosphine).²¹ They introduced a chiral 2,5-disubstituted pyrrolidine unit in *para* position of the biphenyl scaffold, as well as bulky groups on phosphorus to limit rotation around the P-aryl bond (Scheme 5). This extended ligand thereby generated a chiral pocket perfectly suitable for enantioselective reactions, the chiral information being very close to the reacting center. The new catalyst has been applied successfully in the asymmetric cycloisomerizations of enynes.

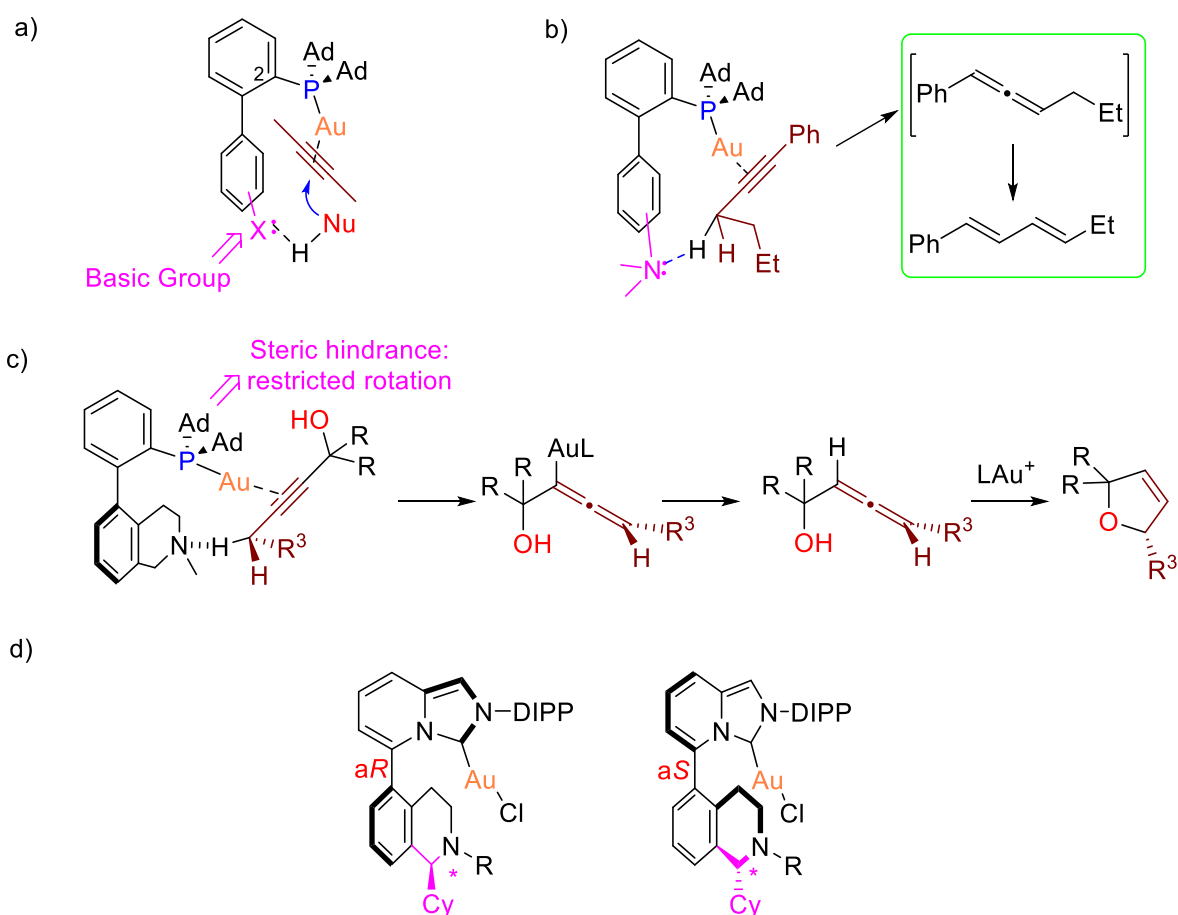


Scheme 5. Echavarren's Design of Extended Chiral Ligands for Monometallic Gold Complexes

2.2. Au(I) complexes of bifunctional chiral ligands

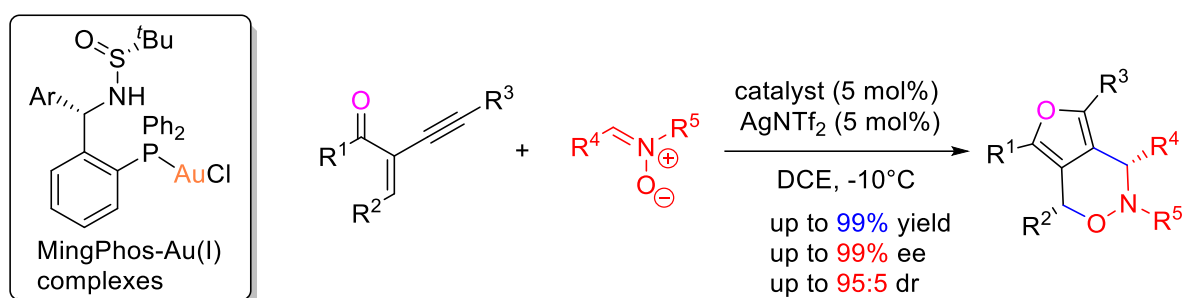
Beyond classical chiral ligands that operate mainly through steric effects, bifunctional ligands have been designed to modulate the catalytic activities or enantioselectivities by addition of another chemical function that can trigger secondary interactions. Recently, gold complexes of chiral ligands displaying either basic amino functions or *H*-bonding units have emerged as extremely efficient catalysts.

For example, in 2014, Liming Zhang reported on the Au(I) complexes of a novel series of bifunctional phosphines displaying a basic group ($X = \text{amine or amide}$) at the C3' position of a biphenyl moiety (Scheme 6a).²² It was demonstrated initially that the basic groups accelerate nucleophilic addition reactions to unsaturated substrates, as they enable suitable interactions with the nucleophiles. Notably, the WangPhos ligand ($X = \text{CO-N(CH}_2)_4$) showed very high reactivity in the addition of acids to alkynes (TON up to 99000, 0.5 mol% catalyst loading). In other instances, the WangPhos ligand facilitates the catalytic reaction by interacting with the unsaturated substrates themselves, as illustrated in Scheme 6b by the isomerization of alkynes into dienes. In the next few years, L. Zhang and coworkers envisioned the use of the same class of ligands in enantioselective gold catalysis and therefore introduced chiral elements on the biaryl backbone (Scheme 6c). For instance, in 2019, they successfully applied a modified WangPhos-type catalyst to the enantioselective synthesis of 2,5-dihydrofurans from propargylic alcohols via the corresponding allenes (Scheme 6c).²⁴ The authors also developed bifunctional NHC gold complexes based on the same design and successfully applied them in asymmetric catalysis (Scheme 6d).²⁵



Scheme 6. Gold Complexes of Bifunctional Ligands and Applications

In 2014, Junliang Zhang and co-workers designed and synthesized a new series of chiral sulfonamide-functionalized phosphines, typified by the MingPhos ligand (Scheme 7).²⁶ As an example, the MingPhos gold complex has been used in the cycloisomerization/nucleophilic addition of 2-activated 1,3-enynes with nitrones. The functional group participates in the stereochemical control, although the configuration of the stereogenic benzylic carbon dictates the configuration of the final product. The catalyst showed high diastereo-, regio- and enantio- selectivities in this reaction and the desired bicyclic furanes were obtained with up to 99% yield, 99% ee and >95:5 diastereomeric ratios. These reactions will be further discussed in this manuscript.



Scheme 7. MingPhos-Au(I) Complexes and Use in Enantioselective Cyclization Reactions

3. The chiral-counterion strategy: Asymmetric Counteranion-Directed Catalysis (ACDC)

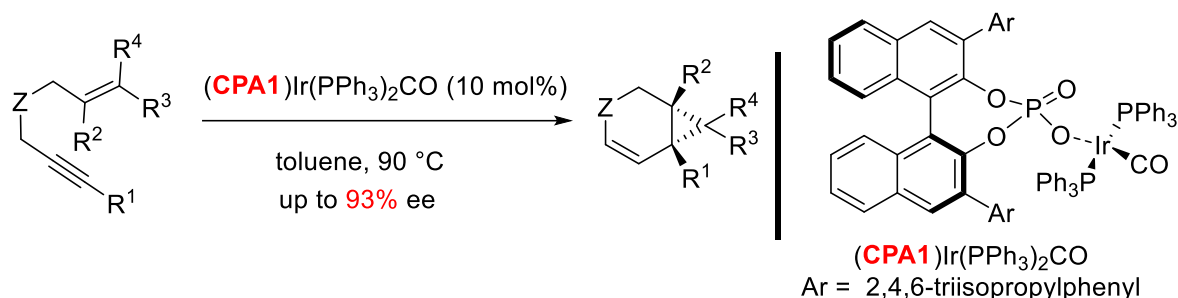
3.1. General information on this strategy

All of the strategies in enantioselective gold catalysis mentioned above rely on specifically designed ligands and involve transfer of the stereochemical information from the ligand backbone to the products. Over the last decade, another strategy emerged based on the non-covalent interaction between a chiral counterion and a cationic achiral metal complex. The method is commonly referred as the “Asymmetric Counteranion-Directed Catalysis”. It was described by List²⁷ as follows: “*Asymmetric counteranion-directed catalysis refers to the induction of enantioselectivity in a reaction proceeding through a cationic intermediate, by means of ion pairing with a chiral, enantiomerically pure anion provided by the catalyst*”. The key role of chiral ion pairs was already well known in the field of phase-transfer catalysis and organocatalysis,²⁸ but remained sporadic in transition metal catalysis.²⁹ Since its early steps, the ACDC strategy has ushered in the vigorous development of successful metal-catalyzed reactions involving a variety of transition metals.^{30,31} With the advent of chiral phosphoric acids as privileged organocatalysts (CPA),³² chiral phosphates have been extensively used as counterions in the ACDC strategy. Selected examples are provided hereafter.

3.2. Selected examples of ACDC in transition metal catalysis

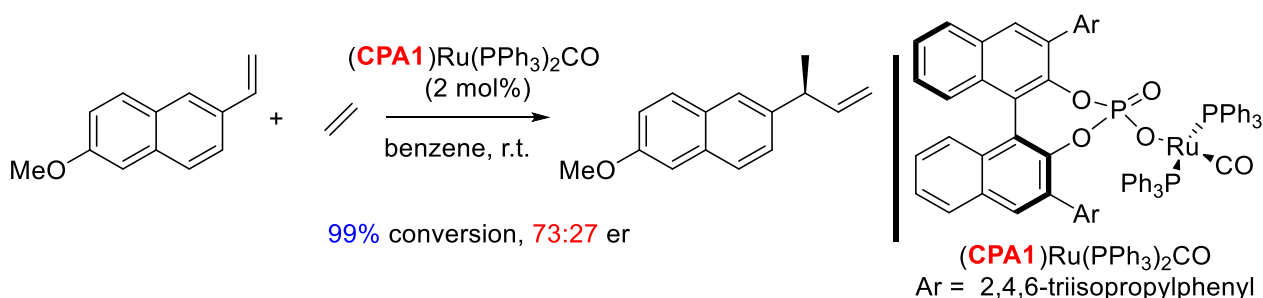
In 2011, Fensterbank, Gandon, Barbazanges and co-workers successfully used chiral iridium phosphates in enantioselective cycloisomerizations (Scheme 8).^{31g} An achiral iridium precursor, the Vaska’s complex

$\text{IrCl}(\text{CO})(\text{PPh}_3)_2$, was reacted with the silver salt of a chiral phosphate to generate the Ir-phosphate catalyst. In the cycloisomerization of 1,6-enynes, the desired bicyclic products were obtained with up to 93% ee, when using the TRIP derived phosphate as the counterion. Meanwhile, IR, ^{31}P NMR and DFT calculations provided strong evidence for the structure of the catalyst and the bonding mode in possible reaction intermediates.



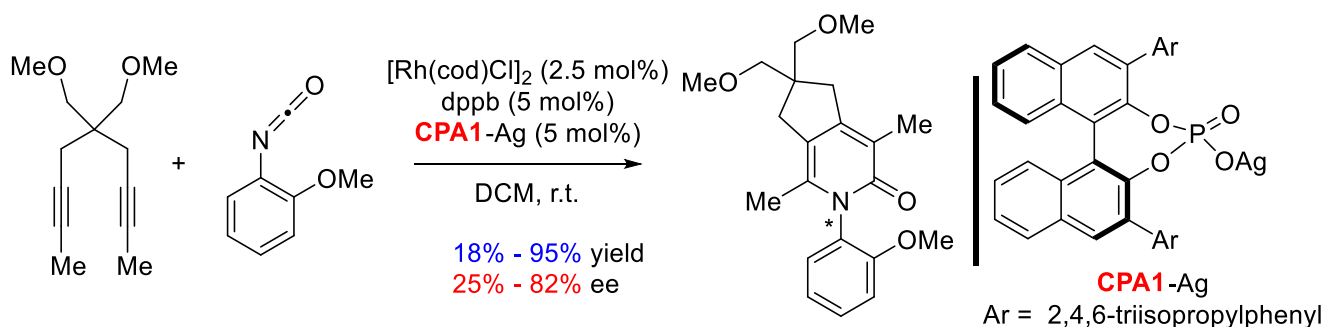
Scheme 8

In parallel studies, the ACDC strategy has been extended to chiral ruthenium catalysts: the List group achieved the asymmetric hydrovinylation of olefins with ethylene, catalyzed by a ruthenium complex displaying the same phosphate counteranion. The catalyst, prepared by the same halide-phosphate exchange reaction, showed excellent reactivity and moderate enantioselectivity. (Scheme 9).³³



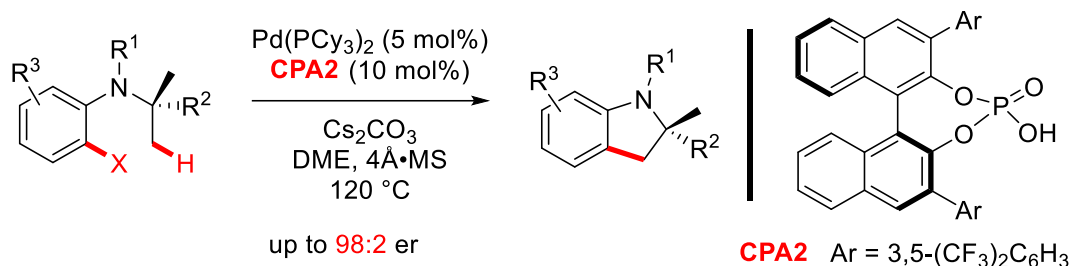
Scheme 9

In 2013, the first rhodium catalyzed enantioselective [2+2+2] cycloadditions of 1,6-diynes with isocyanates, based on the ACDC strategy, were developed by Ollivier and co-workers (Scheme 10).^{31c, 34} The chiral rhodium phosphate was generated *in situ* from the achiral rhodium dimer $[\text{Rh}(\text{COD})\text{Cl}]_2$ and the chiral silver phosphate **CPA1-Ag** salt. It promoted the desired cycloaddition reactions with good yields and enantiomeric excesses up to 82%.



Scheme 10

In 2017, the Baudoin group reported the first use of achiral palladium(0) complexes combined with chiral phosphates to catalyze enantioselective C(*sp*³)-H arylation reactions (Scheme 11).³⁵ In these reactions, the chiral phosphate behaves as the palladium counteranion in Pd(II) intermediates formed after oxidative addition of the substrate to Pd(0). It also behaves as a base favoring the subsequent CH activation step. Finally, the starting halo-anilines were converted into indolines in good yields and enantiomeric excesses, using the perfluoromethylated acid **CPA2** as the co-catalyst.



Scheme 11

3.3. Application of the ACDC strategy in enantioselective Au(I) catalysis

The ACDC strategy has been introduced in the field of gold(I) catalysis in 2007 by F. D. Toste who reported the use of cationic Au(I) complexes displaying achiral ligands and chiral phosphate counteranions.³⁶ Comparison with the classical ligand-based approach shows that the ACDC approach favorably places the source of chiral induction (the chiral phosphate) closer to the reaction center (Figure 5). This facilitates the efficient shaping of the chiral pocket and could potentially favor the enantioselectivity.

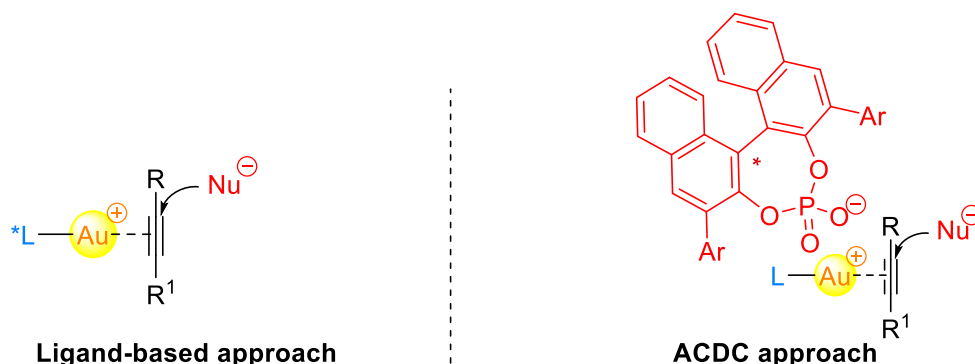
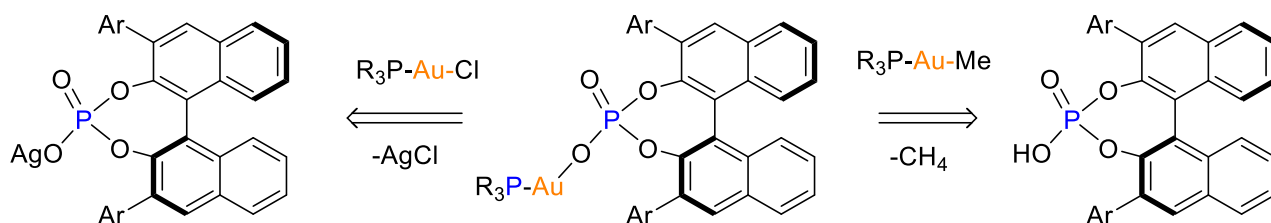


Figure 5. Comparison of Ligand-Based Strategies with the ACDC Strategy in Gold Catalysis

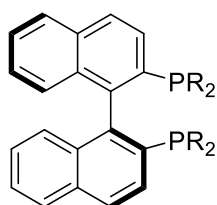
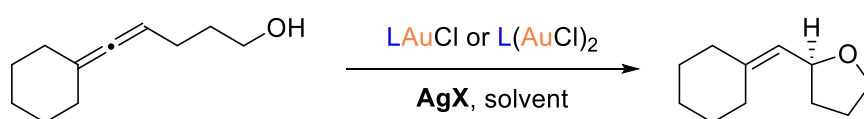
The chiral Au(I) phosphates can be easily prepared by two main protocols: (a) reaction of a phosphine gold chloride with silver phosphate that induces chloride abstraction and counterion metathesis; or alternatively (b) reaction of a (phosphine)Au(methyl) complex with a phosphoric acid, releasing methane and the chiral gold phosphate (Scheme 12).³⁶⁻³⁷



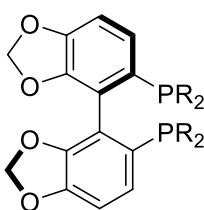
Scheme 12. Formation of Gold(I) Phosphate Complexes

By screening a few ligand/phosphate pairs, F.D. Toste could highlight chiral gold phosphates that demonstrated good reactivity and high enantioselectivity in some reactions, such as the intramolecular hydroalkoxylation of allenes (Table 1).³⁶

Table 1. Optimization of the Catalysts in Intramolecular Hydroalkoxylation of Allenes



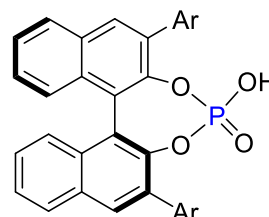
L1, R = Ph
L2, R = 3,5-xlylyl



L3
R = 3,5-(*t*-Bu)₂-4-(CH₃O)-C₆H₂



L4



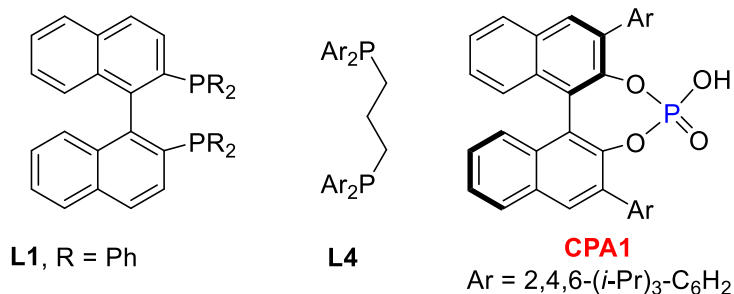
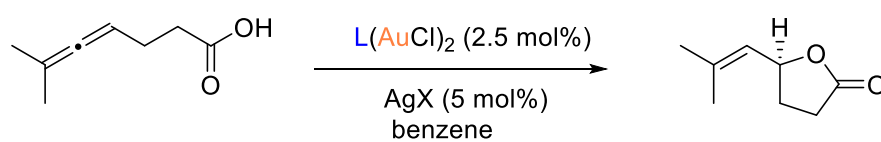
CPA1
Ar = 2,4,6-(*i*-Pr)₃-C₆H₂

entry	L (mol%)	X	solvent	yield (%)	ee (%)
1	L1 (2.5)	BF ₄ ⁽⁻⁾	DCM	52	6
2	L2 (2.5)	BF ₄ ⁽⁻⁾	DCM	68	0
3	L3 (2.5)	BF ₄ ⁽⁻⁾	DCM	79	2
4	L2 (2.5)	4-NO ₂ -C ₆ H ₃ CO ₂ ⁽⁻⁾	DCM	89	8
5	PPh ₃ (5)	CPA1 ⁽⁻⁾	DCM	89	48
6	L4 (2.5)	CPA1 ⁽⁻⁾	DCM	76	65
7	L4 (2.5)	CPA1 ⁽⁻⁾	benzene	90	97

In these reactions, dinuclear gold catalysts derived from BINAP (**L1**, **L2**) or SEGPHOS (**L3**) type ligands were evaluated first and gave very poor enantiomeric excesses, whatever the achiral counterion used (entries 1-4, ee < 10%). The gold phosphate resulting from the reaction of Ph₃PAuCl with **CPA1**-Ag was then used and provided the tetrahydrofuran **6** in 89% yield and 48% ee (entry 5). The reaction was further optimized by changing the ligand to dppp (**L4**) and the solvent to benzene to deliver the target product with 90% yield and 97% ee (entries 6 and 7). These conditions were then successfully applied to the analogous intramolecular hydroamination of allenes.

Moreover, F.D. Toste has considered the possibility of combining chiral phosphines and chiral phosphates in order to highlight matching effects. Indeed, although the phosphine ligand does not directly participate in the construction of a chiral environment, it can modulate the activity and enantioselectivity triggered by the catalyst, by affecting the ion pairing between gold and its counteranion. This effect is illustrated in Table 2 for the intramolecular hydrocarboxylation of allene. When (*R*)-BINAP (**L1**) was used as ligand in a gold complex with an achiral carboxylate counterion, it provided an (*R*)-configured product in moderate 38% ee (entry 1). Also, when the same reaction was performed with the achiral dppp ligand **L4** and the chiral phosphate **CPA1**, it triggered an only low enantioselectivity (12% ee, entry 2). However, a match/mismatch effect was observed with the diastereomeric complexes formed from (*R*)- or (*S*)-BINAP and (*R*)-**CPA1**. Hence, (*R*)-BINAP combined with (*R*)-**CPA1** led to the (*R*)-configured product with a 3% ee (entry 3), while (*S*)-BINAP combined with the same phosphate (*R*)-**CPA1** generated the (*S*)-configured product in 82% ee (entry 4).

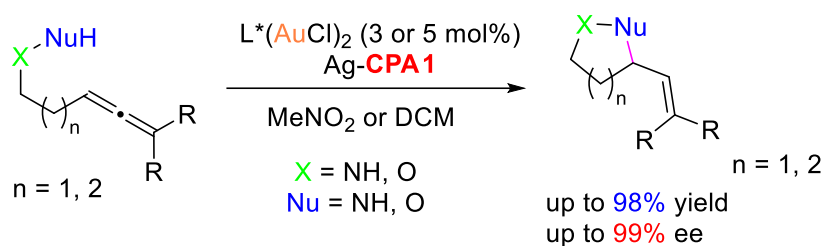
Table 2



entry	L	X	solvent	yield (%)	ee (%)
1	(<i>R</i>)- L1	4-NO ₂ -C ₆ H ₃ CO ₂ ⁽⁻⁾	DCM	80	38 (<i>R</i>)
2	L4	CPA1 ⁽⁻⁾	DCM	89	12 (<i>S</i>)
3	(<i>R</i>)- L1	CPA1 ⁽⁻⁾	DCM	91	3 (<i>R</i>)
4	(<i>S</i>)- L1	CPA1 ⁽⁻⁾	DCM	88	82 (<i>S</i>)

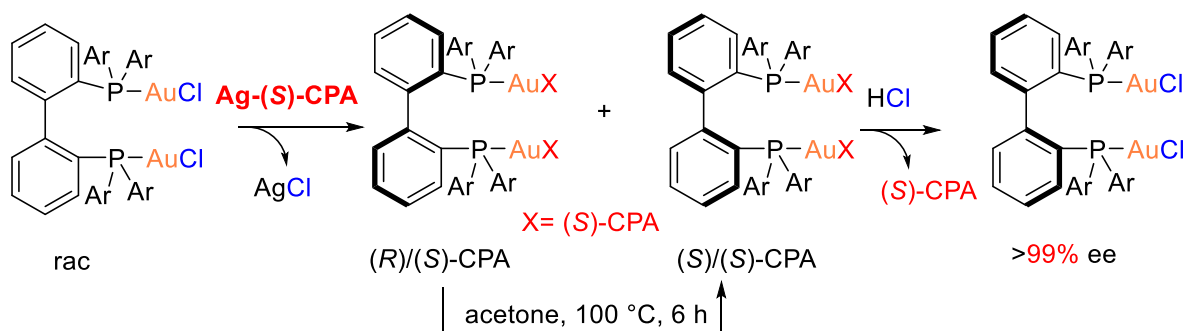
In 2014, Lipshutz observed the same effects when he performed the reaction using an aqueous solution in the presence of surfactants.³⁸

In 2010, the Toste group extended the ACDC strategy to the synthesis of pyrazolidines, tetrahydrooxazines and isoxazolidines through intramolecular hydroamination and hydroalkoxylation reactions. Different chiral counteranions were tested and compared in these reactions. Finally, from each substrate, the desired products could be obtained with excellent yields and enantiomeric excesses using optimized combinations of chiral atropisomeric diphosphines (or achiral dppm) and the chiral TRIP phosphate **CPA1** (Scheme 13).³⁹



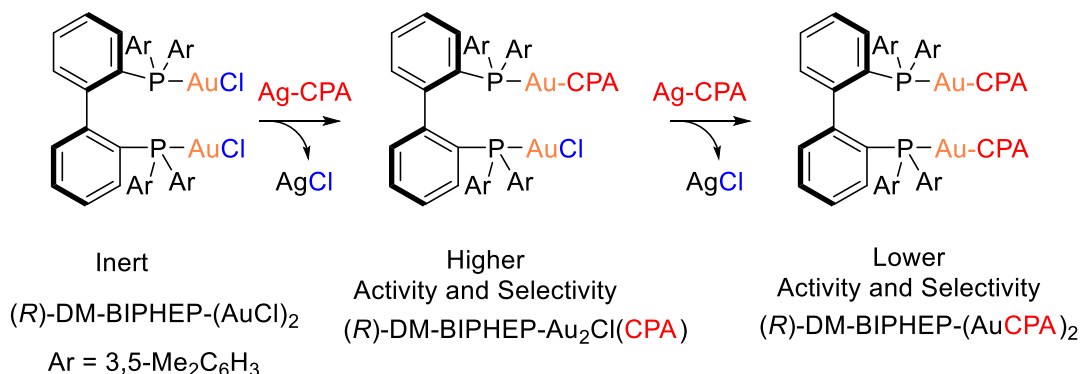
Scheme 13

In 2010, Mikami group reported an original application of chiral Au(I) phosphates.^{14d} They heated the gold complex of a configurationally labile biphenyl-diphosphine with various enantiopure silver phosphates for hours, thereby generating diastereomeric pairs (Scheme 14). They could establish that, under certain conditions, control of the configuration of the chiral axis of the phosphine occurs, leading to a single diastereomer, and turned this process into a dynamic kinetic resolution method. The enantiopure (biphenyl-diphosphine)gold phosphates could be isolated and the corresponding chlorides could be obtained then after treatment of the chiral phosphate with HCl.



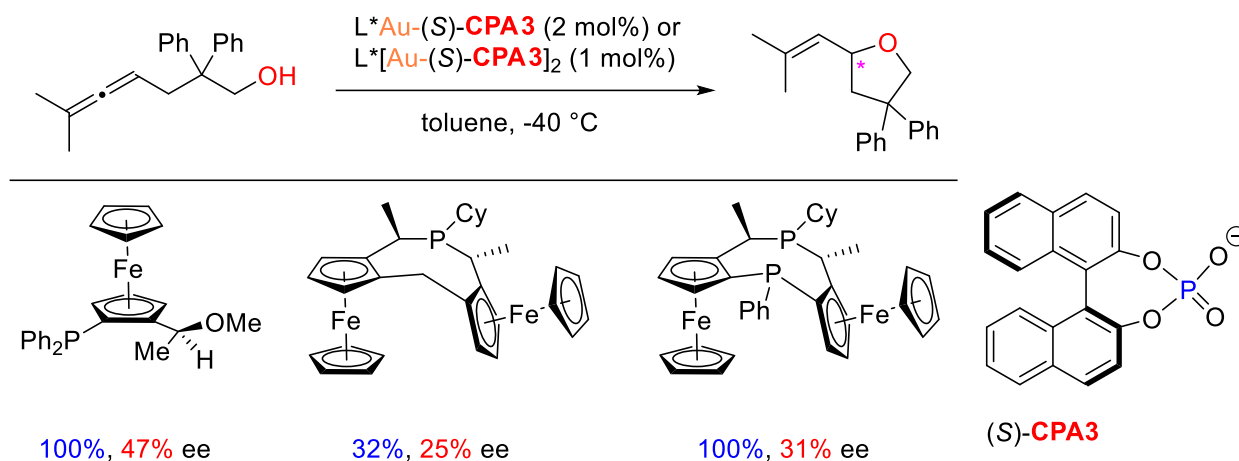
Scheme 14

The same authors investigated then synergistic effects in the intramolecular hydroalkoxylation reactions promoted by dinuclear BIPHEP-gold catalysts with CPA counterions. They found that the mono-activated dinuclear gold complexes show higher enantioselectivity and reactivity than the fully activated or non-activated dinuclear complexes (Scheme 15).^{14c} In the asymmetric cyclohydroalkoxylation of allenes the mono-activated catalysts gave the expected products in good to excellent enantioselectivities (up to 95% ee) when the (*R*)-configured diphosphine is combined with (*S*)-configured phosphates.



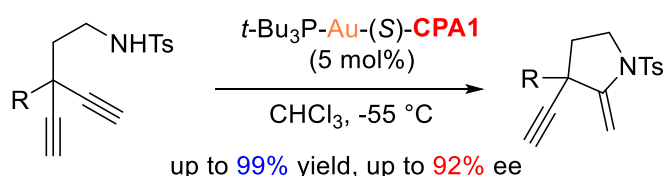
Scheme 15

In 2012, Hii and co-workers synthesized and characterized new ferrocenylphosphine ligands with planar chirality. The ligands were coordinated with gold chloride and chloride abstraction with the silver salt of a BINOL derived phosphate led to the corresponding chiral gold phosphates. These new complexes promoted the intramolecular hydroalkoxylation of allenes with good to excellent yields and led to the corresponding tetrahydrofuranes with up to 47% ee (Scheme 16).⁴⁰



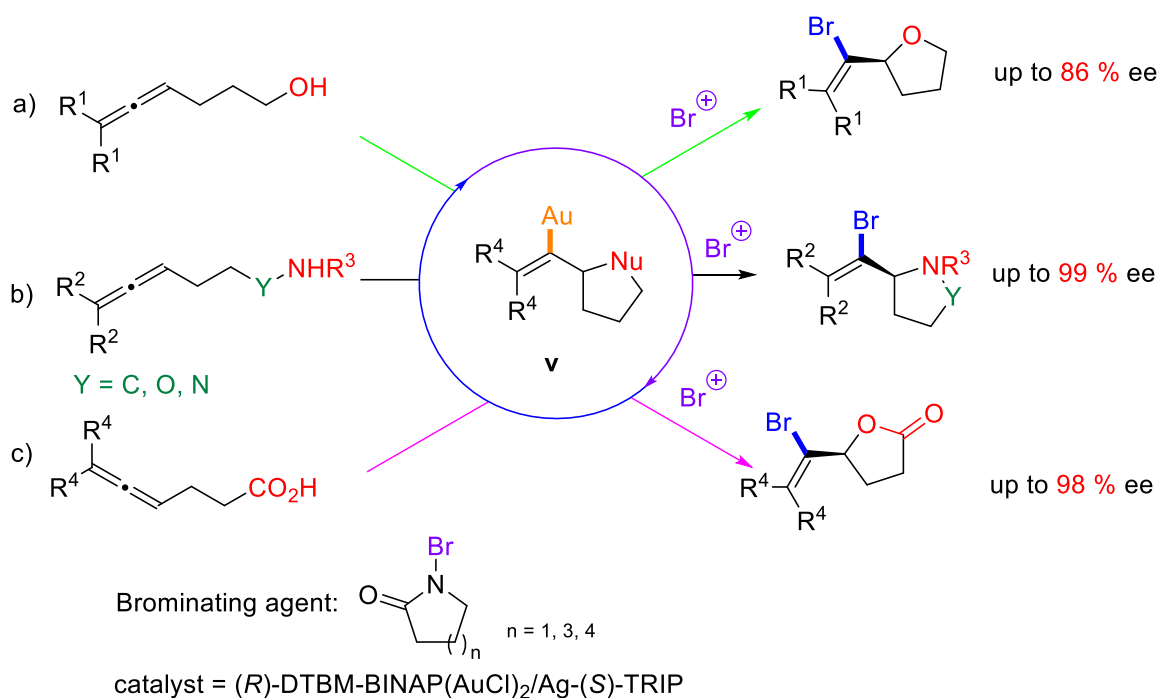
Scheme 16

In 2012, the Czekelius group reported on the gold catalyzed asymmetric intramolecular hydroamidation of 1,4-diyne-amides by applying the ACDC strategy (Scheme 17). In this process, desymmetrization of the prochiral substrate occurs with high enantioselectivity and leads to the desired pyrrolidines with up to 99% yields and 92% enantiomeric excesses. It is worth noting that dinuclear gold complexes of chiral diphosphines catalyze this type of reaction with good yields and very low enantiomeric excesses.⁴¹



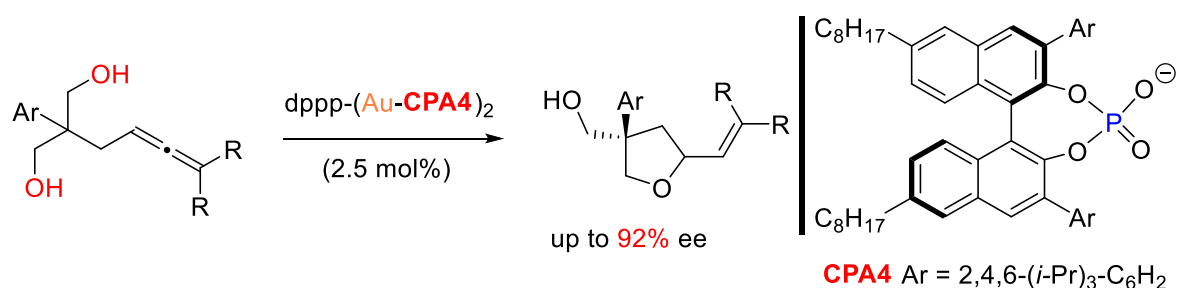
Scheme 17

In 2013, the Toste group found that the vinyl-Au intermediates **v** formed in the intramolecular hydroalkoxylations, hydroaminations and hydrocarboxylation of allenes, can be trapped in the presence of *N*-bromolactams, the addition of $Br^{(+)}$ leading to the brominated olefins shown in Scheme 18.⁴² In this case, the dinuclear (*R*)-DTBM-BINAP gold complex [DTBM = 2,5-di-*tert*butyl-4-methoxyphenyl], combined with the (*S*)-TRIP silver salt led to the corresponding products in excellent yields and enantiomeric excesses. Depending on the substrates, other atropisomeric diphosphines have been used also.



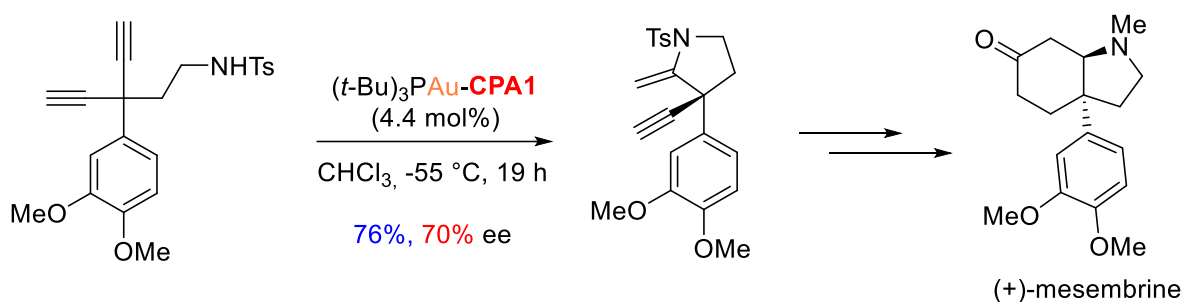
Scheme 18

In 2015, the Toste group disclosed that the bimetallic dppp-gold(I) complex [dppp = bis(diphenylphosphinopropane)] with the chiral phosphate **CPA4** as the counterions is catalytically active in the enantioselective desymmetrization of 1,3-diols via intramolecular hydroalkoxylation of an allene function. The reaction led to substituted tetrahydrofurans with high diastereoisomeric ratios and up to 92% ee (Scheme 19).⁴³



Scheme 19

In 2016, the Czekelius group described the application of the ACDC strategy in the total synthesis of (+)-Mesembrine via a desymmetrization reaction.⁴⁴ The (*R*)-TRIP derived (tris-*tert*-butylphosphine)gold phosphate was used as catalyst in the intramolecular hydroamination of a 1,4-dynamide. The catalyst successfully achieved the selective addition of the protected amine on an alkyne unit, leading to the desymmetrization, hydroamination product **9** in 76% yield and 70% ee. Thus, in this process, a quaternary stereogenic center is created with a satisfying degree of stereocontrol. The obtained product was converted then into the natural alkaloid in six steps (Scheme 20).



Scheme 20

4. The Tethered Counterion Directed Catalysis (TCDC): PhD project

Overall, the short overview in sections 3.2 and 3.3 emphasizes that the ACDC strategy represents a powerful approach to asymmetric transition metal catalysis. In the field of Au(I) catalysis, however, it has been limited mainly to a single class of reactions, the intramolecular hydrofunctionalizations of allenes and its extension to the desymmetrization of diynes. It can be postulated that the ACDC approach enables high enantioselectivity in these reactions since they display at least four very favorable features (see Figure 6): (1) their intramolecular nature; (2) a tight and bulky Au⁽⁺⁾ phosphate⁽⁻⁾ ion pair in the key intermediate; (3) the close proximity between the cationic gold and the carbon center involved in the stereodetermining step; (4) an hydrogen bond possibly formed between the incoming nucleophile and the P=O function of the chiral phosphate. All these features induce steric, conformational and geometrical constraints that contribute to the stereochemical control of these reactions.

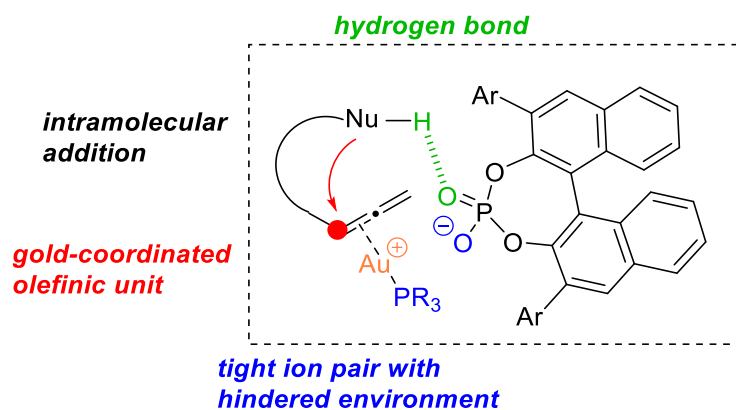


Figure 6. Favorable Features of ACDC Approach

However, unfortunately, the chiral counterion approach has not been applied successfully to other Au(I) catalyzed reactions, possibly because of a loose carbocation-phosphate ion pairs in the stereodetermining step (Figure 7a). The large conformational freedom and moderate steric hindrance of such intermediates will be detrimental to the stereochemical control, leading to poor enantioselectivities. As a representative example, cycloisomerizations constitute a huge domain of Au(I) catalysis,⁴⁵ for which the ACDC strategy is not efficient.^{31g, 37}

In this context, we have proposed a new design for gold catalysts in which gold will be tethered to its chiral phosphate counterion (Figure 7b). This strategy might well inherit the advantages of the ACDC approach, while the presence of the tether will increase the geometrical constraints, decrease flexibility and finally increase stereocontrol. Thus, these new catalysts might solve at least some of the limitations of ACDC in the field of gold catalysis and others. This strategy has been named “Tethered Counterion Directed Catalysis” (TCDC).⁴⁶

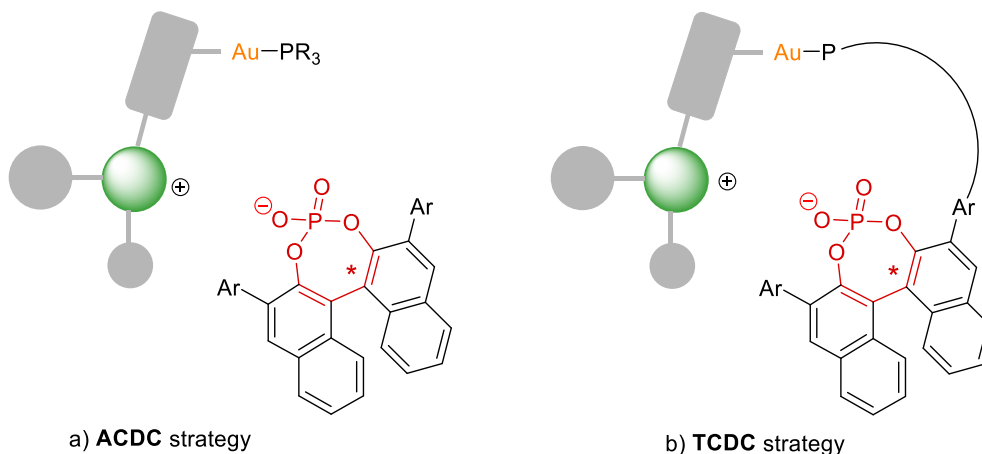


Figure 7. Possible Key Intermediates in ACDC Strategy and TCDC Strategy

In this scenario, we have decided to prepare bifunctional phosphine-phosphoric acid ligands and the corresponding gold complexes of the general formulas **A** or **B** in Figure 8. The targeted corresponding ligands, that we have named **CPAPhos**, display cyclic phosphoric acid functions built on either (*S*)-BINOL or (*S*)-SPINOL backbones, since these scaffolds have largely demonstrated their efficiency in enantioselective catalysis.⁴⁷ The **phosphine** and **phosphoric acid** functions have been tethered by using linkers of various lengths, featuring an *ortho*-phenylene unit and possibly additional CH₂ spacers (X, Y = none or CH₂).

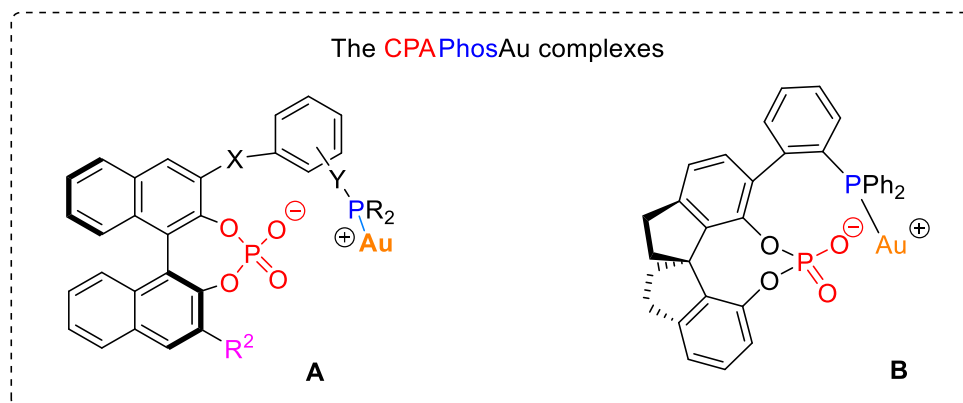


Figure 8. Structure of the Target CPAPhosAu Complexes

In this manuscript we will present first the synthesis and characterization of these two series of bifunctional catalysts (Chapter 1), we will disclose then their applications in selected catalytic reactions, namely in tandem cycloisomerization-nucleophilic addition reactions (Chapter 2). A short chapter will then focus on our preliminary results in the application of the strategy to other reactions (Chapter 3).

Overall, these studies will illustrate the TCDC approach and demonstrate its benefits in enantioselective gold catalysis, in terms of both enantioselectivity and catalytic activity.

Chapter 1: Synthesis of bifunctional chiral phosphine-phosphate Au(I) complexes

In order to test the working hypothesis presented in Section 4 above and validate the TCDC approach, we have prepared several gold(I) complexes of phosphoric acid functionalized phosphines. The synthetic approach is typified hereafter by the synthesis of the first member of the series based on a BINOL chiral platform, then extension of the method to other series will be presented. Note that the target Au(I) complexes CPAPhosAuCl presented below are often qualified as precatalysts, because of the lack of catalytic activity before activation with a silver salt.

1. Synthesis and characterization of the BINOL-derived phosphine-phosphate Au(I) complex CPAPhos^AAuCl

Our first aim has been the synthesis of the gold complex CPAPhos^AAuCl whose structure is shown in Figure 9. The chiral cyclic phosphoric acid unit is made from (*S*)-BINOL [(*S*)-[1,1'-binaphthalene]-2,2'-diol] and the binaphthyl motif bears an *ortho*-diphenylphosphinophenyl substituent attached to its position C3. This motif has been selected because its polyaromatic scaffold is expected to have a rather low degree of conformational freedom and hopefully provide a well-defined chiral pocket for enantioselective catalytic reactions. After investigating the literature reports on the synthesis of analogous scaffolds, a very effective route for the synthesis of these ligands could be determined.

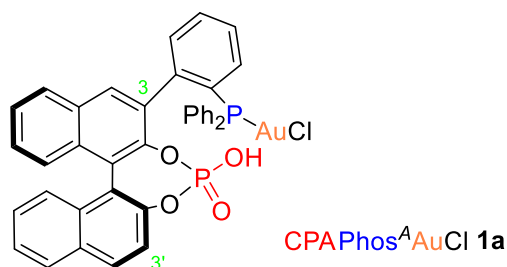
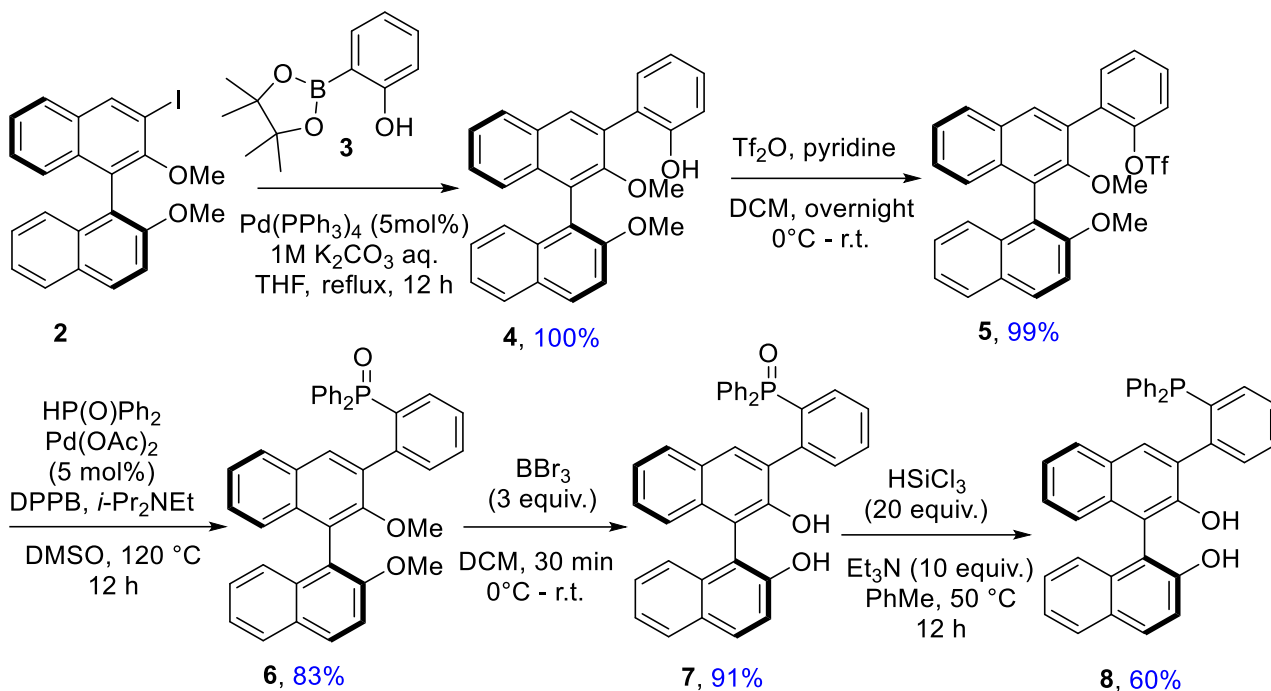


Figure 9. Molecular Structure of the Gold(I) Complex CPAPhos^AAuCl 1a

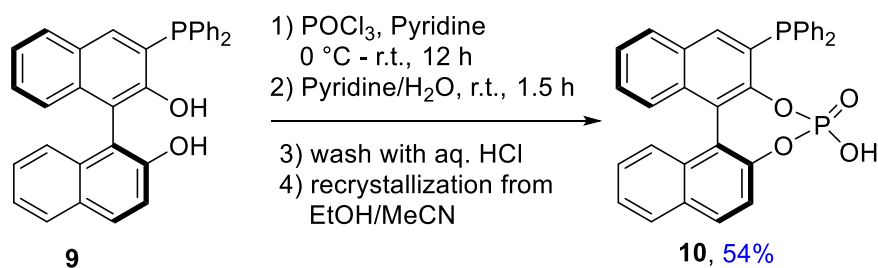
1.1. Synthesis of the gold complex CPAPhos^AAuCl 1a

In 2006, the Sasai group reported the synthesis of the (*S*)-3-(2-(diphenylphosphanyl)phenyl)-[1,1'-binaphthalene]-2,2'-diol **8** in 5 steps (Scheme 21),⁴⁸ using (*S*)-3-iodo-2,2'-dimethoxy-1,1'-binaphthalene **2** as the starting material. The iodide **2** was subjected to a Suzuki coupling with *ortho*-hydroxyphenylboronate **3** and the resulting intermediate **4** was converted into the triflate **5** using triflic anhydride. The desired phosphine oxide **6** was then obtained from **5** by a Pd-promoted phosphination reaction. Finally, a deprotection/reduction sequence led to the trivalent phosphine-diol **8**.



Scheme 21. Synthesis of **8**, according to Sasai⁴⁸

Thus, we guessed that the known phosphine-diol **8** might be a suitable precursor for the targeted phosphine-phosphoric acid ligand *via* a simple phosphorylation step.⁴⁹ It is known indeed from Sawamura *et al.*⁵⁰ that the analogous phosphine-phosphoric acid **10** can be easily prepared from diol **9** by reaction with POCl₃ in pyridine, followed by hydrolysis (Scheme 22). The phosphoric acid **10** was isolated in 54% yield.



Scheme 22. Synthesis of the Phosphine-Phosphoric Acid **10**, according to Sawamura⁵⁰

Thus, based on these literature data, we could define a retrosynthetic approach for the synthesis of catalyst **1a** (Figure 10). The known phosphine diol **8** will be prepared from BINOL, it will be coordinated to gold(I) and reacted then with phosphorus oxychloride to generate the phosphoric acid function. Alternatively, phosphorylation might precede complexation to gold.

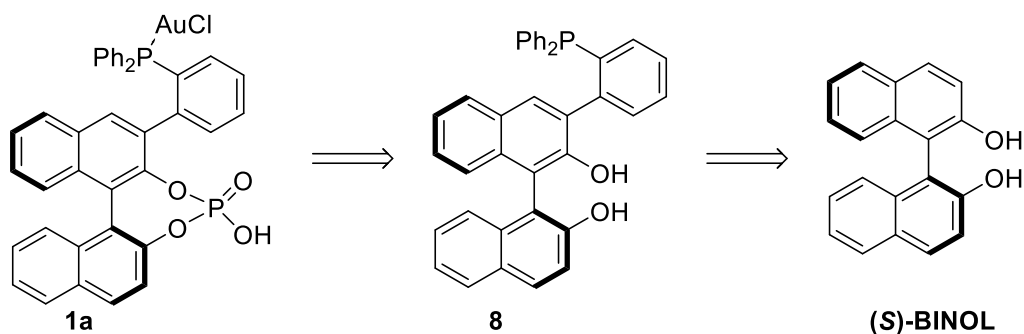


Figure 10. Retrosynthetic Approach to CPAPhos^AAuCl **1a**

We then turn to prepare the compound **8** from (*S*)-BINOL (Figure 11). It is worth noting that (*S*)-BINOL is an ideal starting material for the synthesis of new catalysts due to its easy availability in enantiopure form and cheapness. Compared to the Sasai's approach, we decided to change methyl by methoxymethyl (MOM) as the *O*-protecting groups, and then to introduce a boronate function on the protected BINOL, instead of an iodide. The resulting boronate **12** will serve as the reaction partner to introduce the phosphorus function via a Suzuki coupling.

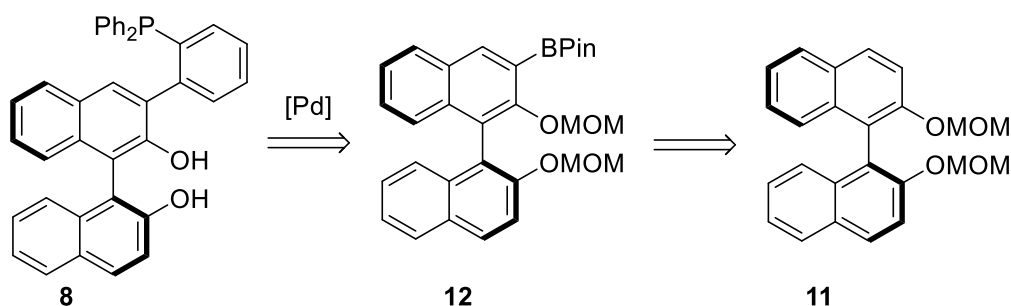
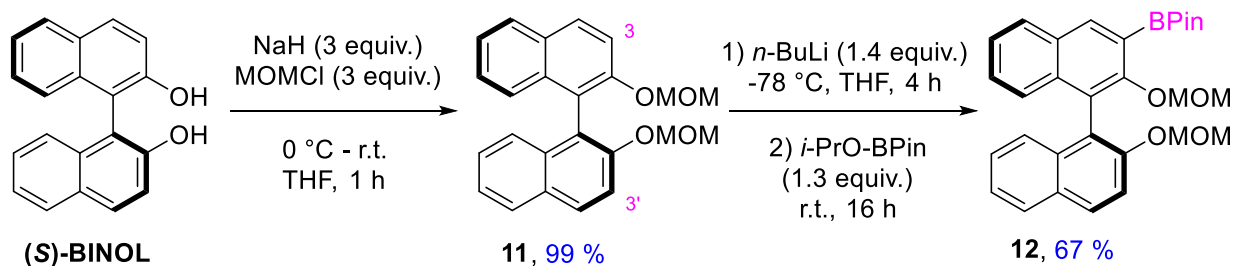


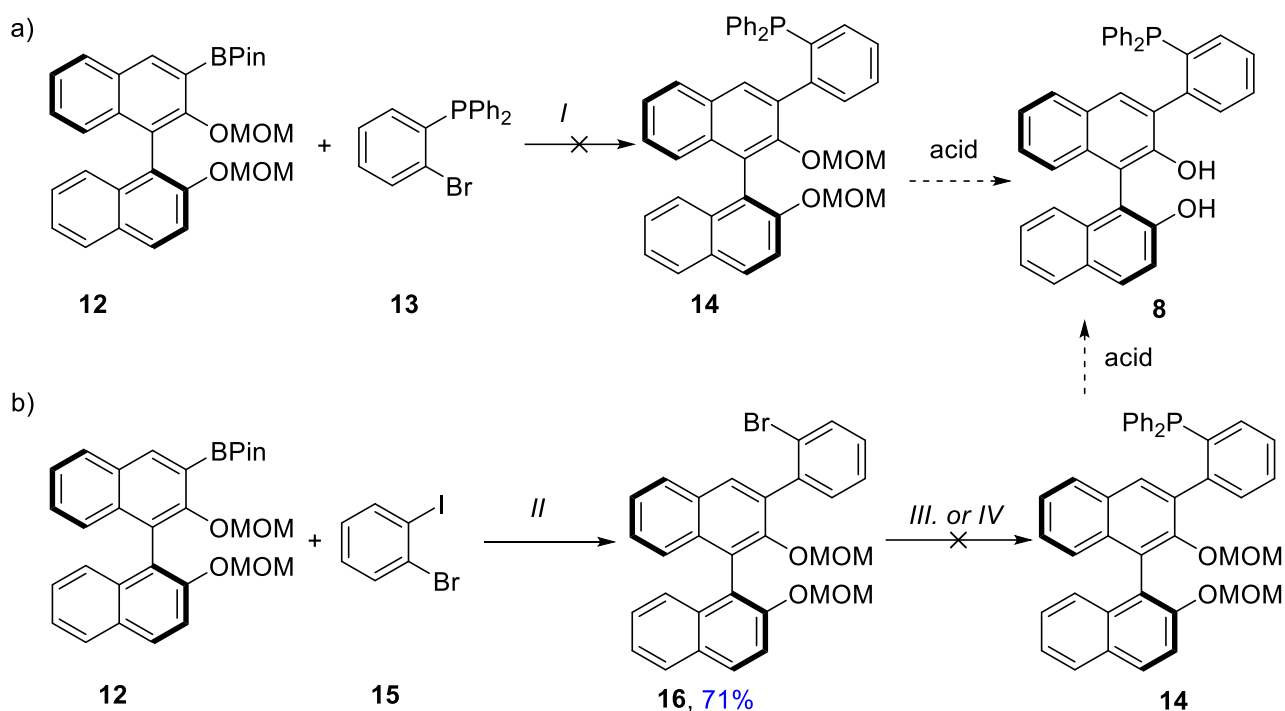
Figure 11. Retrosynthetic Approach to **8**

In order to achieve our goal, we synthesized the 1,3,2-dioxaborolane **12** from (*S*)-BINOL, according to the literature (Scheme 23).⁵¹ After protection of (*S*)-BINOL with methoxymethyl chloride, the boronate function was introduced by lithiation with *n*-BuLi, followed by addition of isopropoxy-pinacolborate (*i*-PrO-BPin). Boronate **12** was obtained in 67% yield. It is worth noting that the methoxymethyl group is a well-known *ortho*-directing group in metalation reactions. Therefore, only the C3 monosubstituted product **12** was obtained in this reaction.



Scheme 23. Synthesis of Boronate **12**

Then we tried to synthesize the trivalent phosphine-diol **8** directly from **12**. Two possible synthetic routes have been proposed (Scheme 24): (a) coupling of the boronate **12** with (*o*-bromophenyl)diphenylphosphine **13**, under palladium catalysis, followed by acidic deprotection; or (b) coupling of **12** with 1-bromo-2-iodobenzene **15**,^{51a, 52} followed by a second coupling reaction with diphenylphosphine or diphenylphosphine chloride and acidic deprotection.⁵³ Both strategies could avoid the formation of phosphine oxide as an intermediate. However, we failed to obtain phosphine **14** from pathway (a) despite many tries. Concerning pathway (b), compound **16** was successfully obtained by Suzuki coupling, using catalytic amounts of Pd(PPh₃)₄, with K₃PO₄ as the base, in DMF (71% yield). However, neither a metalation-phosphination sequence (BuLi, Ph₂PCl),^{53b} nor a palladium promoted coupling between **16** and Ph₂PH²¹ allowed the synthesis of the desired phosphine **14** (Scheme 24 and Table 3).



^a Reaction conditions: *I.* Pd(PPh₃)₄ (5 mol%), K₂CO₃ (3 equiv.), **13** (1.1 equiv.), THF-H₂O (2:1), 100 °C, N₂, 24 h; *II.* Pd(PPh₃)₄ (3 mol%), K₃PO₄ (3 equiv.), DMF, 80 °C, N₂, 23 h; *III.* Pd(dppf)Cl₂ (5 mol%), Ph₂PH (1.1 equiv.), *t*-BuONa (1.2 equiv.), PhMe, 120 °C, N₂, 16h. *IV.* 1) *n*-BuLi; 2) Ph₂PCl (See Table 3 for detail).

Scheme 24. Attempted Strategies for the Synthesis of Phosphine **8**

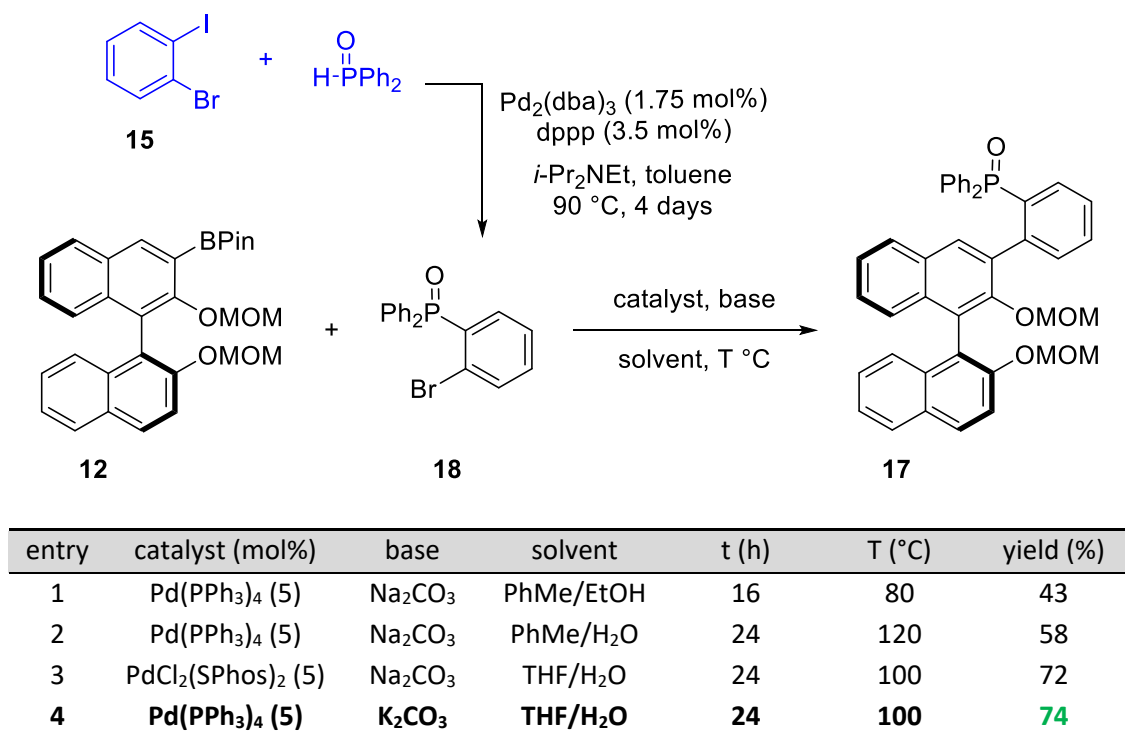
Table 3. Attempts for the Phosphination of **16**^a

entry	reactant (equiv.)	base (equiv.)	T (°C)	solvent	yield
1	Ph ₂ PCl (2.5)	<i>n</i> -BuLi (1.5)	-78	THF	NR
2	Ph ₂ PCl (1)	<i>n</i> -BuLi (1)	-78 to -41	THF	NR
3	Ph ₂ PCl (1)	<i>n</i> -BuLi (1.05)	-20 to r.t.	Et ₂ O	NR
4	Ph ₂ PCl (1.6)	<i>t</i> -BuLi (2.5)	-78	THF	NR

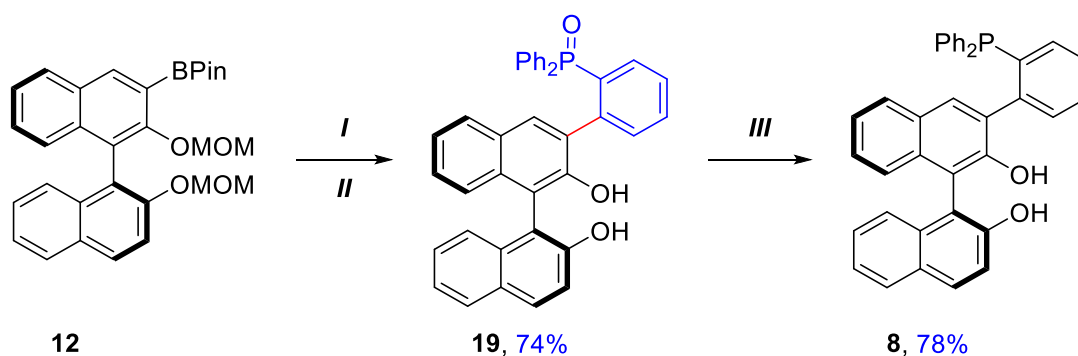
^a Reaction conditions: 1) *n*-BuLi, solvent, 2 h; 2) Ph₂PCL, r.t., 16 h.

Finally, we turned to the synthesis of phosphine oxide **17** (see Table 4) as a precursor for **8**. Based on the previous work of Vitalii Smal in our group (Master student 2017), we have envisioned the Suzuki coupling of boronate **12** with (*o*-bromophenyl)diphenylphosphine oxide **18** as an effective synthetic route to **17**. The phosphine oxide **18** was obtained from 2-bromoiodobenzene **15** and diphenylphosphine oxide as shown in Table 4.⁵⁴ After many attempts, we have determined the optimized conditions for the Suzuki reaction: the coupling was achieved in the presence of a catalytic amount of tetrakis(triphenylphosphine)palladium(0), in the presence of K₂CO₃, in a THF/water mixture, giving **17** in 74% yield.

Table 4. Optimization of the Synthesis of **17**



In further experiments, the Suzuki coupling and *O*-deprotection were performed in a single step (Scheme 25): crude **17** was treated under acidic conditions (*p*-TsoH) to remove the MOM protecting groups, yielding the corresponding diol **19** in 74% overall yield, from **12**. Further reduction of phosphine oxide **19** with an excess trichlorosilane/Et₃N in toluene,^{48,55} led to the desired phosphine **8** in 78% yield.



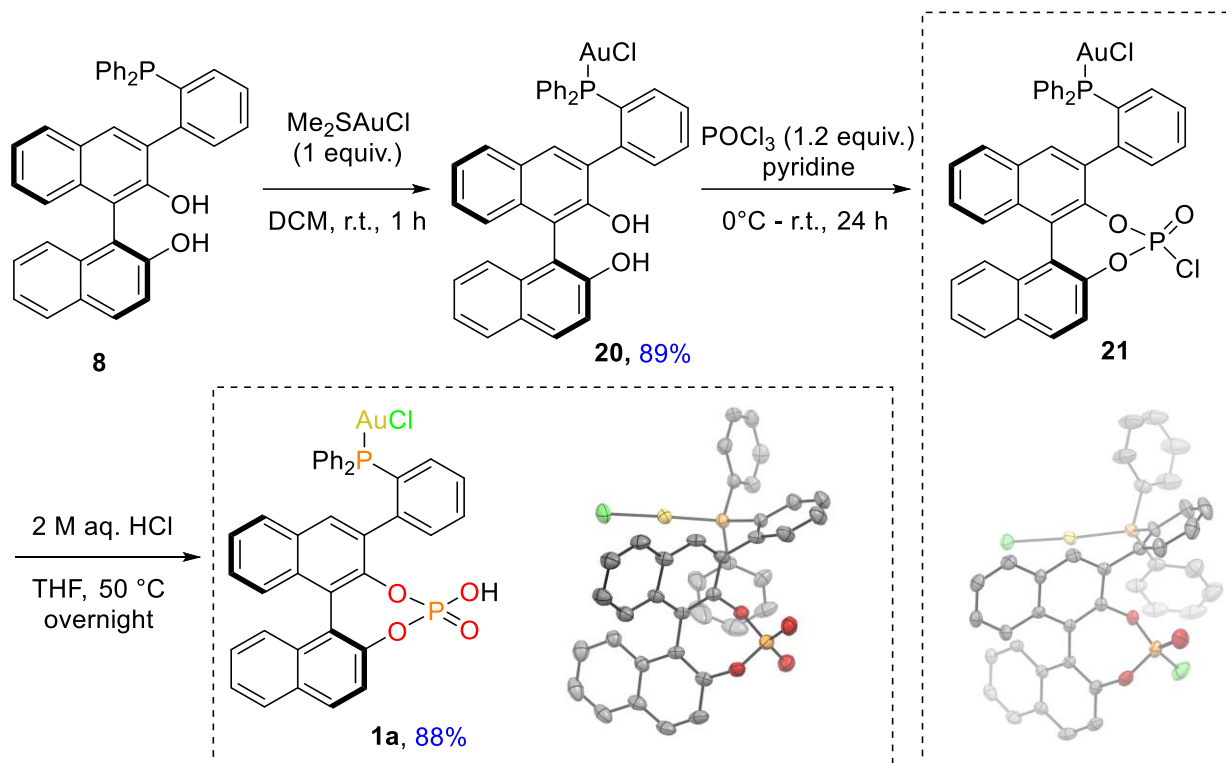
^a Reaction conditions: *I.* Pd(PPh₃)₄ (5 mol%), K₂CO₃ (3 equiv.), **18** (1.1 equiv.), THF/H₂O (2:1), 100 °C, N₂, 24 h; *II.* *p*-TsOH·H₂O (1 equiv.), THF/MeOH (1:1), 60 °C, 3 h; *III.* Cl₃SiH (20 equiv.), Et₃N (10 equiv.), toluene, 90 °C, 24 h.

Scheme 25. Synthesis of the Phosphine-Diol **8**

Overall, this strategy gives access to **8** at a multigram scale. Only the conditions for the reduction of the phosphine oxide remain unsatisfactory, as they require 20 equivalents Cl₃SiH that induce workup difficulties. The optimal solution to shorten the synthetic route would be to avoid the formation of phosphine oxide **19**, but this approach did not succeed so far (Scheme 24).

Having obtained phosphine **8**, we tried first to create a phosphoric acid function from the BINOL unit, under classical conditions (POCl₃, pyridine), but these attempts failed, as only complex mixtures were observed (phosphate-phosphine oxide complex as the major product, Vitalii Smal's work). We decided therefore to coordinate phosphine **8** to gold(I) prior to the phosphorylation step. Complexation has been performed by reaction with chloro(dimethylsulfide)gold(I) (DMS·AuCl), leading to the corresponding phosphine gold(I) chloride **20** in 89% yield. This Au(I) complex was reacted then with phosphorus oxychloride (POCl₃) as the phosphorylating agent, with pyridine as the base, to obtain the phosphorochloridate **21** with full conversion (Scheme 26). Pyridine was removed under vacuum and the residue was washed with 2 M·HCl. This procedure led to a mixture of phosphoryl chloride **21** and the corresponding phosphoric acid CPAPhos^AAuCl **1a**. Further experiments indicated that compound **21** can be easily converted into **1a** by heating with 2 M·HCl in THF at 50 °C. The phosphoric acid **1a** was obtained in 88% yield. Importantly, the whole synthetic route is very straightforward and scalable, thus we could obtain more than 3 g of **1a** after only two weeks of work.

The molecular structures of **21** and **1a** were confirmed by X-ray crystallography: the corresponding ORTEP drawings are shown in Scheme 26. These compounds display standard structural parameters, e.g. almost linear P-Au-Cl moieties (P-Au-Cl angles = 176.6° and 175.0° for **21** and **1a** respectively) and classical bond lengths and angles at the cyclic phosphoric acid moiety (P-O distances = 1.414/1.408 Å for **21** and 1.405/1.390 Å for **1a**; P-O-C angles = 116.72/120.27° for **21** and 116.28/121.72° for **1a**; torsion angles of the binaphthyl moieties = 56.97° and 56.84° for **21** and **1a** respectively).



Scheme 26. Synthesis of 1a from the Phosphine-Diol 8 and X-ray Structures of 21 and 1a

The gold chloride complex **1a** has been fully characterized. Its phosphorus NMR spectrum in CDCl_3 showed the presence of two rotamers in a 4:1 ratio, i.e. two sets of signals at $\delta = 27.7$ and 2.9 ppm for the major isomer, and $\delta = 26.2$ and 4.6 ppm for the minor isomer (Figure 12). The signals at $2.9/4.6$ ppm have been assigned to the phosphoric acid function, while the diphenylphosphino group appears at $27.7/26.2$ ppm. Both signals change significantly in d^5 -pyridine ($\delta = 29.2$ and 6.7 ppm for the major isomer, $\delta = 27.7$ and 7.7 ppm for the minor isomer), which suggests deprotonation of the acid function and, possibly, coordination of pyridine to gold. In d^6 -DMSO two sets of signals were observed at room temperature ($\delta = 26.3$ and 1.8 ppm for the major isomer, $\delta = 25.2$ and 3.1 ppm for the minor isomer), but ^{31}P NMR monitoring showed that at 110°C the signals coalesce into a single set with $\delta = 26.8$ and 1.1 ppm.

This indicates that the two species observed at room temperature are likely to be rotamers of **1a**. It can be postulated that rotation around the phenyl-naphthyl C-C bond is slowed down or prevented by the high steric hindrance of the molecule.

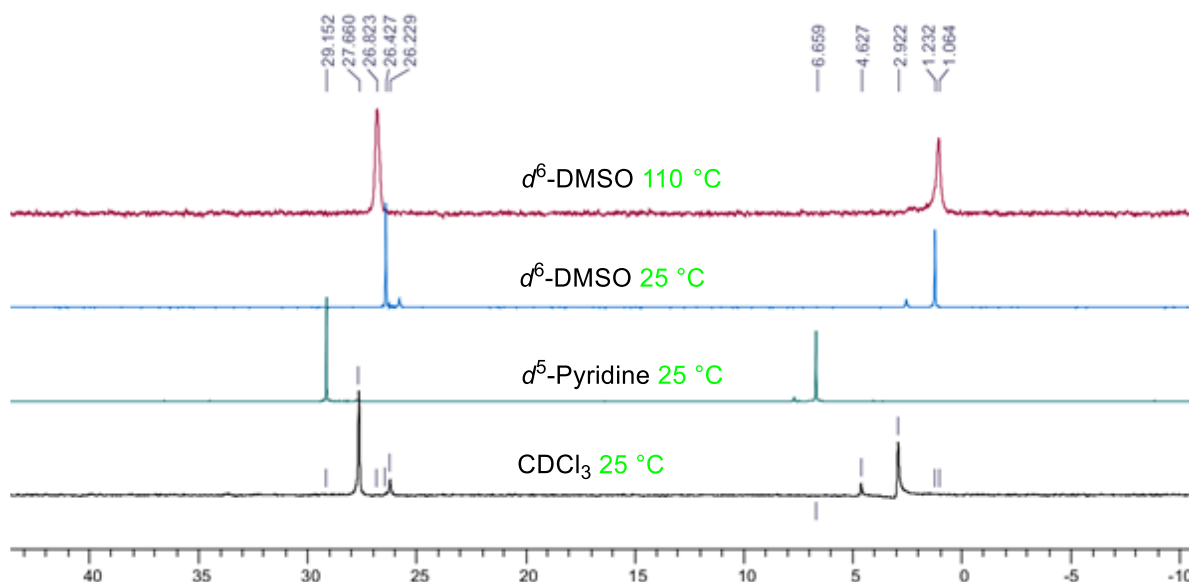
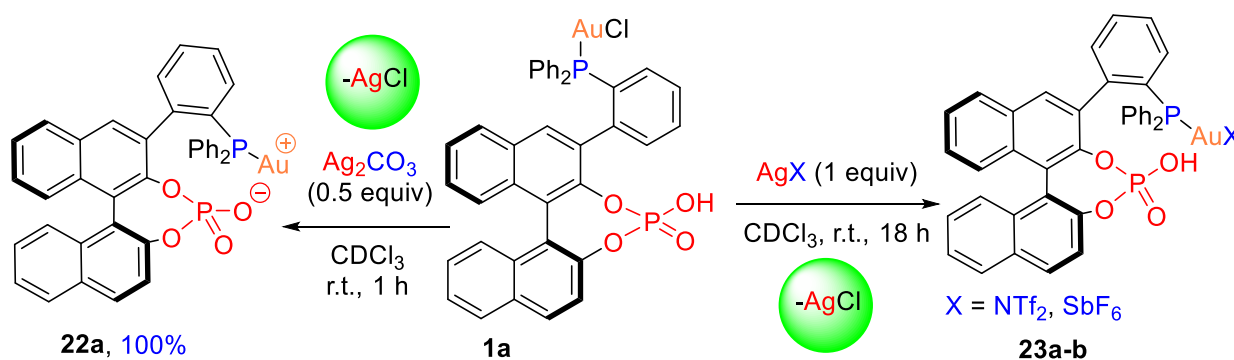


Figure 12. ^{31}P NMR (200 MHz) Spectrum of **1a** in Different Solvents and Temperatures

1.2. Silver-mediated activation of the chiral Au(I) catalyst **1a** to **22a**

Generally speaking, phosphine-gold-chloride complexes are inactive in catalysis. The chloride must be removed to generate cationic gold(I) complexes that are electrophilic enough to ensure coordination and electrophilic activation of unsaturated substrates such as alkynes or allenes. Silver salts such as AgNTf_2 , AgPF_6 , AgSbF_6 and Ag_2CO_3 are common reagents for activating gold(I) catalysts, since abstraction of the chloride is enabled by the formation and precipitation of AgCl . Hence, we have applied this method to remove chloride from complex **1a** (Scheme 27) by using various silver salts. The reactions have been carried out in CDCl_3 and have been monitored *in situ* by ^{31}P NMR.



Scheme 27. Activation of $\text{CPA}^{\text{Phos}}\text{AuCl}$ **1a** with Various Silver Salts

We can see from the ^{31}P NMR spectra in Figure 13 that the chemical shifts of both the phosphoric acid (at 2.9 ppm) and the phosphine (at 27.7 ppm) of **1a** may change after addition of the silver salts. After

addition of AgNTf_2 , the chemical shift of the phosphine switched to 22.9 ppm, while the signal of the phosphoric acid remained at 2.9 ppm, which suggests that only the phosphine gold chloride is affected (Figure 13, **23a**). When AgSbF_6 was added to the gold chloride **1a**, the δ values of both the phosphine and the phosphoric acid were modified, as the chemical shift switched to 20.1 ppm for the phosphine and to 8.8 ppm for the phosphoric acid (Figure 13, **23b**).

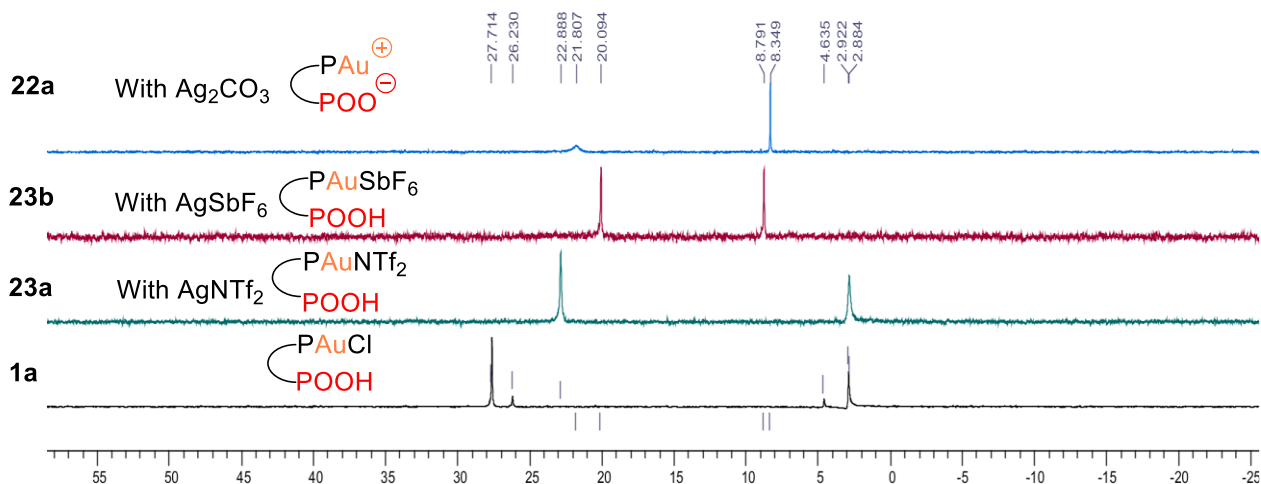
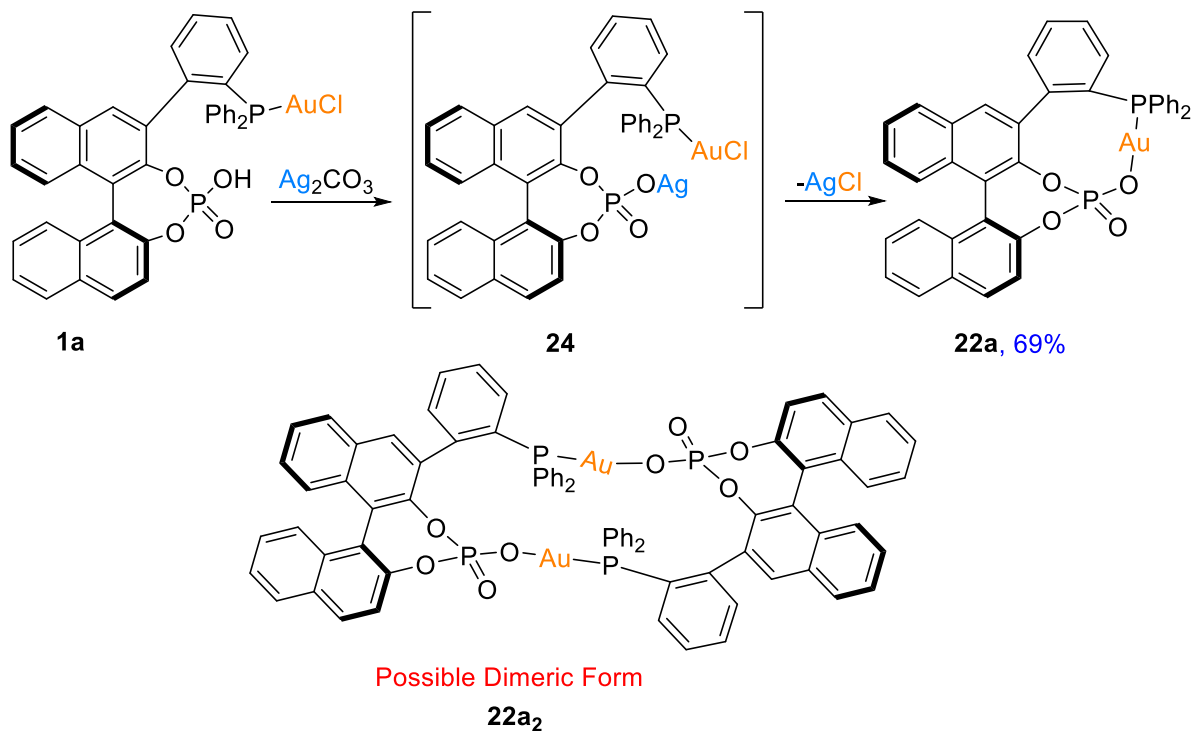


Figure 13. ^{31}P NMR (CDCl_3 , 200 MHz) Monitoring of Chloride Exchange Reactions on **1a** using Silver Salts.

On the other hand, when Ag_2CO_3 was added to the gold chloride **1a**, the chemical shifts switched to 8.3 ppm for the phosphoric acid and to 21.8 ppm for the phosphine unit (Figure 13, **22a**), showing that both phosphorus functions have been modified significantly. Actually, the basic silver carbonate is expected to deprotonate the phosphoric acid function to form the silver phosphate intermediate **24** (Scheme 28). A concomitant intramolecular abstraction of the chloride will lead to the gold phosphate **22a** where the phosphate might behave as either an X-type ligand or a counteranion.³⁷ By increasing the loading of silver base from 0.5 up to 3.0 equivalents, the same result was obtained.

The same experiment was carried out then at a 0.1 mmol (84 mg) scale, with 0.5 equiv. Ag_2CO_3 in DCM, the solid was removed after one hour by filtration, and the target complex **22a** was obtained in 100% yield.

Complex **22a** has been characterized by NMR, but based on NMR data only, we could not exclude that the complex displays actually a dimeric structure, with the phosphine and the phosphate groups coordinated to different gold centers (**22a₂** in Scheme 28), or even an oligomeric structure. Since no X-ray structure could be obtained for complex **22a**, we tried to assess its structure and its monomeric or dimeric nature using other techniques. HRMS (ESI) experiments showed the $[\text{C}_{40}\text{H}_{29}\text{AuNO}_4\text{P}_2]^+$ peak at 846.1232 ($[\text{M}+\text{H}+\text{MeCN}]^+$) that fits well with the calculated mass of the monomeric species (846.1232). The isotopic pattern also confirmed the absence of chloride in the molecular formula. However, these MS data do not establish the molecular structure of **22a** unambiguously, since dimeric species could fragment easily in mass spectrometry experiments. Thus, in order to assess more convincingly the nature of **22a**, DOSY analyses have been carried out, as summarized hereafter.



Scheme 28. Reaction of 1a with Silver Carbonate

1.3. Diffusion-ordered NMR spectroscopy (DOSY) analysis

The diffusion-ordered NMR spectroscopy (DOSY) uses pulsed-field gradient NMR and external calibration curves (ECC) to obtain information about the molecular weight of a given species in solution. In 2018, Bour, Gandon and Dumez reported that DOSY methods can be applied to estimate the molecular weight of gold complexes from their translational diffusion coefficients.⁵⁶ The DOSY technique notably enabled to detect interactions between gold and the substrates from the estimated molecular weights of the adducts. Based on these previous studies, we performed DOSY experiments on complexes **22a** and **1a** to better understand their nature in solution.

The DOSY analysis was carried out on a 600 MHz spectrometer equipped with a TBI probe (Triple Resonance Broad Band Probe) and an Avance III console. DOSY experiments provide the translational diffusion coefficients (D) that are defined according to the Stokes Einstein's equation, as a function of the particle radius, temperature and the viscosity of the medium:

$$D = \frac{k \cdot T}{6\pi \cdot \eta \cdot r}$$

k = Boltzmann constant

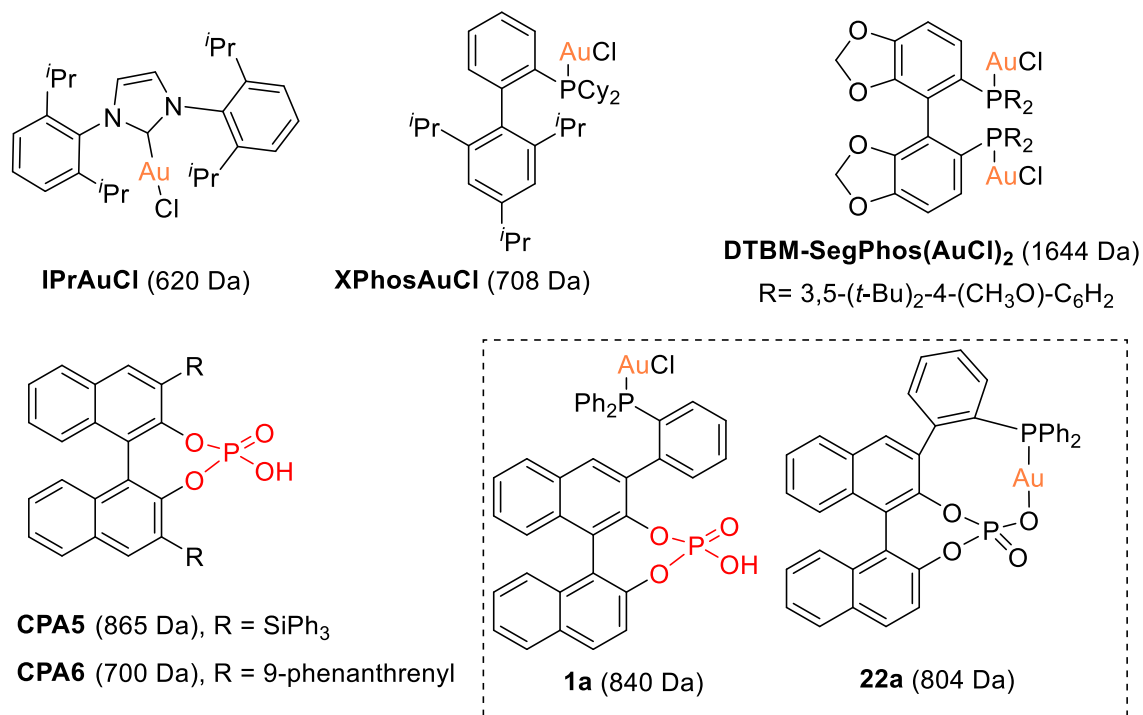
T = temperature

η = dynamic viscosity

r = particle radius

The term $6\pi \eta r$ is called friction or hydrodynamic coefficient f .

To correlate D with the molecular weight reliably, external calibration curves should be worked out by using reference compounds. Thus, we chose the gold complexes **IPrAuCl**, **XPhosAuCl** and **DTBM-Segphos(AuCl)₂** as reference samples in our study (Scheme 29). Also, the phosphoric acids **CPA5** and **CPA6** have been considered, to check if the DOSY experiments are able to detect molecular associations through H -bonding, a process that might occur notably with complex **1a**. Finally, DOSY analyses have been carried out on our complexes **1a** and **22a**. The experiments have been performed in CD_2Cl_2 and in d^5 -pyridine.



Scheme 29. Molecules used in DOSY Experiments, with the Respective Molecular Weights

In Figure 14 hereafter, the logs of the translational diffusion coefficients (D) measured in CD_2Cl_2 are plotted vs the logs of molecular weights (MW), for both our samples and the reference compounds.

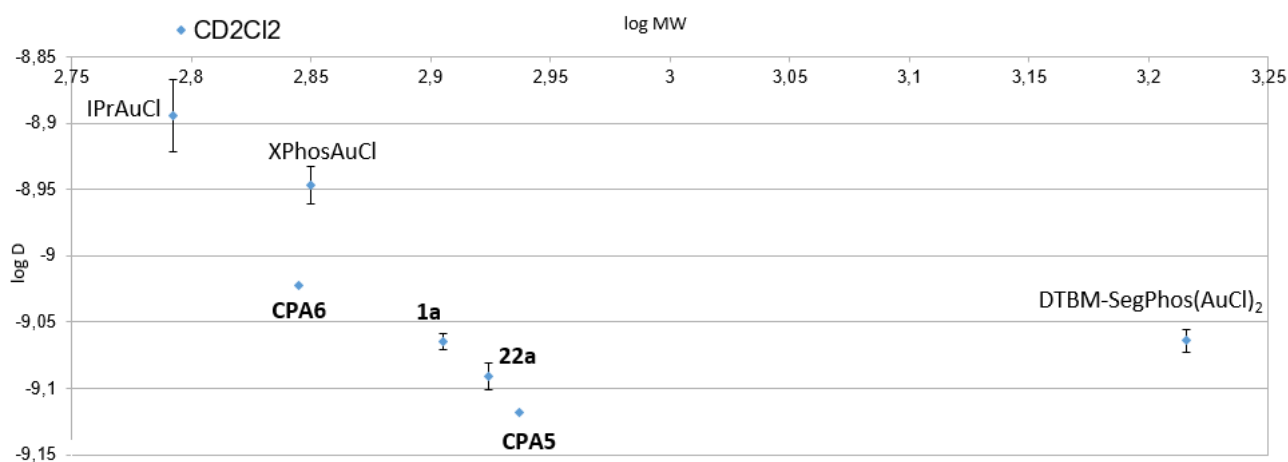


Figure 14. Translational Diffusion Coefficients in CD_2Cl_2 : log D vs log MW (assumed)

In CD_2Cl_2 , the diffusion coefficients of **22a**, **1a**, **CPA5** and **CPA6** are too small to be consistent with the molecular weight of monomeric species (700-860 Da). Their diffusion coefficients are actually of the same order of magnitude as that of **DTBM-SegPhos(AuCl)₂** (1640 Da) or even lower. It can be concluded that these compounds have an apparent molecular weight of about 1600 Da or slightly higher (i.e. approximately twice the MW of the monomer). Therefore, they are likely to be dimeric adducts or bimetallic species. It can be assumed that complex **1a**, although monomeric in the solid state (see X-ray in Scheme 26), generates dimeric adducts in solution by pairing the phosphoric acid functions of two distinct molecules (see Scheme 30 hereafter). On the other hand, complex **22a** might either have the dimeric structure **22a₂** shown in Scheme 28, or dimerize through weak bonds such as π -stacking interactions.

Thus, in order to avoid π -stacking and *H*-bonding effects, DOSY experiments have been carried out then in *d*⁵-pyridine. The observed *D* values (Figure 15) were indeed quite different in this solvent, with respect to CD_2Cl_2 .

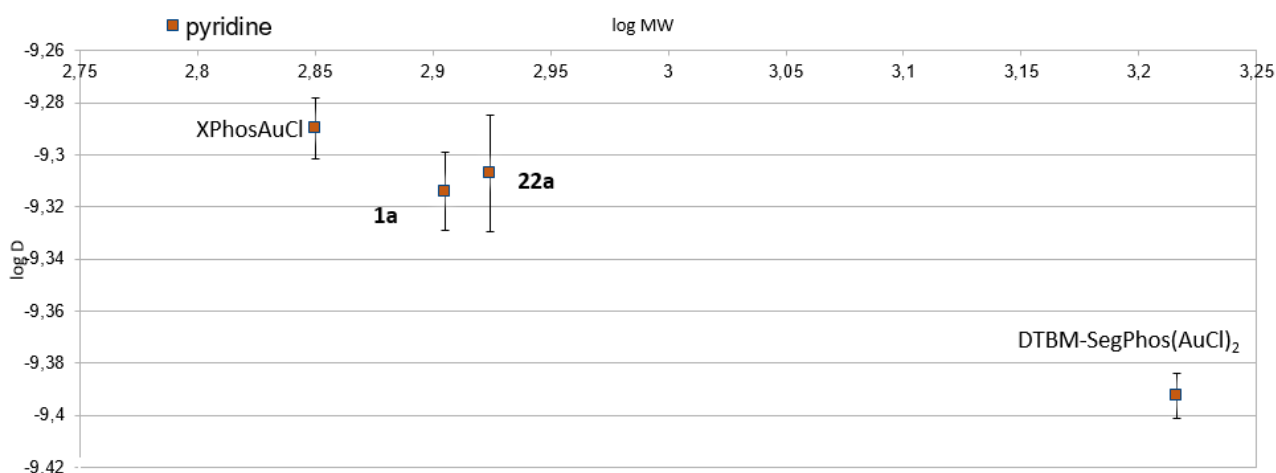


Figure 15. Translational Diffusion Coefficients in *d*⁵-pyridine: log *D* vs log MW (assumed)

Generally speaking, it is expected that diffusion coefficients change as a function of the solvents, since *D* values are inversely proportional to viscosity (η). For a given molecule, the ratio of *D* in two different solvents should be equal to the ratio of viscosities. Thus, since the η values for pyridine and CD_2Cl_2 are 0.95 and 0.437 mPa·s respectively at 20 ° C, the ratio $\frac{D_{\text{pyridine}}}{D_{\text{CD}_2\text{Cl}_2}}$ should be equal to 0.45, if the molecule remains identical in the two media. Figure 16 above plots the $\frac{D_{\text{pyridine}}}{D_{\text{CD}_2\text{Cl}_2}}$ ratios for the four gold complexes **XPhosAuCl**, **DTBM-SegPhos(AuCl)₂**, **22a** and **1a**. For **XPhosAuCl** and **DTBM-SegPhos(AuCl)₂**, the ratios are in good agreement with the calculated 0.45 value, while **22a** and **1a** display significant higher ratios (0.56 and 0.60 respectively). This shows that, apart from viscosity changes, another process intervenes here.

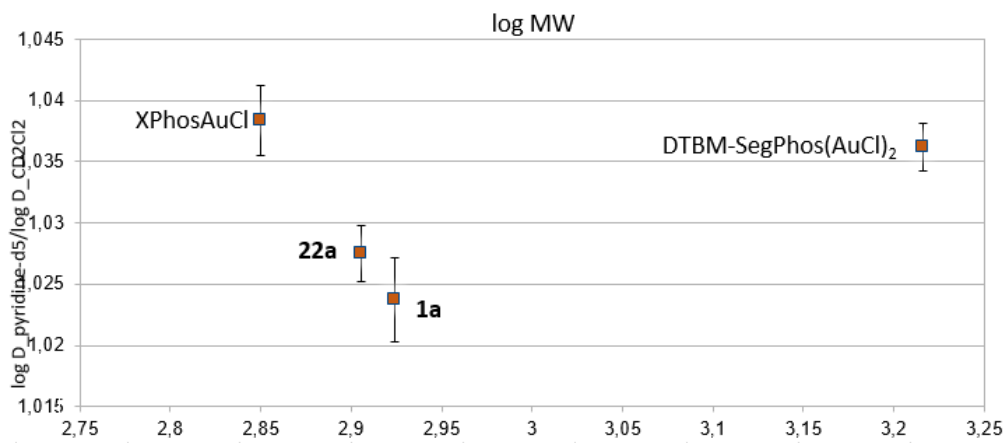
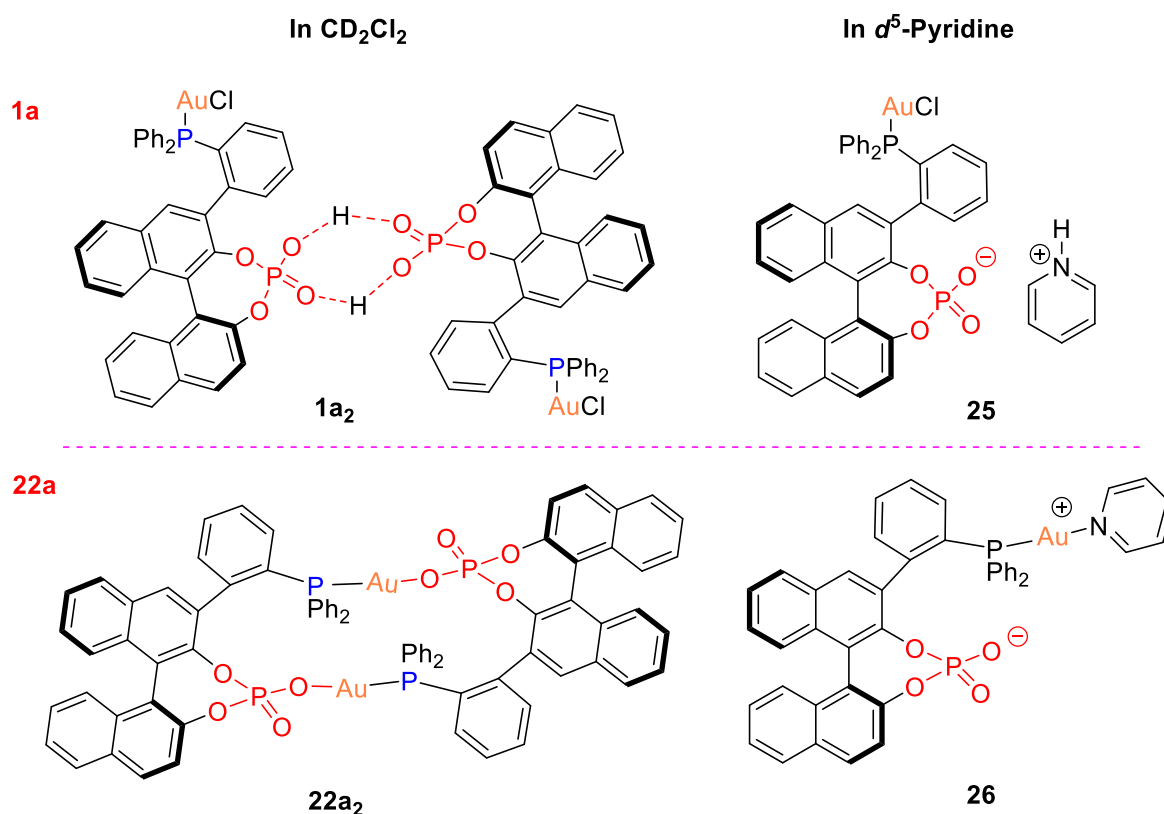


Figure 16

From Figure 15 it can be seen that in pyridine complexes **22a** and **1a** have diffusion coefficients much higher than **DTBM-SegPhos(AuCl)₂** and barely smaller than **XPhosAuCl**. Most notably, these *D* values roughly correlate with the expected molecular weight of monomeric complexes.



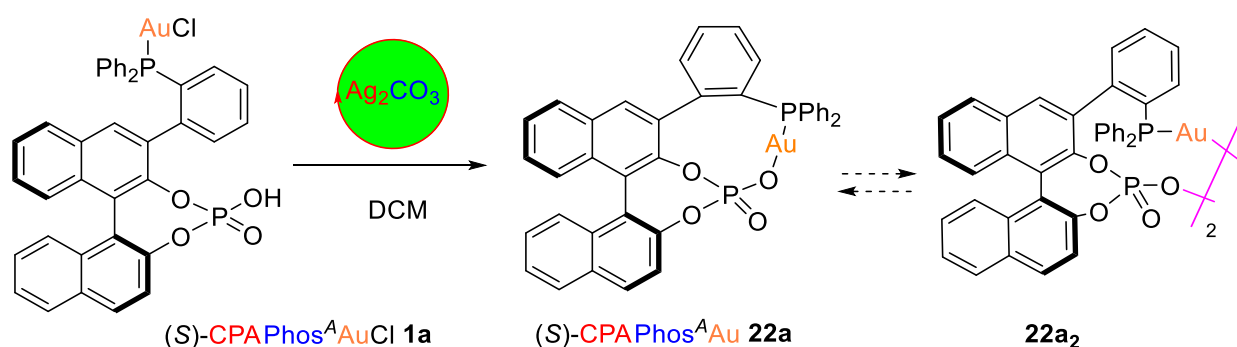
Scheme 30. Postulated Structures from DOSY Experiments in CD_2Cl_2 and d^5 -Pyridine

Overall, these results suggest that the gold complexes **22a** and **1a** change from dimeric to monomeric forms in pyridine. With complex **1a**, pyridine is likely to dissociate the *H*-bonded bridges involving the phosphoric acid function, deprotonate the same group and produce the corresponding pyridinium phosphate **25** in Scheme 30. With **22a**, pyridine might decoordinate the phosphate ligand of the dimeric

species **22a₂**, to generate a monomeric cationic gold species, **26**. It can't be excluded that this pyridine gold complex will be in equilibrium with the monomeric form **22a** (Scheme 29).

1.4. Conclusions

We have designed a new class of chiral gold complexes that contain bifunctional phosphine-phosphoric acid ligands. The first complex of this class, **CPA^APhos^AAuCl 1a**, has been prepared at a gram scale through an efficient and scalable synthetic route that involves 6 main steps, starting from (*S*)-BINOL. Its structure has been ascertained notably by X-ray diffraction studies. We have investigated then the conversion of complex **CPA^APhos^AAuCl** into cationic gold(I) derivatives in the presence of non-basic silver salts, as well as its conversion into the corresponding gold phosphate **CPA^APhos^AAu 22a** by reaction with silver carbonate (Scheme 31).

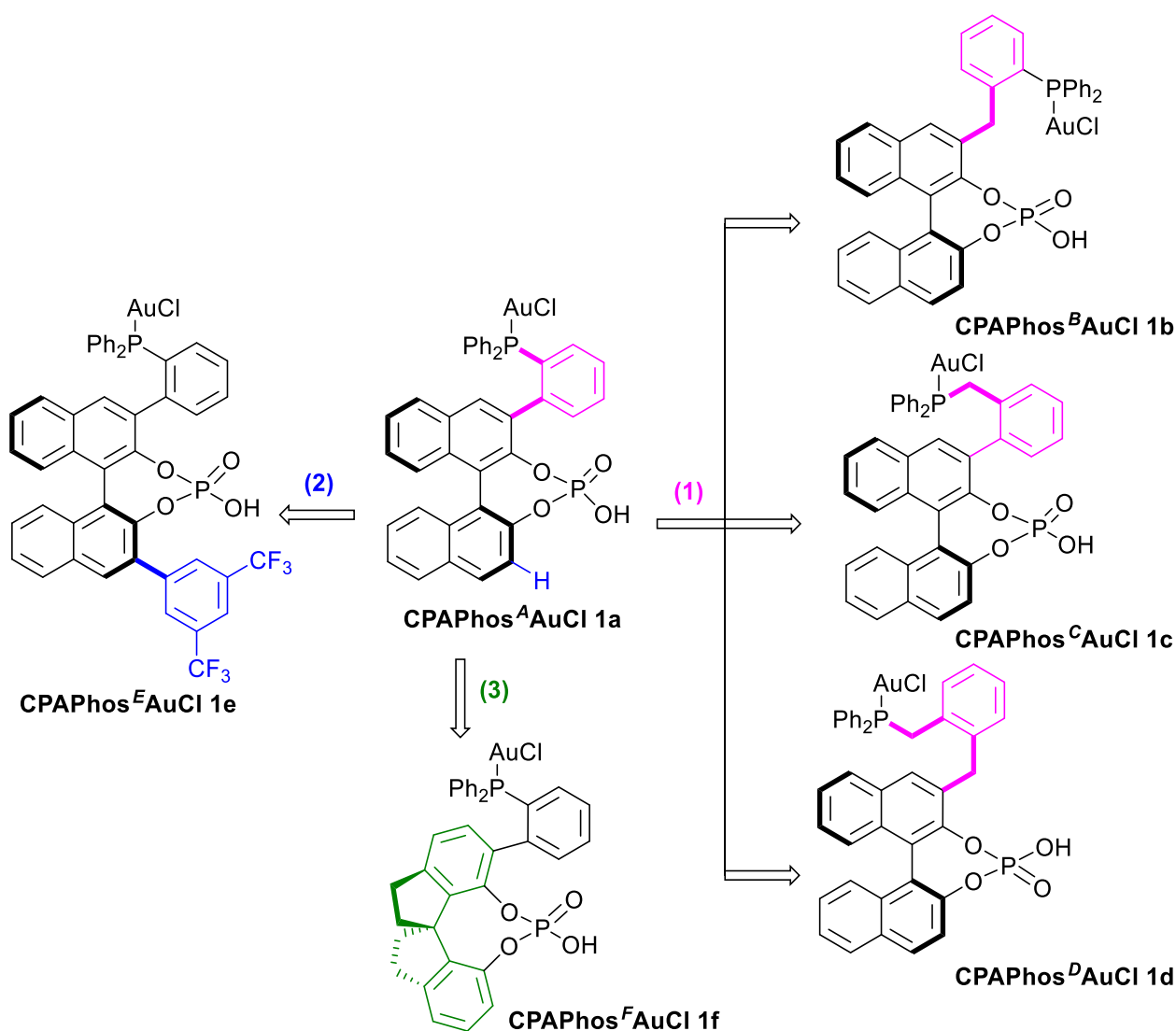


Scheme 31

Although DOSY experiments suggest that complex **22a** might have a dimeric, bimetallic structure **22a₂**, it has been shown that it dissociates easily into monomeric species in the presence of coordinating solvents such as pyridine. We will see later (Chapter 2) that (*S*)-**1a** generates a catalytically active species when activated by Ag_2CO_3 , which means that the dimer is labile enough to be dissociated by either coordinating solvents or substrates. Thus, its possible dimeric structure does not prevent applications in catalysis.

Before disclosing the catalytic applications of this complex, we will show in the next paragraphs that the series of gold complexes of phosphine-phosphoric acid ligands can be extended easily to BINOL derived ligands with different tethers between the phosphine and the phosphoric acid functions, to substituted BINOLs, as well as to SPINOL derived ligands.

2. Synthesis of phosphine-phosphoric acid Au(I) complexes **CPA**Phos^{B-F}AuCl



Scheme 32. Structural Tuning of the Phosphine-Phosphoric Acid Gold(I) Complexes **CPA**PhosAuCl 1

In order to see how the flexibility of the core structure, or steric and electronic effects affect the properties of the newly designed catalysts and the enantioselectivity triggered during catalytic processes, we have prepared a series of gold complexes analogous to CPAPhos^AAuCl 1a (Scheme 32). Key structural variations include: (1) Changing the length of the tether between the BINOL unit and the phosphine function by introducing flexible methylene spacers (CPAPhos^BAuCl 1b, CPAPhos^CAuCl 1c, CPAPhos^DAuCl 1d); (2) Introduction of a bulky and electron-withdrawing 3,5-trifluoromethylphenyl substituent at position C3' of the BINOL moiety (CPAPhos^EAuCl 1e); (3) Replacing the BINOL derived with a SPINOL derived backbone (CPAPhos^FAuCl 1f). These changes are expected to modulate the shape and steric hindrance of the chiral pocket and the electronic properties of the gold catalysts.

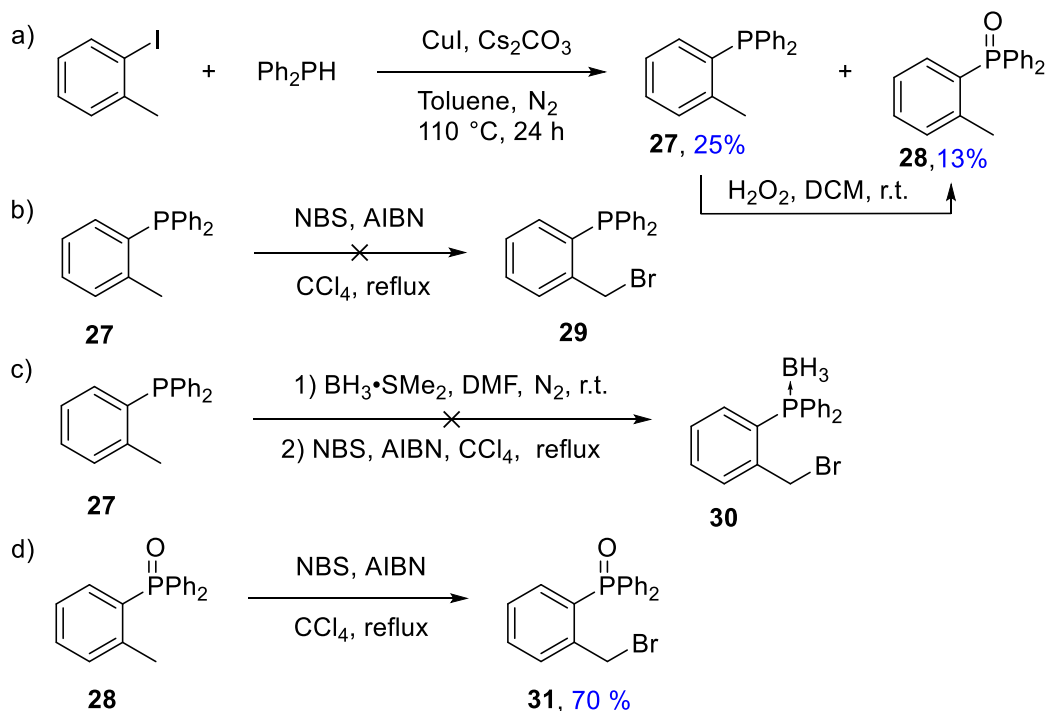
The synthesis of the new complexes are presented hereafter.

2.1. Synthesis of the gold(I) complex CPAPhos^BAuCl **1b**

The only difference between catalysts **1a** and **1b** is the methylene spacer between the BINOL backbone and the arylphosphine. Therefore, the synthetic route to **1b** could follow the same pathway as for the synthesis of **1a** (see Scheme 25), which is based on the coupling between the binaphthyl dioxaborolane **12** and a suitable bromo-functionalized phosphorus derivative.

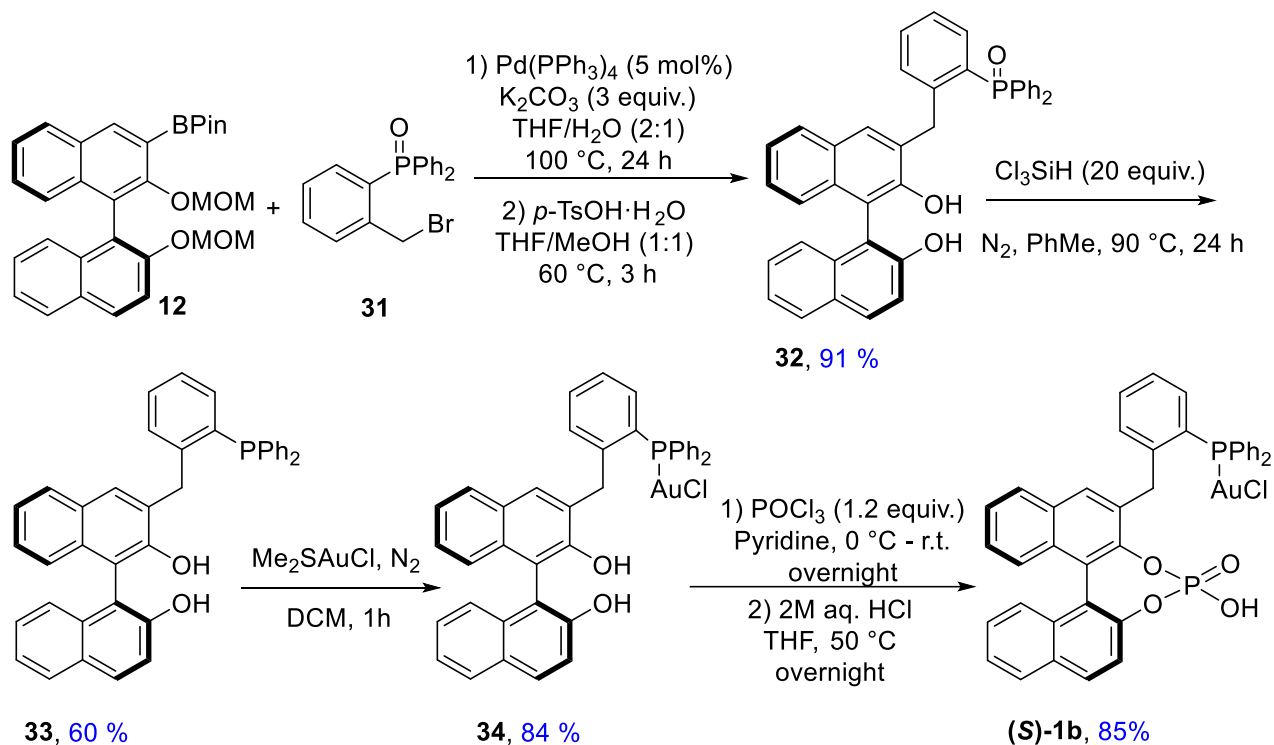
As we did when synthesizing complex **1a**, we first envisioned to use a brominated phosphine derivative as the coupling partner in the reaction with **12**. To this end, we have prepared the *o*-tolyl-diphenylphosphine **27** by CuI promoted coupling of diphenylphosphine with *o*-iodotoluene, that also generated the oxidized product **28** (Scheme 33a, 25% yield)^{54,57}, and we have tested its α -bromination. However, despite many tries, we weren't able to brominate neither the phosphine **27** nor its borane adduct (generated in situ from **27**) to produce the α -bromo-*o*-tolylphosphine derivatives **29** or **30**⁵⁸ (Scheme 33b and c).

Thus, we decided to brominate the phosphine oxide **28**, and the corresponding product **31** was obtained in 70% yield (Scheme 33d). Further investigation showed that the phosphine oxide **28** can be prepared more efficiently from *o*-iodotoluene. After coupling with diphenylphosphine, the mixture was then oxidized with H₂O₂ in DCM to obtain the phosphine oxide **28** in 81% yield in two steps.⁵⁹



Scheme 33. Synthesis of α -Bromo-*o*-Tolylphosphine Derivatives

With the phosphine oxide **31** in hand, we then carried out the reaction sequence in Scheme 34. First, we achieved a Suzuki-type coupling of the dioxaborolane **12** with **31** using 5% Pd(PPh₃)₄ as the catalyst. After an acid promoted deprotection step (MOM removal), the diol **32** was obtained in 91% yield. The phosphine oxide function of **32** was then reduced with trichlorosilane at 90 °C under nitrogen, and the resulting phosphine **33** (60% isolated yield) was coordinated to gold by reaction with DMS·AuCl (84% yield). Finally, phosphorylation of the diol **34** with POCl₃ at room temperature and hydrolysis with dilute hydrochloric acid (2M) led to complex **1b** in 85% yield (Scheme 34).

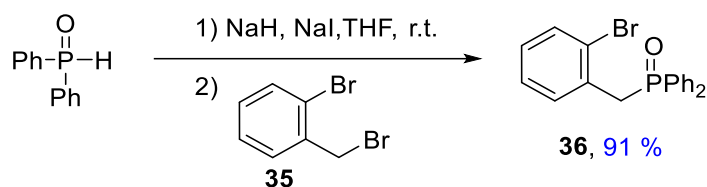


Scheme 34. Synthesis of Complex **1b** from **12**

Overall, the desired complex **(S)-1b** was obtained easily, in 40% total yield from **12**, which demonstrates the robustness of our general synthetic approach. The ³¹P NMR spectrum of **1b** in CDCl₃ shows the expected signals at $\delta = 26.7$ and 3.6 ppm that are diagnostic of the two phosphorus functions. All other NMR data are in agreement with the structural assignment. HRMS (ESI) experiments showed the [C₃₉H₂₈AuO₄P₂]⁺ peak at 819.1115 ([M-Cl]⁺) that fits well with the calculated mass of the monomeric species (819.1123) and [C₃₉H₂₇AuClO₄P₂]⁻ peak at 853.0761 ([M-H]⁻), that fits well with the calculated mass of the monomeric species (853.0744).

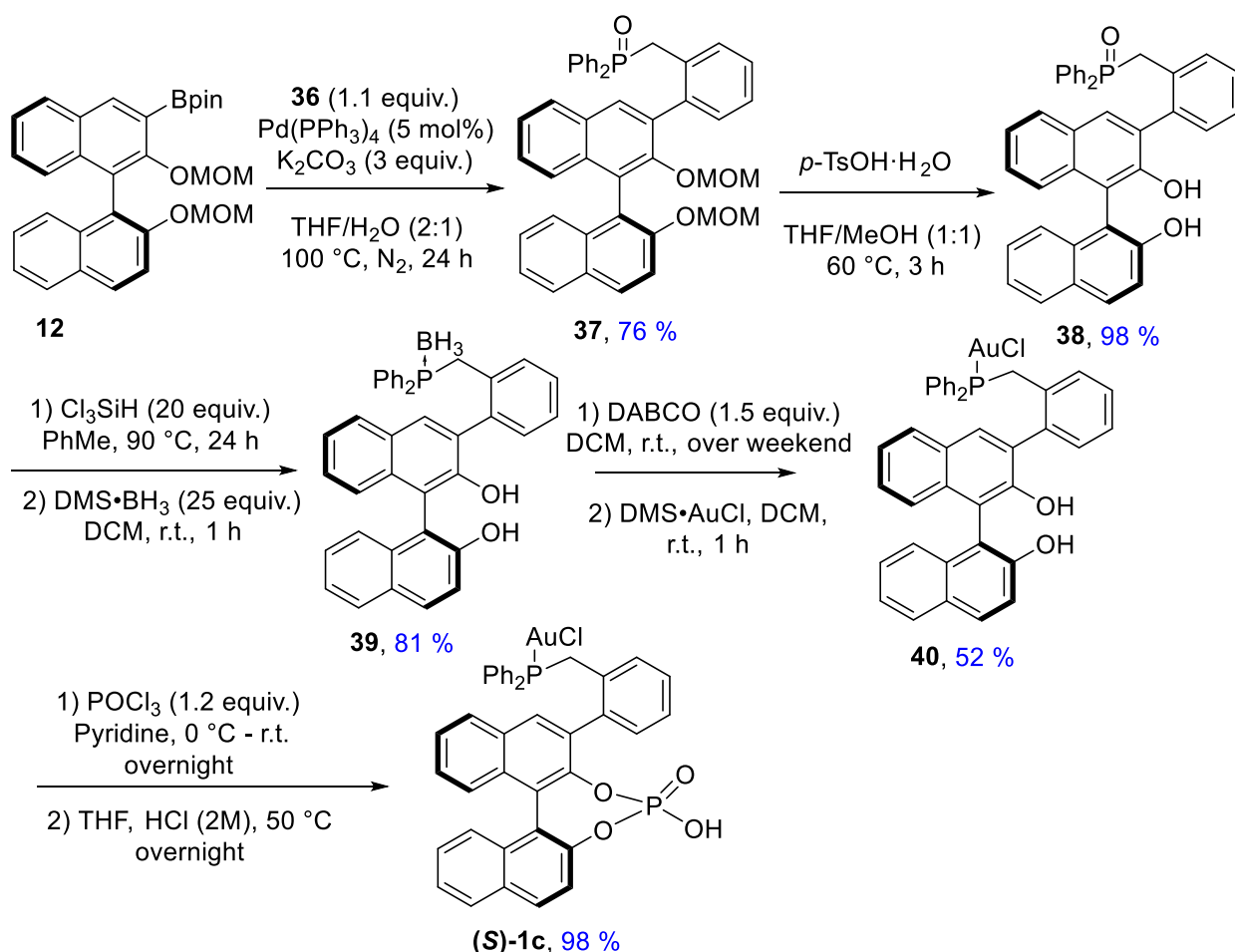
2.2. Synthesis of the gold(I) complex CPAPhos^CAuCl **1c**

Our third synthetic target has been complex **1c** in which the bifunctional ligand displays a CH₂ spacer between the aryl and the diphenylphosphino group. To access this compound by following our well-established approach above, we needed to synthesize the phosphine oxide **36**. In 2018, the Chiba's group reported a simple protocol for preparing diaryl-alkylphosphine oxides using triarylphosphine oxide as the starting materials. The method involves reductive dearylation of the phosphine oxide with NaH-LiI, followed by an alkylation step. Notably, phosphine oxide **36** could be prepared in 89% yield.⁵⁹ We have tested this protocol, however, after several attempts, we failed to obtain the product. We then turned to the usual method that involves alkylation of the metalated diphenylphosphine oxide, and the desired *o*-bromobenzylphosphine oxide **36** was obtained in 91% yield (Scheme 35).



Scheme 35. Synthesis of *o*-Bromobenzyl-Phosphine Oxide **36**

Starting from the *o*-bromobenzyl-diphenylphosphine oxide **36**, complex **1c** was synthesized according to the reaction sequence in Scheme 36: palladium promoted coupling of **36** with the chiral borane **12** led to **37** in 76% yield, subsequent removal of the MOM protecting groups and reduction of the phosphine oxide **38** led to the desired ligand. However, unlike the previous examples, the trivalent phosphine proved to be air-sensitive, since the electron-donating benzyl substituent makes this phosphine more prone to oxidation. Hence, after reduction of **38** with trichlorosilane and cooling of the reaction mixture at room temperature, DMS·BH₃ was added. After workup and purification on silica gel, we could isolate the borane complex **39** in 81% yield in two steps.



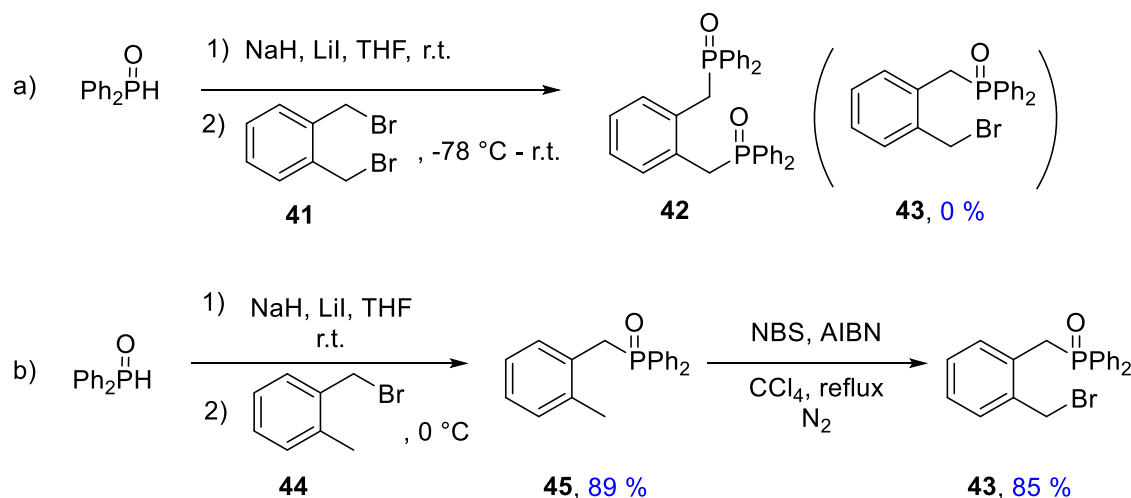
Scheme 36. Synthesis of Complex **1c from **12****

The borane protecting group has been removed by reacting **46** with an excess (1.5 equiv.) DABCO, in DCM at room temperature and the resulting phosphine was reacted *in situ* with DMS·AuCl. The corresponding gold(I) complex **40** was obtained in 52% yield in two steps. After phosphorylation of **40** with

POCl₃ and hydrolysis with 2M HCl, complex **1c** was obtained in 98% yield. The ³¹P NMR spectrum of **1c** in CDCl₃ shows the expected signals (at δ = 31.9 and 2.7 ppm for the major isomer and δ = 30.5 and 3.1 ppm for the minor isomer) that are diagnostic of the two phosphorus functions. HRMS (ESI) experiments showed the [C₃₉H₂₈AuO₄P₂]⁺ peak at 819.1121 ([M-Cl]⁺) that fits well with the calculated mass of the monomeric species (819.1123). And [C₃₉H₂₇AuClO₄P₂]⁻ peak at 853.0729 ([M-H]⁻), that fits well with the calculated mass of the monomeric species (853.0744).

2.3. Synthesis of the gold(I) complex CPAPhos^DAuCl **1d**

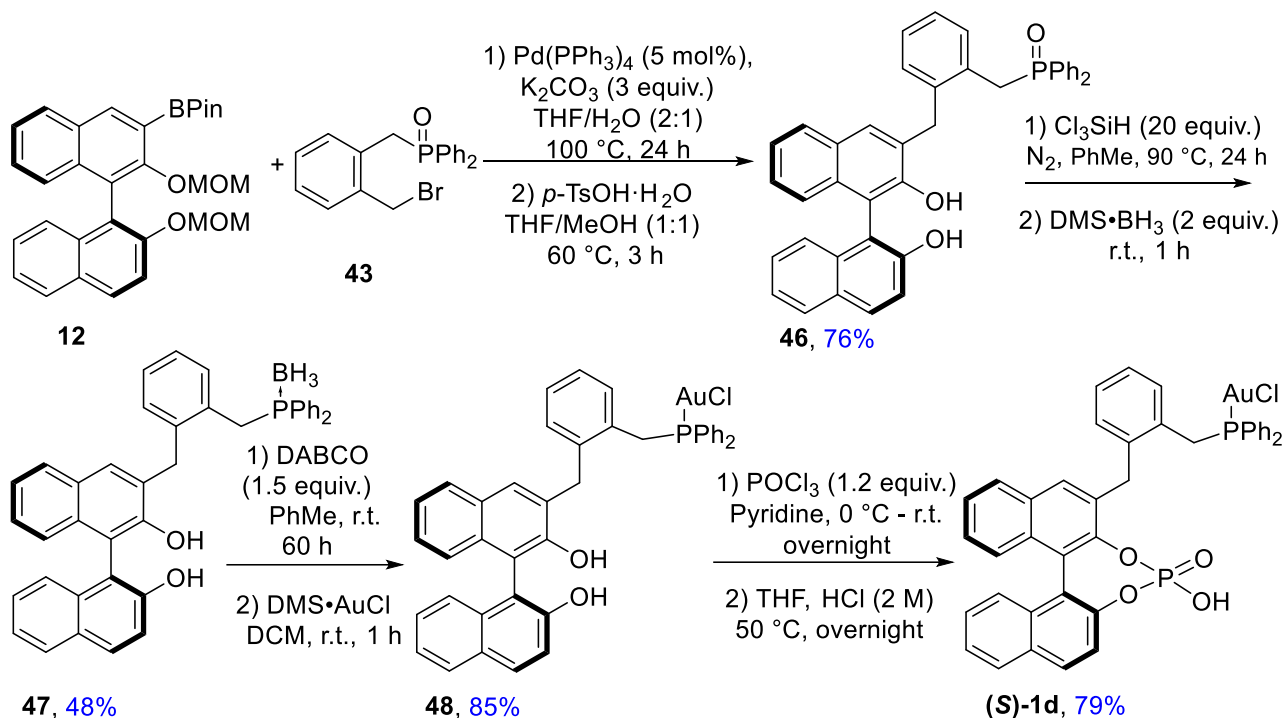
Complex **1d** displays the longest tether between the BINOL unit and the phosphine function, since two CH₂ spacers are included in the tether. In order to prepare this complex, we first synthesized the α-bromoxylylphosphine oxide **43** (Scheme 37).⁵⁸⁻⁵⁹



Scheme 37. Synthesis of the Phosphine Oxide **43**

We tried first to synthesize this phosphine oxide by alkylation of diphenylphosphine oxide with 1,2-bis(bromomethyl)benzene **41**, with NaH as the base. However, under these conditions, only the disubstituted product **42** could be obtained, even adding the suspension of diphenylphosphine oxide and NaH (stirred at r.t. for 1.5 h) in THF dropwise to **41** at -78 °C (Scheme 37a). Therefore, we envisioned to prepare the α-bromo-*o*-xylylphosphine oxide **43** in two steps: alkylation of the secondary phosphine oxide with α-bromoxylene **44**, followed by α-bromination of the resulting phosphine oxide **45** with NBS/AIBN. Through this procedure, the phosphine oxide **43** was obtained in 85% yield (75% yield over two steps, Scheme 37b).

The synthetic route to complex **1d** followed the procedure used for complex **1c** (Scheme 38). Compound **12** was reacted with **43** at 100 °C, under palladium catalysis. After acidic deprotection of the OH functions, the phosphine oxide **46** was obtained in 76% yield. The phosphine oxide **46** was then reduced with Cl₃SiH and the trivalent phosphine was protected with DMS·BH₃. In this process, the base Et₃N is not necessary for the reduction of phosphine oxide. After workup and purification by flash column chromatography, the borane complex **47** was obtained in 48% yield. Then, the borane protecting group was removed by reacting **47** with DABCO at r.t. and the trivalent phosphine was combined with DMS·AuCl *in situ* to obtain the gold complex **48** in 85% yield. Finally, the gold(I) complex was reacted with POCl₃ and, after hydrolysis with a diluted 2M HCl solution, complex **1d** was delivered in 79% yield.



Scheme 38. Synthesis of Complex **1d** from **12**

The ^{31}P NMR spectrum of **1d** in CDCl_3 shows the expected signals at $\delta = 31.0$ and 5.3 ppm that are diagnostic of the two phosphorus functions. All other NMR data are in agreement with the structural assignment. HRMS (ESI) experiments showed the $[\text{C}_{40}\text{H}_{30}\text{AuO}_4\text{P}_2]^+$ peak at 833.1287 ($[\text{M}-\text{Cl}]^+$) that fits well with the calculated mass of the monomeric species (833.1279). And $[\text{C}_{40}\text{H}_{29}\text{AuClO}_4\text{P}_2]^-$ peak at 867.0906 ($[\text{M}-\text{H}]^-$), that fits well with the calculated mass of the monomeric species (867.0901).

Once again the synthetic pathway demonstrated here its remarkable robustness and versatility.

2.4. Synthesis of the gold(I) complex **CPAPhos^FAuCl 1e**

As an additional example of bifunctional phosphine-phosphoric acid we have targeted complex **1e** that displays a 3'-substituted BINOL moiety. It is largely demonstrated that bulky substituents on this position most often improve the enantioselectivity of reactions promoted by chiral BINOL-derived phosphoric acids.⁴⁷ Therefore, we have decided to check if substituents on the BINOL unit might be beneficial in the case of our gold catalysts also, as a result of the increased steric bulk of the phosphoric acid moiety.

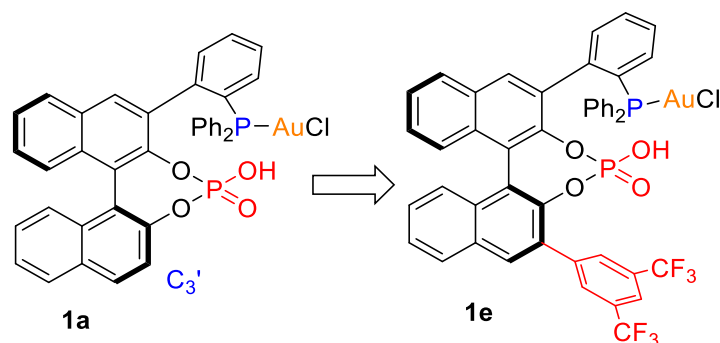
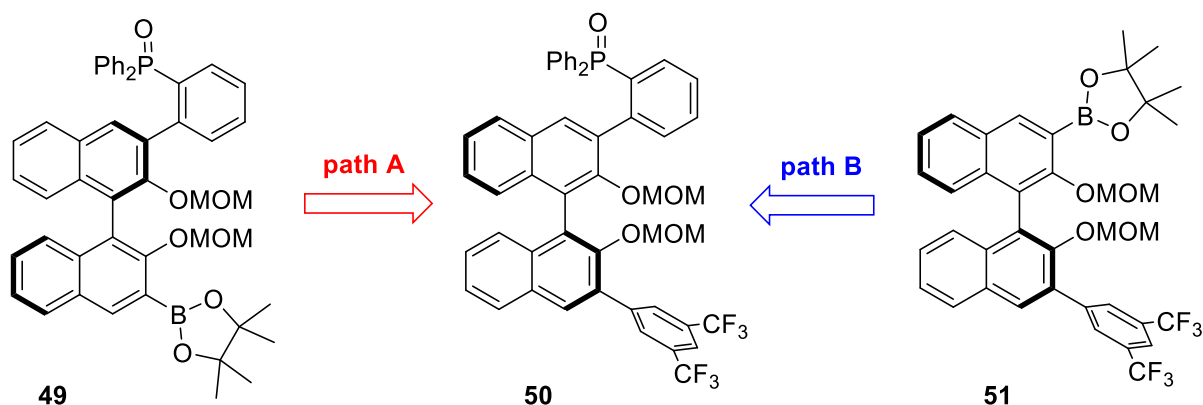


Figure 17. Structure of Complex **1e**

With this aim in mind, we have introduced a 3,5-bis(trifluoromethyl)phenyl substituent on the molecular scaffold of complex **1a** to get the corresponding gold complex **1e** (Figure 17).

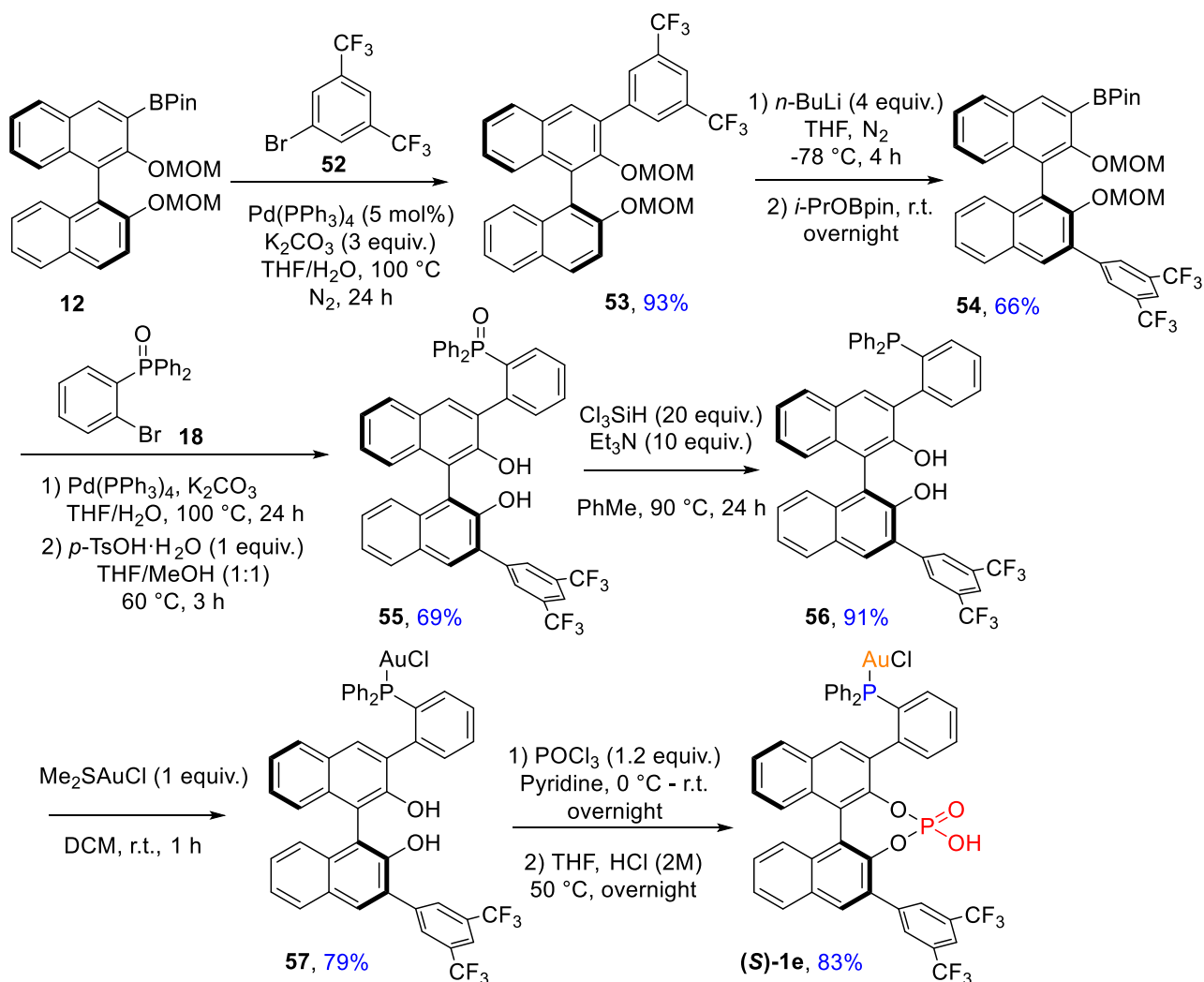
The key intermediate in the synthesis of **1e** is the phosphine oxide **50** that combines the substituted, *O*-protected BINOL and the triarylphosphine unit. Two synthetic routes have been considered to generate complex **50**. Path A involves the boryl-functionalized phosphine oxide **49** as the key intermediate (Scheme 39, left). This path might be highly convenient as far as it would allow to introduce easily a variety of substituents in position C3' of the ligand. Alternatively, **50** can be prepared following path B (Scheme 39, right), that involves introduction of the phosphine oxide function on the 3'-aryl-substituted dioxaborolane **51**, at a late stage.



Scheme 39. Pathways for the Synthesis of Intermediate **50**

We first attempted to prepare **50** through path A, but under the optimized condition for preparing boronic ester **12**, no product **49** was found. This may be because of the presence of P=O, which may result in competitive *ortho*-lithiation.

Afterwards we embarked on path B and we obtained successfully the intermediate phosphine oxide **50** and the desired complex **1e**, as shown in Scheme 40. The synthesis of the phosphine oxide **50** involves two sequential coupling steps. First, a Suzuki coupling was carried out between the dioxaborolane **12** and 1-bromo-3,5-bis(trifluoromethyl)benzene **52** and the corresponding aryl-substituted binaphthyl derivative **53** was obtained in 93% yield. Then a MOM-directed *ortho*-lithiation/borylation sequence introduced a dioxaborolane unit on the free C3' position. The boronate function was engaged in the second Suzuki coupling step with (*o*-bromophenyl)diphenylphosphine oxide **18**, which led to the phosphine-diol **55** after acidic deprotection (69% yield). Reduction of the phosphine oxide **55** and coordination of the trivalent phosphine to gold(I) led to complex **56** in 72% yield over two steps.



Scheme 40. Synthesis of Complex 1e from 12

Finally, phosphorylation of the diol with POCl_3 and hydrolysis with a diluted HCl solution, gave the desired complex **1e** in 83% yield. Complex **1e** was fully characterized by NMR and mass spectroscopy. As shown for complex **1a**, the gold complex **1e** displays two distinct sets of ^{31}P NMR signals ($\delta = 27.7$ and 2.8 ppm for the major isomer and $\delta = 26.2$ and 4.2 ppm for the minor isomer) that indicate the presence of two rotamers in a 9:1 ratio. HRMS (ESI) experiments showed the $[\text{C}_{48}\text{H}_{31}\text{AuF}_6\text{NO}_4\text{P}_2]^+$ peak at 1058.1293 ($[\text{M}+\text{MeCN}-\text{Cl}]^+$) that fits well with the calculated mass of the monomeric species (1058.1288).

2.5. Synthesis of the gold(I) complex CPAPhos^fAuCl **1f**

As a last example, we have envisioned to prepare a bifunctional phosphine-phosphoric acid based on a 1,1'-spirobiindane-7,7'-diol (SPINOL) scaffold (Figure 18). The literature shows indeed that this spiranic structure may be a favorable alternative to BINOL as chiral building block for the synthesis of both ligands⁶⁰ and phosphoric acids⁶¹ for enantioselective organometallic and organocatalysis.

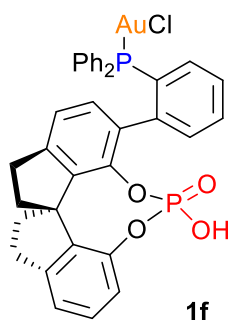


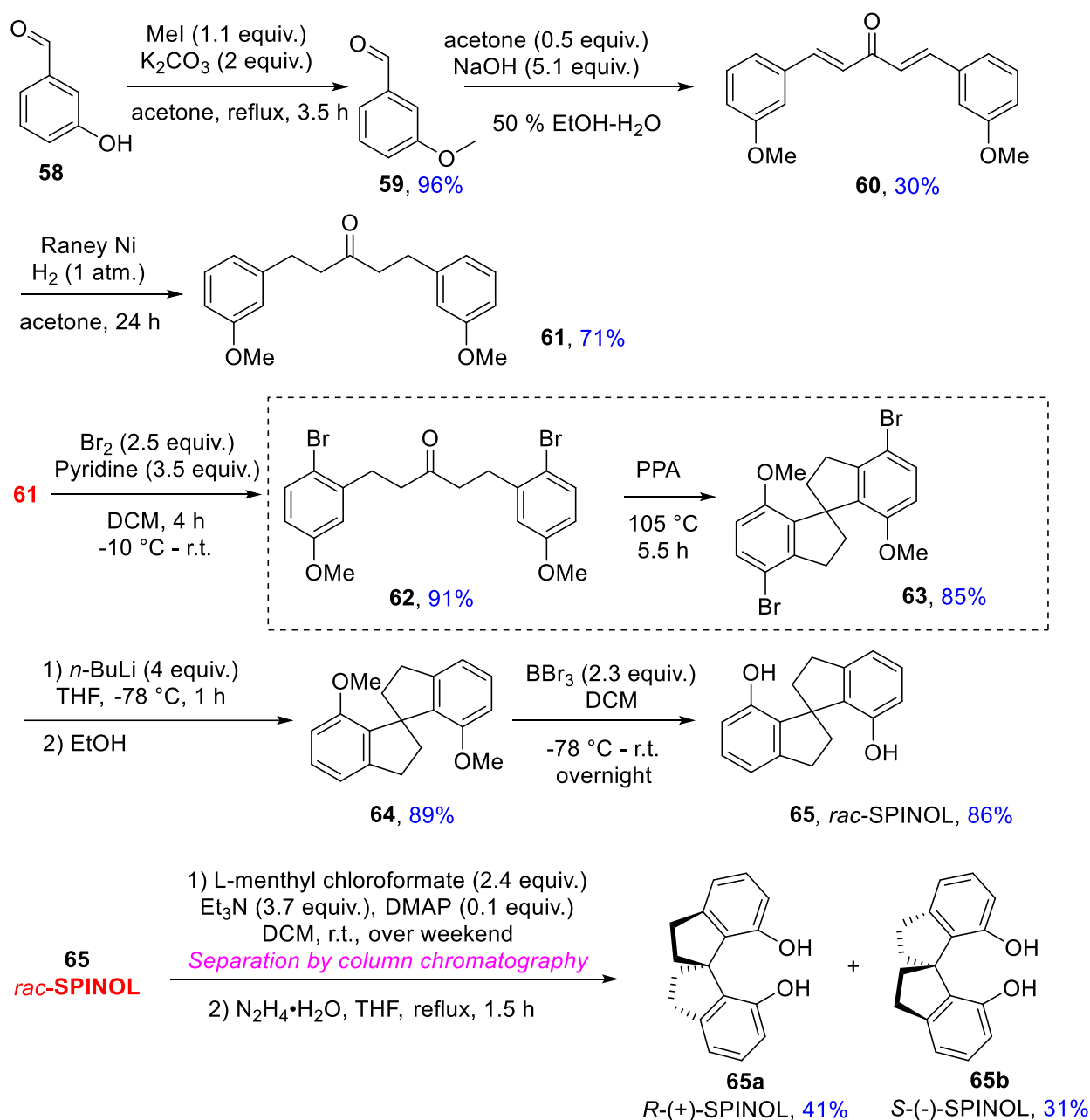
Figure 18. The Targeted (*R*)-SPINOL Derived Gold Complex CPAPhos^FAuCl **1f**

With this aim in mind, we have prepared *rac*-SPINOL in 8 steps according to the literature (Scheme 41).⁶² The key step is the double, intramolecular electrophilic aromatic alkylation taking place on ketone **62** under acid conditions, that will create the spiranic scaffold.

Ketone **62** has been obtained in four steps from 3-hydroxybenzaldehyde **58**. The OH function of the aldehyde has been protected with MeI, then an aldol-type condensation with acetone has been carried out and the resulting ketone **60** (30% yield) has been hydrogenated under 1 atm of H₂, with Ni-Raney as the catalyst, to provide 1,5-bis(3-methoxyphenyl)pentan-3-one **61** in 71% yield. The next step is an electrophilic bromination (Br₂/pyridine in DCM, 91% yield) taking place selectively in *para* position to the MeO group. The role of the bromo-substituents in **62** is to block the *para*-positions so as to achieve the subsequent electrophilic alkylation reaction at the *ortho*-positions selectively. Thus, ketone **62** could be converted into the desired 1,1'-spirobiindane derivative **63** in high yield (85%) using polyphosphoric acid (PPA) as the catalyst.

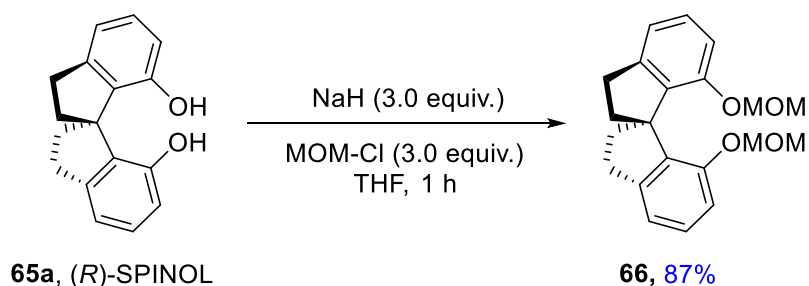
After the cyclization step, the bromine substituents are easily removed by bromine-lithium exchange with *n*-BuLi and subsequent protonation with EtOH. The resulting **64** went through deprotection of the OH functions by removing the methyl groups with BBr₃. The racemic SPINOL **65** was obtained in 86% yield.

Resolution of SPINOL was carried out by forming diastereomeric esters, instead of the reported methods using co-crystallization methods with *Cinchona* alkaloids.⁶³ *Rac*-SPINOL was reacted with enantiomerically pure L-menthyl chloroformate and the resulting diesters were separated by column chromatography on silica gel. Finally, the separated esters have been converted into the corresponding diols by reaction with hydrazine hydrate in refluxing THF. The optically pure (*R*)-SPINOL **65a** and (*S*)-SPINOL **65b** have been obtained in 41% and 31% yields respectively. The enantiomeric purity of the samples has been ascertained by chiral HPLC [Chiralpak AD-H column, heptane:isopropanol = 80:20, 1 mL/min, *t* = 4.6 min (**65a**) or *t* = 6.0 min (**65b**)] and the absolute configuration has been confirmed from optical rotation values [$\alpha_D = +39$ (*c* = 1.08, CHCl₃) for the (*R*)-enantiomer, $\alpha_D = -44$ (*c* = 1.01, CHCl₃) for the (*S*)-enantiomer].



Scheme 41. Synthesis of Enantiopure (R)- and (S)- SPINOL 65

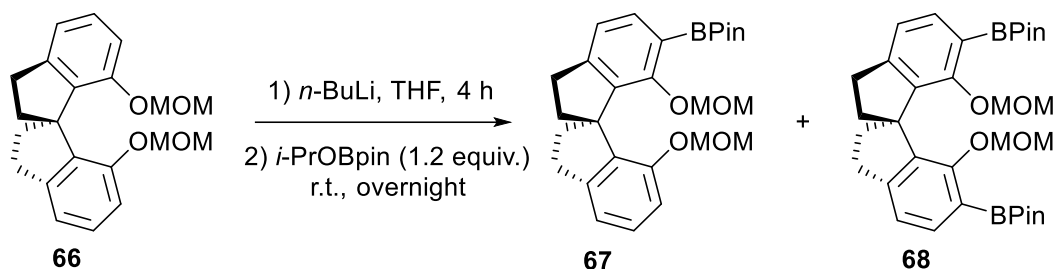
After obtaining the enantiopure SPINOL, the targeted complex **1f** could be synthesized by adapting the approach used for the synthesis for **1a**. The (R)-configured SPINOL **65a** was first deprotonated with NaH and reacted then with MOMCl to give the MOM-protected compound **66** in 87% yield (Scheme 42).



Scheme 42. Synthesis of the MOM-Protected SPINOL 66

As far as we know, the conditions for the borylation of the MOM-protected SPINOL **66** reported in the literature are all about the synthesis of disubstituted products **68**.⁶⁴ Therefore, we had to adapt these conditions to synthesize the monosubstituted borylation product **67**. Thus, we reacted **66** with *n*-BuLi and *i*-PrO-BPin by reducing the amount of *n*-BuLi from 2 to 1.2 equivalents and we could isolate the desired boronate **67** in 42% yield (Table 5, entry 1). Under these conditions, a significant amount of starting material remained unreacted. However, we couldn't find better conditions because larger amounts of *n*-BuLi led to mixtures of starting material, mono- and bis-boronate (Table 5, entry 2).

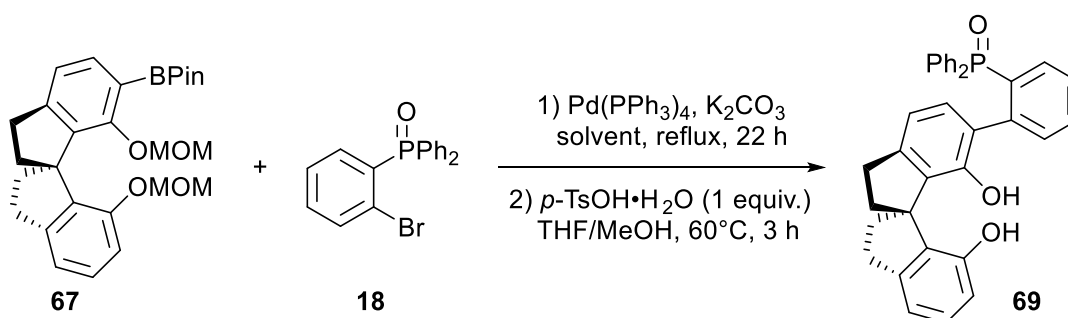
Table 5. Optimization of the Borylation Step (selected results)



entry	<i>n</i> -BuLi	recover (66 , %)	yield (67 , %)	yield (68 , %)
1	1.2 equiv.	35	42	0
2	1.7 equiv.	32	4	12

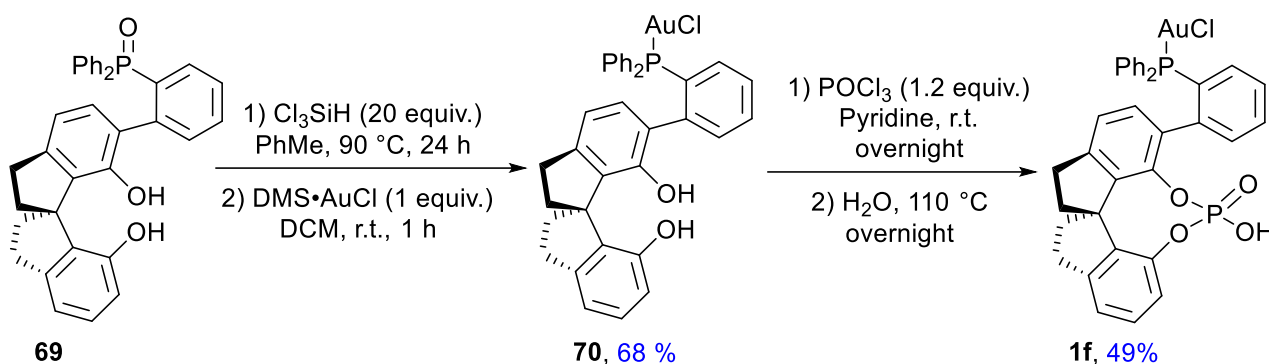
We have investigated then the Suzuki coupling of **67** with the (*o*-bromophenyl)diphenylphosphine **18** (Table 6). When we applied the same conditions as for the synthesis of complex **17** (see Table 4), no product was found after 24 h (entry 1). Then, based on the conditions applied in similar Suzuki coupling reactions on SPINOL derivatives,^{64a} we used a mixture of THF, MeOH and H₂O as the solvent, and increased the amount of the brominated phosphine oxide **18** to 2 equivalents and the loading of the Pd(PPh₃)₄ catalyst to 7.5%. Under these conditions, the coupling product was obtained successfully. After deprotection of the MOM groups with *p*-toluenesulfonic acid, the diol **69** was delivered in 79% yield over two steps (entry 2).

Table 6. Optimization of the Suzuki Coupling Step



entry	ratio (67/18)	Pd(PPh ₃) ₄ (mol%)	K ₂ CO ₃ (equiv)	solvent	yield (%)
1	1.0/1.1	5.0	3.0	THF/H ₂ O	NR
2	1.0/2.0	7.5	3.1	THF/MeOH/H₂O	79

The following steps, i.e. reduction of the phosphine oxide **69** in the absence of Et₃N and coordination to gold(I) are based on the procedures used for the synthesis of complex **1a**. The phosphine-gold(I) complex **70** was obtained in 68% yield in two steps (Scheme 43). After phosphorylation with POCl₃ in pyridine at room temperature, water was added to the crude mixture and the resulting solution was stirred overnight at 110 °C to provide the phosphine-phosphoric acid gold complex **1f** in 49% yield. It can be noticed here that hydrolysis of the intermediate phosphoryl chloride requires harsh conditions and the presence of a base such as pyridine. In the absence of pyridine, acidic hydrolysis of the isolated phosphoryl chloride does not take place even after stirring in 2 M HCl for 3 days at 110 °C.



Scheme 43. Synthesis of the Gold Complex 1f

Complex **1f** was fully characterized by NMR and mass spectroscopy. As shown for complex **1a**, the gold complex **1f** displays two distinct sets of ³¹P NMR signals ($\delta = 23.8$ and -8.6 ppm for the major isomer and $\delta = 25.4$ and -8.4 ppm for the minor isomer) that indicate the presence of two rotamers in a 1:3.8 ratio.

3. Conclusion

In summary, in the first part of this PhD work, we could achieve the synthesis of a new series of gold complexes that display chiral phosphine-phosphoric acid bifunctional ligands. In most cases the multistep synthetic procedures give access to the desired complexes in good yields, at a gram or multigram scale. The method proved rather versatile as it could be applied to the synthesis of ligands with either BINOL- and SPINOL-derived phosphoric acid units. In the BINOL series, several structural modifications could be performed easily, that is changes of the tether connecting the phosphine and the phosphoric acid moieties, as well as addition of a bulky substituent on the BINOL backbone. The six complexes CPA_{Phos}AuCl **1a-f** have been characterized by spectroscopic techniques and the molecular structure of complex **1a** has been confirmed unambiguously by X-ray crystal data. With complex **1a** we have also investigated the removal of the chloride ligand on gold, since this step was supposedly required to activate the gold complex for catalysis. We have demonstrated by DOSY experiments that the resulting gold phosphate should be dimeric in solution, but the dimer dissociates easily into monomeric species.

Experiments performed on the activation of the other precatalysts by silver carbonate showed that the time necessary for the activation of each complexes is influenced by the structure of the catalyst and the solvent. In particular, **1a**, **1e** and **1f** are preferably activated efficiently in DCM. The activation of **1e** and **1f** is however longer than that of **1a**.

In the next chapters, we will report on the catalytic behavior of these gold complexes.

Chapter 2: Application of the TCDC strategy in enantioselective catalysis involving α -alkynyl-ketones

As shown in Chapter 1, we have designed a novel series of Au(I) complexes displaying chiral bifunctional phosphine-phosphoric acid ligands that should allow to demonstrate the TCDC approach. These ligands have been targeted for the potential ability of the corresponding phosphates to form intramolecular ion pairs with cationic gold species, that might represent the resting states of gold catalysts. On the other hand, in catalytic reactions, the gold tethered phosphates might operate then as counteranions for carbocationic intermediates and induce efficient stereocontrol in reactions involving such carbocations.

The first catalytic application that we have envisaged to validate this working hypothesis is the cyclisomerization/nucleophilic addition reaction on 2-alkynyl-enones **71** shown in Figure 19. It relies on the *in situ* formation of intermediate **II**, that displays a carbocation adjacent to a furan ring that would be stabilized by the phosphate, according to the TCDC strategy (Figure 19). The tether connecting gold(I) to the phosphate counteranion should increase the geometrical constraints and bring rigidity, potentially enabling high enantioselectivity in the subsequent reactions.

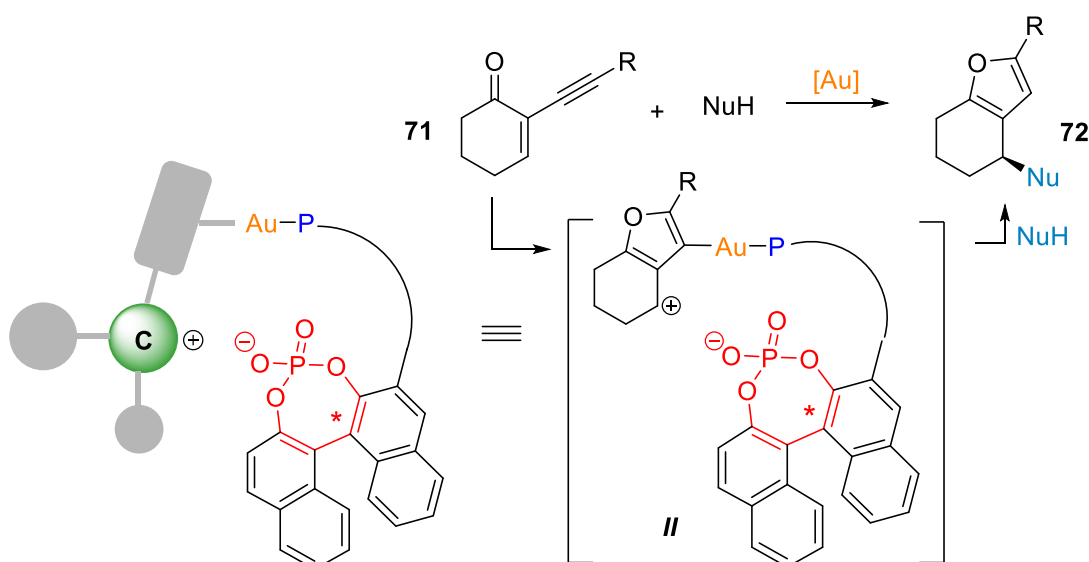


Figure 19. The TCDC Strategy Applied to a Defined Carbocation Intermediate

Thus, addition of nucleophiles to these intermediates should deliver enantioenriched furans which are useful building blocks in organic synthetic chemistry, with applications notably in materials sciences and medicinal chemistry. Analogous furane scaffolds are also widely present in natural products, thus the asymmetric synthesis of furan derivatives of this class is of great general significance (Figure 20).⁶⁵

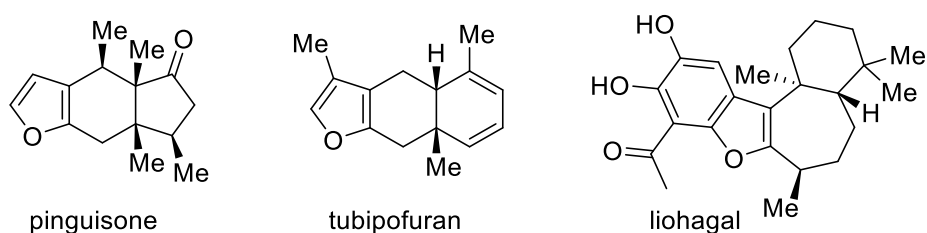
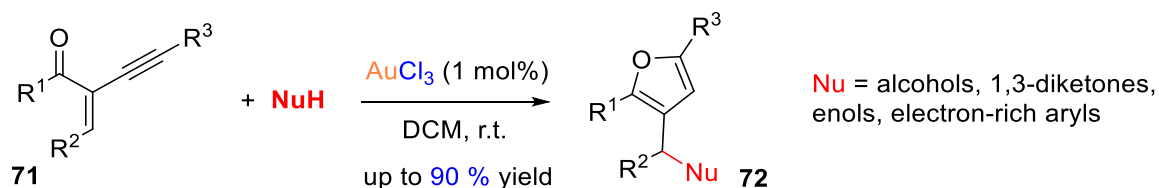


Figure 20. Occurrence of furans in natural products

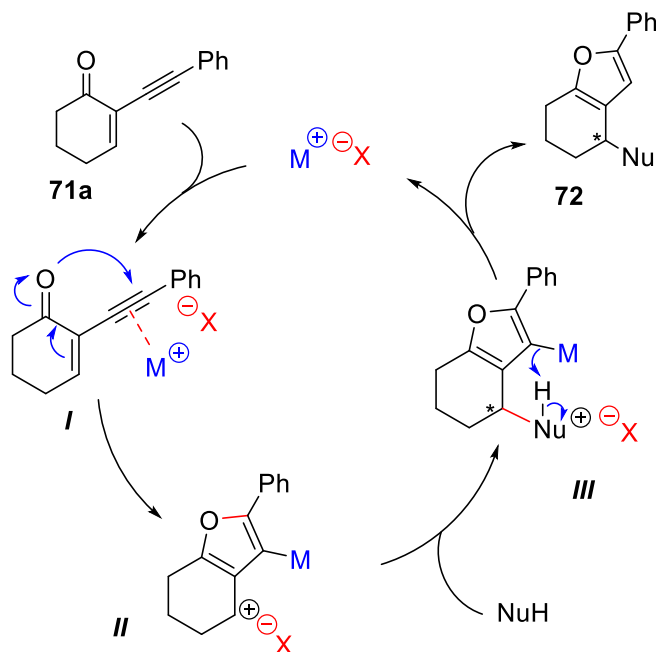
1. Metal promoted tandem cyclization-nucleophilic additions on α -alkynylketones: literature overview

The catalytic reaction above, i.e. the metal-catalyzed formation of furans from α -alkynyl-ketones and nucleophiles, has been investigated extensively.⁶⁶ Pioneering studies have been disclosed in 2004 by Larock, who initially developed the tandem reactions on the 2-alkynyl-ketones **71** using gold(III) chloride as the catalyst. With a diverse range of nucleophiles, such as alcohols, enols or electron-rich arenes, the corresponding polysubstituted furans **72** were obtained in moderate to excellent yields, under mild reaction conditions (Scheme 44).⁶⁷



Scheme 44. Tandem Cyclization/Nucleophilic Additions Promoted by AuCl₃

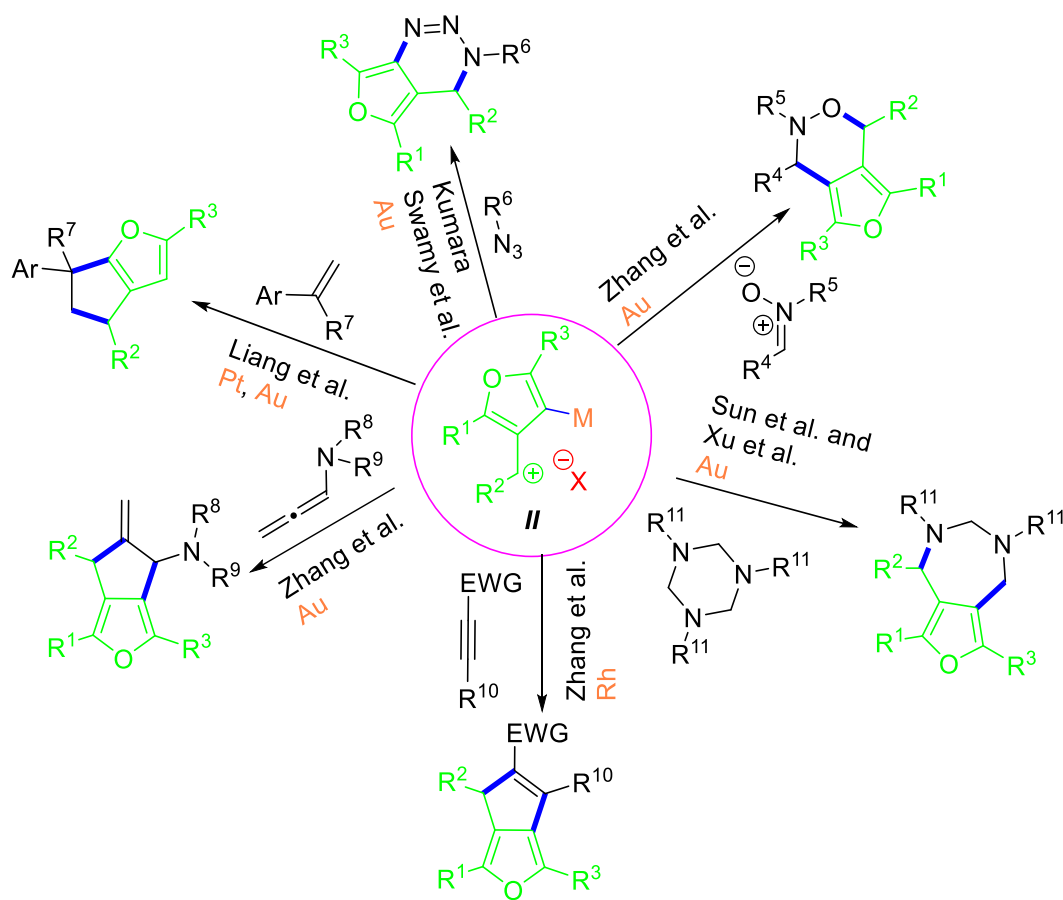
The proposed mechanistic pathway is illustrated below in the case of cyclic ketones (Scheme 45). Coordination of the alkyne unit to the metal induces electrophilic activation and triggers a cyclization process, leading to the carbocationic intermediate **II**. This cation will be trapped then by the nucleophile, leading to intermediate **III**. After protodemetalation of **III**, the catalyst is regenerated and the final furan **72** is delivered.



Scheme 45. Postulated Mechanism for the Tandem Cyclization-Nucleophilic Addition Reactions

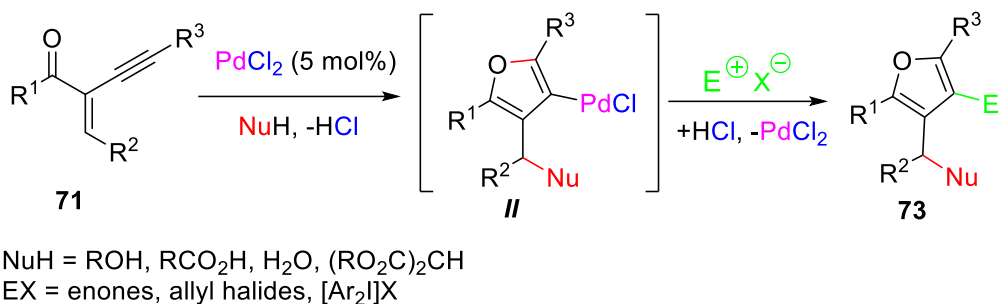
Following the initial disclosures from Larock, a number of research groups embarked in the study of the synthetic potential of this cycloisomerization reaction. In 2005, the Yamamoto group replaced the Au(III) catalyst with Cu(I) and successfully realized the cyclization/nucleophilic addition of 2-alkynyl-enones with alcohols, avoiding the use of moisture sensitive gold(III) chloride.⁶⁸ In 2006, Liang replaced AuCl₃ with the air-stable Bu₄N[AuCl₄]⁶⁹ as catalyst in the same reactions, and Rhim discovered that Pt(II) also catalyze the reaction giving moderate to high yields.⁷⁰

Beyond simple (hetero)nucleophiles, allenamides,⁷¹ nitrones,²⁶ azides,⁷² olefins,⁷³ alkynes,⁷⁴ and imines⁷⁵ can capture intermediate **II** to provide the corresponding furan derivatives *via* either nucleophilic additions or dipolar cyclizations (Scheme 46).^{66b, 76} Further investigations confirmed that, in addition to Au(I) and Au(III),^{69, 77} many other metals such as Pt(II),⁷⁰ Pd(II),⁷⁸ Ag(I),⁷⁹ Cu(I),^{68a, 80} Cu(II)⁸¹ and In(III)⁸² catalyze these reactions efficiently.



Scheme 46

Moreover, Zhang and co-workers have demonstrated that the furyl-metal intermediates **III** in Scheme 45 can be trapped not only with water (protodemetalation), but also with a variety of electrophiles. Thus, they have shown that the Pd(II) promoted, tandem three-component reactions of 2-alkynyl-enones, nucleophiles and electrophiles lead to the tetrasubstituted furans **73** in moderate to good yields (Scheme 47).⁷⁸

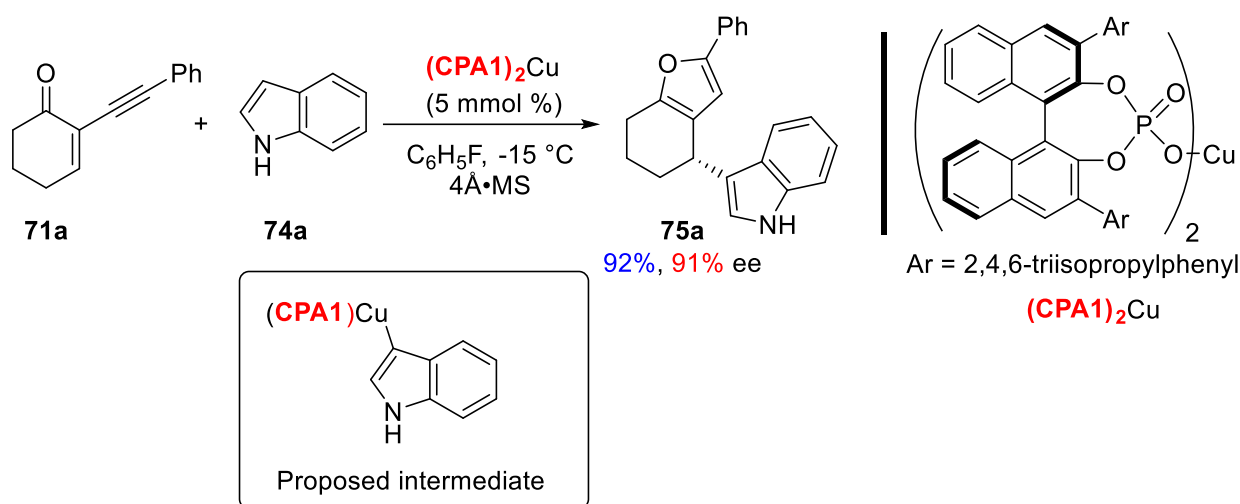


Scheme 47

Enantioselective variants of the reactions above have been developed successfully under metal catalysis, by applying either ligand-based^{26, 71, 83} or counterion-based strategies. For the purposes of this manuscript, we will mention hereafter only enantioselective methods representative of the counterion-based strategies.

Based on the mechanistic hypothesis in Scheme 45 that indicates that the cationic species **II** is a key intermediate, F. D. Toste has envisioned to apply the ACDC approach to these reactions. Indeed, if the X⁽⁻⁾ counterion of intermediate **II** is chiral, it can be anticipated that enantioenriched products will be obtained, although the level of enantioselectivity will strongly depend on the strength of the ion pair between the carbocation and its chiral counterion, among others.

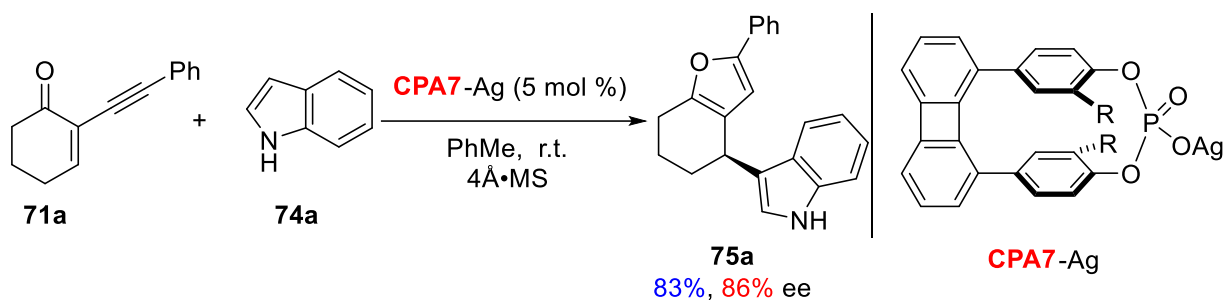
Thus, in 2011 Toste and coworkers reported on the enantioselective tandem reaction of the 2-alkynyl-enone **71a** with indole as the nucleophile,⁸¹ promoted by a TRIP-derived chiral copper(II) phosphate (Scheme 48). Under optimized conditions, they obtained the bicyclic furan **75a** in 94% ee and the method could be extended then successfully to a wide range of C5 and C6-substituted indoles. Of note, the proposed mechanism involves the formation of an indolyl-copper(II) intermediate that plays a crucial role in the reaction. This imposes some limitations in terms of reaction scope. It notably precludes the use of C3-substituted indoles, and 2-methylindole does not react efficiently, probably due to sluggish formation of the copper(II)-indole intermediate.



Scheme 48

Quite interestingly, despite his well-known expertise in the field,^{36, 39, 84} Toste did not mention any attempts of using Au(I) catalysts with chiral phosphate counterions. There is little doubt that such a strategy should have been investigated, therefore the lack of reports likely indicates that the ACDC strategy does not perform well in this specific reaction.

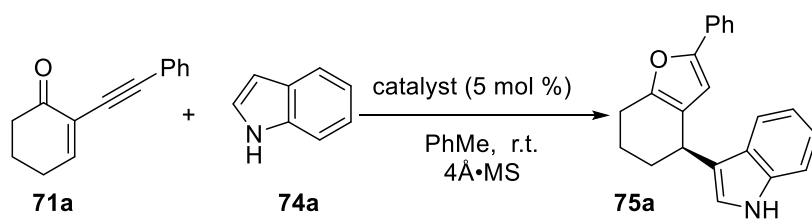
In 2018, in our group, Betzer and Marinetti have reported that the silver(I) salt of a planar chiral phosphoric acid, **CPA7-Ag**, acts as a catalysts in the same reaction, delivering compound **75a** in 83% yield and 86% ee (Scheme 49).⁷⁹ This reaction also is endowed with some limitations, such as the use of unprotected NH-indoles as nucleophiles that is mandatory to get high ees. This suggests that *H*-bonding between the indole and the P=O function of the chiral phosphate plays a key role in the stereochemical control of these Ag(I)-promoted reactions.



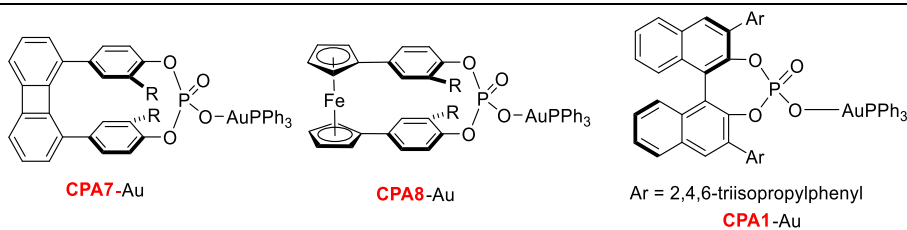
Scheme 49

The same paper also reports the results obtained with some chiral gold(I) phosphates, as shown in Table 7. Entries 1 and 2 show that the planar chiral phosphates **CPA7-Au** and **CPA8-Au** give poor enantioselectivity. Also, when the TRIP derived gold(I) phosphate **CPA1-Au** was used, only a 24% ee was obtained (entry 3). This confirms again that the ACDC approach, under Au(I) catalysis, is not suitable for these reactions.

Table 7. Screening of Gold(I) Phosphates in the Cyclization/Nucleophilic Addition Reaction⁷⁹



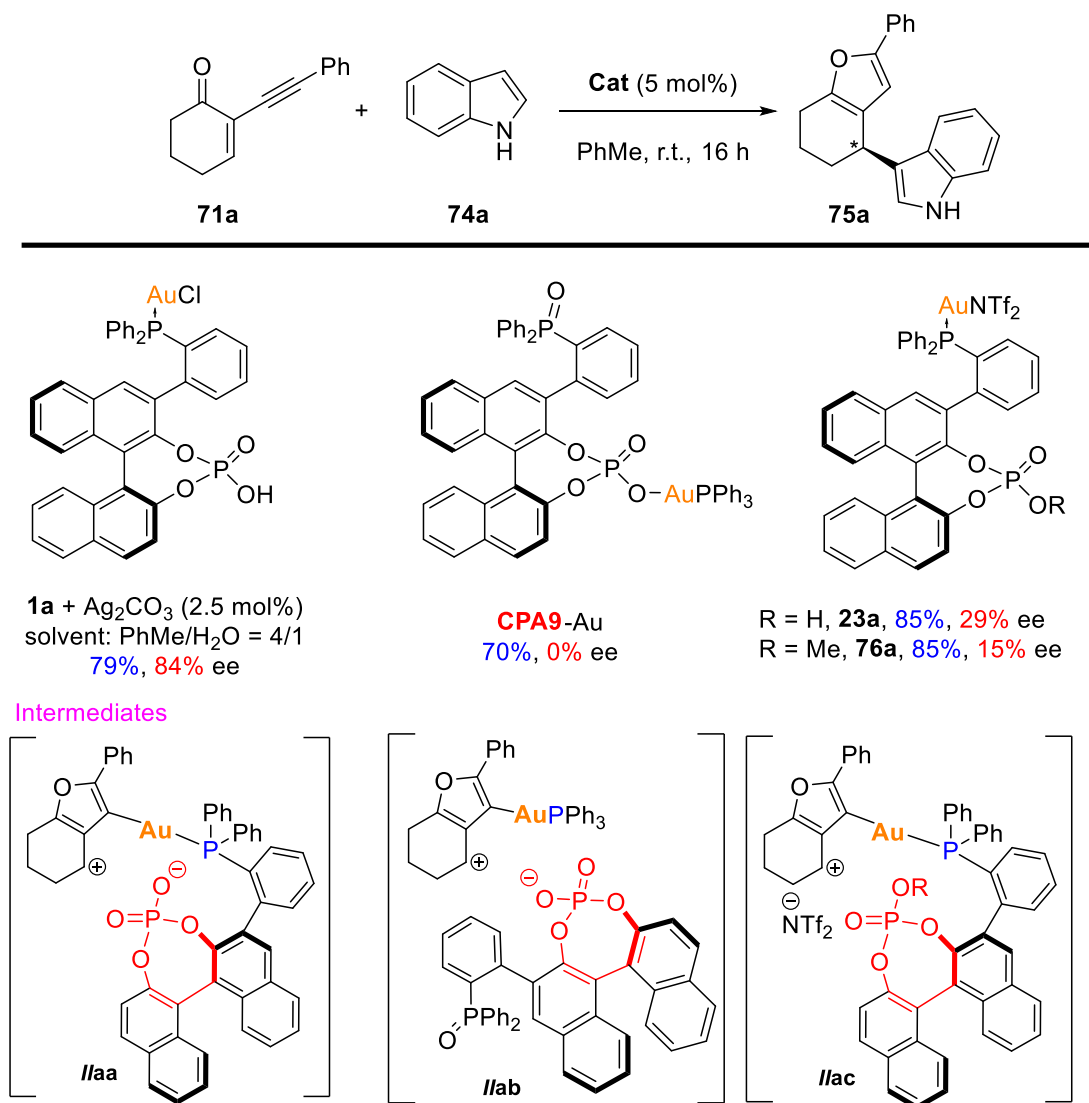
entry	catalyst	yield (%)	ee (%)
1	CPA7-Au	95	1
2	CPA8-Au	70	6
3	CPA1-Au	60	24



2. Application of the TCDC strategy in the cyclization/nucleophilic addition reactions on α -alkynlenones

2.1. Screening of catalysts and reaction conditions

2.1.1. Preliminary catalytic studies with the gold complex **1a** and control experiments



Scheme 50

Having in hand a series of gold-tethered chiral phosphates (see Chapter 1), we have started a systematic screening of these catalysts in a model reaction, the tandem cycloisomerization/nucleophilic addition of indole to 2-(phenylethynyl)cyclohex-2-en-1-one **71a**. Initial experiments have been carried out with the BINOL-derived catalyst **1a**. The two reactants were combined in a 1/1 ratio in a toluene/water 4/1 mixture as the solvent, with a 5 mol% amount of catalyst. Complex **1a** was activated *in situ* by addition of silver carbonate, in the presence of the substrates, and the reaction was completed after stirring at room

temperature for 16 h. After purification by flash column chromatography, **75a** was obtained in 79% yield and 84% ee (Scheme 50). This excellent ee, compared to those obtained with other gold phosphates (Table 7), can be attributed to the tethered structure of intermediate **II** (intramolecular ion pair) that would offer enough rigidity to trigger good enantiodiscrimination.

To validate this hypothesis we have carried out a few control experiments, by screening the three catalysts **CPA9-Au**, **76a** and **23a**. The triphenylphosphine-gold phosphate **CPA9-Au** displays the same molecular skeleton as catalyst **1a**, but the PPh₂ group is oxidized and therefore it can't coordinate to gold. The use of this catalyst resulted in the isolation of the expected product **75a** in 70% yield, but as a racemic mixture. This result confirms that tethering of the phosphate function to gold through the phosphorus ligand is essential. According to our working hypothesis, tethering decreases the conformational freedom and produces well-defined intermediates that enable good stereocontrol.

The second control experiment involves catalyst **23a**, which was prepared *in situ* by activating complex **1a** with the non-basic AgNTf₂. It should combine an untouched phosphoric acid function and an NTf₂⁽⁻⁾ anion as the gold counterion. Despite an excellent catalytic activity, this catalyst delivered **75a** with only 29% ee. Here again, the experiment shows that the catalyst scaffold itself is not able to induce high stereoselectivity, in the absence of a cation-phosphate interaction.

A further evidence was provided by the use of catalyst **76a** that features a methyl phosphate function, instead of a phosphoric acid function. Catalyst **76a** gave the expected furan **75a** with poor enantioselectivity (15% ee).

Overall, these results demonstrate that the structural features of catalyst **1a** are essential to attain high levels of stereochemical induction and definitely validate our design. As an additional remark, it can be emphasized that the chiral phosphoric acid unit of **1a** has been made from a BINOL non-substituted at its C3' position. This contrasts with the established trend showing that high enantioselectivity levels are attained mainly with 3,3'-disubstituted BINOL-based organo- and organometallic catalysts.^{32, 85} It is quite remarkable that the monosubstituted BINOL-based catalyst **1a** can induce such good enantioselectivity.

2.1.2 Optimization of the reaction conditions: solvents and silver salts

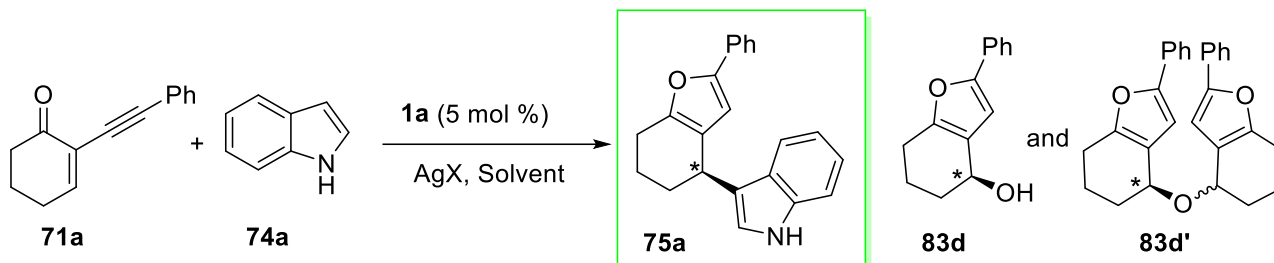
Initial experiments showed that *in situ* activation of **1a** with Ag₂CO₃ in a toluene/water mixture, enables a good catalytic activity in the model reaction in Scheme 50 that involves indole as the nucleophile.

We then screened various solvents to highlight their effects on both the catalytic activity and enantioselectivity. It's worth noting that a competitive addition of water was observed as a side reaction, leading to products **83d** and **83d'** in Table 8. Thus, the toluene/water mixture was replaced firstly with anhydrous toluene and the enantiomeric excess increased to 88% (entry 1). When MeCN was used as solvent in the reaction, only 12% ee was obtained (entry 2), while other solvents such as THF, PhCl and *o*-xylene gave good results, i.e. high conversion rates and enantiomeric excesses of over 80% (entries 3-6).

Based on the results above, anhydrous toluene was chosen as solvent for this reaction. Next, we turned to investigate the influence of the silver salt used to activate the gold catalyst and compare with the use of silver oxide, that led to comparable results (entry 7). Finally, we screened the catalyst loading and, to our surprise, when a 0.2% catalyst was used in this reaction, the enantiomeric excess increased to 96%, with an excellent 75% yield (entry 8). It worth noting that, even when the catalyst loading was decreased to 0.05 mol%, the final product was obtained with 83% yield and 91% ee (entry 9). However, considering the insolubility of silver carbonate in organic solvents and the small scale of these reactions, it becomes difficult, at this catalytic charge, to control the amount of silver salt and the conditions become operationally uneasy.

Therefore, in most of the following experiments we retained the conditions defined in entry 8 as the optimized conditions. The incidental excess of silver carbonate would anyway not be problematic, since silver carbonate does not catalyze the reaction (entry 10).

Table 8. Optimization of the Solvent and Additional Screening of Silver Salt^a



entry	catalyst (mol%)	AgX (mol%)	solvent	yield (%) ^b	ee (%) ^c
1	1a (5)	Ag_2CO_3 (2.5)	PhMe	69	88
2	1a (5)	Ag_2CO_3 (2.5)	MeCN	76	12
3	1a (5)	Ag_2CO_3 (2.5)	THF	29	86
4	1a (5)	Ag_2CO_3 (2.5)	PhCl	82	83
5	1a (5)	Ag_2CO_3 (2.5)	<i>o</i> -xylene	84	86
6	1a (5)	Ag_2CO_3 (2.5)	DMF	76	63
7	1a (5)	Ag_2O (2.5)	PhMe	88	85
8^d	1a (0.2)	Ag_2CO_3 (0.1)	PhMe	75	96
9 ^d	1a (0.05)	Ag_2CO_3 (0.025)	PhMe	83	91
10	-	Ag_2CO_3 (2.5)	PhMe	0	-

^a Reaction conditions: **71a** (0.11 mmol), **74a** (0.1 mmol), solvent (1 mL), under N_2 , r.t. ^b Isolated yields. ^c Determined by chiral HPLC; ^d **71a** (0.55 mmol), **74a** (0.5 mmol), solvent (2.5 mL).

The excellent catalytic activity suggests an especially high stability of the resting state of the catalytically active species **22a** toward decay, possibly due to the tight intramolecular ion pairing between gold and the phosphate (Figure 21).

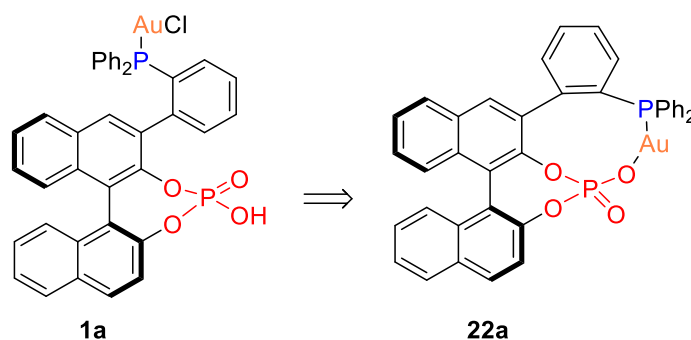


Figure 21

From the bicyclic furan **75a** obtained from entry 8 (with Ag_2CO_3 , in toluene, 96% ee) we could grow single crystals suitable for X-ray diffraction studies. X-ray crystallography showed that **75a** is (*R*)-configured (**Figure 22**). Comparison with HPLC spectra and optical rotations reported by Toste for the same compound also confirms this absolute stereochemistry.⁸¹

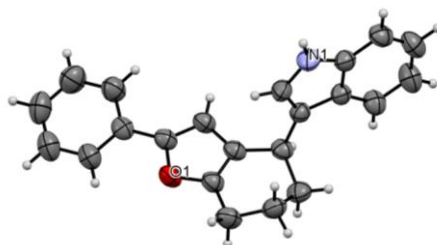


Figure 22. ORTEP View of (*R*)-75a from X-Ray Crystallography

2.1.3 Impact of the protocol used to generate the gold catalyst from **1a**.

In Au(I) catalysis, many factors can influence the efficiency and the outcome of the reactions. The protocol used for the activation of catalyst precursors with silver is particularly tricky, because, beyond the expected activation of the Au(I) complex, the silver salt can either generate or modify the catalytically active species, leading to variable results.⁸⁶ Thus, during the optimization process, we also observed that the protocol used to activate the catalyst has a dramatic impact (Table 9). The following protocols have been investigated:

- 1) Activation of LAuCl **1a** *in situ* by adding AgX in the presence of the starting materials of the catalytic reaction;
- 2) Activation of LAuCl **1a** with AgX in CDCl_3 , (with monitoring of the activation process by ^{31}P NMR), filtration on celite to remove the silver salts and use of the resulting solution in catalytic tests;
- 3) Activation of LAuCl **1a** with AgX in CDCl_3 , filtration on celite and evaporation under vacuum, use of the solid residue as catalyst.

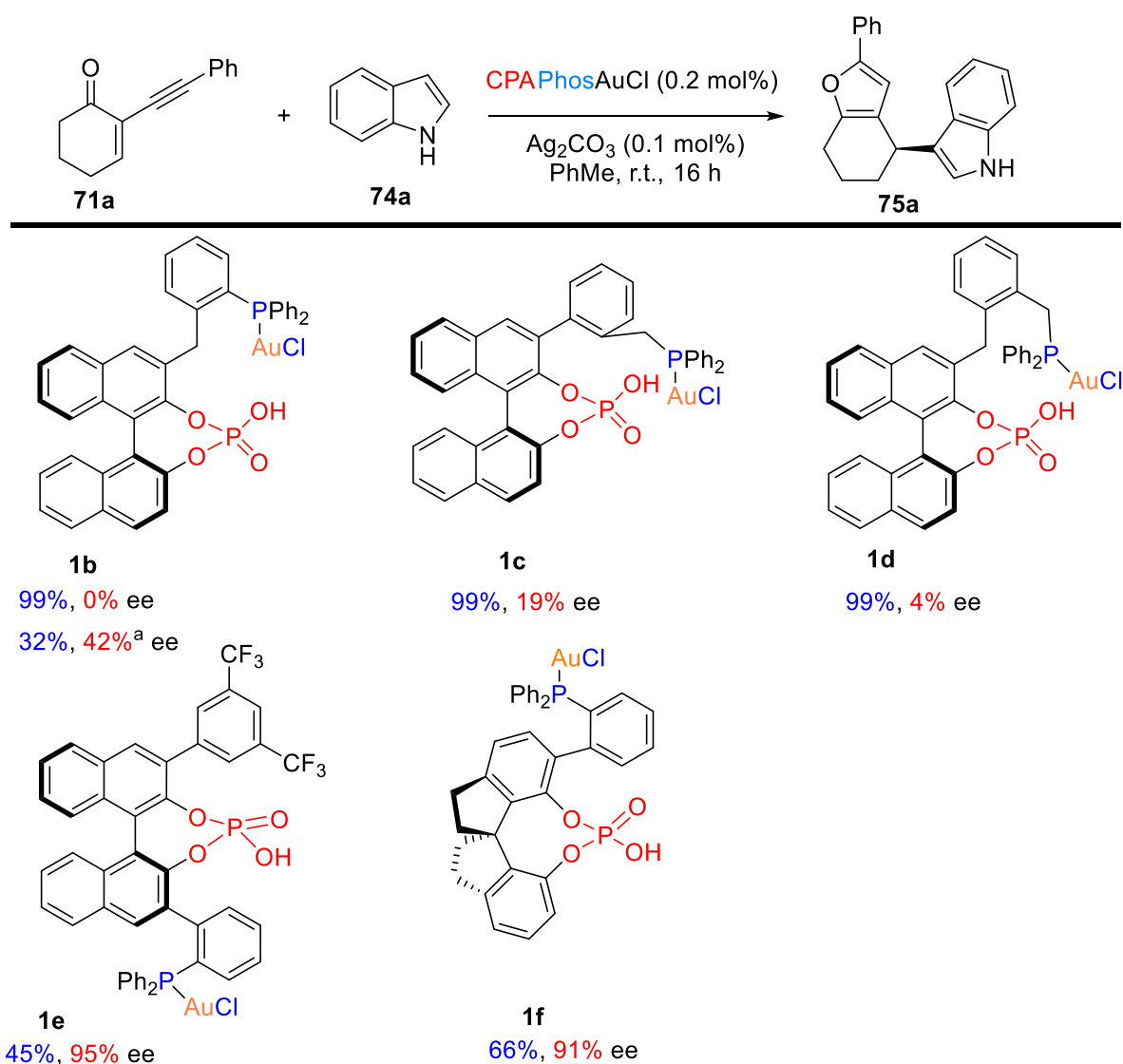
We compared the three protocols in the case of **1a** (entries 1-3) and we found that it is preferable to activate **1a** *in situ*, the two isolation protocols proceeding with the isolation of the catalyst giving lower ees (79% and 26% respectively). This potentially indicates a lack of stability of the catalyst if it is isolated as a solid.

Table 9. Influence of the Catalyst on the Reaction under Different Conditions

entry	LAuCl	AgX (mol%)	yield (%)	ee (%)	protocol
1	1a	Ag_2CO_3 (0.1)	75	96	1
2	1a	Ag_2CO_3 (0.1)	61	79	2
3	1a	Ag_2CO_3 (0.1)	65	26	3

2.1.4 Screening of the phosphine/phosphate catalysts **1a** to **1f**

In order to compare the catalytic activity and selectivity of the six newly prepared phosphine-phosphoric acid catalysts, we have investigated again the model cycloisomerization/addition reaction, under the optimized conditions (Scheme 51). The results showed that all catalysts have very good catalytic activity at low catalytic loadings and that **1a** remains one of the best catalysts in the series. The introduction of a methylene group on the molecular scaffold of **1a**, either between the two aryl groups (**1b**) or between the aryl group and the phosphorus function (**1c**) has a detrimental effect, since the bicyclic furan is obtained with very low ee (0 and 19% respectively). The same effect has been observed when an additional CH₂ tether has been introduced, as in **1d**. We can conclude that the CH₂ tethers induce higher conformational flexibility that decreases the enantiocontrol.



^a Mixture solvent of PhMe/H₂O = 4/1

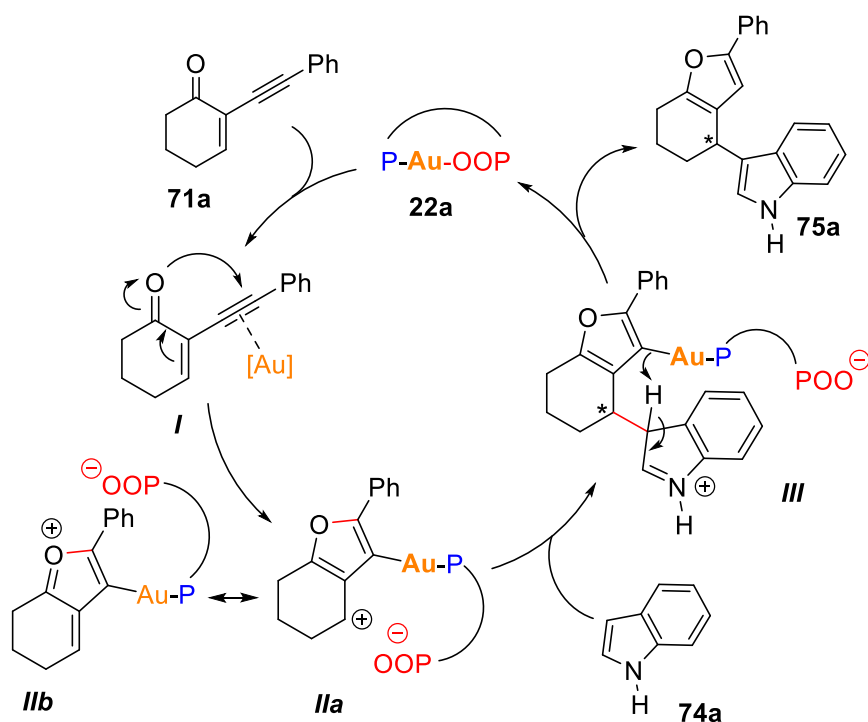
Scheme 51

We then considered catalyst **1e** that displays a 3'-substituted BINOL scaffold. With this catalyst, the final product **75a** was obtained with an excellent 95% ee. Finally, the SPINOL derived complex **1f** also demonstrated excellent catalytic activity and enantioselectivity, giving **75a** with 91% ee (66% yield).

Overall, this demonstrates that the scaffold can be efficiently extended to disubstituted BINOL and SPINOL platforms, while retaining high levels of enantioselectivity. In the model reaction in Scheme 51, these structural changes do not afford major improvements with respect to catalyst **1a**, however, the fine modulation of the catalyst opens favorable perspectives for the optimization of other catalytic reactions.

2.2. DFT Calculations and mechanistic studies

After having obtained the first very impressive results using this new class of catalysts, we turned our attention to the determination of the mechanism of the reaction, in particular relying on DFT calculations. In the postulated mechanism (Scheme 52), the activated gold catalyst **22a** coordinates the triple bond of the alkynyl-enone, which triggers the cycloisomerization of the ketone into the cationic intermediate **II** featuring a phosphate counteranion. The nucleophilic addition of indole to **II** is the enantiodetermining step that leads to intermediate **III**. The protodeauration step proceeds through formal *H*-transfer. It regenerates the gold catalyst and delivers the product **75a**. According to this mechanism, high enantioselectivity levels should result from a tight ion pairing in intermediate **II**, which will bring the chiral phosphate unit close to the prochiral carbon in the enantiodetermining addition step. It can be assumed that the geometrical constraints enforced by tethering gold(I) to phosphate create a more organized spatial arrangement in **II** and enable the excellent stereocontrol.



Scheme 52. Postulated Mechanistic Pathway

For a better understanding of the mechanism, the structure of the resting state of the catalyst, **22a**, has been investigated by DFT calculations at the IEFPCM(toluene)-M06/def2-TZVPP//IEFPCM(toluene)-

M06/def2-SVP level (Dr Gilles Frison, Ecole Polytechnique). It must be noted that **22a**, the cyclic compound formed by coordination of the phosphate to gold, displays three stereogenic elements: the (*S*)-configured binaphthyl, the phosphorus center (central chirality) and the Ph-naphthyl axis (axial chirality). Therefore, this intermediate can generate 4 stereoisomers that differ from their relative configurations. The structures of two diastereomers with the lowest Gibbs energies are shown in Figure 23. Isomer **22aa**, which features a (*S*, *R*, *S_P*)-configuration owns the lowest energy level. When the phosphate coordinates gold with the other oxygen atom (*R_P*), it leads to the (*S*, *S*, *R_P*)-configured structure **22ab**, as the lowest energy epimer, which is 42 kJ·mol⁻¹ higher in energy than **22aa**. In **22ab**, the calculated Au-O bond is longer than in **22aa** (Au-P bond length = 2.088 Å for **22aa** vs 2.152 Å for **22ab**) and the O-Au-P bond angle is significantly smaller (P-Au-O bond angle = 159.88° for **22aa** vs 155.52° for **22ab**). For comparison, we have calculated also the non-tethered (triphenylphosphine)gold(BINOL-phosphate) complex **CPA3-Au**. Calculations estimate its P-Au-O bond angle at 172.9°, i.e. an almost linear geometry for this complex, which is in line with the previously reported X-ray structure (P-Au-O bond angle = 172.7°).³⁷ The P-Au (2.279 Å) and Au-O (2.088 Å) bond lengths of **22aa** are close to those of complex **CPA3-Au** (2.280 Å for P-Au and 2.106 Å for Au-O).

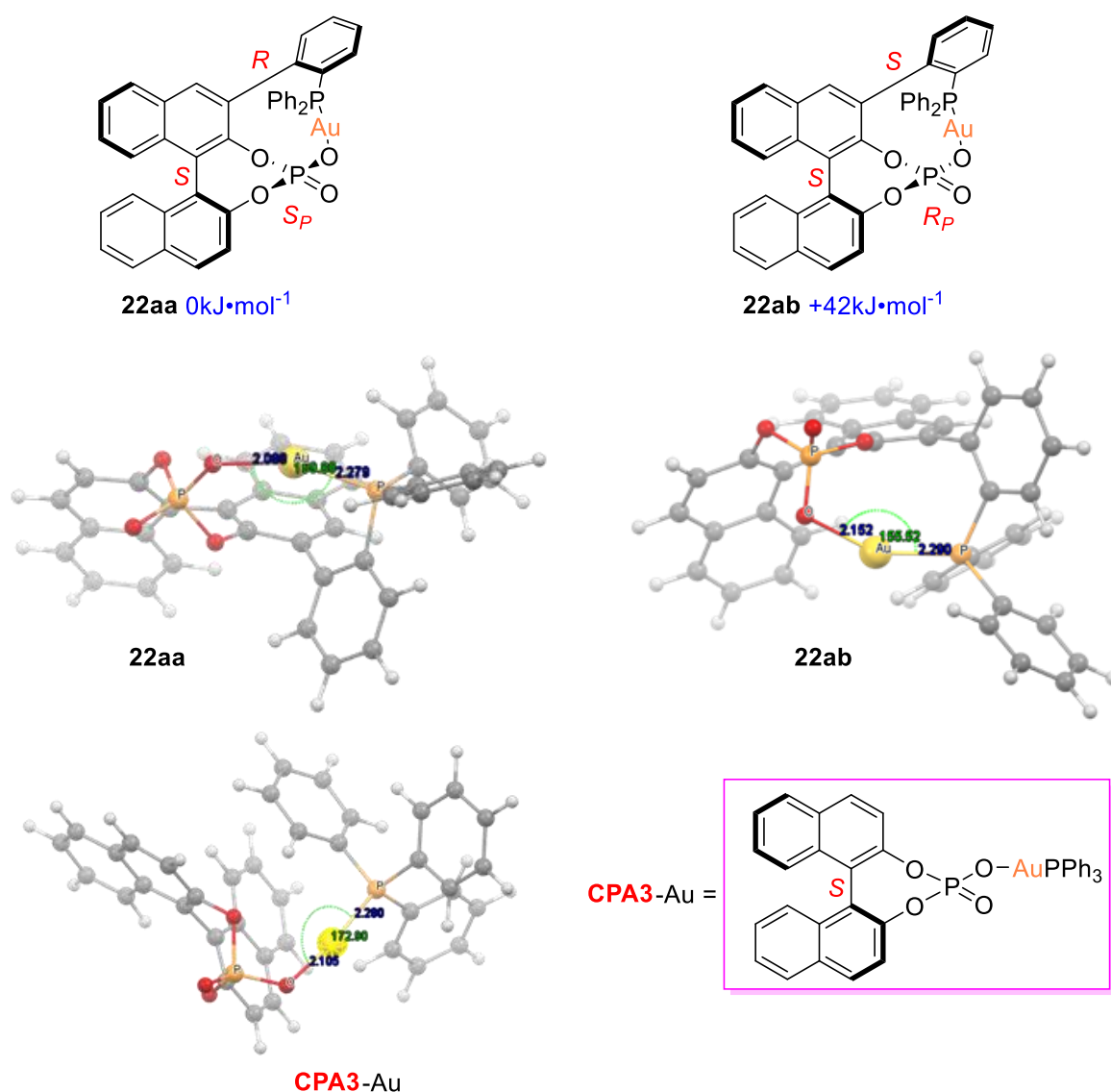


Figure 23. DFT Calculated Structures of 22a and the Triphenylphosphine Complex CPA3-Au

The whole mechanism of the cyclization/addition reaction has been assessed by calculations at the same DFT level. We have computed the structures of all intermediates and transition states, starting from **22a** and the whole energy profile in order to evaluate its feasibility and estimate the influence of the tethered phosphate group on the reaction (Figure 24).

The gold catalyst coordinates the ketone, leading to several isomers with different coordination directions of the alkyne (rotation of the alkyne around the Au-alkyne axis). The most stable intermediates **1a** and **1b** can be formed with a significant release of energy. These intermediates participate then in the cycloisomerization step that leads to the σ -vinyl-Au complex **II**. However, the cycloisomerization of the two isomers display very different energetic pathways. Intermediates **1a,b** generate **IIa,b** through the transition states **TS-I-II** which require +36.6 and +42.6 kJ/mol respectively. The formation of **IIb** is markedly endergonic (+11.1 kJ/mol), while **IIa** is formed with a release of 10.4 kJ/mol (-37.8 kJ/mol with respect to **22a**). The higher energy of intermediate **IIb** can be explained by considering that the phosphate function is clearly opposite to the carbocation, while **IIa** is stabilized by the proximity between the phosphate and the carbocation ($\Delta=28.2$ kJ/mol between the two intermediates). Intermediate **IIa** generates then an adduct with the nucleophilic indole, leading to **II'a** with a release of 11.4 kJ/mol. The subsequent formation of the C-C bond between the carbocation and the indole proceeds with a 27.5 kJ/mol energy barrier and releases 49.4 kJ/mol energy to deliver intermediate **IIIa**. Finally, intermediate **IIIa** undergoes protodeauration and leads to the final product **75a** with a release of 73.1 kJ/mol energy. The starting catalyst **22a** is regenerated.

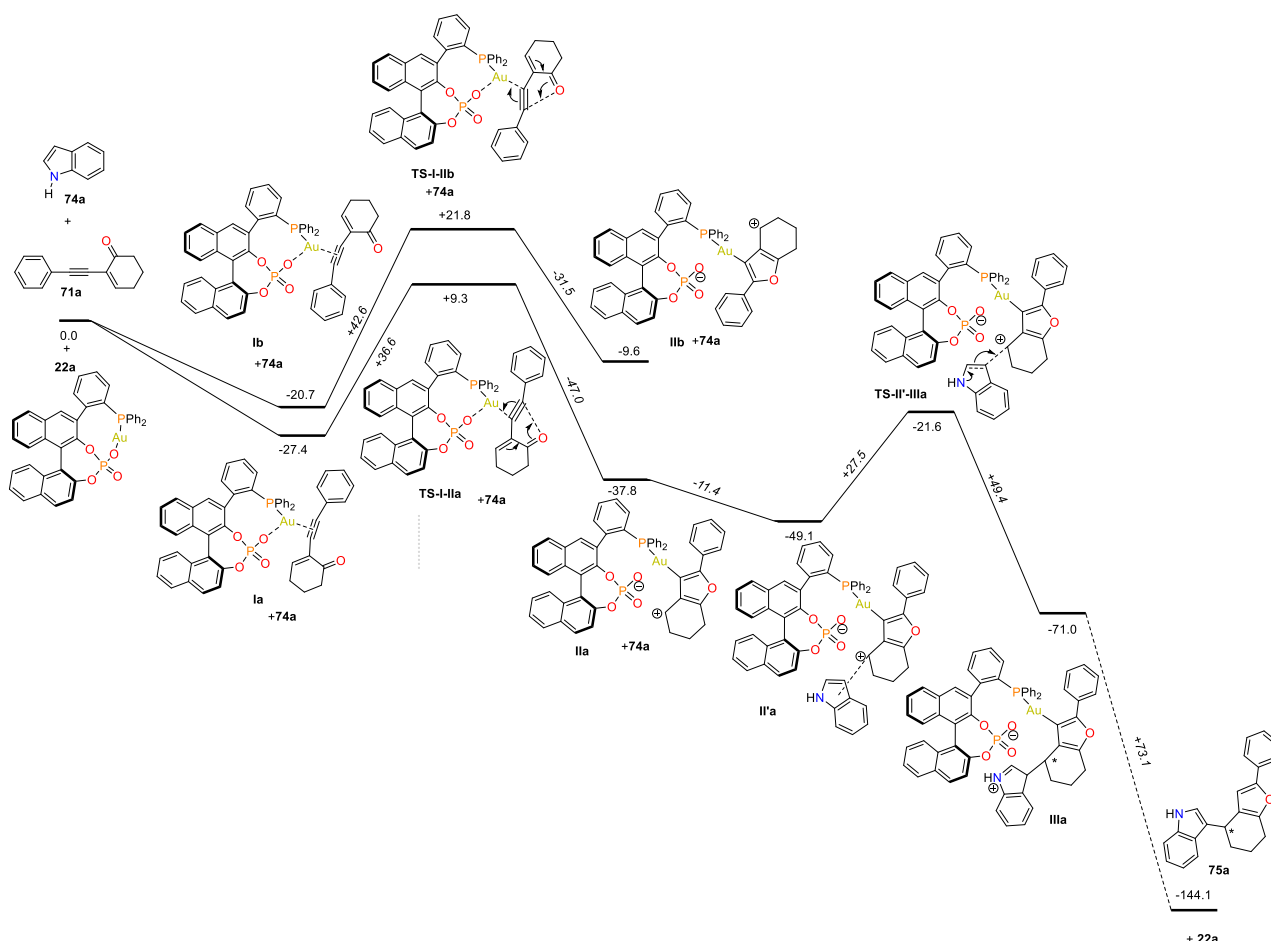
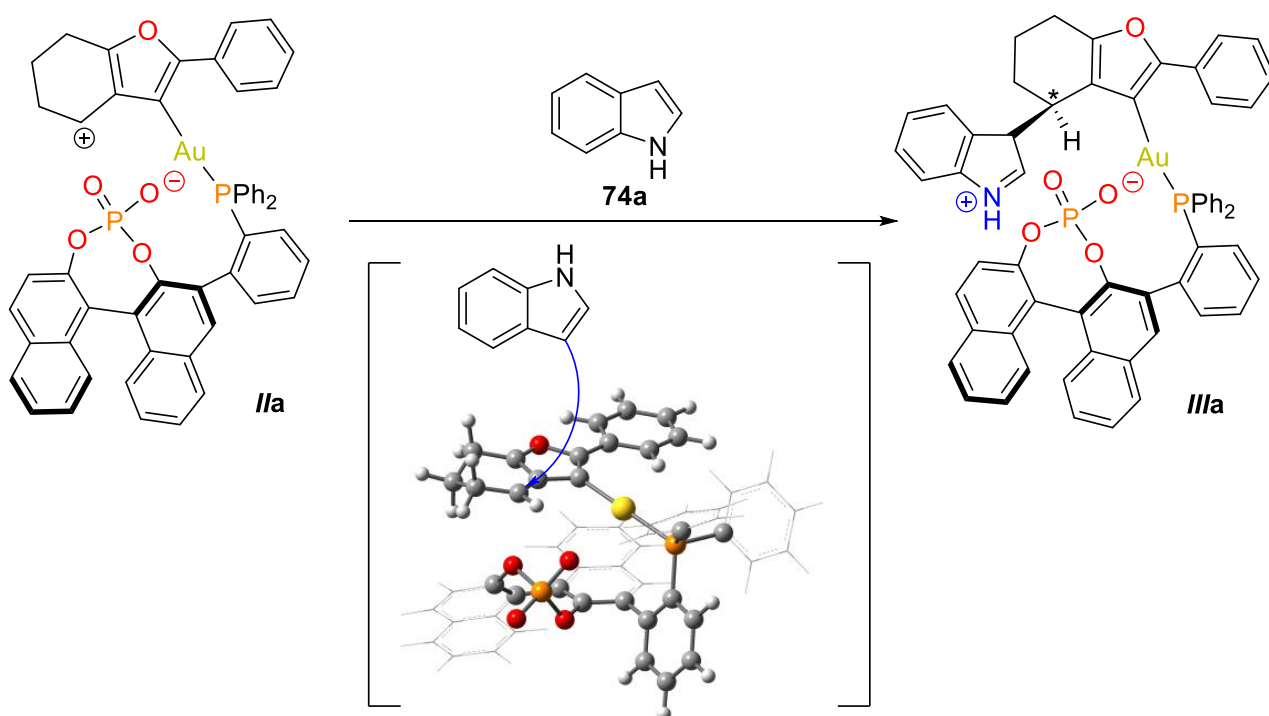


Figure 24. Calculated Reaction Pathway and Intermediates for the Cyclization/Nucleophilic Addition Reaction (Gibbs free energies in kJ·mol⁻¹)

The close examination of the geometry of the key intermediate **IIa** reveals important information on the enantiodiscrimination process. Intermediate **IIa** features an electrostatic pairing between the carbocation and the tethered phosphate group as shown in Scheme 53. The lower side of this carbocationic intermediate is totally hindered by the chiral ligand, and hence the nucleophilic addition of indole should take place from the less hindered face, opposite to the phosphate group, which results in intermediate **III** that lies at -71.0 kJ mol⁻¹ on the free energy surface. The stereochemistry of **III** matches the actual absolute stereochemistry of the final product **75a** that we could determine by X-ray crystallography (Figure 22). This theoretical analysis also shows that the reaction does not involve any *H*-bonding interaction between the NH of the indole and the P=O group of the phosphate. This is in sharp contrast with most processes involving indoles as nucleophiles in reactions promoted by chiral phosphates or phosphoric acids, where *H*-bonding is required to attain a good stereochemical control. This seems to indicate that, in our model reaction, the use of *N*-substituted indoles may be possible, without decreasing the enantioselectivity.



Scheme 53. Optimized Geometry of Intermediate **IIa and Postulated Direction of the Nucleophilic Addition (for clarity, a wireframe representation of some aryl groups is used)**

2.3. Scope of the reaction

2.3.1. Substituted indoles and cyclic enones with variously substituted alkynyl groups

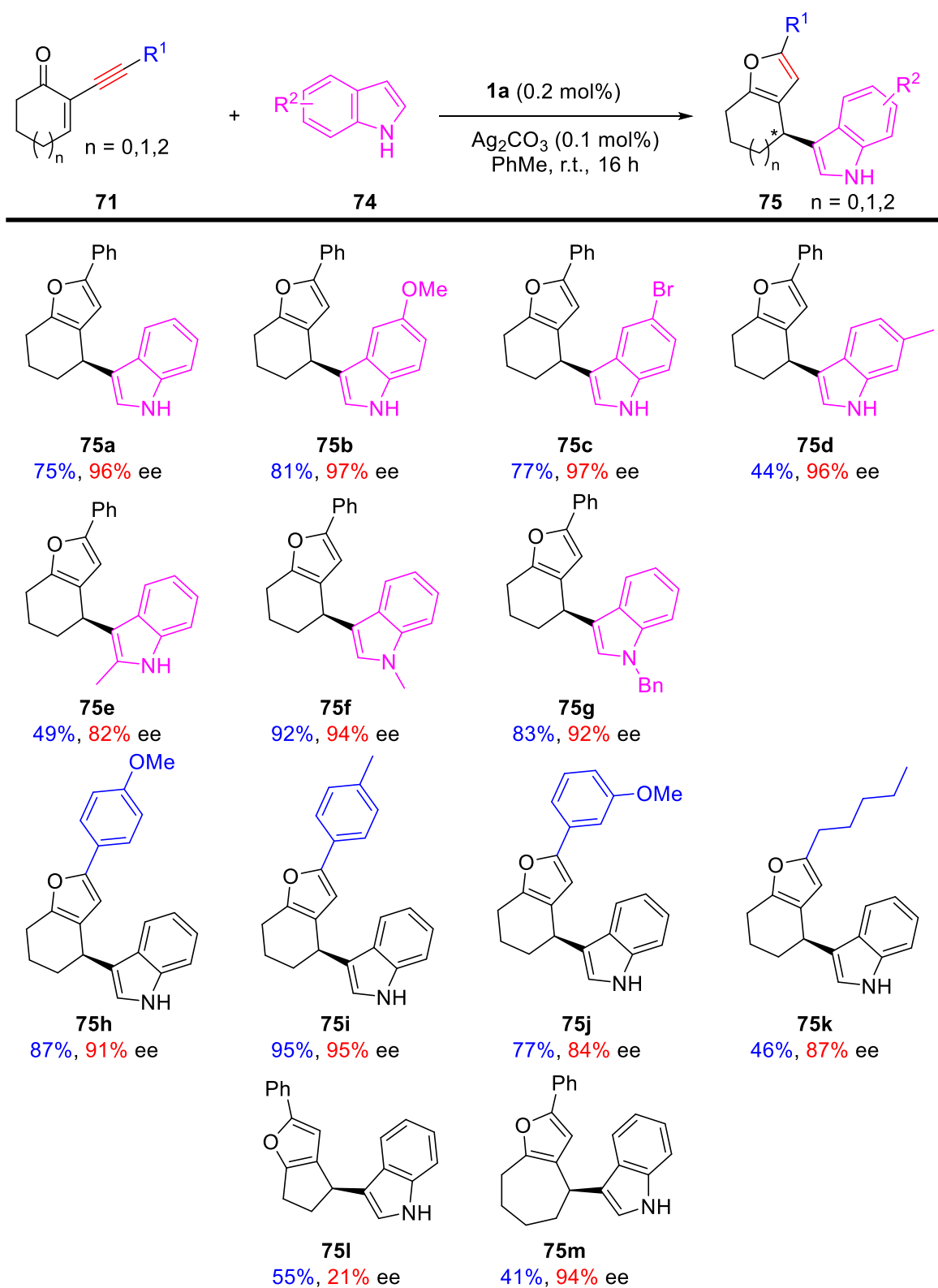
The high enantioselectivity and reactivity of our new catalysts encouraged us to investigate the scope of the tandem cyclization/nucleophilic addition reaction. Various ketones, substituted indoles and even other types of nucleophiles have been considered as shown hereafter. With a better insight in the reaction

mechanism, we next explored the scope of the reaction with respect to the indole nucleophiles (Scheme 54). Under the optimized conditions established before, the reaction tolerated methoxy-, bromo-, and methyl groups on the C5 or C6 positions of indole, delivering the corresponding products **75b/75d** in very high enantiomeric excesses (96-97% ee). The absolute stereochemistry of the products in Scheme 54 has been assigned by analogy with that obtained for **75a** from X-ray crystallography.

When 2-methylindole **74e** was used as the nucleophile, the indole reacted at C3 to produce the corresponding bicyclic furane **75e** with high enantioselectivity (82% ee). This results hence demonstrates a successful extension of the reaction to the use of C2-substituted indoles, which constituted a severe limitation in Toste's approach.⁸⁷

Importantly, *N*-substituted indole derivatives (such as *N*-methyl and *N*-benzyl indoles) reacted cleanly through their C3 positions, which led to the corresponding indolyl-substituted bicyclic furans **75f** and **75g** in excellent yields and enantiomeric excesses (94/92% ee). This result confirms that *H*-bonding between the indole and the chiral phosphate is not required in this process to attain high enantioselectivity, while previous studies showed that *H*-bonding is required in analogous reactions under silver catalysis.⁷⁹

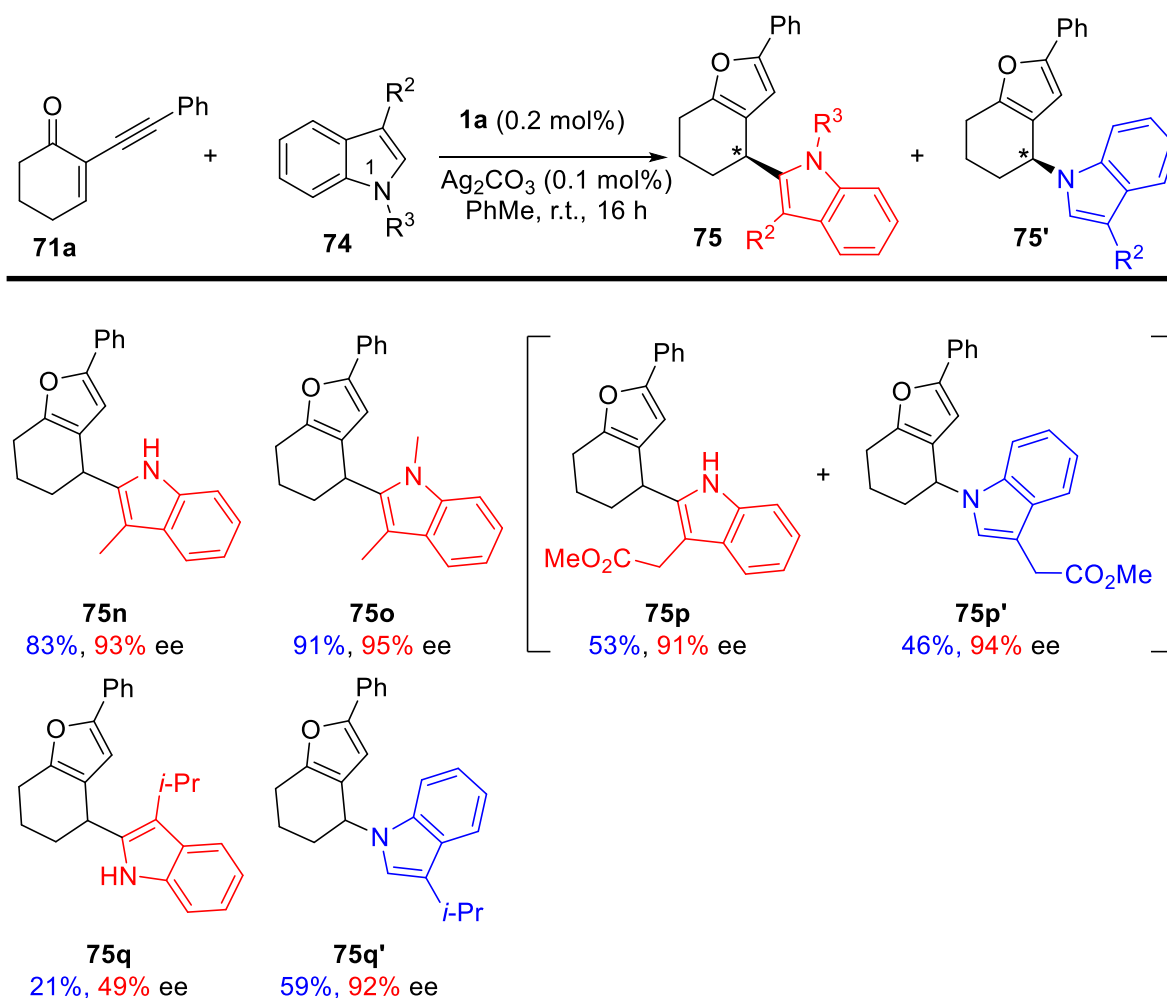
The substituents on the alkynyl unit of the enone were then modified. The phenyl group was replaced by 4-methoxyphenyl-, 4-methylphenyl- and 3-methoxyphenyl groups and these substrates led to high ee's (84-95% ee). We also successfully replaced the aromatic group by an alkyl substituent, **71e** led to the corresponding product **75k** in 46% yield and 87% ee. We next modified the size of the ring of the starting enone, moving from six to five and seven membered rings. To our surprise, the substrate with a five-membered ring **71f** gave only 21% ee, while the cycloheptenone **71g** led to **75m** in 41% yield and 94% ee.



^a Reaction conditions: **71** (0.55 mmol), **74** (0.5 mmol), **1a** (0.2 mol%), Ag_2CO_3 (0.1 mol%), r.t., 16h; ^b Isolated yields; ^c ee determined by chiral HPLC.

Scheme 54. Scope of the Reactions between Indoles and Cyclic α -Alkynyl-Enones^{a,b,c}

2.3.2. C3-substituted indoles



^a Reaction conditions: **71a** (0.55 mmol), **74** (0.5 mmol), **1a** (0.2 mol%), Ag_2CO_3 (0.1 mol%), r.t., 16h; ^b Isolated yields; ^c Determined by chiral HPLC.

Scheme 55. Scope of the Reaction with C3-Substituted Indoles

With the excellent results obtained with various indoles, we tried to push further the scope of the reaction by investigating the possibility of using C3-substituted indoles. This substitution pattern will hopefully orient the addition toward the C2-position of indole, although the nucleophilicity of indoles at C2 is known to be by far inferior to that at C3 (Scheme 55).⁸⁸ The reaction of the model substrate **71a** with the C3 substituted 3-methyl- or 1,3-dimethylindole was carried out under the standard conditions, with a 0.2 mol% of catalyst **1a**, at r.t. for 16h. These indoles demonstrated good reactivity via their C2 position and the reaction produced the corresponding C2-substituted indoles with excellent yields (83/91%) and enantiomeric excesses (93 and 95% ee, respectively).

We next introduced more sterically demanding groups at C3 on the indole ring. Interestingly, when the steric hindrance at C3 increased, competition between addition of the indole via its C2 and via the nitrogen occurred. For example, methyl (3-indolyl)acetate **74j** gave both C2-addition and N-addition products as a 50/50 mixture, both being obtained in excellent ees (91/94% ee). The further increase of the steric hindrance on the indole by means of an isopropyl group, promoted the formation of the N-addition product as the

major product: **75p'** was obtained in 59% yield with 92% ee. Meanwhile, the corresponding C2-substituted product **75q** was obtained in low 21% yield and moderate 49% ee.

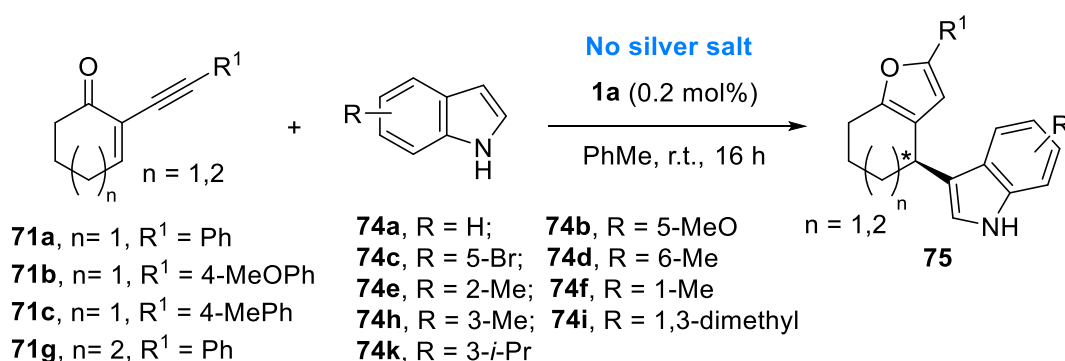
In the case of C3-substituted indoles, we can hence modulate the steric hindrance of the C3 substituent to direct the regioselectivity of the reaction, by keeping high enantioselectivity, at least for the *N*-substituted products.

The whole set of experiments performed so far demonstrate the possibility to engage the three nucleophilic positions of indoles in highly enantioselective cycloisomerization/addition processes.

2.4. Silver-free reactions

Rewordingly, we incidentally found that the silver salt is not systematically required to generate a catalytically active species.

Table 10. Use of Non-Activated 1a in the Enantioselective Cyclization/Addition Reactions



entry	71	74	product	yield (%) ^a	ee (%) ^b	with Ag ₂ CO ₃	
						yield (%)	ee (%)
1	71a	74a	75a	80	92	75	96
2	71a	74b	75b	73	94	81	97
3	71a	74c	75c	30	75	77	97
4	71a	74d	75d	14	88	44	96
5	71a	74e	75e	25	81	49	82
6	71a	74f	75f	40	93	92	94
7	71a	74h	75n	10	85	83	93
8	71a	74i	75o	43	69	91	95
9	71a	74k	75q	2	89	21	49
			75q'	24	86	59	92
10	71b	74a	75h	16	49	87	91
11	71c	74a	75i	12	45	95	95
12	71g	74a	75m	55	95	41	94

^a Isolated yields. ^b Determined by chiral HPLC.

Indeed, during the investigations on the properties of our new catalysts, we found that the catalyst **1a** still shows high reactivity and enantioselectivity in the absence of silver carbonate and any other silver salt. The reactions of ketones **71** and indoles **74**, gave the expected bicyclic furans **75** smoothly (Table 10), with similar ees and slightly diminished yields with respect to reactions performed in the presence of silver carbonate (Table 10, entries 1-9). Only a few divergent results were observed: the 1,3-dimethylindole **74i** gave much lower yield and ee (69% vs 95% ee, Table 10, entry 8). Also the (4-methoxyphenyl)ethynyl-substituted enone **71b** and the 4-methylphenyl-substituted enone **71c** led to much lower ees (Table 10, entries 10-11).

The seven-membered ring **71g** gave the same ee and a slightly higher yield than in the presence of silver (Table 10, entry 12).

In order to investigate in more depth the effect of either simple organic and inorganic bases or silver carbonate on the catalytic activity of the gold catalyst **1a**, we monitored the kinetic profile of the model reaction by ^1H NMR (in CDCl_3) under different conditions (Figure 25). Under the optimized conditions in toluene, i.e. with Ag_2CO_3 as the activating agent, the reaction reached total conversion after 3 h and attained a maximum 80% conversion rate. The silver-free reaction showed on the contrary only 76% conversion after 6.5 h (Figure 25, lines 1 and 2). The reaction rate seems lower in the absence of the silver base. However, when the reaction with **1a** alone was performed in an NMR tube in deuterated benzene, it showed completion after 3 hours without stirring, after a short induction period (Figure 25, line 3). Thus, the non-activated catalyst can perform as good as the activated one, under controlled operating conditions.

When K_2CO_3 was used as a base, the reaction rapidly peaked at a 32% conversion rate (Figure 25, line 4). K_2CO_3 was then replaced by Et_3N , but the reaction didn't work at all (Figure 25, line 5). Thus, the added bases have a detrimental effect on the reaction, unlike silver carbonate.

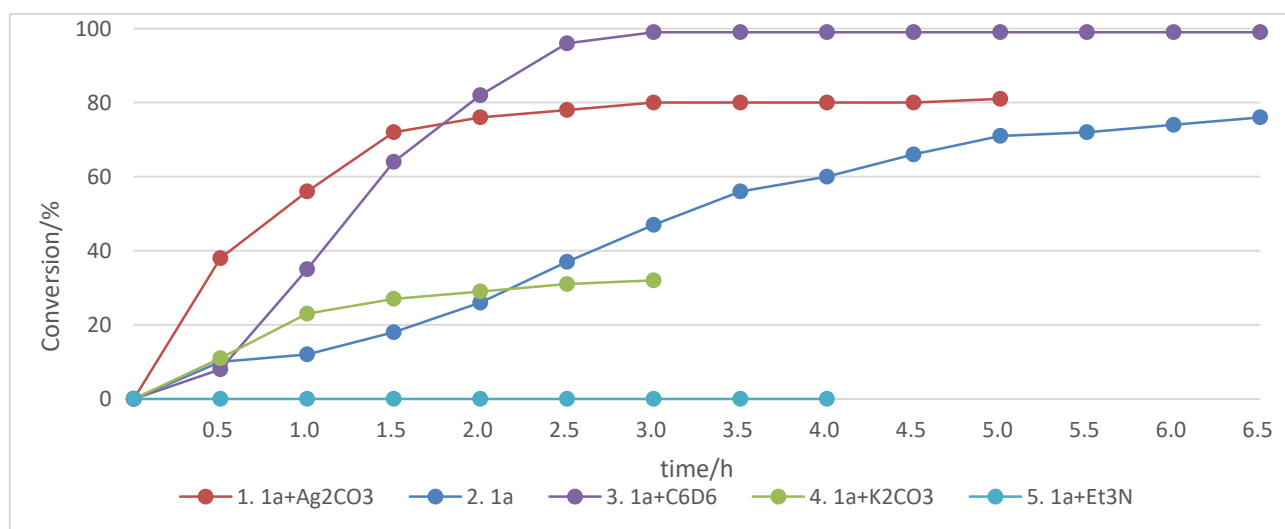
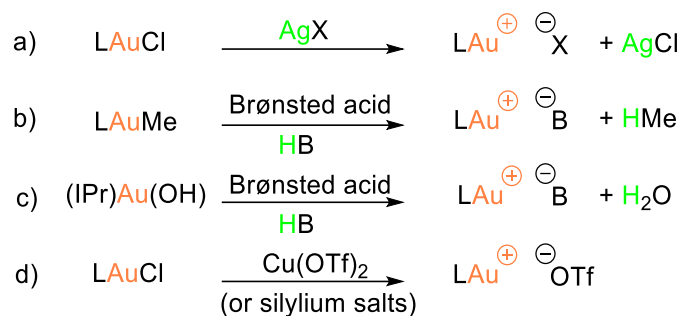


Figure 25. ^1H NMR Monitoring of the Model Catalytic Reaction (**71a** + **74a**) under Various Conditions

Since it is known that the “silver effect” often complicates Au(I) promoted reactions, making them highly dependent on the activation mode and reaction conditions,⁵ silver-free processes are eagerly sought in gold catalysis.⁸⁹ Therefore, as an alternative to silver salts, Lewis or Brønsted acids have been proposed as activating agents, starting from suitable catalyst precursors (Scheme 56). For example, the activation of LAuMe^{6a} or LAu(OH)^{90} precatalysts relies on Brønsted acids, while complexes such as LAuCl can alternatively

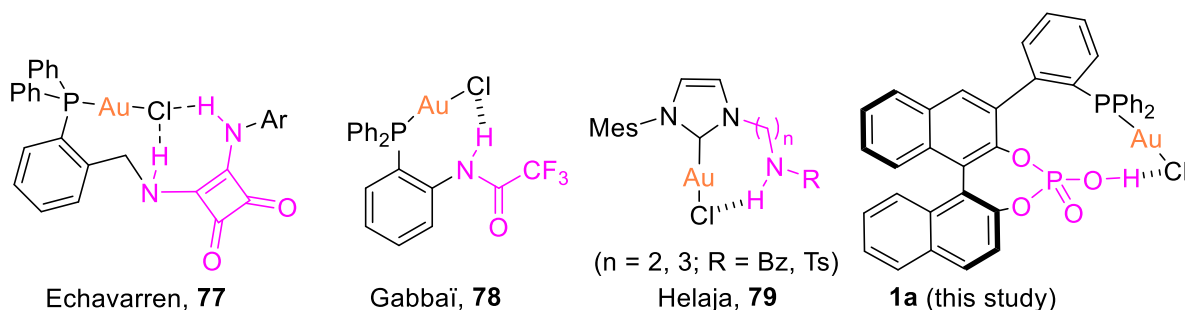
be activated by $\text{Cu}(\text{OTf})_2$ ⁹¹ or silylium ions.⁹² Except for LAuCl complexes, the preparation, storage and use of other type of gold precatalysts may be rather challenging.



L = phosphine or NHC
 X = OTf, BF₄, SbF₆, NTf₂, etc.

Scheme 56. Methods for the Activation of Gold Complexes

Thus, the search for silver free catalysts still represents a rapidly growing field. In 2015, Li and co-workers have discovered that the neutral gold complex IPrAuCl shows high catalytic activity in the gold-catalyzed hydration of alkynes without preactivation.⁹³ Recently, Echavarren disclosed a study focused on the activation of gold chloride complexes by *H*-bonding.⁹⁴ The concept here is to design gold complexes with bifunctional ligands that are capable of self-activation by intramolecular *H*-bonding between gold chloride and the thiourea moiety of the ligand. This concept was preceded by Gabbaï and Helaja using monodentate *H*-bond donors (Scheme 57).⁹⁵



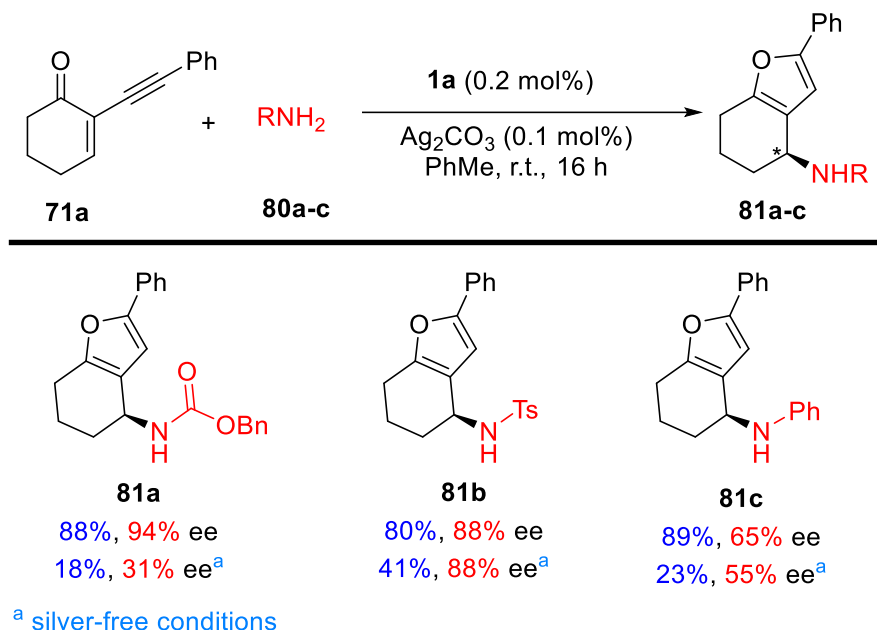
Scheme 57

Based on these literature data, it seems likely that our new catalysts self-activate via the same principle of an intramolecular *H*-bonding between the P-OH function (phosphoric acid function) and the Au-Cl function (Scheme 57). Later in this manuscript, we will show that this self-activation effect is applicable to other reactions and may be even more pronounced when the reactions are performed in DCM.

2.5. Extension of the cyclization/nucleophilic addition reaction to other nucleophiles

In this section, we will show that other nucleophiles than indoles can be used in this reaction, such as carbamates, anilines, tosylamide, alcohols, phenol or water, while delivering the corresponding addition products with high ees.

2.5.1. Nitrogen nucleophiles



Scheme 58. Reactions of the α -Alkynyl Cyclohexenone **71a** with *N*-Nucleophiles

The carbamate **80a**, tosylamide **80b** and aniline **80c** were tested as nucleophiles in the tandem cyclization/addition reactions, as shown in Scheme 58. Both CbzNH_2 and TsNH_2 resulted in high yields and ees. Aniline **80c** also worked well under the optimized condition, leading to *N*-substituted product **81c** in 89% yield and 65% ee.

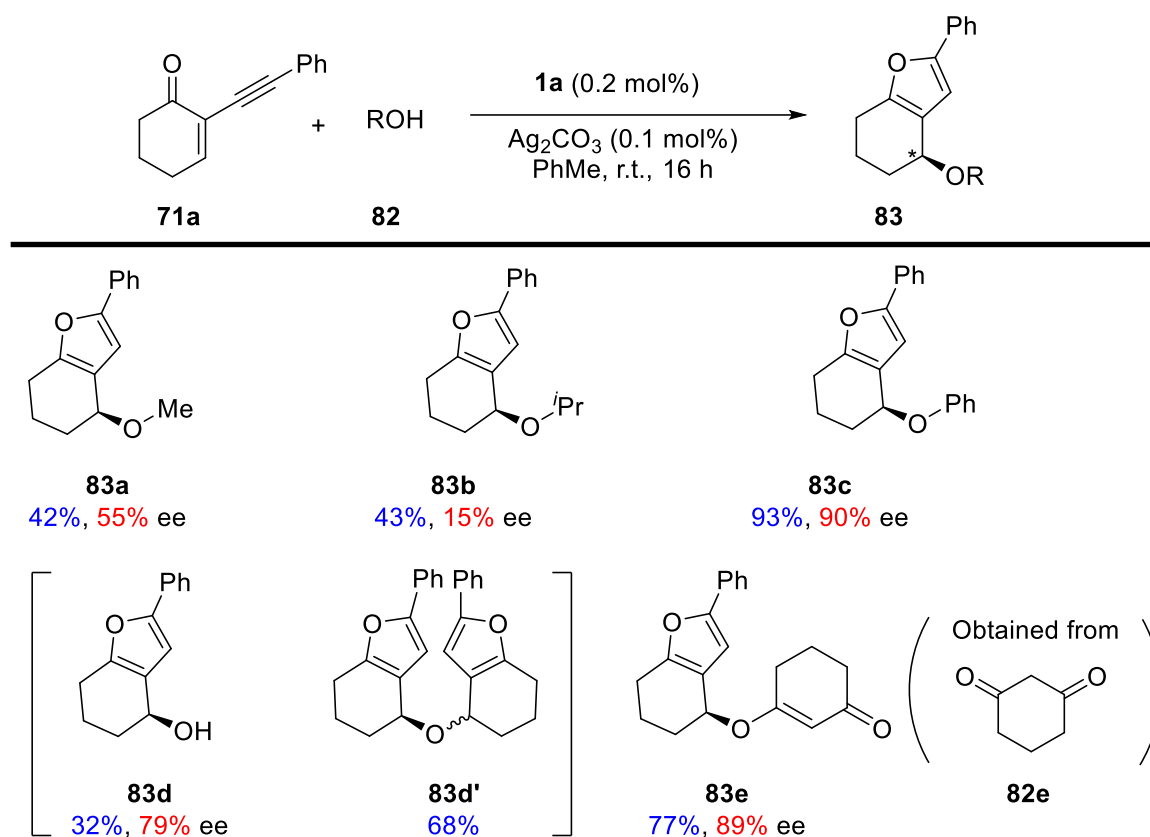
We then applied the silver-free protocol, but lower enantiomeric excesses or yields were obtained in all cases. The tosylamide **80b** gave the same 88% ee and the aniline **80c** gave a little bit lower 55% ee. To our surprise, the carbamate **80a** gave only 31% ee under silver-free conditions.

2.5.2. Oxygen nucleophiles

We next investigated a series of oxygen nucleophiles, such as alcohols, PhOH , a diketone and water. Other oxygen nucleophiles, namely naphthols, will be discussed later in Section 2.6. We initially applied the optimized conditions: the reactions were carried out in toluene in the presence 0.2 mol% of **1a** and 0.1 mol% of silver carbonate (Scheme 59).

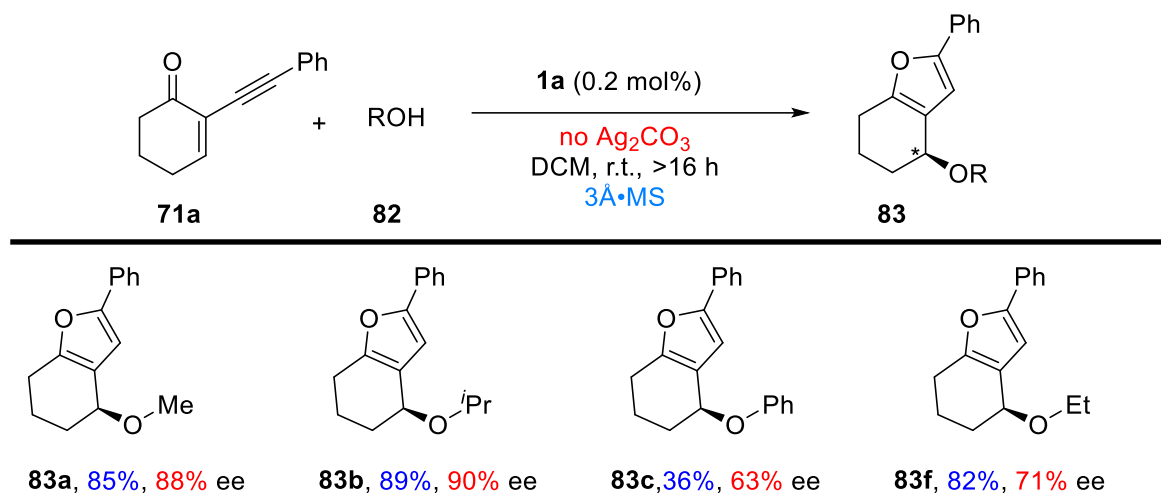
Aliphatic alcohols such as methanol and isopropanol successfully resulted in the *O*-alkylation products. However, both the yields and the ees were moderate. Phenol **82c** gave excellent results, with 90% isolated yield and 93% ee. When water was added as the nucleophile, a 79% ee was obtained for the secondary

alcohol **83d**. However, the reaction also produced the two dimeric compounds **83d'** (two diastereomers), resulting from the nucleophilic addition of the hydroxylated product **83d** to the carbocationic intermediate (**III**) of the cyclization reaction. Finally, the diketone **82e** was used in this reaction which resulted in the *O*-addition product **83e** in 77% yield and 89% ee.



Scheme 59. Reactions of the α -Alkynyl Cyclohexenone **71a with *O*-Nucleophiles**

We next investigated some of these reactions using silver-free conditions (Scheme 60). The reactions were carried out in DCM and molecular sieves was added, in order to limit the formation of the OH-addition product **83d** and the dimeric derivatives **83d'**. Interestingly, these conditions resulted in higher yields and enantioselectivities, with the exception of the reaction involving phenol as the nucleophile. The additions of MeOH, EtOH and *i*-PrOH led to 88%, 71% and 90% ee respectively. This demonstrated again the high synthetic potential of this simple approach.



Scheme 60. Reactions of the α -Alkynyl-Cyclohexenone **71a** with *O*-Nucleophiles under Silver-Free Conditions

2.5.3. Other attempted reactions

In order to check the applicability of our catalytic system in analogous reactions, we spent considerable time to investigate other nucleophiles, as shown in Scheme 61. However, most of them did not give the cycloisomerization/nucleophilic addition process starting from enone **71a**, with a 5 mol% of **1a** and silver carbonate in toluene.

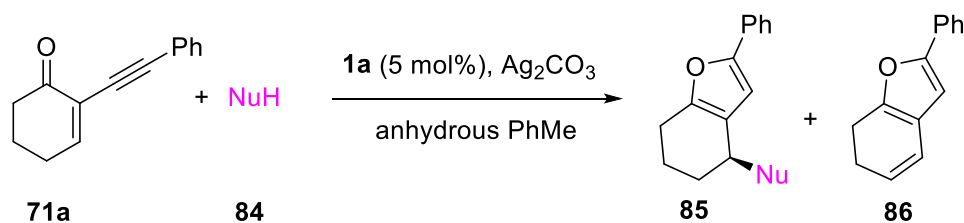
Allyltrimethylsilane, trimethylsilyl cyanide, ammonia and nitromethane did not act as nucleophiles. In many cases, the unsaturated product **86** was obtained instead of the expected addition products. This likely accounts for the weak nucleophilicity of these reactants that cannot effectively add to the carbocationic intermediate **II** (Scheme 54), thereby giving the $\text{H}^{(+)}$ elimination product.

Among the unsuccessful nucleophiles, we can mention the *O*- and *N*- bis-nucleophile, 2-aminophenol **84a** that showed no regioselectivity and led to a complex mixture.

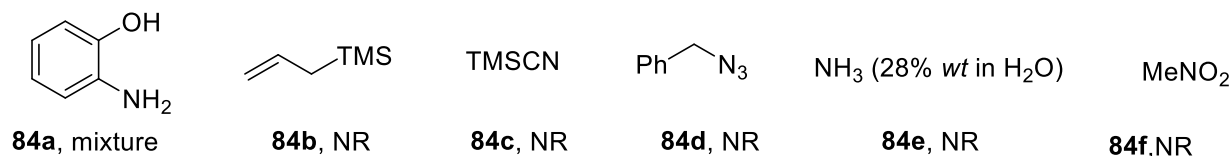
According to the literature, olefins,⁷³ allenamides⁷¹ and benzoisoxazole⁹⁶ might lead to the corresponding tricyclic derivatives **85g**, **85h** and **85i** via cycloaddition reactions. Unfortunately, none of these reactions proceeded as expected.

A special case aroused from the reaction of *N*-*tert*-butoxycarbonyl- α -(phenylsulfonyl)isobutylhydroxylamine **84j**. This compound is known to be precursor to an *N*-Boc nitron⁹⁷ that could have led to the 1,3-dipolar cycloaddition product **85j**. To our surprise, we isolated instead a compound resulting from the formal addition of SO_2Ph , **85j'** with a 93% ee. Considering that the formation of the nitron proceeds via the extrusion of $\text{PhSO}_2^{(-)}$, it is not so surprising that the latter can act as the nucleophile. This is an interesting result considering that the PhSO_2 -addition products have never been reported in these reactions.

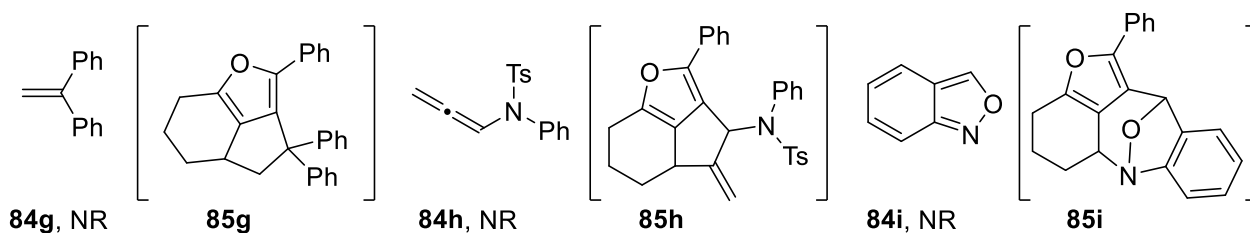
We consequently tried to carry out the same reaction sequence using benzenesulfinic acid. The addition product **85j'** was obtained in 88% yield but with only 34% ee. We postulated that the acidic PhSO_2H ⁹⁸ might regenerate the phosphoric acid function of the catalyst, which in turn leads to lower ee's. Therefore, we replaced the acid PhSO_2H with its salt PhSO_2Na . The reaction did not proceed, probably because of the low solubility of the salt. We are still trying to determine a suitable protocol to access these derivatives efficiently.



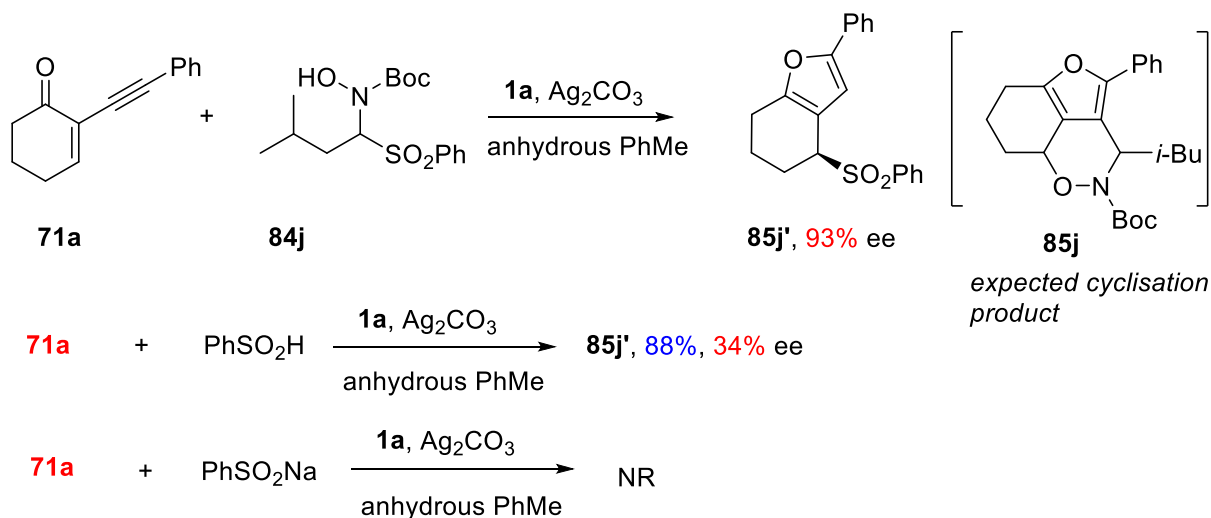
1) Miscellaneous nucleophiles



2) Cycloaddition attempts



3) Reaction with a *N*-Boc nitron precursor

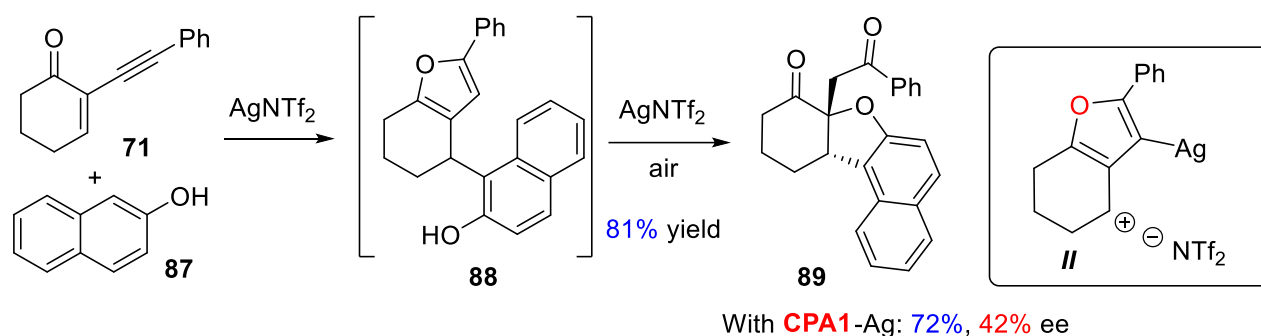


Scheme 61. Other Unsuccessful Nucleophiles

2.6. Application of the cyclization/addition method in reactions involving naphthols

In order to expand further the scope of the tandem cyclization/nucleophilic addition reaction, we have considered naphthols as potential nucleophiles, because naphthols are important and versatile starting materials in a number of catalytic reactions. Among others, they have been investigated previously as nucleophiles in the process targeted in our study, but using different catalysts. In 2020, the Xu and Ren group

discovered that silver salts catalyze the reaction of ketone **71** with 2-naphthol **87** to compound **88** as a reaction intermediate (Scheme 62).⁹⁹



Scheme 62. Naphthols as Nucleophiles in the Ag(I) Promoted Cyclization/Addition Reaction

The nature of the product indicates that 2-naphthol acts as a C-nucleophile in the tandem reaction. Interestingly, when the reaction was carried out in the presence of air, **88** was oxidized to **89** that was isolated in 81% yield. It was proposed that the silver salt plays a role in this oxidation step, though this issue remains rather unclear. When a chiral silver phosphate (**CPA1**-Ag) was used as the catalyst, the final product was obtained in 72% yield, with a low 42% ee.

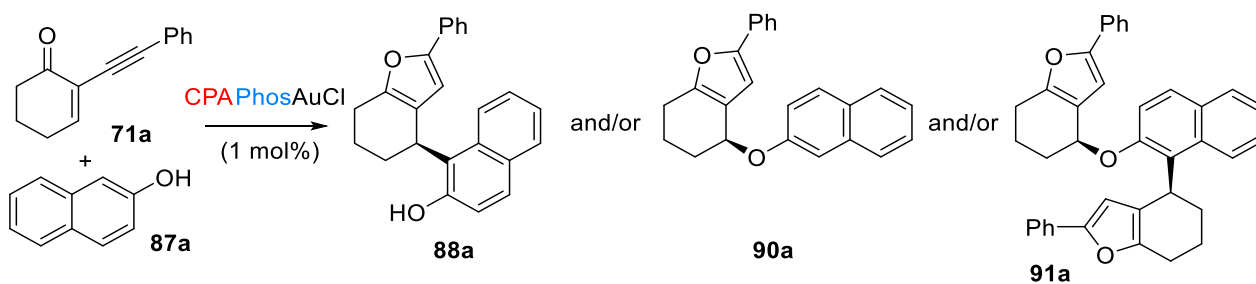
Considering the poor ee obtained in this reaction under silver catalysis, we saw an opportunity to extend the use of our gold catalysts to reactions involving nucleophilic addition of naphthols. This part of the project was developed in collaboration with Yunliang Yu, as a part of his PhD project. Yunliang Yu being the main contributor, the results of this study will be summarized briefly.

2.6.1. Cyclization/addition reactions with 2-naphthol as nucleophile

We first selected 2-naphthol as the nucleophile in the reaction with **71a** and we looked for suitable reaction conditions (Scheme 63). The optimization of this reaction turned out to be much more complex than expected, therefore this study especially highlighted the relevance of having in hand several precatalysts, as well as to possibly apply the silver-free strategy.

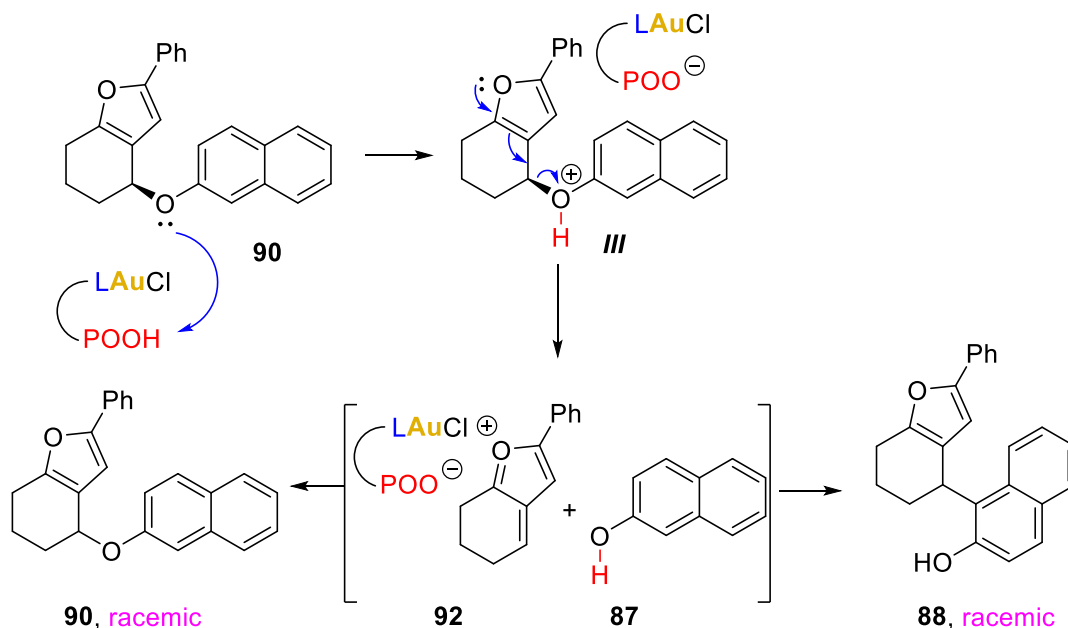
As main outcomes of this work, we discovered that:

- The addition of silver carbonate is not necessary in this reaction.
- The best solvent is DCM.
- The disubstituted BINOL-based catalyst **1e** is much more active than the monosubstituted derivative **1a**.
- The 2-naphthol can act as both O- and C-nucleophile. As a result, both addition products **88a** and **90a** can be obtained. Moreover, the C-addition product **88a** can also further act as a nucleophile, leading ultimately to the disubstituted naphthol **91a**.



Scheme 63. Au(I) Promoted Cyclization/Nucleophilic Addition Reactions Involving 2-Naphthol

- In the presence of catalyst **1e** or **1a**, the *O*-addition product **90a** racemizes over the time and converts to the racemic *C*-addition product **88a**. Extensive studies established that this rearrangement proceeds via protonation of the naphthyl ether **90** by the acidic catalyst, which generates a good leaving group. Extrusion of naphthol from **III** generates a carbocation with the chiral phosphate as counterion. This highly electrophilic species may then undergo addition of the naphthol via either *C*- or *O*-additions. However, this addition step is barely enantioselective, because the phosphoric acid behaves as a non-tethered organocatalyst and does not trigger efficient enantiodiscrimination (Scheme 64).



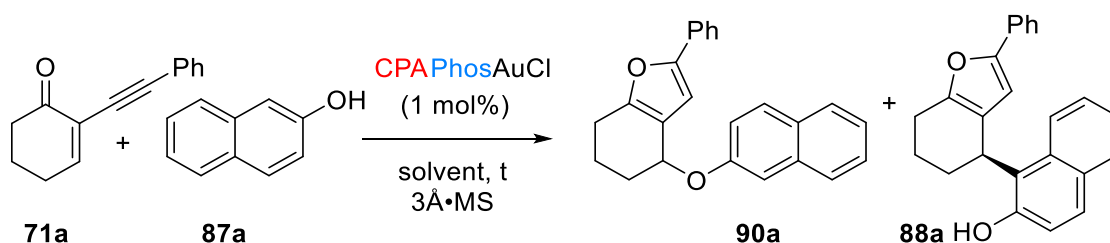
Scheme 64. Acid-Catalyzed Naphthol Elimination and Subsequent Nucleophilic Additions (ee eroding pathway)

- The whole process hence generates both *C*-addition and *O*-addition products, resulting from both enantioselective and non-enantioselective pathways. The acid-promoted process results in a decrease of the enantiomeric excesses of both products, if the reaction time is not controlled. It is of note that the doubly substituted product **91a** can result from the reaction of enone **71a** with either the enantioenriched *C*-addition product **88a** (obtained from the Au-catalyzed process) or the *C*-addition product with lower ee, obtained from the stereochemistry-eroding acid-promoted pathway.
- After extensive studies of all reaction pathways, we could establish conditions for the control of the regioselectivity of the reaction, as well as the enantioselectivity for each product (Table 11). The reaction

performed in DCM at room temperature with catalyst **1a** takes less than two minutes and generates the *O*-addition product **90a** in 85% ee and the *C*-addition product **88a** in 96% ee (entry 1). This reaction is not regioselective, but these conditions can be used if both products are needed in high ees. The same reaction performed with **1e** (1 mol%) over 1 min favors the formation of the *C*-addition product **88a**, that is obtained in 91% ee (entry 2). Finally, we were delighted to find that reactions performed in dioxane or diethyl ether generate preferentially the *O*-addition product but, most remarkably, with inversion of the stereochemistry of its stereogenic carbon (entries 3-4). This is an interesting case of enantiodivergence mediated by the solvent,¹⁰⁰ though we have currently no insight on the origin of this phenomenon. On the contrary, the *C*-addition product **88a** does not undergo a switch of the enantioselectivity mediated by the solvent.

The stoichiometric ratio between the starting naphthol and the enone is not discussed here, but it is also an important parameter, especially if the formation of the 'dimer' **91a** is targeted.

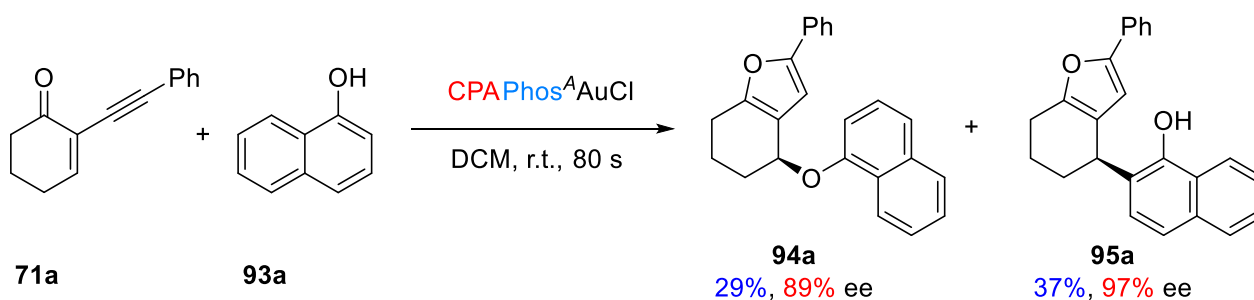
Table 11. Optimization of the Enantioselective Cycloisomerization/Addition Reaction with 2-Naphthol



entry	catalyst	solvent	t	T (°C)	ratio 90a/88a	ee (90a , %)	ee (88a , %)
1	1a	DCM	80s	r.t.	55/45	85	96
2	1e	DCM	60s	r.t.	40/60	33	91
3	1e	dioxane	overnight	15 °C	78/22	82 (-)	ND
4	1e	Et ₂ O	1.5 h	15 °C	70/30	84.5 (-)	90

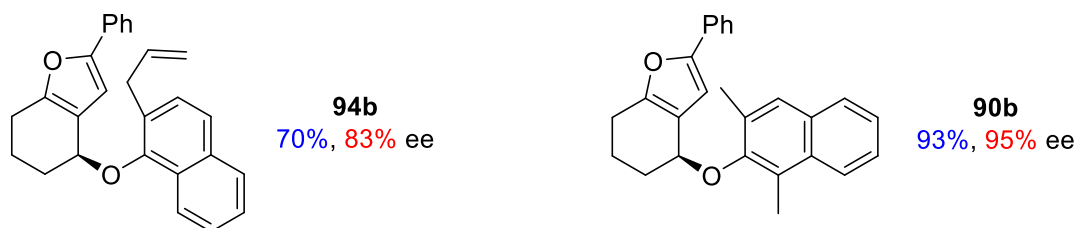
2.6.2. Cyclization/addition reaction with 1-naphthol and substituted naphthols

On the basis of the optimized conditions above, the extension of the reaction to 1-naphthol has been investigated using enone **71a** and 1 mol% **1a** as the catalyst. The reaction led to the *O*-addition product **94a** in 29% yield and 89% ee and to the *C*-addition product **95a** in 37% yield and 97% ee (Scheme 65).



Scheme 65. Au-Promoted Cyclization/Addition Reaction with 1-Naphthol as the Nucleophile

A number of other reactions were performed with 2-substituted 1-naphthols and 3-substituted 2-naphthols. These reactions are much easier, considering that only *O*-addition can proceed. Excellent enantioselectivities were obtained using **1e** (0.2 mol%) as the catalyst in PhMe at 0 °C, as demonstrated by the representative examples shown in Scheme 66.

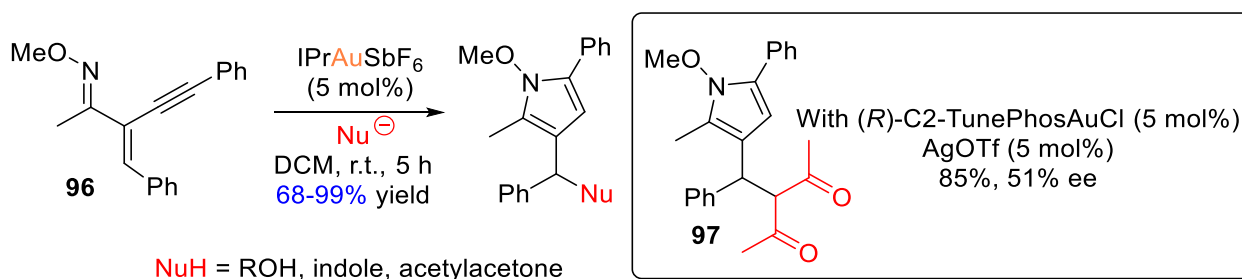


Scheme 66. Representative Examples of Products Obtained using Naphthols as Nucleophiles

The two *O*-addition products **94b** and **90c** were obtained in excellent yields and enantioselectivities.

2.7. Application of the cyclization/nucleophilic addition reactions to conjugated oximes

As shown so far in this manuscript, we have extensively used α -alkynylenones as starting materials in the Au-promoted cyclization/addition reaction. In 2012, Zhang and co-workers extended this class of reactions to acyclic α -alkynylenone oximes using alcohols or indole as nucleophiles and obtained the corresponding pyrroles in good yields using IPrAuSbF₆ as a catalyst (Scheme 67).¹⁰¹ As far as we know, a single attempt has been reported toward enantioselective variants: using (*R*)-C2-TunePhos as the chiral ligand, the reaction of the acyclic *O*-methyl oxime **96** with acetylacetone as the nucleophile led to the corresponding pyrrole **97** in 85% yield and 51% ee.

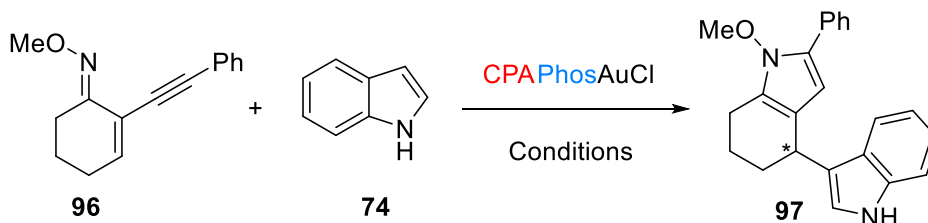


Scheme 67. Tandem Cyclization/Nucleophilic Additions on Enone Oximes

Hence, we tried to apply our new catalysts to the reaction of the cyclic α -alkynylenone oxime **96** with indole, to check whether we could obtain enantioenriched products. We first applied the previously optimized conditions (reactions in toluene at room temperature, with Ag₂CO₃ as the base), but only 13% conversion was obtained (Table 12, entry 1). Then we increased the reaction temperature to 90 °C, the conversion rate increased to 65% and the desired bicyclic pyrrole was obtained with low 21% ee (entry 2). This result made us to further investigate the reaction conditions by increasing the catalyst loading to 1 mol%,

but we did not observe any improvement (entry 3). When we replaced toluene with DCM, both catalysts **1a** and **1e**, gave the desired product, however, the enantiomeric excesses did not improve significantly (entries 4-5). Then we studied the effect of the temperature and we found that decreasing the reaction temperature to 0°C decreases the ee slightly, while a 35% ee was obtained at 40 °C (entry 7). Facing such low enantioselectivity levels, finally we checked if silver carbonate alone or the phosphoric acid function might be responsible for the catalytic activity. The control experiments in entries 9 and 10 showed that this is not the case, since neither Ag₂CO₃ nor diphenylphosphoric acid promote this reaction.

Table 12. Optimization of the reactions between Oximes and Indole^a



entry	cat.	[Ag]	T (°C)	solvent	yield (%) ^b	ee (%) ^c
1	1a (0.2)	Ag ₂ CO ₃	r.t.	PhMe	13 ^d	-
2	1a (0.2)	Ag ₂ CO ₃	90	PhMe	65 ^d	21
3	1a (1.0)	Ag ₂ CO ₃	r.t.	PhMe	9 ^d	23
4	1a (0.2)	Ag ₂ CO ₃	r.t.	DCM	61	25
5	1e (0.2)	Ag ₂ CO ₃	r.t.	DCM	51	24
7	1a (0.2)	Ag ₂ CO ₃	0	DCM	40	19
8	1a (0.2)	Ag ₂ CO ₃	40	DCE	63	35
9	1a (0.2)	Ag ₂ CO ₃	60	DCE	64	34
10	-	Ag ₂ CO ₃	r.t.	DCM	NR	-
11	dpp ^e	-	r.t.	DCM	NR	-

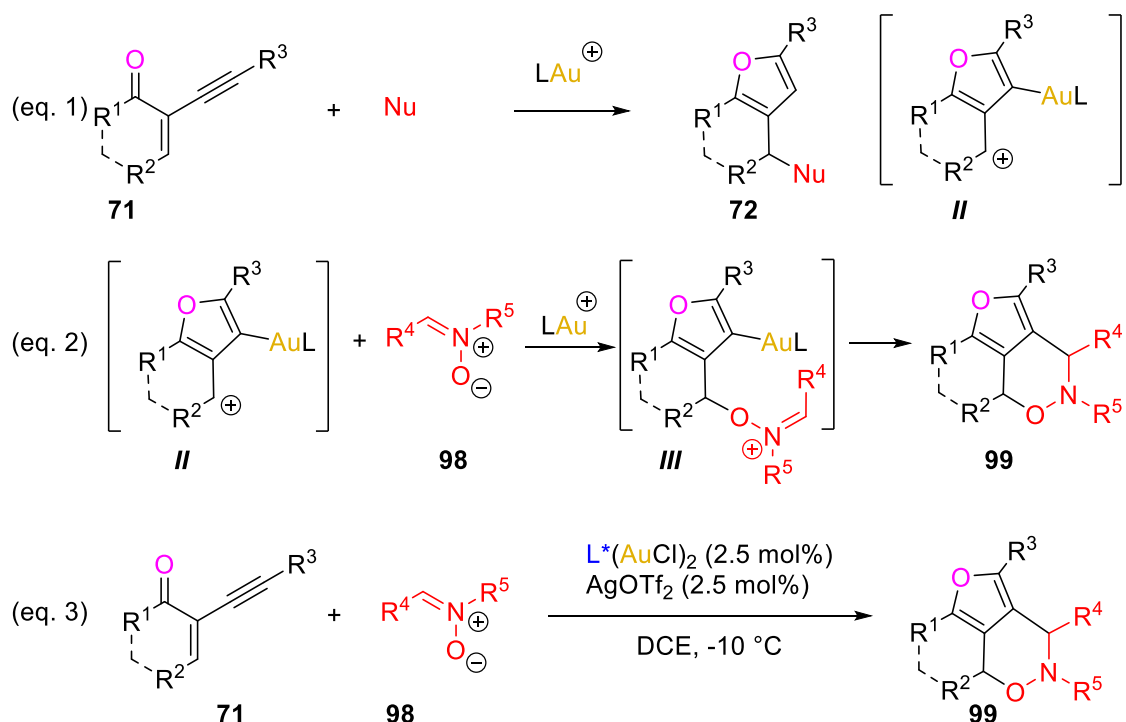
^a Reaction condition: **96** (0.11 mmol), **74** (0.1 mmol), solvent (0.5 mL); ^b Isolated yield; ^c Determined by chiral HPLC; ^d Conversions determined by ¹H NMR; ^e dpp = diphenylphosphoric acid.

At this point, we did not optimize this reaction further, although other conditions such as silver free conditions might have been tested.

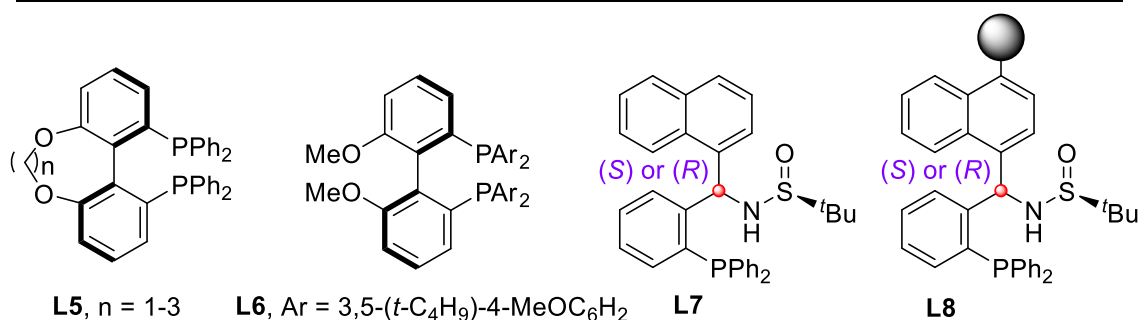
3. The TCDC strategy in the cyclization/formal cycloaddition reactions involving nitrones

As described above, our gold catalysts can efficiently promote the cycloisomerization of 2-alkynyl enones leading to the key intermediate **II**, which is further trapped by a nucleophile to provide the corresponding bicyclic furans (Scheme 68, eq. 1). In recent years, the Zhang's group has shown that these cationic intermediates can also be trapped by nitrones acting as nucleophiles. Addition of a nitron **98** leads to the iminium intermediates **III** that undergoes then the intramolecular cleavage of the vinyl-gold(I) bond to release the cyclic product **99**. The final product results from a formal [3+3] cycloaddition reaction (eq. 2).^{66a}

Zhang also successfully realized the asymmetric variant of these cyclization/cycloaddition reactions and obtained a series of enantioenriched fused bicyclic derivatives (eq. 3). These reactions proceeded well with the TUNEPHOS and BIPHEP ligands **L5** and **L6**.^{26b, 83a} In 2014, the same author developed a new series of chiral sulfonamide functionalized monophosphines, the MingPhos ligands **L7**, and applied them in the same reaction.^{26a} Finally, the MingPhos ligands were successfully immobilized on a polystyrene resin, which led to heterogeneous chiral catalysts that proved as efficient as homogeneous catalysts in this reaction and could be recycled up to eight times.¹⁰²

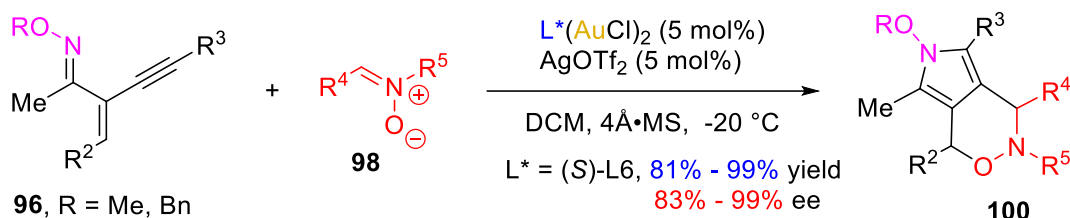


Zhang, 2010 L* = (R)-L5, 74% - 99% yield, 28% - 98% ee
 L* = (R)-L6, 51% - 99% yield, 4% - 98% ee
 Zhang, 2014 L* = (R)-L7, 85% - 99% yield, 92% - 98% ee
 L* = (S)-L7, 85% - 99% yield, 93% - 99% ee
 Zhang, 2015 L* = (R)-L8, 74% - 88% yield, 90% - 96% ee
 L* = (S)-L8, 81% - 87% yield, 94% - 99% ee



Scheme 68. Gold Promoted Cyclizations/Nitronium Additions According to Zhang and Co-Workers

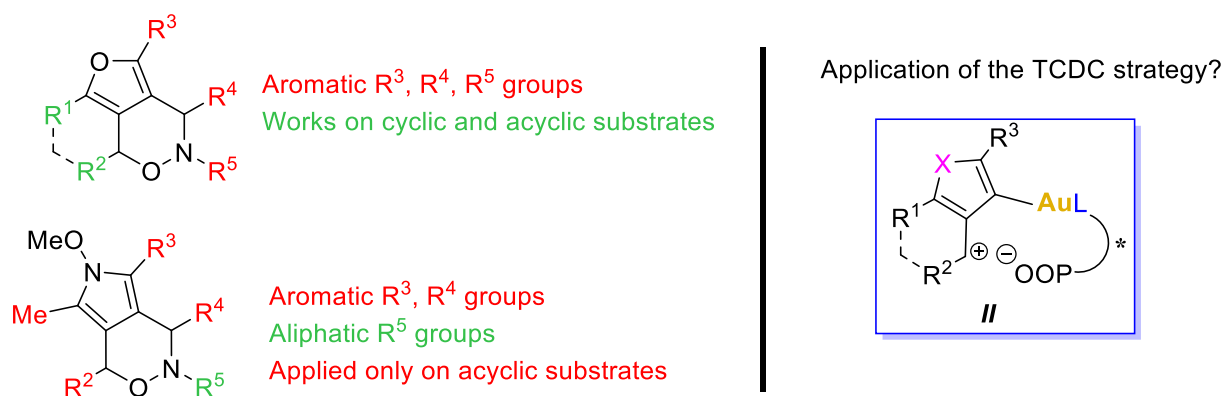
In 2018, Zhang implemented this reaction to the oxime equivalents of 2-alkynyl enones,¹⁰³ which led to enantioenriched pyrrolo[3,4-*d*][1,2]oxazines (Scheme 69). The best chiral ligand for this reaction proved to be the MeO-DTBM-BIPHEP **L6**, that yielded the targeted compounds in very high ees.



Scheme 69. Enantioselective Cyclization/Addition Reactions between Enone Oximes and Nitrones

It is clear from the literature that this reaction sequence from ketones or oximes is already well-established under enantioselective conditions. A close look however highlights a number of limitations, such as: 1) These reactions have been performed almost exclusively on nitrones derived from aromatic aldehydes ($\text{R}^4 = \text{Ar}$). 2) Similarly, they have been investigated only on nitrones derived from PhNHOH ($\text{R}^5 = \text{Ph}$). 3) Reactions performed from substrates with an aliphatic R^3 substituent lead to low ees. 4) The reaction tolerates oximes with aliphatic R^5 groups, but it has not been demonstrated on cyclic starting materials (Scheme 70).

In this context, we wondered what would be the input of the TDCD strategy in this class of reactions. Intermediates **II** formed by the reaction of the starting 2-alkynyl enones **71** (and their oxime analogs **96**) may offer new opportunities to potentially extend the scope to nitrones derived from aliphatic aldehydes and/or aliphatic *N*-hydroxylamines.



Scheme 70. Scope and Limitations of the Established Methods in the Gold Promoted Cyclizations/Nitrone Additions

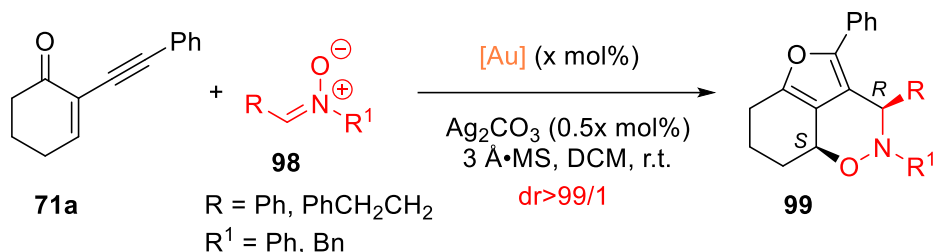
3.1. Optimization of the reaction of 2-alkynylenones with nitrones

To verify our hypothesis, we chose ketone **71a** and diphenylnitrone **98a** as starting materials (Table 13). After checking that silver carbonate alone has no catalytic activity (entry 1), we used **1a** as catalyst (5 mol%) and obtained the corresponding product **99aa** smoothly with good 69% yield, as a single diastereomer and in 67% enantiomeric excess (entry 2). The presence of molecular sieves decreased the yields and the enantioselectivities (entry 3 vs entry 2 and entry 5 vs entry 4). However, with a ratio nitrone/ketone of 2/1, a good 82% yield and 80% ee was obtained (entry 4).

We then replaced the aryl-substituted nitrone **98a** with nitrone **98b** derived from an aliphatic *N*-hydroxylamine. To our surprise, an excellent 97% enantioselectivity was obtained either in the presence or absence of molecular sieves (entries 6-7). Further variations of the ratio between the nitrone and the ketone

and optimization of the catalyst loading showed that 0.2 mol% catalyst is sufficient for this reaction to proceed in high yield (74%) and enantioselectivity (98% ee) (entry 10). Interestingly, under the same conditions, catalyst **1e** gives the same enantioselectivity and higher yield than **1a**, indicating a higher catalytic activity (entry 11). The comparison of NMR data of compounds **99** obtained from nitrones **98a** and **98b** with Zhang's data^{26a, 83a} established a *syn* stereochemistry and a (3*R*, 8*aS*) absolute configuration.

Table 13. Optimization of the Catalytic System using Nitrones^a



entry	98	[Au] (mol%)	98/71a ratio	3 Å-MS	yield (%) ^b	ee (%) ^c
1 ^d	98	-	1.1/1	-	0	-
2	 98a	1a (5)	1.1/1	-	69	67
3		1a (5)	1.1/1	+	59	54
4		1a (5)	2/1	-	84	80
5		1a (5)	2/1	+	69	55
6		1a (5)	1.1/1	+	47	97
7	 98b	1a (5)	1.1/1	-	65	97
8		1a (5)	1/1.5	-	88	98
9		1a (1)	1/1.5	-	80	98
10		1a (0.2)	1/1.5	-	74	98
11		1e (0.2)	1/1.5	-	89	98
12		1a (5)	1.1/1	+	81	93
13	 98c	1a (5)	1/1.5	-	88	95
15		1a (1)	1/1.5	+	91	93
16		1a (1)	1/1.5	-	79	98
17		1e (1)	1/1.5	+	87	99
18		1a (0.2)	1/1.5	+	0	-
19		1e (0.2)	1/1.5	+	16	91

^a Reaction conditions: DCM (1 mL), under N₂, r.t. ^b Isolated yields. ^c Determined by chiral HPLC; ^d Ag₂CO₃ (2.5 mol%).

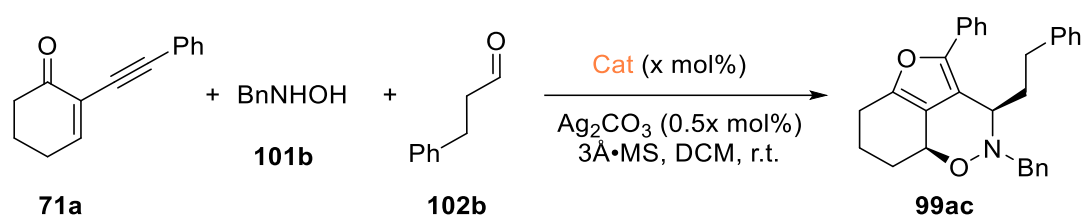
We then explored the reaction of a nitronium substituted with two alkyl groups (**98c**) and obtained the corresponding product **99ac** in 93% ee and 81% yield, at a 5% catalyst loading (entry 12). Further optimization indicated that: 1) the catalyst loading can be decreased to 1 mol% (entries 15-19); 2) **1e** leads to better results than **1a** (entries 15-17) and 3) there is again a detrimental effect of the molecular sieves on the reaction if **1a** is used, while **1e** tolerates well the presence of molecular sieves (entries 16-17). Considering the importance to operate in the absence of water, this is an interesting observation.

These preliminary results reveal highly promising perspectives in terms of scope and enantioselectivities. Again, it is striking to be able to run enantioselective gold catalysis with such low catalyst loadings. It is also worth mentioning that all the products were obtained with total diastereoselectivity, as single diastereoisomers.

Since the formation of a nitron from an aldehyde and a hydroxylamine takes place easily in DCM, we hypothesized that one pot formation of the nitron might be conceivable and would result in a considerably simplified procedure.

We first considered a one-pot, sequential procedure. The reaction was carried out by stirring first the *N*-benzylhydroxylamine **101b**, 3-phenylpropanal **102b** and 3 Å·MS in DCM at room temperature for 3 h. Ketone **71a**, catalyst **1a** and silver carbonate were then added and further stirring at room temperature for 16 h provided the product **99ac** in 72% yield and 96% ee (Table 14, entry 1). In the absence of 3 Å·MS, the enantiomeric excess was the same but the yield decreased to 65%, due to the competitive addition of water (1 equiv generated from the reaction of the aldehyde and the hydroxylamine) to the cycloisomerized cationic intermediate (entry 2). These good results encouraged us to further investigate one-pot reactions and very good results (95% yield and 98% ee) were obtained (entry 3). Catalyst **1e** (0.3 mol% catalyst loading) showed again a higher reactivity and enantioselectivity than **1a** in this reaction, leading to the product **99ac** in 96% yield and 99% ee (entries 4-5).

Table 14. Optimization of the One-Pot Catalytic Reaction



entry	Cat (mol%)	protocol	yield (%) ^a	ee (%) ^b
1	1a (1)	sequential ^c	72	96
2	1a (1)	sequential ^{c,d}	65	96
3	1a (1)	<i>in situ</i> ^e	95	98
4	1a (0.3)	<i>in situ</i> ^{e,f}	31	89
5	1e (0.3)	<i>in situ</i> ^e	96	99

^a Isolated yields. ^b Determined by chiral HPLC. ^c The aldehyde **102b** (1 equiv.) and hydroxylamine **101b** (1 equiv.) were stirred for three hours in DCM in the presence of 3 Å MS before addition of the ketone **71a** (1.5 equiv.), **1a** (1 mol%) and Ag₂CO₃ (0.5 mol%) and further stirred for 16 h. ^d in the absence of 3 Å MS. ^e Aldehyde **102b** (1 equiv.), hydroxylamine **101b** (1 equiv.) ketone **71a** (1.5 equiv.), **1a** (1 mol%) and Ag₂CO₃ (0.5 mol%) were stirred in DCM in the presence of 3 Å MS for 24 h. ^f 89 h.

With this optimization study, we have established a **highly efficient enantioselective Au(I)-catalyzed multicomponent reaction**. In general, multicomponent reactions are considered good atom- and step-economy processes for green synthetic chemistry and have attracted lot of attention.¹⁰⁴ Until now, scientists have developed many classical multicomponent name reactions, such as Biginelli, Debus-Radziszewski, Gewald, Hantzsch, Kabachnik-Fields, Passerini or Ugi reactions. However, as far as Au(I)-catalysis is concerned,

very little is known in the field of multicomponent reactions. The single well established case of multicomponent Au(I)-catalysed reaction is the coupling of aldehydes, amines and alkynes, known as the A³ coupling.¹⁰⁵ However, there are seemingly no reports on enantioselective Au(I)-catalyzed multicomponent reactions, despite sporadic attempts.¹⁰⁶ Considering the promising preliminary results above, we felt that this method might be highly relevant and we committed ourselves to investigate its scope more extensively.

3.2. Scope of the reaction

We have investigated the scope and limitations of the reaction between enones and nitrones by considering various aldehydes and hydroxylamines as nitrone precursors, as well as variously substituted enones.

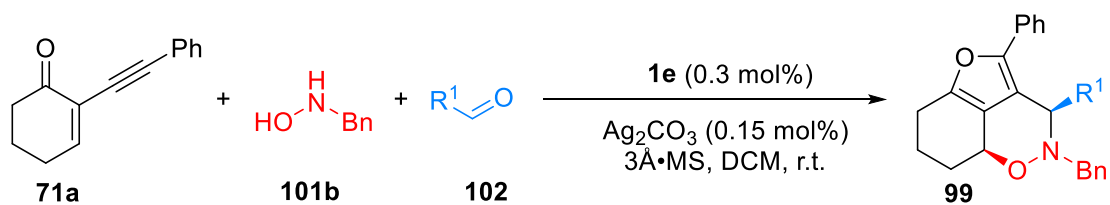
3.2.1. Aliphatic aldehydes

Considering that aliphatic aldehydes have not been used as nitrone precursors in the numerous studies reported by Junliang Zhang,¹⁰⁷ we first focused on this class of aldehydes using ketone **71a** as the reaction partner. We applied the above-mentioned optimized conditions, i.e. the one-pot procedure in the presence of **1e** (0.3 mol%), silver carbonate, molecular sieves in DCM at room temperature (Scheme 71). In addition to 3-phenylpropanal, isovaleraldehyde led the corresponding product **99ad** in 81% yield and 98% ee. The cyclopropanecarbaldehyde also released the corresponding product **99ae** in 81% yield and 94% ee.

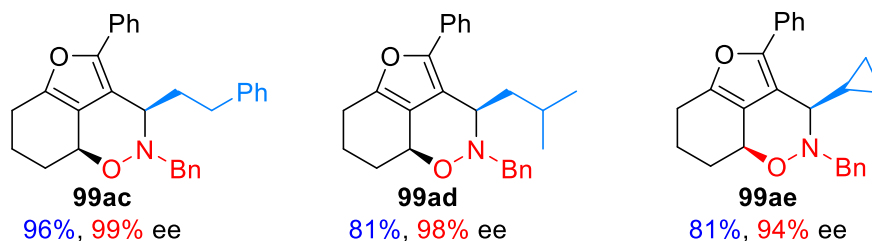
We next introduced heteroatoms in the aliphatic chain of the aldehyde in order to reach more functionalized products. Benzyloxyacetaldehyde **102e** furnished **99af** in 85% yield and 99% ee. To our surprise though, *N*-(Fmoc)-aminopropionaldehyde **102g** delivered the corresponding product **99ah** smoothly but without any enantioselectivity.

Unsaturated aldehydes such as pent-4-enal **102h** delivered the cycloaddition product **99ai** in 61% yield and 97% ee. This reaction shows an interesting chemoselectivity considering that the π -Lewis acidic Au(I) complex might cause activation of the olefin and hamper the reaction outcome. Other unsaturated aldehydes such as pent-4-ynal **102j** and hexa-4,5-dienal **102i** however didn't deliver satisfactory results under the optimized condition. The coordination of the Au(I) complex to the unsaturated system is likely to decrease here the catalyst activity.

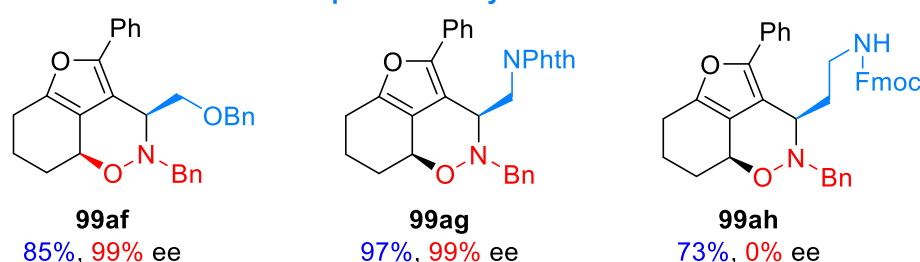
Some simple aliphatic aldehydes also failed to participate in the reaction, such as propionaldehyde **102k**, isobutyraldehyde **102l**, cyclohexanecarbaldehyde **102m** and cyclopentanecarbaldehyde **102n**. The steric hindrance of the latter may be responsible for this lack of reactivity.



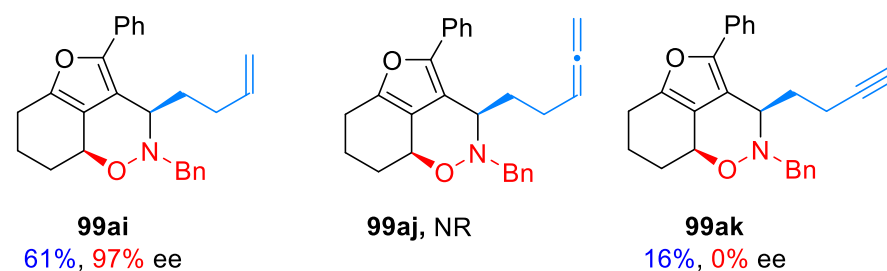
- Non-functionalized aliphatic aldehydes



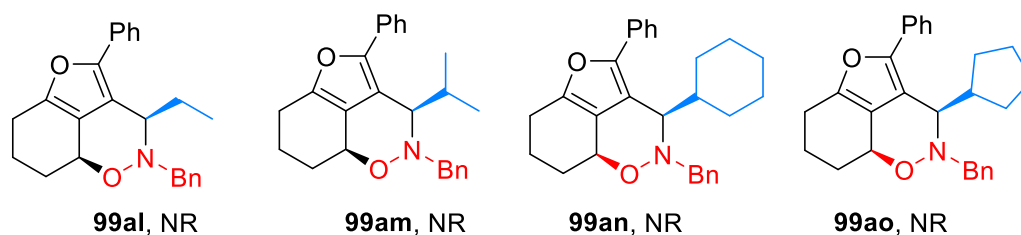
- Heteroatom-functionalized aliphatic aldehydes



- Unsaturated aliphatic aldehydes



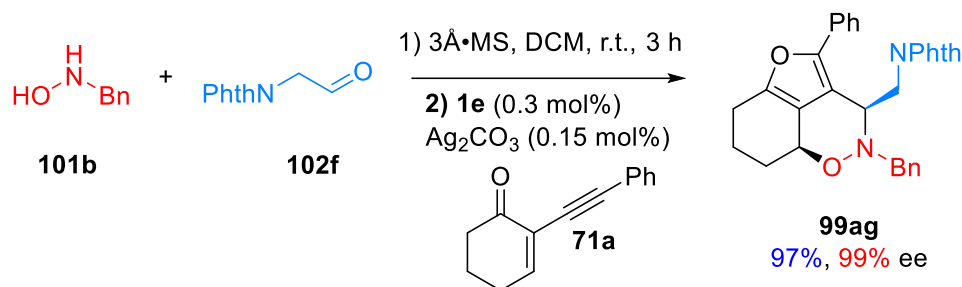
- Unsuccessful aliphatic aldehydes



Scheme 71. Scope of the Enantioselective Multicomponent Reaction using Aliphatic Aldehydes

Annoyed by the lack of enantioselectivity observed with *N*-(Fmoc)-aminopropionaldehyde **102g** (see compound **99ah**) we hypothesized that the NH function might be responsible for a detrimental *H*-bonding. Therefore, we focused on the *N*-phthalimido-protected acetaldehyde **102f** (Scheme 71), which however did not lead to a high conversion in the one-pot conditions. We then considered a one-pot procedure in the sequential manner. The nitron was hence formed *in situ* from the aldehyde **102f** and *N*-benzyloxyamine **101b**, before addition of the ketone **71a**, silver carbonate and **1e**. With these conditions,

the product **99ag** was obtained in 97% yield and 99% ee. This excellent result also suggests that the reaction conditions can be crucial for the success of these multicomponent reactions.

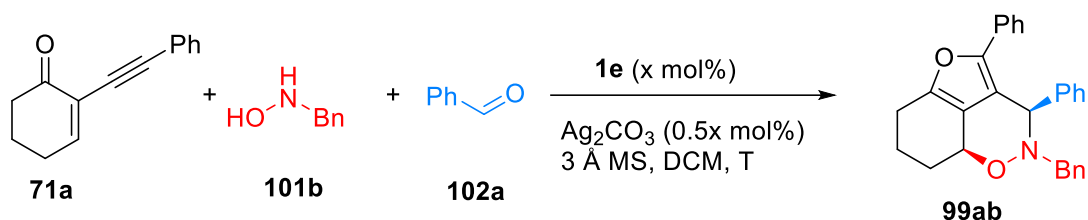


Scheme 72. Scope of the Enantioselective Multicomponent Reaction using Aliphatic Aldehydes

3.2.2. Aromatic aldehydes

We then turned to expand the scope of the reaction to aromatic aldehydes using ketone **71a** and *N*-benzylhydroxylamine **101b**, and first used benzaldehyde **102a** (Table 15, entry 1). Only the corresponding nitron **98b** (generated from benzaldehyde and benzylhydroxylamine), ketone **71a** and trace of product **99ab** were found in the reaction mixture. This indicates that the nitron derived from aromatic aldehydes are less nucleophilic than their aliphatic analogs. The catalyst loading was then increased to 0.5 mol% and the corresponding product **99ab** was delivered in 50% with excellent 99% enantioselectivity (entry 2). By heating the reaction to 40 °C under a 0.5 mol% catalyst loading, the corresponding product **99ab** was obtained in 83% yield and 98% ee (entry 3).

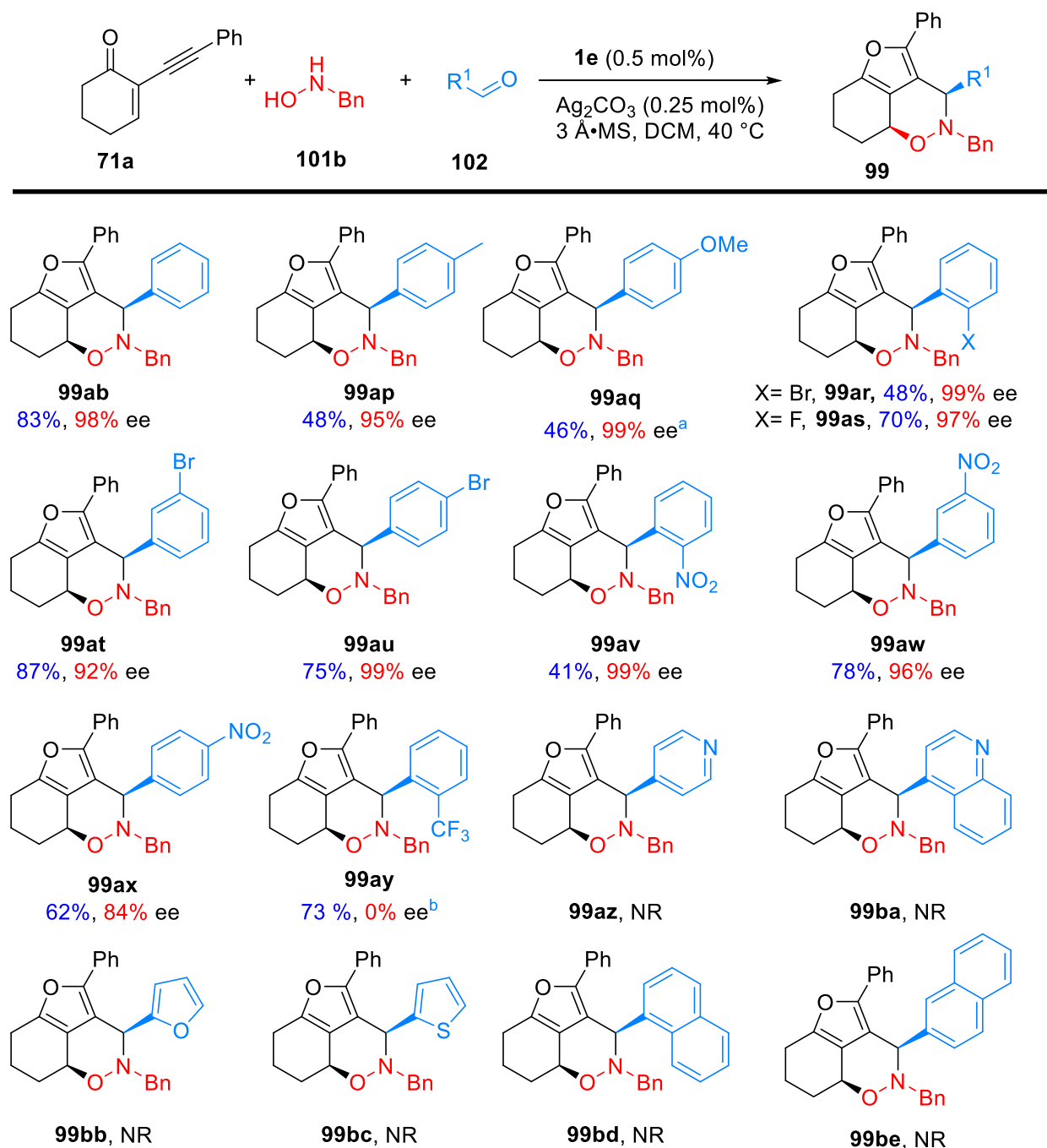
Table 15. Optimization of Aromatic Aldehyde in Cycloisomerization/Nucleophilic Addition Reaction



entry	1e (mol%)	Ag_2CO_3 (mol%)	T (°C)	yield (%) ^b	ee (%) ^c
1	0.3	0.15	r.t.	trace	-
2	0.5	0.25	r.t.	50	99
3	0.5	0.25	40	83	98

^a Reaction conditions: Solvent (1 mL), under N_2 , 48 h. ^b Isolated yields. ^c Determined by chiral HPLC.

Various aromatic aldehydes were then applied in this reaction (Scheme 73). Substituent effects on the aryl were investigated, with both electron-donating and electron withdrawing substituents, introduced at the *ortho*, *meta* and *para* positions. Excellent results were globally obtained, most of the products being obtained with ees higher than 90%. Major features of the reaction are:



^a pregeneration of nitrone; ^b 0.3 mol% catalyst

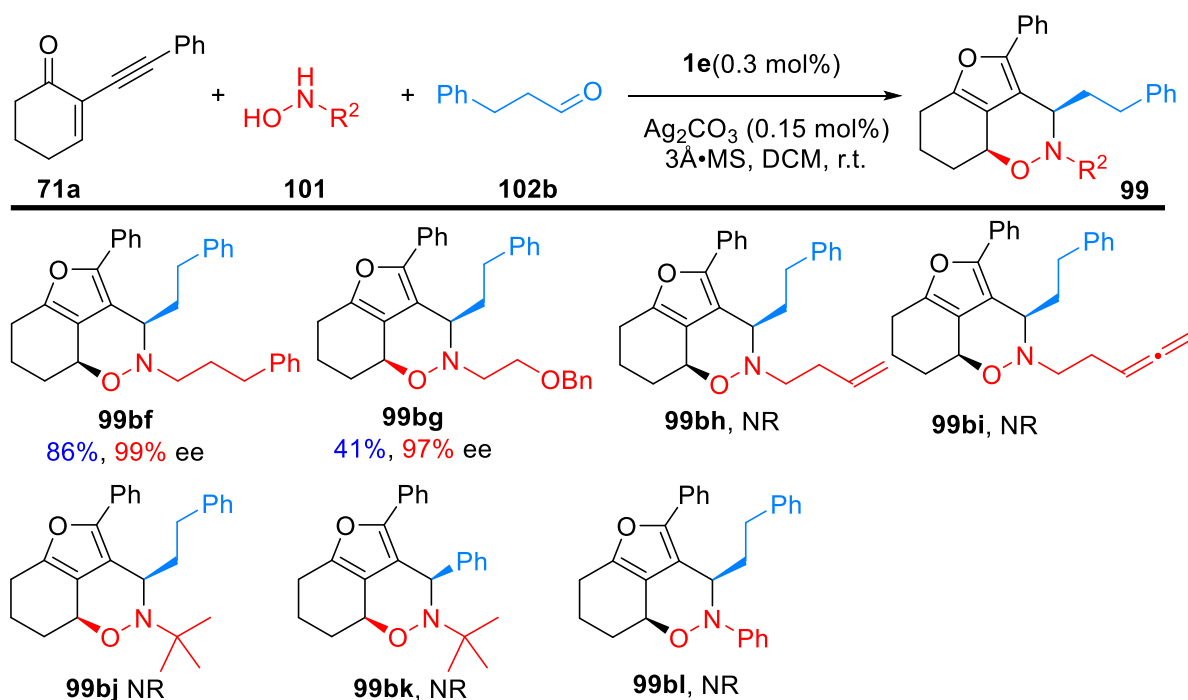
Scheme 73. Scope of the Enantioselective Multicomponent Reaction using (*het*)-Aromatic Aldehydes

- The reaction tolerates EDG and EWG, the only notable exception being the use of 2-trifluoromethyl benzaldehyde that, unexpectedly led to 0% ee.
- The use of highly electron-rich aldehydes such as *p*-methoxybenzaldehyde imposes a one-pot, sequential protocol, with the formation of the nitrone prior to the addition of the catalyst and ketone, to ensure satisfactory results (**99aq**, 46% yield, 99% ee).
- The investigation of heterocyclic aromatic aldehydes did not meet any success. It is conceivable that nitrogen-based aryl groups coordinate the cationic gold catalyst because of their Lewis basicity. However, furyl or thienyl groups did not participate in the reaction for unclear reasons.
- 1- and 2-naphthaldehydes also did not react under these conditions.

The reaction is consequently endowed with a number of limitations. Further investigations using sequential protocols will figure out whether these limitations can be overcome. Despite these limitations, the method appeared powerful for a large number of classical aromatic aldehydes and led to excellent results with a low catalyst loading.

3.2.3. Nature of the hydroxylamine

We next investigated different hydroxylamines under the optimized conditions, with a focus on aliphatic hydroxylamines, which have never been used in this reaction (Scheme 74). Both *N*-(3-phenylpropyl)hydroxylamine **101c** and the *N*-(2-(benzyloxy)ethyl)hydroxylamine **101d** afforded excellent enantiomeric excesses in the reactions (**99bf**, 99% ee and **99bg**, 97% ee). The unsaturated hydroxylamines **101e** and **101f** however failed to deliver the corresponding products, supposedly for the same reasons than that with unsaturated aliphatic aldehydes. Similarly, the bulky *t*-BuNHOH **101g** did not react under these conditions, whether it is from dihydrocinnamaldehyde or benzaldehyde. It should be noted that the reaction from the isolated corresponding nitron did not proceed either. Finally, phenylhydroxylamine **101a** (which is used in most reported studies) failed to provide the corresponding cycloisomerization/nucleophilic addition products under the multicomponent conditions.



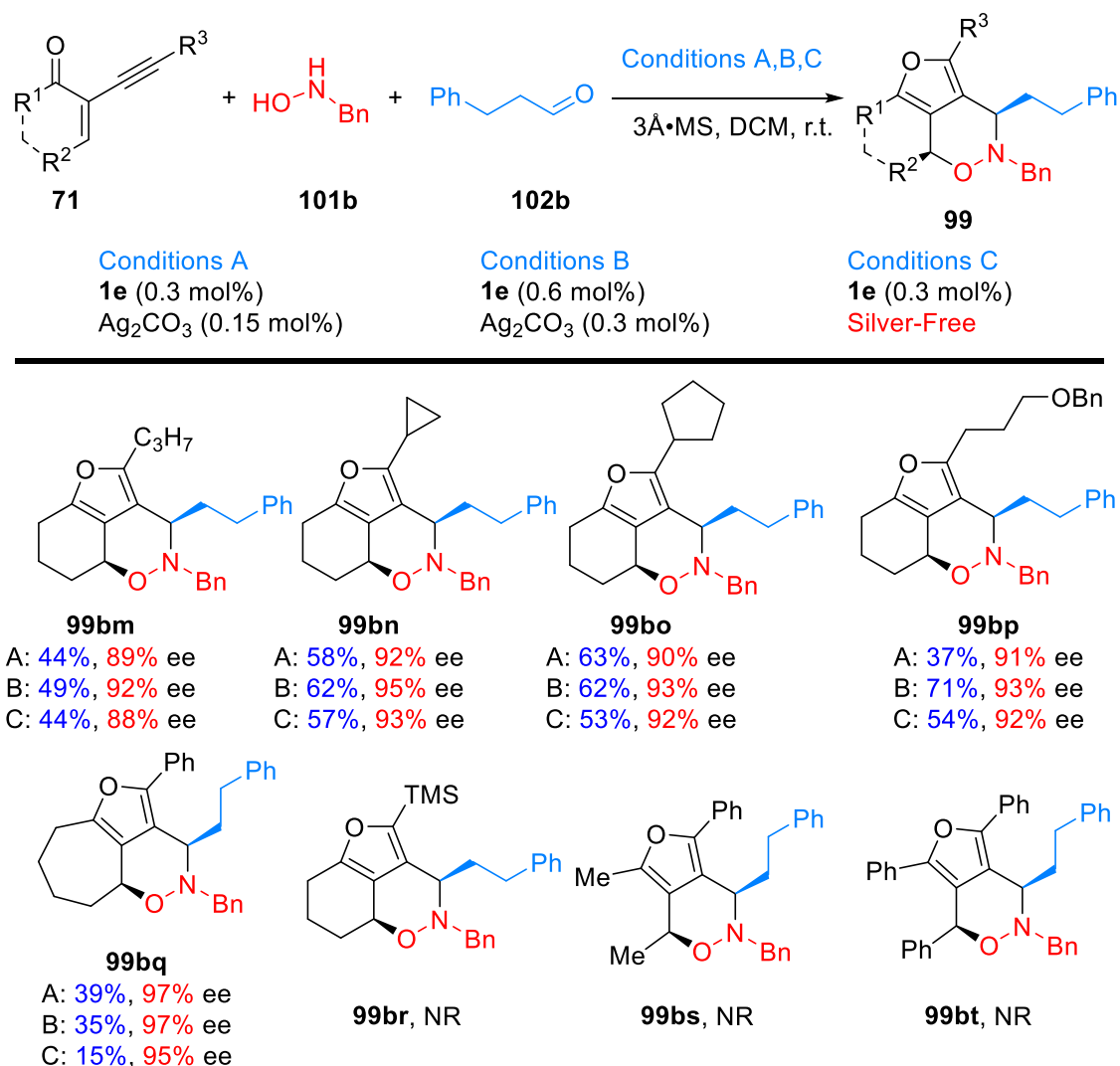
Scheme 74. Scope of the Enantioselective Multicomponent Reaction using Diverse Hydroxylamines

3.2.4. Variation of the ketone

Finally, we varied the ketone partner in the multicomponent reaction under different conditions (Scheme 75). Conditions A are classical conditions established for most of our previous substrates. The catalyst loading was also doubled to 0.6 mol% in conditions B. More importantly, we screened here silver-

free conditions (Conditions C). Ketones **71h-71k** substituted with alkynes bearing an aliphatic R³ substituent were first screened. The reaction tolerated linear *n*-C₃H₇- **71h**, cyclopropyl- **71i**, cyclopentyl- **71j**, or (benzyloxy)propyl- **71k** ketones, that all led to the corresponding products with moderate to good yields and excellent enantiomeric excesses using the three conditions. This confirmed at this stage that silver-free conditions lead to the target compounds in a similar range of yields and enantioselectivities and hence are applicable to multicomponent reactions too.

We next have further modified the size of the ketone ring. The seven-membered ring ketone **71g** delivered the corresponding product **99bq** in moderate yields with the three conditions but very high enantioselectivities (95-97% ee). The ketone **71l**, substituted with a TMS group, did not afford any product.

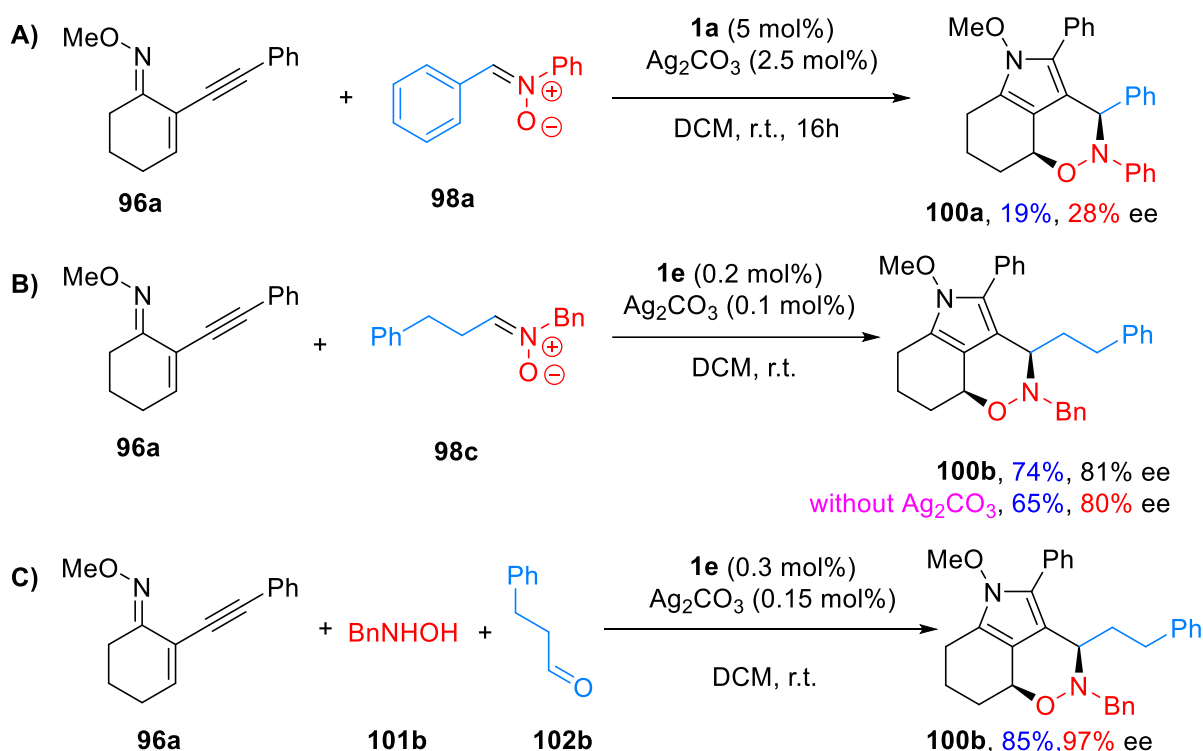


Scheme 75. Scope of the Enantioselective Multicomponent Reaction using Different Yne-Ketones

We finally screened acyclic ketones **71m** and **71n**, that have been classically used in the chemistry developed from 2-alkynyl enones.¹⁰⁷ However, using our series of catalysts, we did not obtain any products from these acyclic ketones. This probably highlights one of the most important limitation of our method.

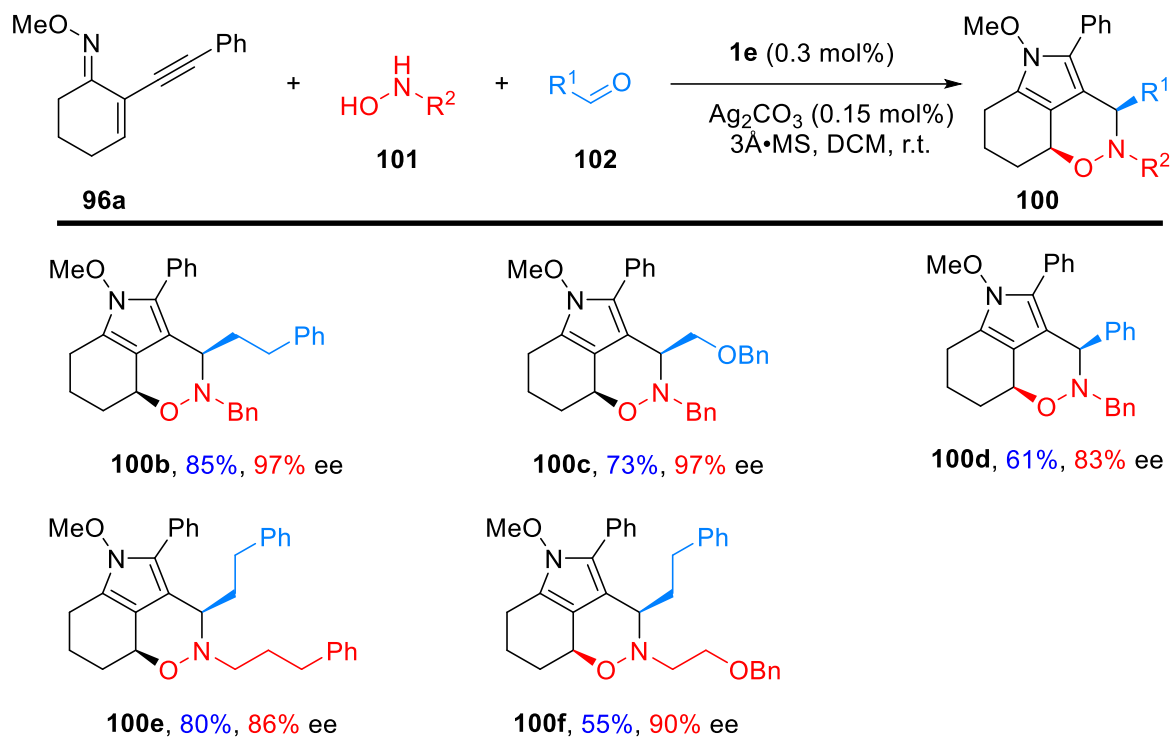
3.3. Application to a reaction variant: Reaction of oxime and nitron

We then turned to investigate the extension of the method to the reactions of oximes **96** and nitrones **98**, initially reported by Zhang in enantioselective Au(I) catalysis^{103, 108} (Scheme 76). The reaction was first attempted from oxime **96a** and nitron **98a** in the presence of 5 mol% of **1a**. These conditions resulted in the formation of **100a** in poor yield (19%) and ee (28%) (Scheme 76A). With the experience gathered on the multicomponent reaction using ketones, we then replaced the nitron **98a** with the nitron **98c** and used catalyst **1e** and then obtained better results, with the isolation of **100b** in 74% yield and 81% ee (Scheme 76B). Further investigation showed that silver-free conditions lead to comparable result (65% yield and 80% ee). Finally, we established that the reaction performed all *in situ* lead to 82% yield and 81% ee. This provides again the opportunity to work in an enantioselective multicomponent manner.



Scheme 76. The TCDC Strategy in the Cycization/Cycloaddition of 2-Alkynyl Oximes with Nitrones

With the collaboration of Nazarii Sabat, post-doctoral researcher in the group, we screened a range of aldehydes and hydroxylamines under the multicomponent conditions (Scheme 77). Benzylhydroxylamine was used in combination with dihydrocinnamaldehyde, benzyloxyacetaldehyde and benzaldehyde using 0.3 mol% of **1e**. The three corresponding products were obtained in high yields and enantioselectivities. Finally, both *N*-(3-phenylpropyl)hydroxylamine **101c** and the *N*-(2-(benzyloxy)ethyl)hydroxylamine **101d** were engaged in the reaction using dihydrocinnamaldehyde, which afforded compound **100e** (in 80% yield and 86% ee) and **100f** (in 55% yield and 90% ee).



Scheme 77

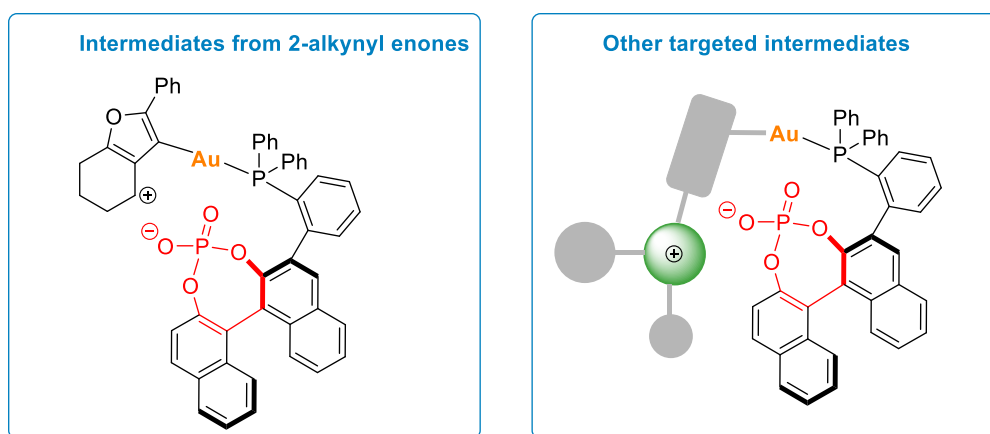
4. Conclusion

In conclusion, these different studies provide clear evidence that tethering of a phosphine and a phosphoric acid function (TCDC strategy), represents a promising new approach in enantioselective Au(I) catalysis. By combining the chiral counterion strategy and the remote cooperative group strategy, this design has enabled unprecedented enantioselectivity levels to be attained in a number of synthetically useful reactions, with catalyst loadings that contrast that classically used in cationic Au(I) catalysis. While in gold catalysis the ACDC strategy was hitherto limited to intramolecular processes in a focused reaction class (cyclization of heteroatoms to allenes), the counterion tethering approach allowed us to successfully develop several intermolecular reactions, some being in a multicomponent enantioselective manner, which is unprecedented.

Tethering of the phosphate counterion also produced a rare example of phosphine gold chloride complex that does not require activation by silver salts, presumably by assistance of *H*-bonding from the phosphoric acid function (see Scheme 57). In the context of the literature, this is also a highly significant advance to the field.

Chapter 3: Application of the TCDC strategy in reactions involving other scaffolds

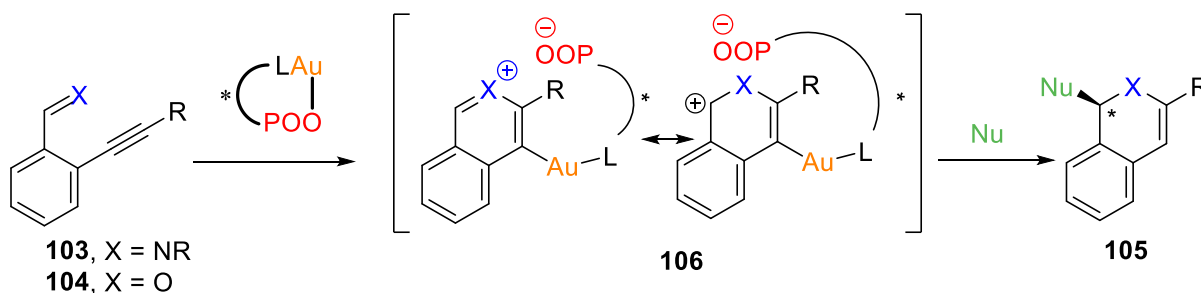
In the Chapter 2 of this manuscript, we have demonstrated the use of the newly designed CPA_{Phos}AuCl as catalysts in reactions involving 2-alkynyl enones. These catalysts have outperformed classical Au(I) complexes, in terms of scope, catalyst loadings or chemoselectivity. These reactions were perfectly well suited for the TCDC strategy, with the stabilization of the carbocation resulting from the cycloisomerization step by the phosphate (Scheme 78). However, we anticipated that this new class of catalysts might be applicable in other reactions, via other cationic intermediates. The following studies summarize briefly our efforts in that direction.



Scheme 78

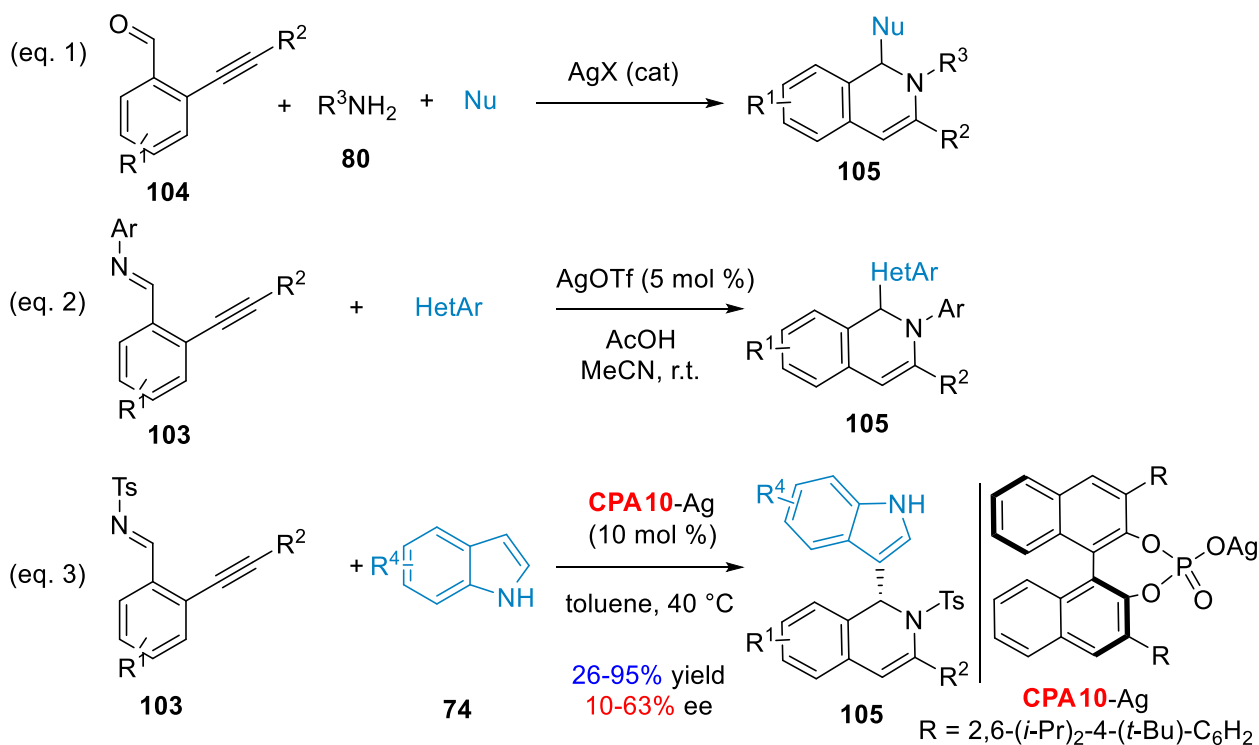
1. Cyclizations of imines combined with nucleophilic trapping

In our first attempts to extend the TCDC concept in other reactions using our chiral Au(I) complexes, we hypothesized that *O*-alkynyl arylaldehydes or arylimines **103/104** could be suitable substrates, via a coordination with the Au(I) catalyst and cyclization to intermediates **106** (Scheme 79), potentially stabilized by the chiral phosphate counterion. A nucleophile could then add to these intermediates to deliver 1,2-dihydroisoquinoline or isochromene derivatives with enantioselectivity. We first have targeted preferentially 1,2-dihydroisoquinolines.



1.1. Bibliographic precedents

This 6-*endo*-dig cyclization to 1,2-dihydroisoquinolines has numerous precedents, pioneered by Wu using silver catalysis. Numerous nucleophiles such as unsaturated ketones, phosphonates, imidazoles, ketones or indoles could be used successfully (Scheme 80, eq. 1).¹⁰⁹ Interestingly, most of these studies proceeded via a multicomponent approach, with the *in situ* imine formation, and could be extended to metal free conditions.¹¹⁰

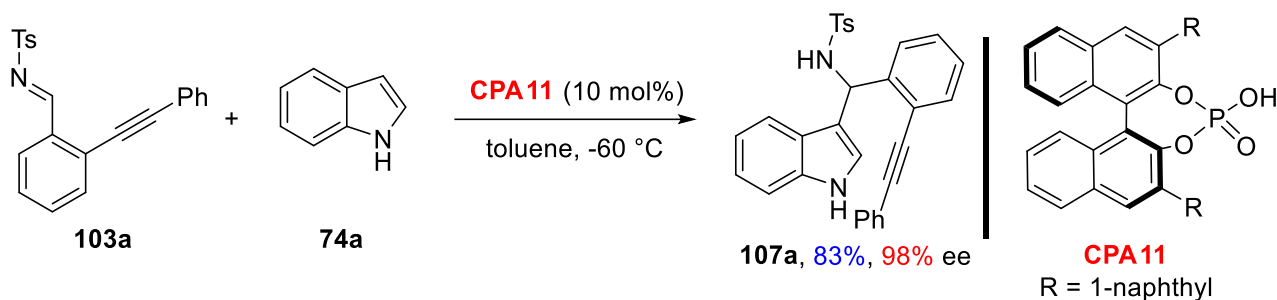
Scheme 80. Silver-Catalyzed Cyclization of *Ortho*-Alkynylaryldimines

With a long-lasting interest in related cyclization from aldehyde derivatives or other precursors,¹¹¹ Brachet and Belmont recently investigated the cyclization of *ortho*-alkynylaryldimine derivatives using Ag catalysts, with the concomitant addition of heterocyclic nucleophiles (Scheme 80, eq. 2).¹¹² The starting imines are here substituted with aryl groups, leading to the target products in essentially good yields using AgOTf as the catalyst, with the presence of acetic acid.

In 2012, You and his co-workers used electron-poor *N*-Ts imines **103** under enantioselective silver catalysis, using chiral silver phosphates **CPA10-Ag** as catalysts and indoles **74** as nucleophiles (Scheme 80, eq. 3).¹¹³ This strategy however lacked efficiency in terms of enantioselectivities, with ees ranging from 10% to 59% (with the exception of 7-fluoroindole leading to 89% ee) and proceeded with chiral phosphate with extended bulky groups.

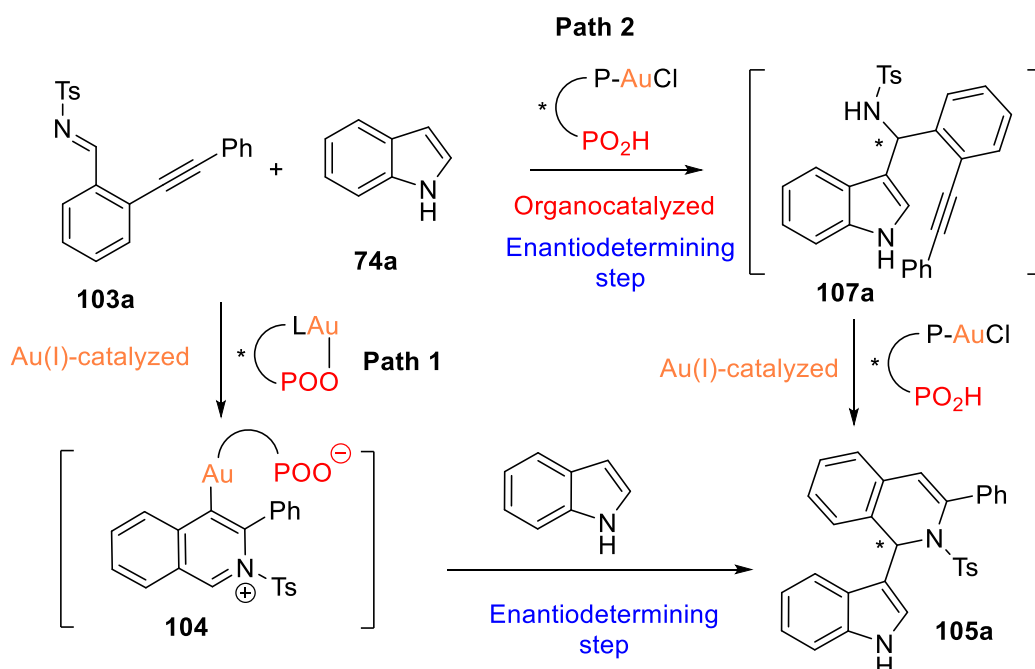
In this context, we tried to apply our catalysts in this reaction, expecting a significant increase in the enantioselectivity of the process.

1.2. Results and discussion



Scheme 81. Organocatalyzed Friedel-Crafts Addition of Indole to Imine 103a by You

In 2007, the You group¹¹⁴ found that chiral phosphoric acids **CPA11** can catalyze the Friedel-Crafts additions of indoles to imines and deliver the corresponding product **107a** in good 83% yield and 98% ee (Scheme 81).

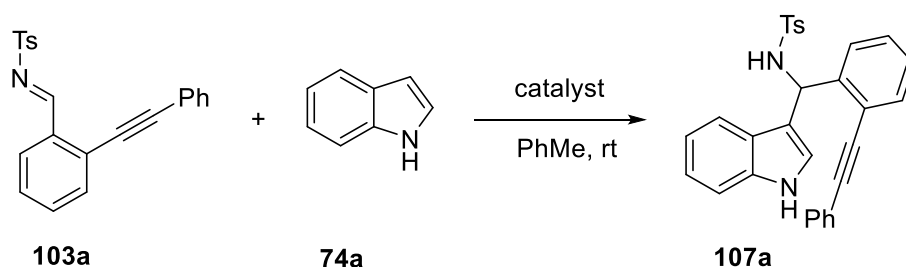


Scheme 82. Competing Organocatalyzed and Au(I)-Catalyzed Pathways

Due to the presence of the phosphoric acid function, our catalysts may act as potential organocatalysts in a competitive Friedel-Crafts reaction. Therefore, if our catalysts are not activated correctly by the silver-salt, the formation of the target product could result from two competitive pathways: 1) the expected tandem cycloisomerization/nucleophilic addition reaction (Path 1) and/or 2) the organocatalytic Friedel-Crafts addition reaction followed by a Au(I)-catalyzed hydroamination (Path 2) (Scheme 82). Both pathways would certainly not proceed with the same level of enantioselectivity, each having very different enantiodetermining steps.

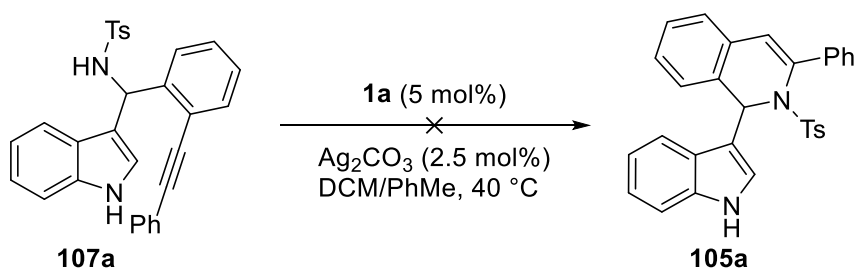
For this reason, we first investigated **1a** and **1e** as organocatalysts, in order to know the magnitude of enantioselectivity that the competing organocatalyzed pathway would provide. *N*-Ts imine **103a** and indole **74a** were chosen as representative starting materials and organocatalyzed conditions with **1a** and **1e** were applied in toluene at room temperature (Table 16, entries 1-2). Only product **107a** was found in these reactions, which proves that the bifunctional Au(I) complex acts as an organocatalyst in this process by virtue of its phosphoric acid function. Among the two catalysts, **1e** gave the best enantioselectivity (36% ee) in this reaction. With its 3,3'-disubstitution pattern on the BINOL platform, this is not surprising considering its resemblance with classical chiral phosphoric acids. These tests also showed that the further Au(I)-catalyzed hydroamination did not proceed, meaning that the precatalyst does not self-activate to an active Au(I) catalyst.

Table 16. Friedel-Crafts Addition of Indole to Imine 103a Catalyzed by 1a and 1e



entry	catalyst (mol%)	yield (%) ^b	ee (%) ^c
1	1a (5)	88	12
2	1e (5)	55	36

We next submitted the secondary amine **107a** to a Au(I)-catalyzed hydroamination using **1a** activated with silver carbonate. This reaction did not proceed and left the starting material unchanged (Scheme 83). This result established that even if **105a** is obtained in high enantioselectivity in subsequent assays, it will not originate from the competing Path 2, because: 1) the organocatalyzed step proceeds in low ee (Table 16) and 2) the TCDC strategy is not suitable for the cyclization of **107a** to **105a**, even in the presence of silver salt (Scheme 83).

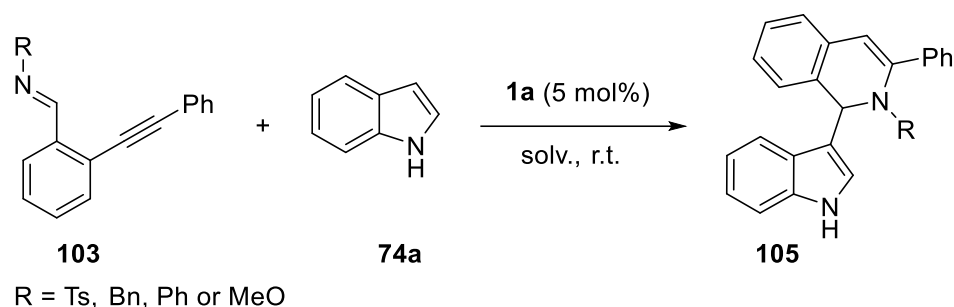


Scheme 83. Cyclization Attempt from 107a to 105a

Imines with tosyl-, benzyl-, phenyl- or methoxy- group (oxime) have next been used, in order to determine the influence of this group on the reaction (Table 17). Among all, only the tosyl- substituted imine **103a** delivered the corresponding 1,2-dihydroisoquinoline product **105a** in 57% yield and 60% ee (entry 1). The phenyl-sustituted imine **103c** delivered the corresponding 1,2-dihydroisoquinoline products **105c** in 41%

and 14% ee (entry 3). No 1,2-dihydroisoquinoline derivatives were found when benzyl- or methoxy-substituted imines were used. The tosyl group hence appeared the best for further investigations.

Table 17. Screening of the Protection Group^a

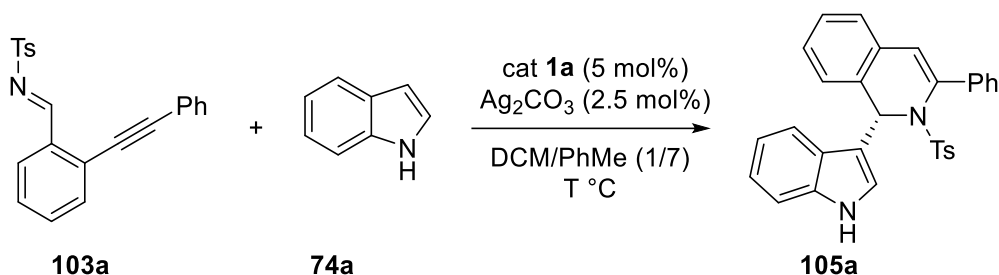


entry	R	solvent	yield (%) ^b	ee (%) ^c
1	Ts	PhMe	57	60
2	Bn	PhMe	NR	-
3	Ph	DCM/PhMe (1/3)	41	14
4	MeO	DCM	NR	-

^a Reaction conditions: **103** (0.05 mmol), **74a** (0.044 mmol), DCM (1 mL), under N₂, r.t. ^b Isolated yields. ^c Determined by chiral HPLC

We next optimized the reaction conditions, varying the temperature and the imine/indole ratio, using a mixture of PhMe and DCM as the solvent (Table 18). A blank test first showed that Ag₂CO₃ does not catalyze the reaction (Table 18, entry 1). In all subsequent assays, the catalyst, indole and Ag₂CO₃ were stirred at room temperature in DCM for 1 h, and then imine and PhMe were added to the mixture. When these conditions were applied at 40 °C, product **105a** was obtained in 38% yield and 85% ee (entry 2). We then attempted to improve the yield by increasing the reaction temperature or changing the ratio of indole and imine, but these assays were unsuccessful (entries 3-6). Comparison of the HPLC data and optical rotation with that reported by You¹¹³ established the absolute configuration for the major enantiomer.

Table 18. Optimization of Cycloisomerization/Nucleophilic Addition Reaction^a



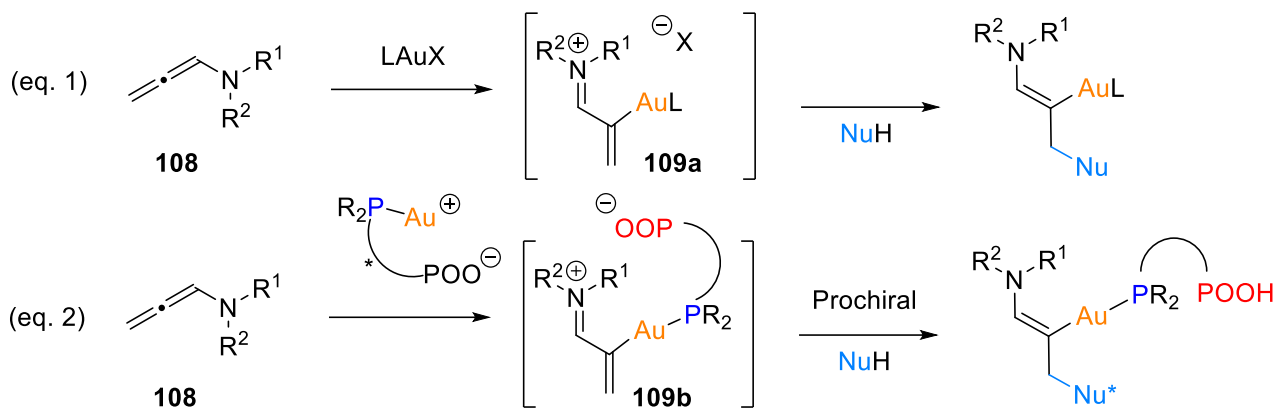
entry	T (°C)	imine/indole	yield (%) ^b	ee (%) ^c
1 ^d	40	1.1/1	NR	-
2	40	1.1/1	38	85
3	50	1.1/1	50	56
4	80	1.1/1	39	41
5 ^e	40	1.5/1	43	75
6 ^f	40	1/2.4	41	74

^a Reaction conditions: **103a** (0.055 mmol), **74a** (0.05 mmol), solvent (1 mL), under N_2 , r.t.; ^b NMR yields. ^c Determined by chiral HPLC; ^d In the absence of **1a**. ^e **103a** (0.075 mmol), **74a** (0.05 mmol), solvent (1 mL), under N_2 , r.t.; ^f **103a** (0.05 mmol), **74a** (0.12 mmol), solvent (1 mL), under N_2 , r.t.

The results obtained so far indicate that the cycloisomerization product **105a** result a purely Au(I)-catalyzed mechanistic pathway, because we were able to reach high enantiomeric excess (up to 85% ee). This hence validates the use of the TCDC strategy in this class of reaction. Further efforts need to be engaged in that direction to develop an efficient, enantioselective version of this reaction.

2. Activation of allenamides combined with naphthol dearomatization

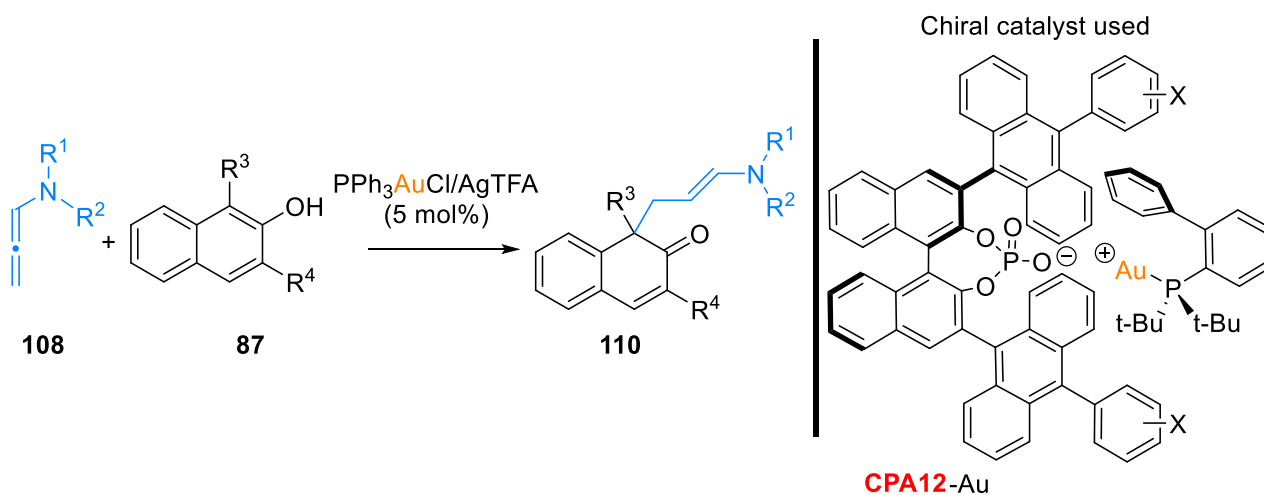
Allenamides **108** play an important role as unsaturated compounds in Au(I) catalysis.¹¹⁵ They are known to coordinate gold(I) complexes, leading to an intermediate iminium vinylgold species **109a**, that can undergo nucleophilic additions (Scheme 84, eq. 1). The transposition of this activation mode to the CPA_{Phos}AuCl complexes indicate that such an activation would result in the formation of the intermediate iminium **109b** potentially stabilized by the phosphate function (Scheme 84, eq. 2). This intermediate would feature the rigidity and well-defined shape necessary to allow further enantioselective processes, i.e. if a nucleophilic addition occurs with the concomitant formation of a stereogenic center from a prochiral nucleophile. The allenamide chemistry could hence benefit from the TCDC strategy in Au(I) catalysis.



Scheme 84. Activation of Allenamides with Au(I) Complexes

2.1. Bibliographic precedents in Au(I) catalysis

In 2018, Bandini and his co-worker discovered the dearomatization reactions of substituted 2-naphthols **87** with allenamides **108** in the presence of gold(I). They obtained various dearomatized products **110** in moderate to excellent yields (44%-98%) (Scheme 85).¹¹⁶ Very recently, during the drafting of this work, a chiral version was developed by the same group using chiral Au(I) phosphates **CPA12-Au**.¹¹⁷ This method requires highly complex catalytic system combining a JohnPhos ligand with 3,3'-polyacenes BINOL-based phosphates. Moderate to good ees were obtained, with however a narrow scope of the reaction (limited to $R^1 = \text{Ph}$, $R^2 = \text{Ts}$).

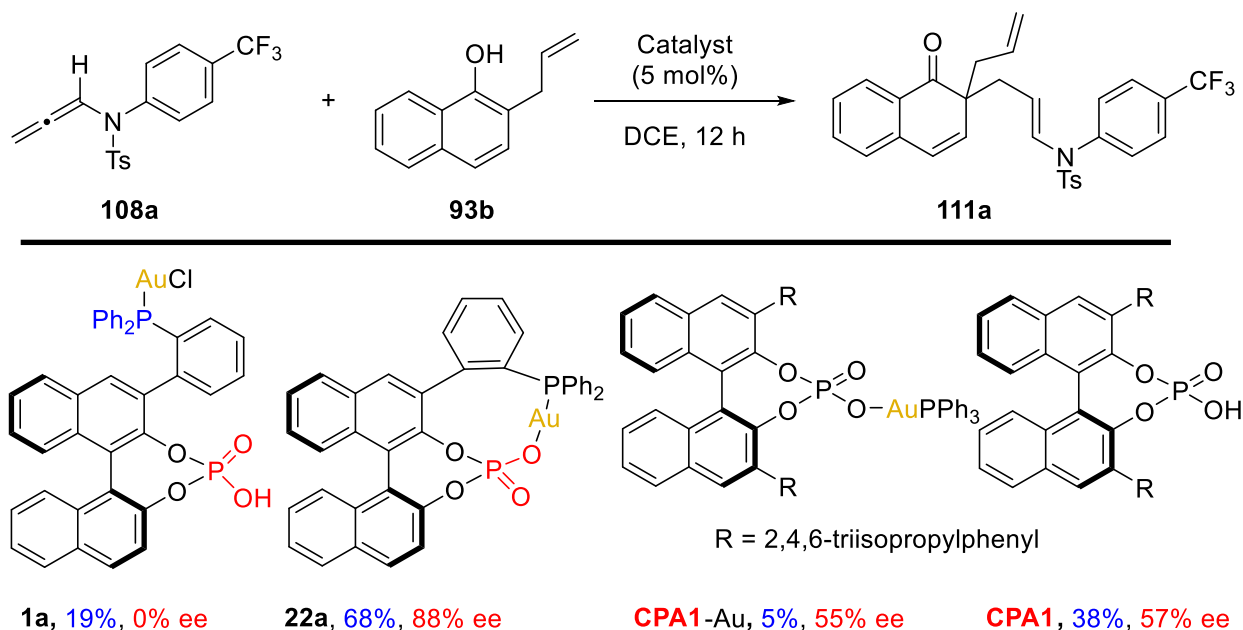


Scheme 85. Dearomatization of Naphthols with Allenamides by Bandini

We hence selected the Au(I)-catalyzed dearomatization reactions of substituted 1- and 2-naphthols with allenamides as a benchmark reaction to investigate the TCDC strategy suitability in allenamide chemistry. This work was mainly performed by Yunliang Yu, in the course of his PhD, and will hence be here only briefly summarized to illustrate the extended use of our method.

2.2. Main results obtained

During the optimization process of 2-naphthols with allenamides, Yunliang Yu used several catalysts to compare their enantioinduction abilities in the dearomatization reaction (Scheme 86).

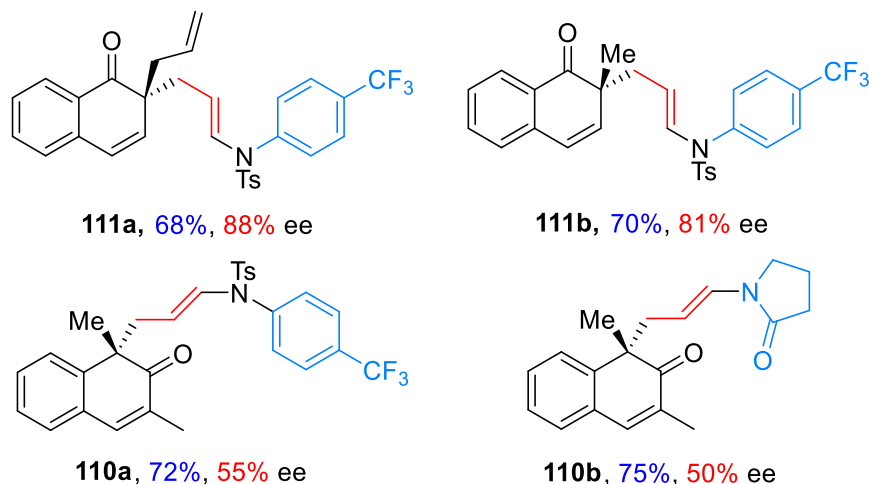


Scheme 86. Dearomatization of 2-allyl 1-naphthol with allenamide 108a

This highlighted that:

- 1) **1a** does not self-activate to an active Au(I) catalyst in the reaction conditions.
- 2) The TCDC strategy (**1a** + Ag₂CO₃) is more efficient (68% yield, 88% ee) than ACDC strategy with Au(I) phosphates (5% yield, 55% ee).
- 3) This reaction is also organocatalyzed by chiral phosphoric acids. This was already known from the literature,¹¹⁸ but implies to make sure of the efficient activation of the precatalyst to avoid competing organocatalyzed pathway.

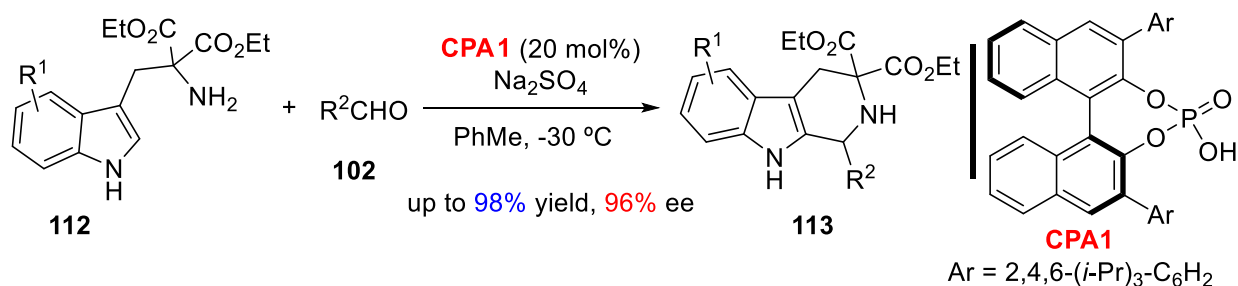
We next applied the TCDC strategy to the dearomatization of 1- and 2-naphthols with allenamides, and two dozens of dearomatized products **111** and **110** were obtained in moderate to good yields (up to 91%) and enantiomeric excesses (up to 92%). Representative examples are given below (Scheme 87).



Scheme 87. Representative Examples Obtained via the TCDC Strategy

3. The TCDC strategy in (*iso*)-Pictet-Spengler reactions

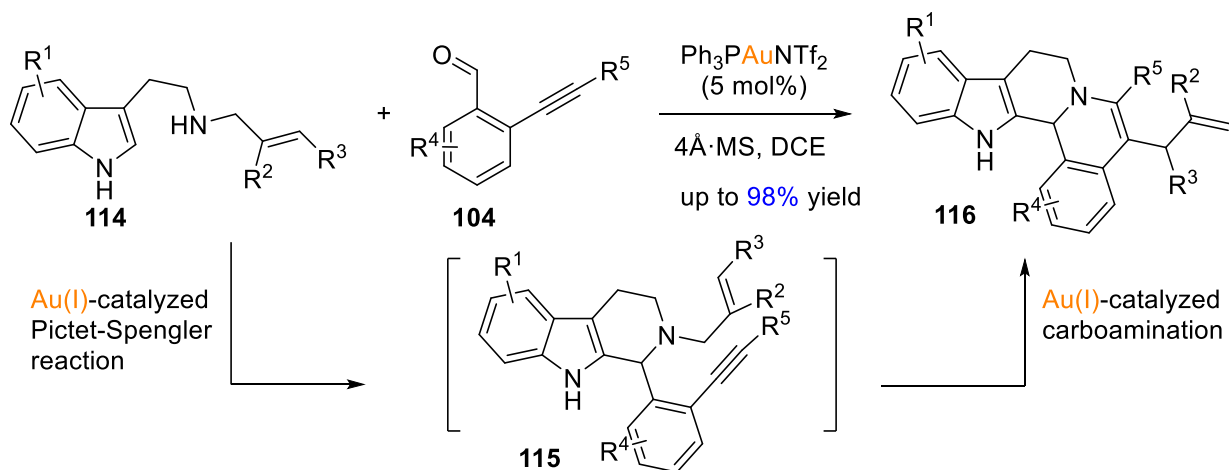
The Pictet-Spengler reaction, which was developed by Amé Pictet and Theodor Spengler in 1911,¹¹⁹ is undoubtedly the most important method for the synthesis of tetrahydro- β -carbolines.¹²⁰ Considering the bioactivities of these heterocycles and derived natural and non-natural products, the study of enantioselective Pictet-Spengler reactions is of great significance.^{120c, 121}



Scheme 88. Organocatalyzed Enantioselective Pictet-Spengler Reactions by List

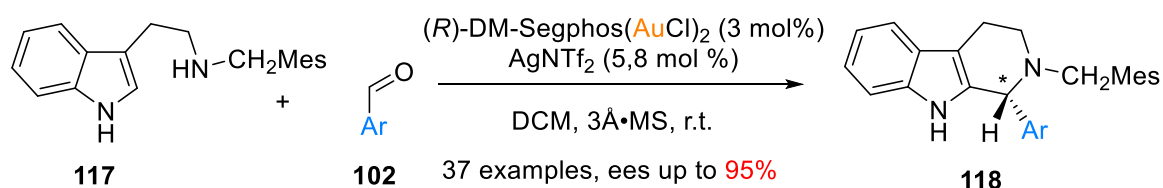
The Pictet-Spengler reaction is most often catalyzed by a Brønsted acid. With the advent of organocatalysis,⁴⁷ numerous methods were developed using chiral thioureas and chiral phosphoric acids.¹²¹ This was pioneered by List in 2006, who showed that catalytic amounts of chiral phosphoric acid catalyzed the reaction of tryptamine derivatives **112** with aldehydes to deliver tetrahydro- β -carbolines **113** in high yields and enantioselectivities (Scheme 88).¹²²

In the context of a project related to the study of Au(I)-catalyzed carboamination reactions, our group incidentally discovered in 2015 that Au(I) catalysts showed high catalytic activity in Pictet-Spengler reactions.¹²³ In the absence of any acidic catalyst, Au(I) complexes catalyzed Pictet-Spengler reactions from aromatic *ortho*-alkynylaldehydes **104** and *N*-allyl tryptamines **114** followed by a carboamination reaction and which afforded pentacyclic products **116** with high yields (Scheme 89).



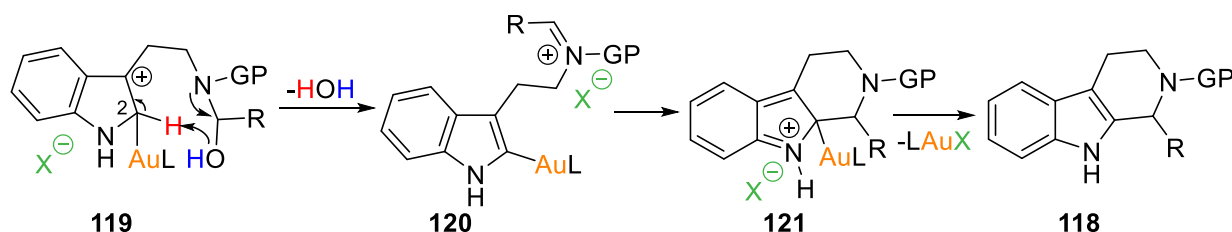
Scheme 89. Discovery of the Au(I)-Catalyzed Pictet-Spengler Reactions

Because the catalytic activities of Au(I) complexes was totally counter-intuitive in such a reaction, investigations were pursued, which eventually led to the establishment of the enantioselective Au(I) -catalyzed version of this reaction (Scheme 90).¹²⁴ The successful formation of compounds **118** in high yields and enantioselectivities was achieved.



Scheme 90. Enantioselective Au(I)-Catalyzed Pictet-Spengler Reactions

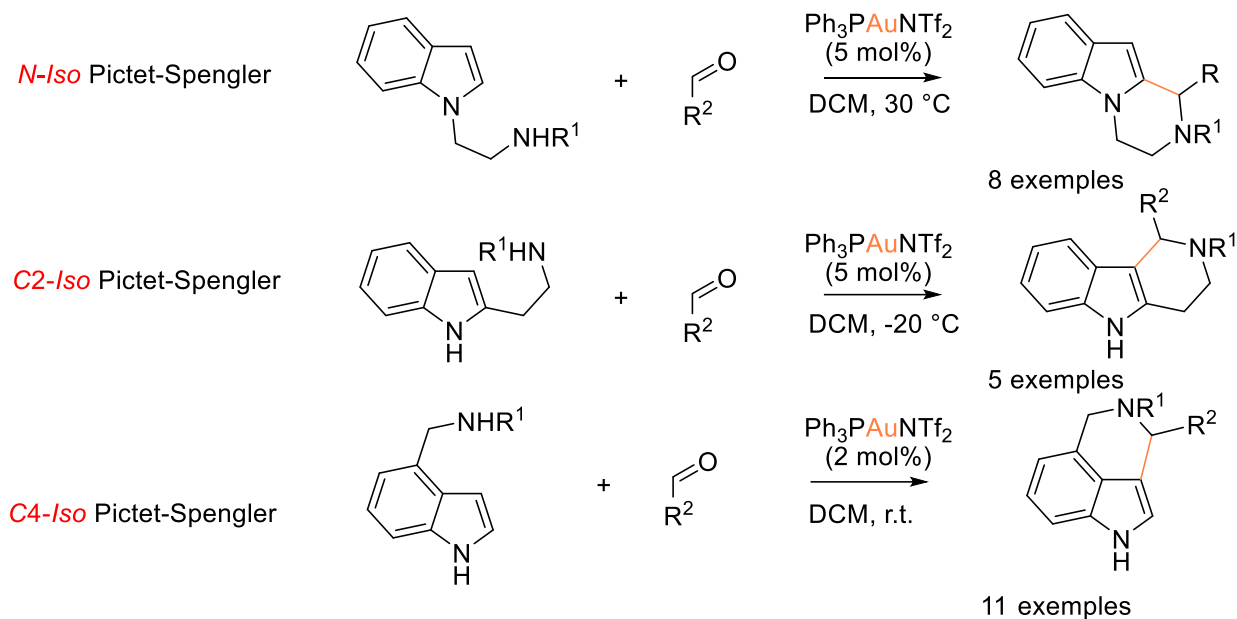
Facing this unprecedented reactivity, mechanistic investigations and DFT calculations established that this reaction occurs by an original mechanism where coordination of the Au(I) complex on the electron-rich indole of the initially formed hemiaminal **119** ultimately leads to an aurated indole-iminium intermediate **120** that undergoes the classical $\text{C}2$ addition of the indole ring to the iminium, leading to **121**. Deauration step regenerates the catalyst and releases product **118** (Scheme 91).



Scheme 91. Mechanism Proposal for Au(I)-Catalyzed Pictet-Spengler Reactions

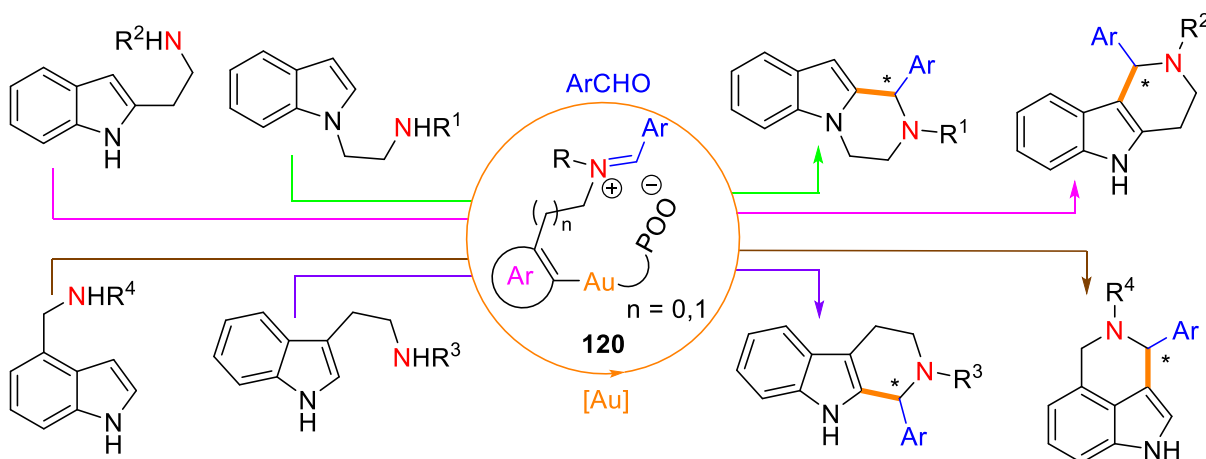
Given this reactivity in the classical Pictet-Spengler reaction, it was not to exclude that Au(I) complexes could act as catalysts in the analogous Pictet-Spengler reactions performed using regioisomeric “tryptamines”. In collaboration with Nicolas Glinsky-Olivier and Pierre Milcendeau, PhDs in the group, we

have indeed showed that this reactivity can be extended to *N*-*iso*, *C2*-*iso* and *C4*-*iso* Pictet-Spengler reactions using the Gagosz catalyst, which led to a series of 1,2,3,4-tetrahydropyrazino[1,2-*a*]indoles, tetrahydro- γ -carbolines and 1,3,4,5-tetrahydropyrrolo[4,3,2-*de*]isoquinolines (Scheme 92).¹²⁵



Scheme 92. Au(I)-Catalyzed *Iso*-Pictet-Spengler Reactions Developed in the Group

The investigation of the enantioselective Au(I) catalyzed version of these reactions with classical chiral diphosphine ligands however failed. We tried to apply the TCDC strategy in the four versions of the gold catalyzed (*iso*)-Pictet-Spengler reactions, thinking that intermediates **120** may be formed in the reactions and that the intramolecular linkage between the Au(I) and the chiral phosphate may shape well-defined, rigid intermediates suitable for a high enantioselectivity (Scheme 93).

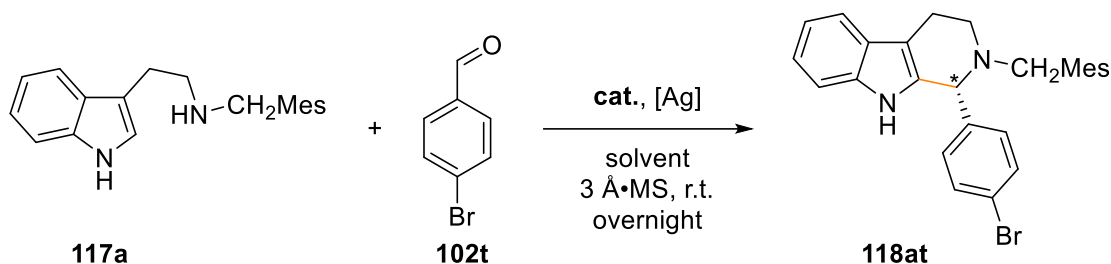


Scheme 93. The Four Different Versions of (*Iso*)-Pictet-Spengler Reactions using CPAPhosAuCl Complexes

The most significant results were obtained in the classical Pictet-Spengler reaction. We applied catalysts **1a** and **1e** in the reaction of *N*-2,4,6-trimethylbenzyl tryptamine **117** and 4-bromobenzaldehyde. A blank test

showed that Ag_2CO_3 has no catalytic activity in this reaction (Table 19, entry 1). Because our Au(I) complexes are also organocatalysts by virtue of their phosphoric acid function, the catalytic activity of **1a** was evaluated in the absence of a silver salt, leading to the formation of **118at** in 73% ee, with a low 22% conversion (entry 3). This result reflects for the stereochemical induction induced by the catalyst if it is not suitably activated by the silver salt. In the presence of Ag_2CO_3 , the gold catalyzed reaction proceeded in 42% yields and 57% ee (entry 3). Finally, a comparison with the catalytic activity of **1e** was performed, which conducted to lower values, both in terms of yield and enantioselectivity (entry 4). The absolute configuration of the stereogenic center of the major enantiomer was attributed as *R*, by comparison with the data obtained in our previous studies.¹²⁴

Table 19. Optimization of Pictet-Spengler Reaction



entry	cat.	[Ag]	solvent	conv. (%)	ee (%)
1	-	Ag_2CO_3	DCM	0	-
2	1a	-	PhMe	22	73
3	1a	Ag_2CO_3	DCM	42	57
4	1e	Ag_2CO_3	DCM	33	34

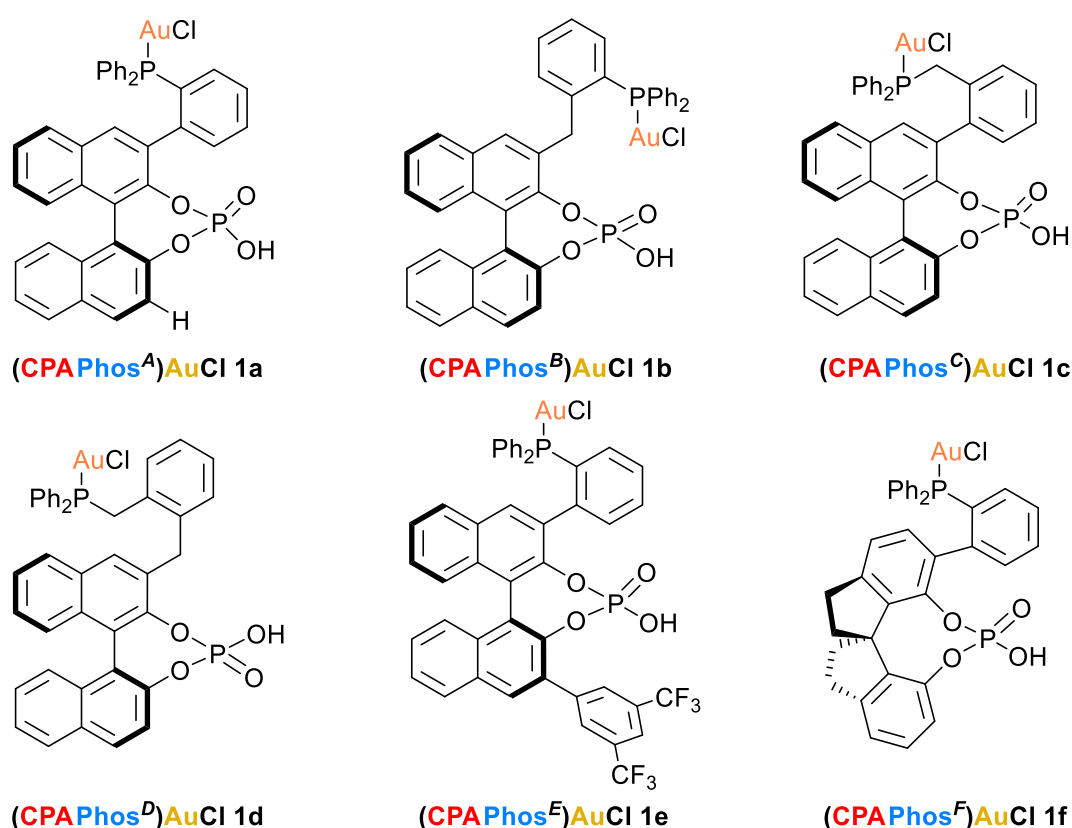
These preliminary results obviously compare unfavorably with classical catalytic approaches of the literature. However, they constitute an exciting basis for further research in Pictet-Spengler and related reactions, by extending the use of the TCDC strategy to another type of *in situ* formed intermediates.

4. Conclusion

In this chapter, we have briefly shown that the Tethered Counterion-Directed Catalysis (TCDC) strategy is applicable to diverse classes of reactions, such as the cyclization of *ortho*-alkynylarylaldimines, the dearomatization of naphthols with allenamides and the Pictet-Spengler reaction. These reactions evolve via very different intermediates highlighting the potential of this catalytic strategy for diverse applications, even if lot of efforts are still to do in that direction.

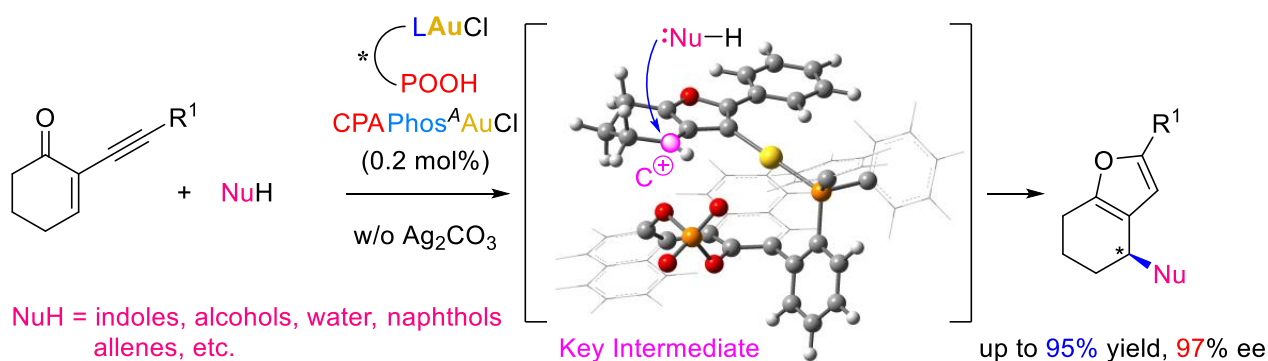
General Conclusion and Perspectives

The Asymmetric Counteranion Directed Catalysis (ACDC) is undoubtedly a spearhead approach in enantioselective catalysis. However, it is underdeveloped as far as Au(I) catalysis is concerned. In this context, in order to overcome the current limitations, we have developed a new strategy, the Tethered Counteranion Directed Catalysis (TCDC), that involves the design of chiral Au(I) complexes with a tether connecting the gold atom with a chiral phosphate. Thus, we have successfully designed and synthesized a series of chiral gold complexes (**1a-f**) displaying bifunctional phosphine-phosphoric acid ligands that we have named **CPAPhos** (Scheme 94). The phosphoric acid units are based on (*S*)-BINOL or (*R*)-SPINOL skeletons. The bifunctional chiral phosphate gold complex **1a** has been characterized by X-ray diffraction studies, DFT calculations, NMR, IR, HRMS and DOSY analysis.



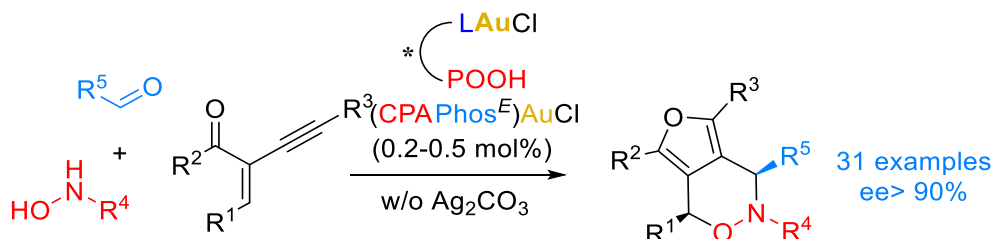
Scheme 94. The (CPAPhos)AuCl Complexes Prepared in this PhD Work

The new gold(I) catalysts were used then successfully in enantioselective catalytic reactions. We initially investigated the cycloisomerization reaction of cyclic 2-alkynyl enones, combined with the addition of various nucleophiles, including indoles, alcohols and others (Scheme 95). Catalysts **1a**, **1e** and **1f** showed excellent catalytic activities and enantioselectivities in this reaction (up to 95% yield and 97% ee were obtained with only 0.2% catalyst loading). DFT calculations provided a model to understand the high enantioselectivity obtained in these reactions. They suggested that the attack of the nucleophile takes place selectively on one face of the key carbocationic intermediate. The absolute configuration of the product predicted by these DFT calculations is fully consistent with the results obtained experimentally.



Scheme 95. Cycloisomerization/Nucleophilic Additions on 2-Alkynyl Enones

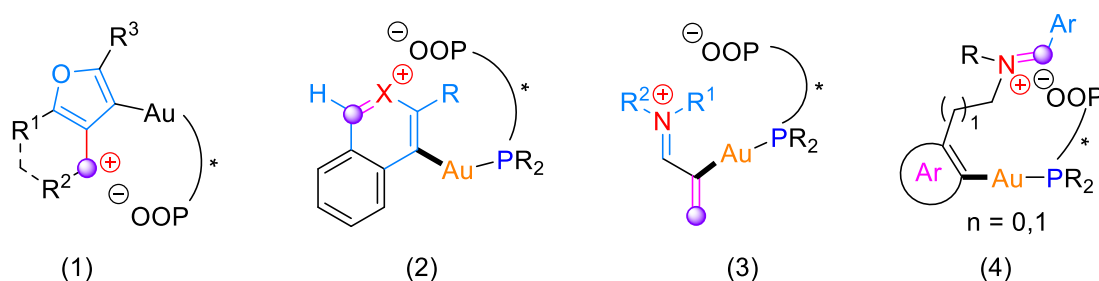
We have shown next that the reaction of 2-alkynyl enones with nitrones can be catalyzed by $(\text{CPA})\text{Phos}^{\text{F}}\text{AuCl}$ with high enantioselectivities (Scheme 96). Remarkably, multicomponent conditions have been established, allowing the *in situ* formation of the nitron. This constitutes, to our knowledge, the first example of multicomponent enantioselective Au(I)-catalyzed reactions.



Scheme 96. Cycloisomerization of 2-Alkynyl Enones Combined with the [3+2] Cycloaddition of Nitrones

Further investigations showed that the $(\text{CPA})\text{Phos}\text{AuCl}$ complexes can catalyze also other enantioselective reactions whose development is still in progress.

Overall, we have been able so far to apply the TCDC approach to reactions that generate four distinct types of intermediates. The cycloisomerizations of 2-alkynyl enones and 2-alkynyl arylaldehydes generate the cation-phosphate ion pairs (1) and (2), while dearomatization of naphthols with allenamides and Pictet-Spengler type cyclizations involve the iminium-phosphate pairs (3) and (4) respectively (Scheme 97). In the future, we intend to expand the applications of the TCDC strategy to reactions involving analogous intermediates in order to reveal the full potential of this innovative method.



Scheme 97. Intermediates Generated in the Catalytic Reactions Described in this PhD Work

Another important finding of this work is that (CPA Phos)AuCl complexes do not systematically require a silver salt for the activation of gold chloride to its cationic, catalytically active form. Considering the non-innocent role played by the silver salts in gold catalysis, this discovery is a strong asset in the development of our approach. We still need to establish whether the silver-free TCDC strategy can be extended to most gold-catalyzed reactions or not.

It is worth noting that the use of the CPA Phos ligands may not be restricted to Au(I). The CPA Phos ligands might coordinate a number of transition metals such as Pd, Ir, Rh or Ru (not exhaustively) to form catalytically active metal complexes (CPA Phos)M (M: Metals), either in the acyclic or cyclic forms. The coordination of CPA Phos ⁴ to Rh and Ir has been investigated recently by Yunliang Yu in our group. Yunliang successfully prepared the corresponding complexes (CPA Phos)Rh(cod), (CPA Phos)Ir(cod) and (CPA Phos)Ir(PPh₃)(CO). Studies on the use of these new complexes in asymmetric catalysis are in progress (Figure 26).

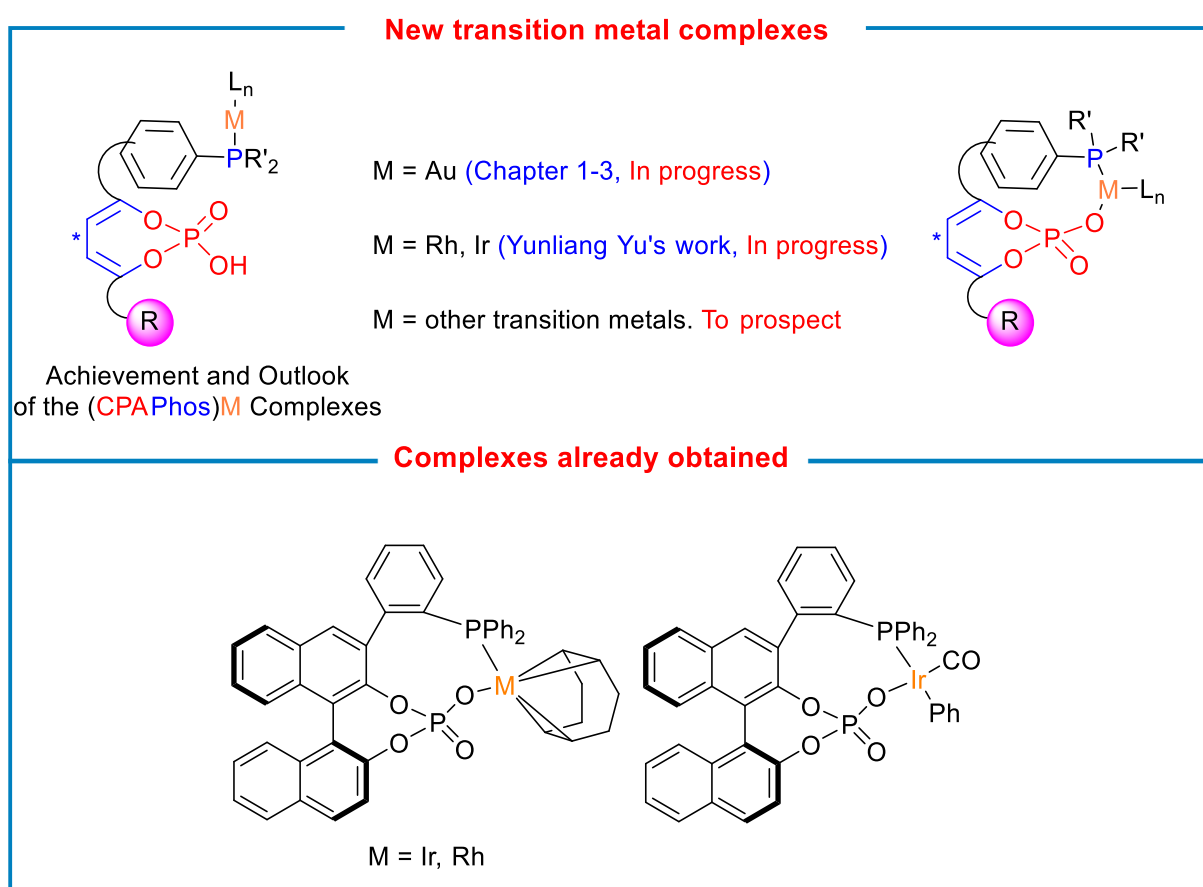


Figure 26. Extension of the TCDC Strategy to Other Transition Metal Complexes

Finally, this work demonstrates that tethering of a gold complex to its phosphate counterion generates robust catalysts with high catalytic activity. At the same time, it can improve significantly the enantioselectivity levels of selected catalytic reactions, by creating additional conformational constraints in a variety of reaction intermediates.

This proof of concept opens new perspectives in enantioselective catalysis, as far as the catalyst design can be extended easily to other classes of ligands and to other metals..

Experimental section

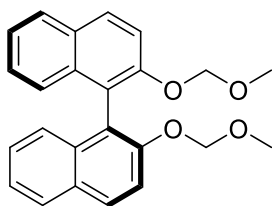
General methods

Unless otherwise noted, all of the reactions were performed under N₂ atmosphere, the solvents were distilled under N₂, and the separations were carried out under flash-chromatographic conditions on silica gel (Redi Sep prepacked column, 230-400 mesh) with use of a CombiFlash Companion. Reagent-grade chemicals were obtained from diverse commercial suppliers (Sigma-Aldrich, Acros Organics, TCI and Alfa-Aesar) and were used as received. *n*-BuLi was used as commercially available solutions and titrated before use. ¹H NMR (300 and 500 MHz), ³¹P (120 MHz and 200 MHz) and ¹³C (75 and 125 MHz) NMR spectra were recorded on Bruker Advance spectrometers. The chemical shifts (δ) are reported in part per million (ppm) and coupling values (*J*) are given in hertz (Hz). Multiplicities are abbreviated as follows: s (singlet), d (doublet), t (triplet), q (quadruplet), bs (broad singlet), dd (doublet of doublet), dt (doublet of triplet), m (multiplet). Infrared spectra (IR) were recorded on a Perkin-Elmer FT-IR system using diamond window Dura SamplIR II and the data are reported in reciprocal centimeters (cm⁻¹). Optical rotations were measured on a Anton Paar MCP 300 polarimeter at 589 nm. $[\alpha]_D$ is expressed in deg.cm³.g⁻¹.dm⁻¹ and *c* is expressed in g/100 cm³. Melting points were recorded in open capillary tubes on a Büchi B-540 apparatus and are uncorrected. High resolution mass spectra (HRMS) were recorded using a Micromass LCT Premier XE instrument (Waters) and were determined by electrospray ionization (ESI) with a TOF analyzer.

Chapter 1. Synthesis of bifunctional chiral phosphine-phosphate Au(I) complexes

1. Synthesis and Characterization of 1a

Synthesis of (S)-2,2'-bis(methoxymethoxy)-1,1'-binaphthalene (11)

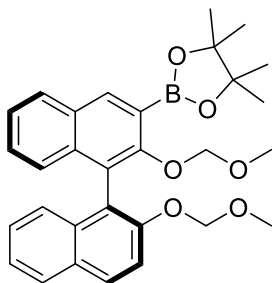


(S)-BINOL (14.3 g, 50.0 mmol, 1.0 equiv.) was dissolved in 80 mL of anhydrous THF and added dropwise to a suspension of NaH (60% wt in mineral oil, 6.0 g, 150 mmol, 3 equiv.) in 80 ml of anhydrous THF at 0 °C. The reaction mixture was stirred for 1 h at room temperature and then MOM-Cl (11.4 mL, 150 mmol, 3 equiv.) was added dropwise at 0 °C. The reaction mixture was stirred for another 3 hours at room temperature. When the reaction was completed, it was quenched with saturated aqueous NaHCO₃ and extracted twice with CH₂Cl₂. Combined organic layers were then dried over MgSO₄ and evaporated. The crude product was used directly for further synthesis without purification (18.5 g, 49.4 mmol, 99%).

IR (neat) ν_{\max} = 3057, 2956, 2901, 2826, 1621, 1592, 1506, 1237, 1147, 1031, 1011, 920, 809, 749. ¹H NMR (CDCl₃, 300 MHz) δ (ppm) = 7.92 (d, *J* = 9.0 Hz, 2H), 7.84 (d, *J* = 8.3 Hz, 2H), 7.55 (d, *J* = 9.0 Hz, 2H), 7.33-

7.28 (m, 2H), 7.22-7.14 (m, 4H), 5.05 (d, $J = 6.8$ Hz, 2H), 4.94 (d, $J = 6.8$ Hz, 2H), 3.11 (s, 6H). ^{13}C NMR (CDCl_3 , 75 MHz) δ (ppm) = 152.8, 134.2, 130.0, 129.5, 128.0, 126.5, 125.7, 124.2, 121.4, 117.4, 95.3, 56.0.

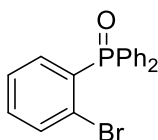
Synthesis of (*S*)-2-(2,2'-bis(methoxymethoxy)-[1,1'-binaphthalen]-3-yl)-4,4,5,5-tetramethyl-1,3,2-dioxaborolane (**12**)



To a solution of (*S*)-2,2'-bis(methoxymethoxy)-1,1'-binaphthalene **11** (7.84 g, 21 mmol, 1.0 equiv.) in 140 mL of anhydrous THF, *n*-BuLi (19.6 mL, 29.4 mmol, 1.4 equiv.) was added dropwise at -78 °C. The reaction mixture was stirred at -78 °C for 4 hours, then isopropoxy-pinacolborate (5.6 mL, 27.3 mmol, 1.3 equiv.) was added to the flask and the resulting solution was allowed to warm to room temperature. It was stirred overnight at room temperature and then quenched with water and extracted with DCM. Combined organic layers were dried over MgSO_4 and evaporated. The crude product was purified by flash column chromatography on silica gel (eluent: 100% heptane to heptane:DCM = 2:1) yielding the product **12** as a white solid (7.03 g, 14.1 mmol, 67%).^{51b}

IR (neat) ν_{max} = 3411, 3054, 2956, 2825, 1909, 1622, 1592, 1436, 1241, 1146, 1014, 988, 923, 696. **^1H NMR (CDCl_3 , 300 MHz)** δ = 8.49 (s, 1H), 7.92 (d, $J = 8.9$ Hz, 2H), 7.82 (d, $J = 8.1$ Hz, 1H), 7.55 (d, $J = 9.0$ Hz, 1H), 7.39-7.29 (m, 2H), 7.27-7.17 (m, 4H), 5.15 (d, $J = 6.8$ Hz, 1H), 4.93 (d, $J = 7.0$ Hz, 1H), 4.89 (d, $J = 5.8$ Hz, 1H), 4.84 (d, $J = 5.8$ Hz, 1H), 3.11 (s, 3H), 2.40 (s, 3H), 1.39 (s, 12H). **^{13}C NMR (CDCl_3 , 75 MHz)** δ (ppm) = 156.9, 153.1, 139.4, 135.9, 134.5, 130.5, 129.8, 129.5, 128.7, 127.7, 127.5, 126.5, 126.3, 126.1, 125.5, 124.8, 124.1, 121.8, 116.9, 100.2, 100.1, 95.2, 84.0, 56.0, 55.9, 25.0. **HRMS (ESI):** m/z : calcd for $\text{C}_{30}\text{H}_{33}\text{BNaO}_6^+$ 523.2262 [$\text{M}+\text{Na}$] $^+$, found, 523.2313. **$[\alpha]_{\text{D}}$** = -68 (c 1.16, CHCl_3).

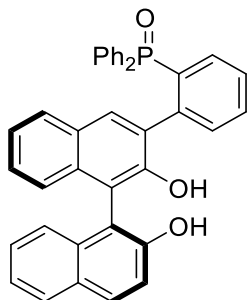
Synthesis of (2-bromophenyl)diphenylphosphine oxide (**18**)⁵⁴



Diphenylphosphine oxide (4.81 g, 23.8 mmol, 1.0 equiv.) was dissolved in PhMe (60 mL), and then $\text{Pd}_2(\text{dba})_3$ (0.38 g, 0.4 mmol, 1.75 mol%), 1,3-bis(diphenylphosphino)propane (0.34 g, 0.8 mmol, 3.5 mol%), then bromiodobenzene (3.36 mL, 26.2 mmol, 1.1 equiv.), and *i*-Pr $_2$ NEt (4.9 mL, 29.7 mmol, 1.25 equiv.) were added and the mixture stirred at 90 °C for 4 days. After cooling to room temperature, water was added and the solution was extracted with DCM. Organic layers were dried over MgSO_4 , filtered and evaporated under vacuum. The crude product was purified by flash column chromatography (Hept: EA = 4:1 to EA), giving product as a pale yellow solid (6.0 g, 16.8 mmol, 64%).

$^1\text{H NMR}$ (CDCl_3 , 500 MHz) δ = 7.75-7.65 (m, 5H), 7.58-7.53 (m, 2H), 7.60-7.45 (m, 4H), 7.41-7.30 (m, 3H). $^{13}\text{C NMR}$ (CDCl_3 , 75 MHz) δ = 136.1 (d, $J_{\text{C-P}}$ = 10.4 Hz), 135.0 (d, $J_{\text{C-P}}$ = 7.7 Hz), 133.6 (d, $J_{\text{C-P}}$ = 2.2 Hz), 133.2 (d, $J_{\text{C-P}}$ = 104.3 Hz), 132.3 (d, $J_{\text{C-P}}$ = 9.9 Hz), 132.1 (d, $J_{\text{C-P}}$ = 2.7 Hz), 131.9 (d, $J_{\text{C-P}}$ = 107.6 Hz), 128.7 (d, $J_{\text{C-P}}$ = 12.6 Hz), 127.1 (d, $J_{\text{C-P}}$ = 11.5 Hz), 127.1 (d, $J_{\text{C-P}}$ = 4.9 Hz). $^{31}\text{P NMR}$ (CDCl_3 , 200 MHz) δ = 30.6.

Synthesis of (S)-2-(2,2'-dihydroxy-[1,1'-binaphthalen]-3-yl)phenyl) diphenylphosphine oxide (**19**)⁴⁸

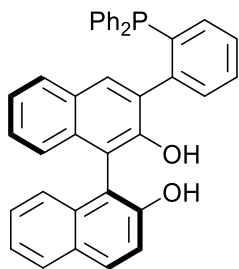


(2-bromophenyl)diphenylphosphine oxide **18** (3.25 g, 9.2 mmol, 1.1 equiv.) and $\text{Pd}(\text{PPh}_3)_4$ (0.48 g, 0.42 mmol, 5 mol%) were added to a flask, followed by anhydrous, degassed THF (100 mL) and H_2O (50 mL). The mixture was stirred at room temperature for 10 min. To this solution were added (S)-2-(2,2'-bis(methoxymethoxy)-[1,1'-binaphthalen]-3-yl)-4,4,5,5-tetramethyl-1,3,2-dioxaborolane **12** (4.78 g, 8.3 mmol, 1.0 equiv.) and K_2CO_3 (3.45 g, 24.9 mmol, 3 equiv.), and the solution was stirred at 100 °C for 24 h. After cooling to room temperature, water was added and the reaction mixture was extracted twice with methyl *tert*-butyl ether. The combined organic layers were dried over MgSO_4 , filtered and concentrated under vacuum.

The crude product was dissolved in a mixture of THF/MeOH 1:1 (80 mL), then *p*-TsOH· H_2O (1.58 g, 8.3 mmol, 1 equiv.) was added to this solution and reaction mixture was stirred at 60 °C for 3 hours. After that, it was cooled down to room temperature and solvents were evaporated under reduced pressure. Water was added and the reaction mixture was extracted twice with DCM. The combined organic layers were dried over MgSO_4 , filtered and concentrated under vacuum. The crude product was purified by flash column chromatography (eluent: 100% heptane to heptane/ethyl acetate, 30/70) giving the product **19** as a white solid (3.43 g, 6.1 mmol, 74%).

IR (neat) ν_{max} = 3058, 1619, 1467, 1438, 1142, 750. $^1\text{H NMR}$ (CDCl_3 , 500 MHz) δ = 8.11 (bs, 1H), 7.83 (d, J = 8.8 Hz, 1H), 7.77 (d, J = 8.2 Hz, 1H), 7.67 (dd, J_1 = 11.6 Hz, J_2 = 7.6 Hz, 2H), 7.61 (t, J = 7.6 Hz, 1H), 7.58-7.54 (m, 1H), 7.46 (t, J = 6.9 Hz, 1H), 7.42-7.30 (m, 4H), 7.29-7.06 (m, 12H), 6.97 (s, 1H), 6.93 (d, J = 7.9 Hz, 1H), 5.74 (s, 1H). $^{13}\text{C NMR}$ (CDCl_3 , 125 MHz) δ = 154.0, 151.4, 143.6 (d, $J_{\text{C-P}}$ = 7.3 Hz), 134.5, 133.9, 133.5 (d, $J_{\text{C-P}}$ = 13.7 Hz), 133.0, 132.6 (d, $J_{\text{C-P}}$ = 1.8 Hz), 132.5 (d, $J_{\text{C-P}}$ = 9.2 Hz), 132.4 (d, $J_{\text{C-P}}$ = 158.5 Hz), 132.2 (d, $J_{\text{C-P}}$ = 2.7 Hz), 132.0 (d, $J_{\text{C-P}}$ = 10.1 Hz), 131.9, 131.9, 131.4, 131.3, 131.3, 131.2 (d, $J_{\text{C-P}}$ = 106.3 Hz), 130.5, 130.1, 130.1, 129.0 (d, $J_{\text{C-P}}$ = 50.4 Hz), 128.7 (d, $J_{\text{C-P}}$ = 11.9 Hz), 128.4 (d, $J_{\text{C-P}}$ = 12.8 Hz), 128.3 (d, $J_{\text{C-P}}$ = 6.4 Hz), 127.4 (d, $J_{\text{C-P}}$ = 12.8 Hz), 126.7, 126.8, 125.4, 123.7, 123.3, 120.2, 115.4, 113.1. $^{31}\text{P NMR}$ (CDCl_3 , 200 MHz) δ = 30.5. **HRMS (ESI)**: m/z : calcd for $\text{C}_{38}\text{H}_{28}\text{O}_3\text{P}^+$ 563.1771 [$\text{M}+\text{H}$] $^+$, found, 563.1770. $[\alpha]_{\text{D}} = +71$ (c 0.76, CHCl_3), *lit* +86 (c 0.6, CHCl_3).

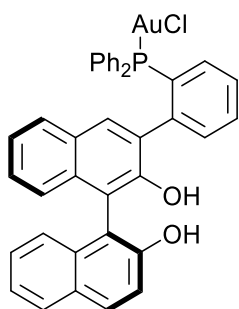
Synthesis of (S)-3-(2-(diphenylphosphaneyl)phenyl)-[1,1'-binaphthalene]-2,2'-diol (**8**)⁴⁸



(S)-3-(2-(2,2'-dihydroxy-[1,1'-binaphthalen]-3-yl)phenyl)diphenylphosphine oxide **19** (3.43 g, 6.1 mmol, 1.0 equiv.) was dissolved in toluene (100 mL) at 0 °C, and then Et₃N (8.5 mL, 61 mmol, 10 equiv.) and Cl₃SiH (12.5 mL, 122.1 mmol, 20 equiv.) were added to the solution dropwise at 0 °C. The reaction was then stirred at 90 °C for 24 h. After cooling to room temperature, the reaction solution was quenched with 2M·NaOH and then PhMe was evaporated under reduced pressure. 2M·NaOH was added to dissolve the precipitated solid and then extracted twice with DCM, dried over MgSO₄ and evaporated. The crude product was purified by flash column chromatography (eluent: heptane to DCM) giving the product **8** as a white solid (2.61 g, 4.7 mmol, 78%).

IR (neat) ν_{\max} = 3510, 3053, 1619, 1596, 1434, 1138, 734. **¹H NMR (CDCl₃, 500 MHz)** δ = 7.94 (d, J = 8.8 Hz, 1H), 7.87 (d, J = 7.9 Hz, 1H), 7.64-7.57 (m, 1H), 7.55-7.42 (m, 3H), 7.40-7.15 (m, 17H), 7.11-7.03 (m, 2H), 5.71 (bs, 1H), 5.15 (bs, 1H). **¹³C NMR (CDCl₃, 125 MHz)** δ = 153.2, 150.1, 143.2 (d, J_{C-P} = 30.2 Hz), 138.2 (d, J_{C-P} = 30.2 Hz), 136.9 (d, J_{C-P} = 8.2 Hz), 136.7 (d, J_{C-P} = 9.2 Hz), 134.1, 134.0, 133.8 (d, J_{C-P} = 19.2 Hz), 132.3, 131.2, 130.5, 130.3 (d, J_{C-P} = 3.7 Hz), 129.6, 129.5, 128.8, 128.6, 128.5, 128.5, 128.5, 127.6, 127.5, 127.2, 125.1, 124.9, 124.2, 123.9, 118.1 (d, J_{C-P} = 82.5 Hz), 112.1, 112.0. **³¹P NMR (CDCl₃, 120 MHz)** δ = -10.6, -12.3. **HRMS (ESI):** m/z : calcd for C₃₈H₂₈O₂P⁺ 547.1821 [M+H]⁺, found, 547.1801. [α]_D = -80 (c 0.94, CHCl₃), *lit* -73 (c 0.6, CHCl₃).

Synthesis of (S)-3-(2-(2,2'-dihydroxy-[1,1'-binaphthalen]-3-yl)phenyl)diphenylphosphine gold(I) chloride (**20**)

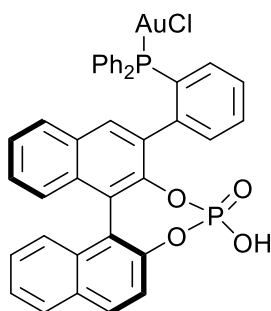


(S)-3-(2-(diphenylphosphaneyl)phenyl)-[1,1'-binaphthalene]-2,2'-diol **8** (2.63 g, 4.8 mmol, 1.0 equiv.) and Me₂S·AuCl (1.41 g, 4.8 mmol, 1.0 equiv.) were dissolved in dry DCM (130 mL), and then the reaction solution was stirred at room temperature for 1 h. The solvent was evaporated and the crude product was purified by flash column chromatography (Heptane-DCM), yielding the product **20** as a white solid (3.4 g, 4.4 mmol, 89%).

IR (neat) ν_{\max} = 3515, 3405, 3057, 2926, 1619, 1597, 1437, 1131, 748. **¹H NMR (CDCl₃, 500 MHz)** δ = 7.87 (d, J = 8.8 Hz, 1H), 7.79 (d, J = 7.9 Hz, 1H), 7.63-7.61 (m, 1H), 7.58-7.49 (m, 4H), 7.50-7.47 (m, 1H), 7.46-7.40

(m, 4H), 7.39-7.34 (m, 3H), 7.34-7.23 (m, 5H), 7.23-7.16 (m, 4H), 7.00 (d, $J = 8.2$ Hz, 1H), 6.53 (bs, 1H), 4.90 (bs, 1H). ^{13}C NMR(CDCl_3 , 125 MHz) $\delta = 154.3, 150.2, 144.0$ (d, $J_{\text{C-P}} = 15.6$ Hz), 134.8 (d, $J_{\text{C-P}} = 5.5$ Hz), 134.5 (d, $J_{\text{C-P}} = 13.7$ Hz), 134.3 (d, $J_{\text{C-P}} = 13.7$ Hz), 134.2, 133.7 (d, $J_{\text{C-P}} = 8.2$ Hz), 133.5, 133.1, 132.1 (d, $J_{\text{C-P}} = 1.8$ Hz), 131.7 (d, $J_{\text{C-P}} = 1.8$ Hz), 131.6, 131.5 (d, $J_{\text{C-P}} = 1.8$ Hz), 130.9 (d, $J_{\text{C-P}} = 62.3$ Hz), 129.9, 129.6 (d, $J_{\text{C-P}} = 12.8$ Hz), 129.4, 129.2 (d, $J_{\text{C-P}} = 11.9$ Hz), 129.0, 128.7, 128.6, 128.6, 128.2, 128.1, 127.8, 127.4, 124.9, 124.8, 124.1, 123.8, 119.4, 113.6, 110.4. ^{31}P NMR (CDCl_3 , 200 MHz) $\delta = 24.2$. HRMS (ESI): m/z : calculated for $\text{C}_{40}\text{H}_{30}\text{AuNO}_2\text{P}^+$: 784.1680 $[\text{M}+\text{MeCN}-\text{Cl}]^+$, found, 784.1688; m/z : calcd for $\text{C}_{38}\text{H}_{26}\text{AuClO}_2\text{P}^-$ 777.1030 $[\text{M}-\text{H}]^-$, found, 777.1016. $[\alpha]_{\text{D}} = -149$ (c 1.07, CHCl_3).

Synthesis of (S)-(2-(2,2'-diyl hydrogen phosphate-[1,1'-binaphthalen]-3-yl)phenyl) diphenylphosphine gold(I) chloride (1a)



(S)-(2-(2,2'-dihydroxy-[1,1'-binaphthalen]-3-yl)phenyl)diphenylphosphine gold(I) chloride **20** (3.4 g, 4.3 mmol, 1.0 equiv.) was added to 10 mL pyridine, then POCl_3 (0.48 mL, 5.11 mmol, 1.2 equiv.) was added to the solution dropwise under 0 °C. The resulting solution was stirred at room temperature for 24 h. After completion, it was quenched with water and the solvent were removed under vacuum. 2M-HCl and THF were added, and the reaction mixture was stirred overnight at 50 °C. After cooling to room temperature, the reaction solution was extracted with DCM and H_2O . Crude product was purified by flash column chromatography (eluent: DCM-MeOH-AcOH = 9:1:0.1) giving the product **1a** as a brown solid (3.15 g, 3.7 mmol, 88%).

m.p.: 256.2-261.5 °C. **IR (neat)** $\nu_{\text{max}} = 3515, 3405, 3056, 2925, 1619, 1436, 1214, 1131, 748$. **HRMS (ESI):** m/z calcd for $\text{C}_{40}\text{H}_{29}\text{AuNO}_4\text{P}_2^+$ 846.1232 $[\text{M}+\text{MeCN}-\text{Cl}]^+$, found, 846.1245; m/z calcd for $\text{C}_{38}\text{H}_{25}\text{AuClO}_4\text{P}_2^-$ 839.0588 $[\text{M}-\text{H}]^-$, found, 839.0587. $[\alpha]_{\text{D}} = +15$ (c 1.03, CHCl_3).

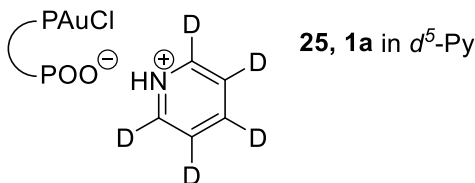
-NMR data in d^6 -DMSO:

^1H NMR (d^6 -DMSO, 343K, 500 MHz) $\delta = 8.13$ -8.07 (m, 2H), 8.06 (d, $J = 6.6$ Hz, 1H), 8.03 (d, $J = 8.2$ Hz, 1H), 7.86 (d, $J = 8.2$ Hz, 1H), 7.72 (t, $J = 7.6$ Hz, 2H), 7.62 (d, $J = 6.3$ Hz, 1H), 7.60-7.48 (m, 7H), 7.43 (d, $J = 8.8$ Hz, 1H), 7.40 (d, $J = 9.1$ Hz, 1H), 7.37-7.28 (m, 4H), 7.18-7.10 (m, 2H), 7.00 (bs, 2H), 6.24 (bs, 1H). ^{13}C NMR (d^6 -DMSO, 343K, 125 MHz) $\delta = 146.9$ (d, $J_{\text{C-P}} = 9.2$ Hz), 144.9 (d, $J_{\text{C-P}} = 10.1$ Hz), 141.5 (d, $J_{\text{C-P}} = 13.7$ Hz), 133.8 (d, $J_{\text{C-P}} = 7.3$ Hz), 133.6 (d, $J_{\text{C-P}} = 13.7$ Hz), 133.3 (d, $J_{\text{C-P}} = 13.7$ Hz), 132.9 (d, $J_{\text{C-P}} = 6.4$ Hz), 131.8, 131.5, 131.3 (d, $J_{\text{C-P}} = 5.5$ Hz), 131.2, 131.0 (d, $J_{\text{C-P}} = 116.4$ Hz), 130.7, 130.3, 129.8, 129.5, 129.4, 129.1 (d, $J_{\text{C-P}} = 11.0$ Hz), 128.4, 128.4 (d, $J_{\text{C-P}} = 12.8$ Hz), 128.0 (d, $J_{\text{C-P}} = 9.2$ Hz), 127.6, 127.6, 127.4 (d, $J_{\text{C-P}} = 12.8$ Hz), 126.9 (d, $J_{\text{C-P}} = 15.6$ Hz), 126.4, 125.9, 125.6, 125.2, 124.9, 121.7, 121.0, 120.7, 120.3.

^{31}P NMR (d^6 -DMSO, 343 K, 200 MHz) $\delta = 26.4, 1.2$ (major isomer) and 25.8, 2.5 (minor isomer).

^{31}P NMR (d^6 -DMSO, 383 K, 200 MHz) δ = 26.8, 1.1.

-NMR data in deuterated pyridine:



^1H NMR (d^5 -Pyridine, 500 MHz) δ = 11.86 (bs, 1H), 9.26 (t, J = 6.3 Hz, 1H), 7.97 (s, 1H), 7.88 (d, J = 8.0 Hz, 1H), 7.84 (t, J = 7.7 Hz, 1H), 7.82-7.75 (m, 3H), 7.72 (d, J = 8.7 Hz, 1H), 7.63 (dd, J_1 = 13.2 Hz, J_2 = 7.7 Hz, 2H), 7.53 (t, J = 6.9 Hz, 1H), 7.49-7.33 (m, 9H), 7.20 (t, J = 7.6 Hz, 1H), 7.15 (dd, J_1 = 12.1 Hz, J_2 = 7.9 Hz, 1H), 6.99 (t, J = 6.8 Hz, 2H), 6.92 (t, J = 6.9 Hz, 1H). ^{13}C NMR (d^5 -Pyridine, 125 MHz) δ = 148.6 (d, $J_{\text{C-P}}$ = 10.1 Hz), 144.1 (d, $J_{\text{C-P}}$ = 13.7 Hz), 136.9 (d, $J_{\text{C-P}}$ = 7.3 Hz), 135.6 (d, $J_{\text{C-P}}$ = 14.7 Hz), 134.7, 134.7 (d, $J_{\text{C-P}}$ = 13.7 Hz), 134.1, 133.9, 133.7 (d, $J_{\text{C-P}}$ = 4.6 Hz), 133.5, 132.8, 132.4, 132.1, 131.7, 131.6 (d, $J_{\text{C-P}}$ = 62.3 Hz), 131.3, 130.7, 130.3 (d, $J_{\text{C-P}}$ = 11.9 Hz), 130.3, 129.9, 129.8, 129.7 (d, $J_{\text{C-P}}$ = 11.0 Hz), 129.4, 129.0 (d, $J_{\text{C-P}}$ = 10.1 Hz), 128.8, 128.7, 128.3, 127.8, 127.6, 127.3, 126.2, 126.0, 123.1. ^{31}P NMR (d^5 -Pyridine, 200 MHz) δ = 29.2, 6.7.

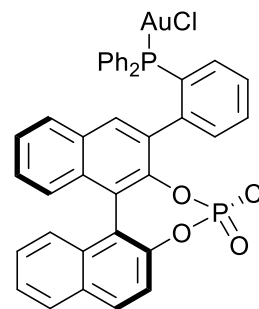
-NMR data in CDCl_3 :

^1H NMR (CDCl_3 , 500 MHz) δ = 8.30 (s, 1H), 8.04 (d, J = 8.2 Hz, 1H), 7.90 (d, J = 8.2 Hz, 2H), 7.77-7.72 (m, 1H), 7.58-7.48 (m, 5H), 7.46-7.39 (m, 3H), 7.35-7.19 (m, 8H), 6.97 (dd, J_1 = 11.9 Hz, J_2 = 7.9 Hz, 1H), 6.73-6.66 (m, 2H), 6.66-6.60 (m, 1H), 6.53 (bs, 1H). ^{31}P NMR (CDCl_3 , 200 MHz) δ = 27.7, 2.9 (major isomer), 26.2, 4.6 (minor isomer).

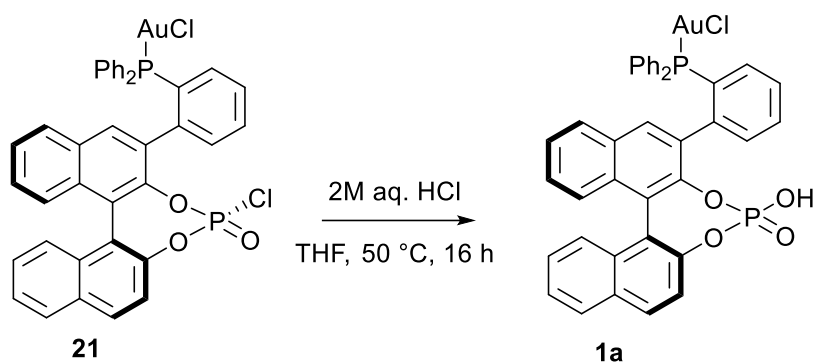
Isolation of the intermediate phosphoroyl chloride **21**

In some reaction batch for the synthesis of **1a**, one of the intermediate phosphoroyl chloride diastereoisomer was showed to be poorly reactive towards hydrolysis and could be isolated and characterized.

Data for (*S*)-(2-(2,2'-diylchlorogenphosphate-[1,1'-binaphthalen]-3-yl)phenyl) diphenylphosphine gold(I) chloride **21**: m.p.: 193.4-194.2 °C. IR (neat) ν_{max} = 3056, 2961, 2925, 2854, 1591, 1437, 1413, 1310, 1242, 1208, 1101, 1082, 970, 954, 904, 821, 876, 750, 693. ^1H NMR (CDCl_3 , 500 MHz) δ = 8.37 (s, 1H), 8.09 (d, J = 8.2 Hz, 1H), 8.03 (d, J = 8.8 Hz, 1H), 7.97 (d, J = 8.2 Hz, 1H), 7.85 (t, J = 6.3 Hz, 1H), 7.71 (t, J = 7.6 Hz, 1H), 7.62-7.55 (m, 2H), 7.52-7.45 (m, 5H), 7.45-7.40 (m, 3H), 7.40-7.31 (m, 4H), 7.25 (d, J = 9.1 Hz, 1H), 7.07 (dd, J_1 = 12.0 Hz, J_2 = 8.2 Hz, 1H), 6.74-6.69 (m, 3H). ^{13}C NMR (CDCl_3 , 125 MHz) δ = 146.1 (d, $J_{\text{C-P}}$ = 11.9 Hz), 143.9 (d, $J_{\text{C-P}}$ = 11.9 Hz), 141.1 (d, $J_{\text{C-P}}$ = 12.8 Hz), 134.9 (d, $J_{\text{C-P}}$ = 14.7 Hz), 134.6 (d, $J_{\text{C-P}}$ = 14.7 Hz), 134.1 (d, $J_{\text{C-P}}$ = 7.3 Hz), 133.8, 133.2 (d, $J_{\text{C-P}}$ = 6.4 Hz), 132.6, 132.2, 131.9, 131.9, 131.9, 131.7, 131.7, 131.5, 130.9 (d, $J_{\text{C-P}}$ = 1.8 Hz), 129.8, 129.6, 129.4 (d, $J_{\text{C-P}}$ = 11.9 Hz), 129.0, 128.9 (d, $J_{\text{C-P}}$ = 8.2 Hz), 128.9, 128.8, 128.6, 128.4, 128.0, 127.5, 127.0 (d, $J_{\text{C-P}}$ = 68.7 Hz), 126.8, 122.1, 121.8, 121.8, 119.6 (d, $J_{\text{C-P}}$ = 2.7 Hz). ^{31}P NMR (CDCl_3 , 200 MHz) δ = 26.8, 9.2. HRMS (ESI): m/z calcd for $\text{C}_{40}\text{H}_{28}\text{AuClINO}_3\text{P}_2^+$ 864.0893 [$\text{M}+\text{MeCN}-\text{Cl}$] $^+$, found, 864.0898.

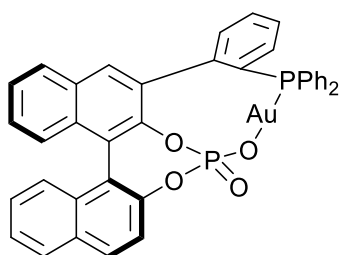


This compound **21** could be submitted to hydrolysis according to the following procedure.



To a solution of **21** (436 mg, 0.51 mmol) in THF (30 mL) was added 2M·HCl (30 mL). The resulting mixture was then stirred overnight at 50 °C. After cooling to room temperature, the THF was removed under vacuum and the resulting solution was extracted with DCM. Organic layers were dried over MgSO₄, filtered and evaporated under vacuum. The crude product was purified by flash column chromatography, giving product **1a** as a brown solid (350.0 mg, 0.42 mmol, 82%).

Synthesis of **22a**



To a suspension of Ag₂CO₃ (13.8 mg, 0.05 mmol, 0.5 equiv.) in DCM (5 mL), **1a** (84.1 mg, 0.1 mmol, 1 equiv.) was added. The mixture was stirred at room temperature for 1 h. Then the suspension was filtered on celite. The filter was rinsed with DCM and evaporated under vacuum. The product **22a** was obtained as an amorphous grey solid (100%).

IR (neat) ν_{\max} = 3656, 3410, 3054, 2923, 2852, 1621, 1592, 1509, 1480, 1436, 1417, 1330, 1263, 1227, 1101, 1080, 1052, 997, 967, 950, 869, 850, 816, 749, 712, 694. **HRMS (ESI):** m/z calcd for C₄₀H₂₉AuNO₄P₂⁺ 846.1232 [M+H+MeCN]⁺, found, 846.1232; **HRMS (ESI):** m/z calcd for C₃₉H₂₆AuO₆P₂⁻ 849.0876 [M+HCOO]⁻, found, 849.0867. [α]_D = +39 (c 1.12, CHCl₃).

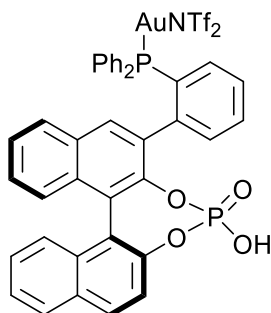
-NMR data in *d*⁵-Pyridine

¹H NMR (*d*⁵-Pyridine, 500 MHz) δ = 8.12-7.98 (m, 3H), 7.92 (d, J = 8.9 Hz, 1H), 7.89 (d, J = 8.2 Hz, 1H), 7.82-7.74 (m, 3H), 7.70 (td, J_1 = 7.6 Hz, J_2 = 1.8 Hz, 2H), 7.57 (d, J = 9.2 Hz, 1H), 7.50-7.44 (m, 3H), 7.44-7.32 (m, 7H), 7.30-7.27 (m, 1H), 7.20-7.08 (m, 4H). **¹³C NMR (*d*⁵-Pyridine, 125 MHz)** δ = 152.0 (d, J_{C-P} = 9.2 Hz), 149.4 (d, J_{C-P} = 8.2 Hz), 144.8 (d, J_{C-P} = 14.7 Hz), 136.4, 135.8 (d, J_{C-P} = 13.7 Hz), 135.6, 135.4 (d, J_{C-P} = 5.5 Hz), 134.7 (d, J_{C-P} = 12.8 Hz), 134.2 (d, J_{C-P} = 8.2 Hz), 133.8, 133.2, 133.1, 133.1 (d, J_{C-P} = 128.3 Hz), 132.1, 131.8 (d, J_{C-P} = 45.8 Hz), 130.9, 130.5 (d, J_{C-P} = 11.9 Hz), 130.4 (d, J_{C-P} = 79.7 Hz), 129.9, 129.9, 129.6, 129.3, 129.0, 128.7 (d, J_{C-P} = 9.2 Hz), 127.9, 127.4, 127.1, 126.7, 125.9, 125.0, 124.9 (d, J_{C-P} = 127.4 Hz), 123.8, 123.5, 122.8. **³¹P NMR (*d*⁵-Pyridine, 200 MHz)** δ = 22.9, 8.6.

-NMR data in CDCl₃

¹H NMR (CDCl₃, 500 MHz) δ = 7.80 (d, *J* = 8.2 Hz, 1H), 7.76 (d, *J* = 8.9 Hz, 1H), 7.65 (bs, 2H), 7.52-7.23 (m, 16H), 7.20-7.10 (m, 2H), 7.00-6.85 (m, 3H). ³¹P NMR (CDCl₃, 200 MHz) δ = 21.8, 8.3.

Synthesis of (S)-(2-(2,2'-diyl hydrogen phosphate-[1,1'-binaphthalen]-3-yl)phenyl) diphenylphosphine gold(I) bis(trifluoromethanesulfonyl)imide (23a)



To a suspension of AgNTf₂ (16.8 mg, 0.030 mmol) in toluene (1 mL), **1a** (16.8 mg, 0.020 mmol) was added. The mixture was stirred overnight at room temperature. Then the suspension was filtered on celite. The filter was rinsed with DCM and evaporated under vacuum. The product **23a** was obtained as an amorphous grey solid (17.8 mg, 0.016 mmol, 82%).

IR (neat) ν_{\max} = 3061, 1592, 1438, 1401, 1353, 1209, 1198, 1131, 1082, 1060, 1028, 958, 900, 830, 751. $[\alpha]_D = +170$ (*c* 1.16, CHCl₃). HRMS (ESI): *m/z* calcd for C₄₀H₂₉AuNO₄P₂⁺ 846.1232 [M-NTf₂+H+MeCN]⁺, found, 846.1224.

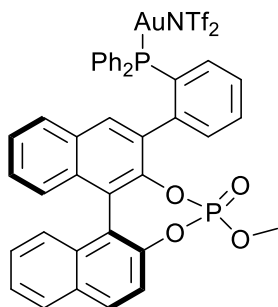
-NMR data in CDCl₃

¹H NMR (CDCl₃, 500 MHz) δ = 8.32 (s, 1H), 8.17 (d, *J* = 8.2 Hz, 1H), 7.95 (d, *J* = 8.2 Hz, 1H), 7.92 (d, *J* = 8.8 Hz, 1H), 7.65-7.59 (m, 2H), 7.59-7.52 (m, 3H), 7.52-7.37 (m, 6H), 7.37-7.28 (m, 3H), 7.27-7.18 (m, 3H), 6.96 (dd, *J*₁ = 12.3 Hz, *J*₂ = 7.9 Hz, 1H), 6.60-6.52 (m, 1H), 6.50-6.38 (m, 2H), 5.69 (bs, 1H). ¹³C NMR (CDCl₃, 125 MHz) δ = 146.2 (d, *J*_{C-P} = 5.5 Hz), 143.7 (d, *J*_{C-P} = 4.6 Hz), 142.0 (d, *J*_{C-P} = 12.8 Hz), 135.3 (d, *J*_{C-P} = 14.7 Hz), 134.4 (d, *J*_{C-P} = 13.7 Hz), 133.3 (d, *J*_{C-P} = 7.3 Hz), 133.1 (d, *J*_{C-P} = 8.2 Hz), 132.6 (d, *J*_{C-P} = 108.1 Hz), 132.5 (d, *J*_{C-P} = 1.8 Hz), 132.5, 131.6, 131.5 (d, *J*_{C-P} = 46.7 Hz), 131.5 (d, *J*_{C-P} = 1.8 Hz), 131.4, 130.7 (d, *J*_{C-P} = 6.4 Hz), 129.8 (d, *J*_{C-P} = 12.8 Hz), 129.3, 129.0, 128.9, 128.9, 128.6, 128.0, 127.8 (d, *J*_{C-P} = 20.2 Hz), 127.8, 127.4, 127.3 (d, *J*_{C-P} = 20.2 Hz), 127.0, 126.7, 126.4, 124.4 (d, *J*_{C-P} = 67.8 Hz), 123.4, 121.6 (d, *J*_{C-P} = 103.6 Hz), 120.8, 119.5, 118.3. ³¹P NMR (CDCl₃, 200 MHz) δ = 22.9, 2.9.

-NMR data in deuterated pyridine

¹H NMR (d⁵-Pyridine, 500 MHz) δ = 11.45 (bs, 1H), 8.05-7.97 (m, 3H), 7.93-7.80 (m, 3H), 7.75 (td, *J*₁ = 7.6 Hz, *J*₂ = 1.8 Hz, 1H), 7.69-7.28 (m, 15H), 7.25 (d, *J* = 7.5 Hz, 1H), 7.19 (d, *J* = 7.6 Hz, 1H), 7.11 (d, *J* = 8.5 Hz, 1H). ³¹P NMR (d⁵-Pyridine, 200 MHz) δ = 22.8, 7.6 (major isomer), 27.9, 7.1 (minor isomer).

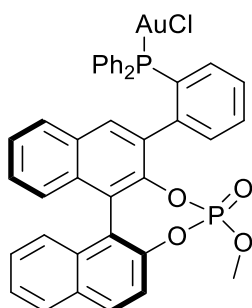
Synthesis of 76a



76b (16.7mg, 0.02 mmol, 1.0 equiv.) and AgNTf₂ (7.5 mg, 0.02 mmol, 1.0 equiv.) were added to 1 mL CDCl₃, the resulting solution was then stirred at room temperature for 2 h. The reaction solution was filtered and evaporated, giving product **76a** as a white solid (18.8 mg, 0.02 mmol, 79%).

IR (neat) ν_{\max} = 3059, 2961, 2927, 2856, 1537, 1438, 1400, 1354, 1300, 1261, 1210, 1193, 1131, 1102, 1055, 975, 957, 895, 830, 751, 693. **¹H NMR (CDCl₃, 500 MHz)** δ = 8.35 (s, 1H), 8.15 (d, J = 8.2 Hz, 1H), 7.96 (d, J = 8.8 Hz, 1H), 7.95 (d, J = 7.6 Hz, 1H), 7.85 (t, J = 6.3 Hz, 1H), 7.74 (t, J = 7.6 Hz, 1H), 7.59 (t, J = 7.6 Hz, 1H), 7.55 (t, J = 7.6 Hz, 1H), 7.55 (s, 1H), 7.51-7.42 (m, 5H), 7.38 (t, J = 7.6 Hz, 1H), 7.36 (t, J = 7.6 Hz, 1H), 7.29 (d, J = 8.8 Hz, 2H), 7.27-7.21 (m, 3H), 6.98 (dd, J_1 = 12.6 Hz, J_2 = 7.9 Hz, 1H), 6.58 (t, J = 6.9 Hz, 1H), 6.48 (t, J = 6.6 Hz, 2H), 3.71 (d, J = 11.7 Hz, 3H). **¹³C NMR (CDCl₃, 125 MHz)** δ = 146.9 (d, J_{C-P} = 11.0 Hz), 143.2 (d, J_{C-P} = 8.2 Hz), 141.9 (d, J_{C-P} = 12.8 Hz), 135.2 (d, J_{C-P} = 15.6 Hz), 134.4 (d, J_{C-P} = 13.7 Hz), 134.2 (d, J_{C-P} = 7.3 Hz), 132.9 (d, J_{C-P} = 9.2 Hz), 132.8, 132.6 (d, J_{C-P} = 106.3 Hz), 132.4 (d, J_{C-P} = 2.7 Hz), 131.9 (d, J_{C-P} = 2.7 Hz), 131.8 (d, J_{C-P} = 1.8 Hz), 131.6, 131.3, 131.3, 130.6 (q, J_{C-P} = 2.7 Hz), 129.7 (d, J_{C-P} = 11.9 Hz), 129.1, 128.9 (d, J_{C-P} = 10.1 Hz), 128.8 (d, J_{C-P} = 12.8 Hz), 128.4, 128.1, 128.0, 127.7 (d, J_{C-P} = 54.1 Hz), 127.3, 127.3, 126.9, 126.9, 126.2, 124.8 (d, J_{C-P} = 67.8 Hz), 122.2, 121.0, 120.8, 119.6 (d, J_{C-P} = 2.7 Hz), 118.3, 55.5 (d, J_{C-P} = 4.6 Hz). **³¹P NMR (CDCl₃, 200 MHz)** δ = 23.0, 2.3. **HRMS (ESI):** m/z calcd for C₄₁H₃₁AuNO₄P₂⁺ 860.1388 [M+MeCN-NTf₂]⁺, found, 860.1387. **[α]_D** = +28 (c 1.83, CHCl₃).

Synthesis of 76b



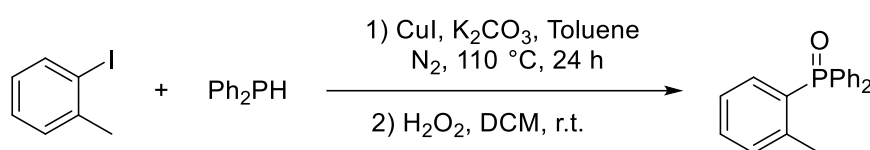
(S)-(2-(2,2'-diylchlorogenphosphate-[1,1'-binaphthalen]-3-yl)phenyl) diphenylphosphine gold(I) chloride **21** (122 mg, 0.14 mmol, 1.0 equiv.) was added to methanol (5 mL), the result solution was then stirred overnight at 35 °C. The methanol was removed and the crude product was purified by flash column chromatography, giving product **76b** as a white solid (69.0 mg, 0.08 mmol, 57%).

IR (neat) ν_{\max} = 3056, 2958, 2923, 2856, 1620, 1592, 1437, 1300, 1218, 1187, 1101, 1051, 993, 974, 955, 892, 829, 750, 694. **¹H NMR (CDCl₃, 500 MHz)** δ = 8.27 (s, 1H), 8.01-7.95 (m, 3H), 7.93 (d, J = 8.2 Hz, 1H), 7.71 (t, J = 7.6 Hz, 1H), 7.56-7.47 (m, 5H), 7.47-7.39 (m, 4H), 7.39-7.31 (m, 4H), 7.30-7.24 (m, 1H), 7.20 (d, J = 8.5

Hz, 1H), 7.05 (dd, $J_1 = 11.6$ Hz, $J_2 = 7.9$ Hz, 1H), 6.82-6.72 (m, 3H), 3.66 (d, $J = 11.7$ Hz, 3H). ^{13}C NMR (CDCl_3 , 125 MHz) $\delta = 147.0$ (d, $J_{\text{C-P}} = 11.0$ Hz), 143.6 (d, $J_{\text{C-P}} = 8.2$ Hz), 141.6 (d, $J_{\text{C-P}} = 12.8$ Hz), 134.8 (d, $J_{\text{C-P}} = 8.2$ Hz), 134.6 (d, $J_{\text{C-P}} = 9.2$ Hz), 134.4 (d, $J_{\text{C-P}} = 8.2$ Hz), 133.4, 133.2 (d, $J_{\text{C-P}} = 7.3$ Hz), 132.5 (d, $J_{\text{C-P}} = 43.1$ Hz), 131.9 (d, $J_{\text{C-P}} = 1.8$ Hz), 131.7 (d, $J_{\text{C-P}} = 1.8$ Hz), 131.6 (d, $J_{\text{C-P}} = 2.7$ Hz), 131.3, 131.1, 131.1, 131.0, 130.5 (d, $J_{\text{C-P}} = 143.0$ Hz), 129.5, 129.4, 129.3, 128.8, 128.7, 128.6, 128.6, 128.2, 127.8 (d, $J_{\text{C-P}} = 135.6$ Hz), 127.7, 127.6, 127.2, 126.8, 126.4 (d, $J_{\text{C-P}} = 64.2$ Hz), 122.2, 121.3, 119.7 (d, $J_{\text{C-P}} = 2.7$ Hz), 55.8 (d, $J_{\text{C-P}} = 5.5$ Hz). ^{31}P NMR (CDCl_3 , 200 MHz) $\delta = 27.2$, 1.2. HRMS (ESI): m/z calcd for $\text{C}_{41}\text{H}_{31}\text{AuNO}_4\text{P}_2^+$ 860.1388 $[\text{M}+\text{MeCN}\cdot\text{Cl}]^+$, found, 860.1390; m/z calcd for $\text{C}_{38}\text{H}_{25}\text{AuClO}_4\text{P}_2^-$ 839.0588 $[\text{M}\cdot\text{CH}_3^+]^-$, found, 839.0576.

2. Synthesis and Characterization of 1b

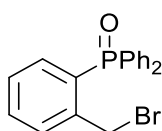
Synthesis of diphenyl(o-tolyl)phosphine oxide (**28**)¹²⁶



To a flask were added iodotoluene (530 mg, 2.4 mmol, 1.2 equiv.), Ph_2PH (0.35 mL, 2 mmol, 1 equiv.), K_2CO_3 (141.6mg, 3 mmol, 1.5 equiv.), CuI (38.1 mg, 0.2 mmol, 10 mol%) and PhMe (5 mL) under N_2 , then the mixture was allowed to heat to 110 °C for 24h. After the reaction solution cooling to room temperature, filtered with DCM to remove any insoluble residues. Then H_2O_2 (0.26 mL, 3 mmol, 1.5 equiv.) was added to the solution, several minutes later, the color of the solution turned brown, and then saturated $\text{Na}_2\text{S}_2\text{O}_3$ (aq.) was added to the mixture to quench the reaction and then extracted with DCM and H_2O , dried over MgSO_4 , filtered and concentrated under vacuum. The residue was purified by silica gel chromatography (hetp to 3:7 hetp/EtOAc) and gave product **28** in 81% yield (473 mg, 1.62 mmol).

^1H NMR (CDCl_3 , 500 MHz) $\delta = 7.62$ (dd, $J_1 = 11.9$ Hz, $J_2 = 7.6$ Hz, 4H), 7.49 (t, $J = 7.3$ Hz, 2H), 7.50 (td, $J_1 = 7.6$ Hz, $J_2 = 2.4$ Hz, 4H), 7.36 (t, $J = 7.3$ Hz, 1H), 7.23 (dd, $J_1 = 7.3$ Hz, $J_2 = 4.0$ Hz, 1H), 7.08 (t, $J = 6.4$ Hz, 1H), 7.00 (dd, $J_1 = 13.7$ Hz, $J_2 = 7.3$ Hz, 1H), 2.42 (s, 3H). ^{13}C NMR (CDCl_3 , 75 MHz) $\delta = 143.1$ (d, $J_{\text{C-P}} = 7.7$ Hz), 133.3 (d, $J_{\text{C-P}} = 6.0$ Hz), 132.6 (d, $J_{\text{C-P}} = 95.0$ Hz), 131.9, 131.8, 131.7, 131.6 (d, $J_{\text{C-P}} = 2.7$ Hz), 130.6 (d, $J_{\text{C-P}} = 103.2$ Hz), 128.4 (d, $J_{\text{C-P}} = 12.1$ Hz), 125.0 (d, $J_{\text{C-P}} = 12.6$ Hz), 21.5 (d, $J_{\text{C-P}} = 4.4$ Hz). ^{31}P NMR (CDCl_3 , 200 MHz) $\delta = 31.9$. HRMS (ESI): m/z : calculated for $\text{C}_{19}\text{H}_{17}\text{OP}$: $[\text{M}+\text{H}]^+$, 293.1090, found: 293.1094.

Synthesis of (2-(bromomethyl)phenyl)diphenylphosphine oxide (**31**)

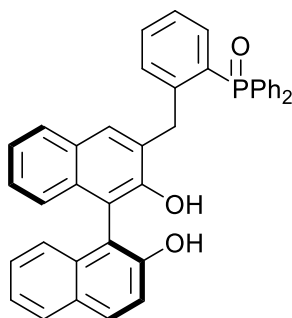


Diphenyl(o-tolyl)phosphine oxide (29.2 mg, 0.1 mmol, 1 equiv.), NBS (17.7 mg, 0.15 mmol, 1.5 equiv.) and AIBN (1.6 mg, 0.01 mmol, 10 mol%) were dissolved in CCl_4 (3 mL) under N_2 , the resulting solution was allowed to heat to reflux over weekend. After the reaction solution cooling to room temperature, water was added and the solution was extracted with DCM. Organic layers were dried over MgSO_4 , filtered and

evaporated under vacuum. The crude product was purified by flash column chromatography (Hept to Hept:EA = 1:1), giving product **31** as a white solid (26 mg, 0.07 mmol, 70%).

$^1\text{H NMR}$ (CDCl_3 , 500 MHz) δ = 7.66 (dd, J_1 = 11.9 Hz, J_2 = 7.3 Hz, 5H), 7.59-7.47 (m, 7H), 7.24 (t, J = 7.3 Hz, 1H), 7.03 (dd, J_1 = 13.7 Hz, J_2 = 7.6 Hz, 1H), 5.00 (s, 2H). $^{31}\text{P NMR}$ (CDCl_3 , 200 MHz) δ = 32.3. HRMS (ESI): m/z : calculated for $\text{C}_{19}\text{H}_{16}\text{BrOP}$: $[\text{M}+\text{H}]^+$, 371.0195, found: 371.0203.

Synthesis of (S)-2-((2,2'-dihydroxy-[1,1'-binaphthalen]-3-yl)methyl)phenyl)diphenylphosphine oxide (**32**)¹²⁷

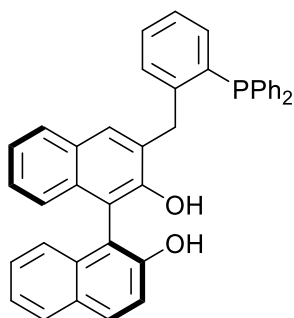


(2-(bromomethyl)phenyl)diphenylphosphine oxide **31** (40.7 mg, 0.11 mmol, 1.1 equiv.) and $\text{Pd}(\text{PPh}_3)_4$ (5.8 mg, 0.005 mmol, 5 mol%) were added to a flask, followed by anhydrous, degassed THF (2 mL) and H_2O (1 mL). The mixture was stirred at room temperature for 10 min. To this solution were added (S)-2-(2,2'-bis(methoxymethoxy)-[1,1'-binaphthalen]-3-yl)-4,4,5,5-tetramethyl-1,3,2-dioxaborolane **12** (50 mg, 1 mmol, 1.0 equiv.) and K_2CO_3 (41.5 mg, 0.3 mmol, 3 equiv.), and the solution was stirred at 100 °C for 24 h. After cooling to room temperature, water was added and the reaction mixture was extracted twice with methyl *tert*-butyl ether. The combined organic layers were dried over MgSO_4 , filtered and concentrated under vacuum.

The crude product was dissolved in a mixture of THF/MeOH 1:1 (80 mL), then *p*-TsOH· H_2O (19.0 mg, 0.1 mmol, 1 equiv.) was added to this solution and reaction mixture was stirred at 60 °C for 3 hours. After that, it was cooled down to room temperature and solvents were evaporated under reduced pressure. Water was added and the reaction mixture was extracted twice with DCM. The combined organic layers were dried over MgSO_4 , filtered and concentrated under vacuum. The crude product was purified by flash column chromatography giving the product **32** as a white solid (60.5 mg, 0.09 mmol, 91%).

IR (neat) ν_{max} = 3524, 3058, 1622, 1437, 1344, 1272, 1151, 1132, 1096, 748 cm^{-1} . $^1\text{H NMR}$ (CDCl_3 , 500 MHz) δ = 9.18 (s, 1H), 7.80-7.74 (m, 4H), 7.63-7.59 (m, 4H), 7.51-7.48 (m, 3H), 7.42-7.38 (m, 5H), 7.29 (d, J = 8.9 Hz, 1H), 7.26-7.20 (m, 2H), 7.14-7.08 (m, 3H), 7.04-7.01 (m, 2H), 6.93 (dd, J_1 = 14.0 Hz, J_2 = 7.6 Hz, 1H), 5.46 (s, 1H), 4.50 (d, J = 15.6 Hz, 1H), 4.41 (d, J = 15.6 Hz, 1H). $^{13}\text{C NMR}$ (CDCl_3 , 125 MHz) δ = 153.0, 151.9, 145.0 (d, $J_{\text{C-P}}$ = 7.7 Hz), 134.0, 133.8, 133.3 (d, $J_{\text{C-P}}$ = 13.2 Hz), 132.7 (d, $J_{\text{C-P}}$ = 2.2 Hz), 132.5, 132.4, 132.2 (d, $J_{\text{C-P}}$ = 9.9 Hz), 131.7 (d, $J_{\text{C-P}}$ = 98.3 Hz), 131.7 (d, $J_{\text{C-P}}$ = 10.4 Hz), 131.5, 131.0, 129.8, 129.5 (d, $J_{\text{C-P}}$ = 102.6 Hz), 129.4 (d, $J_{\text{C-P}}$ = 11.5 Hz), 128.8 (d, $J_{\text{C-P}}$ = 12.1 Hz), 128.7, 128.1, 127.7, 126.4 (d, $J_{\text{C-P}}$ = 7.1 Hz), 126.2 (d, $J_{\text{C-P}}$ = 12.6 Hz), 125.4, 124.9, 123.5, 123.2, 118.1, 115.4, 113.9, 36.5 (d, $J_{\text{C-P}}$ = 4.9 Hz). $^{31}\text{P NMR}$ (CDCl_3 , 200 MHz) δ = 36.0. HRMS (ESI): m/z : calculated for $\text{C}_{39}\text{H}_{29}\text{O}_3\text{P}$: $[\text{M}+\text{H}]^+$, 577.1927, found, 577.1941. $[\alpha]_{\text{D}} = -2$ (1.48, CHCl_3).

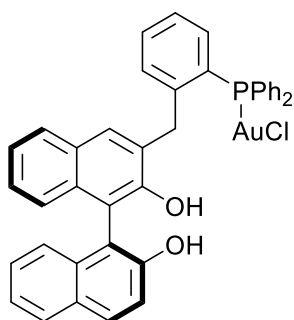
Synthesis of (S)-2-((2,2'-dihydroxy-[1,1'-binaphthalen]-3-yl)methyl)phenyl)diphenylphosphine (33)



(S)-2-((2,2'-dihydroxy-[1,1'-binaphthalen]-3-yl)methyl)phenyl)diphenylphosphine oxide **32** (1.06 g, 1.83 mmol, 1.0 equiv.) was dissolved in toluene (37 mL) at 0 °C, and then Cl₃SiH (3.75 mL, 36.64 mmol, 20 equiv.) were added to the solution dropwise at 0 °C. The reaction was then stirred at 90 °C for 24 h. After cooling to room temperature, the reaction solution was quenched with 2M·NaOH and then THF was evaporated under reduced pressure. 2M·NaOH was added to dissolve the precipitated solid and then extracted twice with DCM, dried over MgSO₄ and evaporated. The crude product was purified by flash column chromatography (eluent: heptane to DCM) giving the product **33** as a white solid (0.61 g, 1.09 mmol, 60%).

IR (neat) ν_{\max} = 3524, 3059, 3013, 1620, 1596, 1435, 1215, 752. **¹H NMR (CDCl₃, 500 MHz)** δ = 7.90 (d, J = 9.2 Hz, 1H), 7.84 (d, J = 7.9 Hz, 1H), 7.59 (d, J = 8.2 Hz, 1H), 7.44 (s, 1H), 7.34-7.23 (m, 16H), 7.19-7.15 (m, 2H), 7.12 (d, J = 8.2 Hz, 1H), 7.03 (d, J = 8.5 Hz, 1H), 6.98 (d, J_1 = 7.6 Hz, J_2 = 4.3 Hz, 1H), 5.22 (s, 1H), 4.97 (s, 1H), 4.50 (dd, J_1 = 35.4 Hz, J_2 = 16.5 Hz, 2H). **¹³C NMR (CDCl₃, 75 MHz)** δ = 153.0, 151.7, 144.9 (d, J_{C-P} = 25.8 Hz), 136.8, 136.7, 136.4 (d, J_{C-P} = 12.1 Hz), 134.2, 134.1 (d, J_{C-P} = 19.8 Hz), 133.0 (d, J_{C-P} = 95.0 Hz), 131.7, 131.7, 131.5, 130.2 (d, J_{C-P} = 4.9 Hz), 129.7, 129.7, 129.6, 129.4, 129.4, 128.8 (d, J_{C-P} = 10.4 Hz), 128.7 (d, J_{C-P} = 9.3 Hz), 128.6 (d, J_{C-P} = 2.2 Hz), 128.2, 127.6, 126.9 (d, J_{C-P} = 7.1 Hz), 124.5, 124.1 (d, J_{C-P} = 5.5 Hz), 124.0, 117.9, 111.5, 110.8, 35.2 (d, J_{C-P} = 23.1 Hz). **³¹P NMR (CDCl₃, 200 MHz)** δ = -14.7. $[\alpha]_D = -33$ (1.21, CHCl₃).

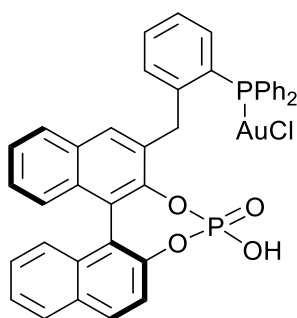
Synthesis of (S)-2-((2,2'-dihydroxy-[1,1'-binaphthalen]-3-yl)methyl)phenyl)diphenylphosphine gold(I) chloride (34)



(S)-2-((2,2'-dihydroxy-[1,1'-binaphthalen]-3-yl)methyl)phenyl)diphenylphosphine **33** (232.5 mg, 0.4 mmol, 1.0 equiv.) and Me₂S·AuCl (122.2 mg, 0.4 mmol, 1.0 equiv.) were dissolved in dry DCM (15 mL), and then the reaction solution was stirred at room temperature for 1 h. The solvent was evaporated and the crude product was purified by flash column chromatography (Heptane-DCM), yielding the product **34** as a white solid (267.3 mg, 0.34 mmol, 84%).

IR (neat) ν_{\max} = 3520, 3403, 3059, 3009, 1619, 1596, 1214, 1147, 1102, 750. **$^1\text{H NMR (CDCl}_3, 500 \text{ MHz)}$** δ = 7.93 (d, J = 8.9 Hz, 1H), 7.85 (d, J = 7.9 Hz, 1H), 7.67 (d, J = 7.9 Hz, 1H), 7.60-7.42 (m, 12H), 7.39 (d, J = 8.9 Hz, 1H), 7.35-7.22 (m, 6H), 7.12 (t, J = 9.2 Hz, 2H), 6.92 (dd, J_1 = 12.5 Hz, J_2 = 7.9 Hz, 1H), 6.20 (s, 1H), 5.08 (s, 1H), 4.50 (d, J = 17.4 Hz, 1H), 4.18 (d, J = 17.4 Hz, 1H). **$^{13}\text{C NMR (CDCl}_3, 75 \text{ MHz)}$** δ = 153.9, 151.1, 143.3, 135.2 (d, $J_{\text{C-P}}$ = 14.3 Hz), 134.5 (d, $J_{\text{C-P}}$ = 14.3 Hz), 133.7 (d, $J_{\text{C-P}}$ = 7.7 Hz), 133.1, 133.0 (d, $J_{\text{C-P}}$ = 8.8 Hz), 132.4 (d, $J_{\text{C-P}}$ = 2.7 Hz), 132.3 (d, $J_{\text{C-P}}$ = 9.9 Hz), 131.5, 130.2, 129.6, 129.5 (d, $J_{\text{C-P}}$ = 22.0 Hz), 129.3, 129.2, 128.8, 128.4 (d, $J_{\text{C-P}}$ = 24.2 Hz), 128.3, 128.3, 127.6, 127.5, 127.4, 127.2 (d, $J_{\text{C-P}}$ = 26.3 Hz), 124.4, 124.3 (d, $J_{\text{C-P}}$ = 14.3 Hz), 123.9, 118.8, 112.0, 110.8, 35.6 (d, $J_{\text{C-P}}$ = 11.5 Hz). **$^{31}\text{P NMR (CDCl}_3, 200 \text{ MHz)}$** δ = 26.7. $[\alpha]_{\text{D}}$ = -86 (0.96, CHCl₃).

Synthesis of (S)-(2-(2,2'-dihydroxyphosphate-[1,1'-binaphthalen]-3-yl)methyl)phenyl)diphenylphosphine gold(I) chloride (**1b**)

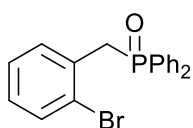


(S)-(2-(2,2'-dihydroxy-[1,1'-binaphthalen]-3-yl)phenyl)diphenylphosphine gold(I) chloride **34** (555 mg, 0.7 mmol, 1.0 equiv.) was added to 15 mL pyridine, then POCl₃ (0.08 mL, 0.84 mmol, 1.2 equiv.) was added to the solution dropwise under 0 °C. The resulting solution was stirred at room temperature for 24 h. After completion, it was quenched with water and the solvent were removed under vacuum. 2M·HCl and THF were added, and the reaction mixture was stirred overnight at 50 °C. After cooling to room temperature, the reaction solution was extracted with DCM and H₂O. Crude product was purified by flash column chromatography (eluent: DCM-MeOH-AcOH = 9:1:0.1) giving the product **1b** as a brown solid (506.4 mg, 0.6 mmol, 85%).

IR (neat) ν_{\max} = 3059, 2922, 2852, 1733, 1619, 1591, 1462, 1437, 1234, 1215, 1102, 1023, 954, 890, 749. **$^1\text{H NMR (CDCl}_3, 500 \text{ MHz)}$** δ = 7.91-7.90 (m, 2H), 7.76 (d, J = 8.2 Hz, 1H), 7.59-7.52 (m, 5H), 7.47-7.20 (m, 15H), 7.15-7.12 (m, 1H), 6.87-6.82 (m, 1H), 5.59 (s, 1H), 4.69 (d, J = 16.8 Hz, 1H), 4.57 (d, J = 17.1 Hz, 1H). **$^{31}\text{P NMR (CDCl}_3, 120 \text{ MHz)}$** δ = 26.3, 3.6. **HRMS (ESI): m/z :** calculated for C₃₉H₂₈AuO₄P₂⁺: [M-Cl]⁺, 819.1123, found, 819.1115, [M-H]⁻, 853.0744, found, 853.0761. $[\alpha]_{\text{D}}$ = +116 (0.80, CHCl₃).

3. Synthesis and Characterization of **1c**

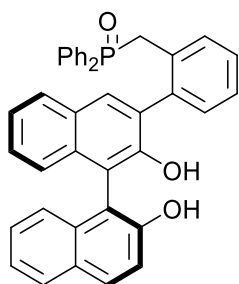
Synthesis of (2-bromobenzyl)diphenylphosphine oxide (**36**)



To a solution of diphenylphosphine oxide (404 mg, 2 mmol, 1 equiv.) in THF (10 mL) was added 60% NaH (168 mg, 4.2 mmol, 2.1 equiv.) slowly under N₂, the suspension was stirred at room temperature for 1.5 h, then 1-bromo-2-(bromomethyl)benzene (550 mg, 2.2 mmol, 1.1 equiv.) was added. The resulting solution was stirred at room temperature for another 3 h, and then extracted with DCM and H₂O. Combined organic layers were then dried over MgSO₄ and evaporated. The crude product was used directly for further synthesis without purification (680 mg, 1.83 mmol, 91%).

¹H NMR (CDCl₃, 500 MHz) δ = 7.73 (m, 4H), 7.58 (d, *J* = 7.3 Hz, 1H), 7.52-7.49 (m, 2H), 7.43-7.41 (m, 4H), 7.21 (t, *J* = 7.3 Hz, 1H), 7.03 (t, *J* = 7.6 Hz, 1H), 3.9 (d, *J* = 14.0 Hz, 2H). ³¹P NMR (CDCl₃, 200 MHz) δ = 29.9

Synthesis of (S)-2-(2,2'-dihydroxy-[1,1'-binaphthalen]-3-yl)benzyl)diphenylphosphine oxide (**38**)

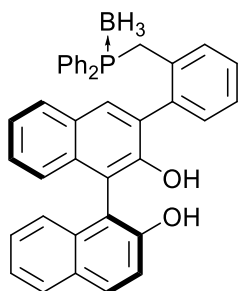


(2-bromobenzyl)diphenylphosphine oxide **36** (1.63 g, 4.4 mmol, 1.1 equiv.) and Pd(PPh₃)₄ (0.23 g, 0.2 mmol, 5 mol%) were added to a flask, followed by anhydrous, degassed THF (80 mL) and H₂O (40 mL). The mixture was stirred at room temperature for 10 min. To this solution were added (S)-2-(2,2'-bis(methoxymethoxy)-[1,1'-binaphthalen]-3-yl)-4,4,5,5-tetramethyl-1,3,2-dioxaborolane (2.3 g, 4 mmol, 1.0 equiv.) **12** and K₂CO₃ (1.66 g, 12 mmol, 3 equiv.), and the solution was stirred at 100 °C for 24 h. After cooling to room temperature, water was added and the reaction mixture was extracted twice with methyl *tert*-butyl ether. The combined organic layers were dried over MgSO₄, filtered and concentrated under vacuum. The residue was purified by silica gel chromatography (hep to 3:7 hep/EtOAc) and gave product **37** as 76% yield (2.03 g, 3.04 mmol).

The product **37** was dissolved in a mixture of THF/MeOH 1:1 (40 mL), then *p*-TsOH·H₂O (0.58 g, 3.04 mmol, 1 equiv.) was added to this solution and reaction mixture was stirred at 60 °C for 3 hours. After that, it was cooled down to room temperature and solvents were evaporated under reduced pressure. Water was added and the reaction mixture was extracted twice with DCM. The combined organic layers were dried over MgSO₄, filtered and concentrated under vacuum. The crude product was purified by flash column chromatography (eluent: 100% heptane to heptane/ethyl acetate, 30/70) giving the product **38** as a white solid (1.72 g, 2.98 mmol, 98%).

IR (neat) ν_{max} = 3514, 3059, 3020, 1623, 1436, 1214, 1174, 749. [α]_D = -4.95 (c 1.07, CHCl₃). ³¹P NMR (CDCl₃, 200 MHz) δ = 31.0.

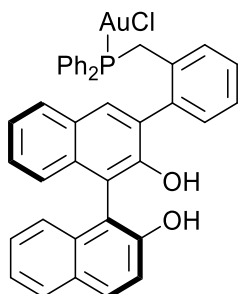
Synthesis of (S)-(2-(2,2'-dihydroxy-[1,1'-binaphthalen]-3-yl)benzyl)diphenylphosphine borane (39)



(S)-(2-(2,2'-dihydroxy-[1,1'-binaphthalen]-3-yl)benzyl)diphenylphosphine oxide **38** (288.3 mg, 0.5 mmol, 1.0 equiv.) was dissolved in toluene (5 mL) at 0 °C, and then Cl₃SiH (1.1 mL, 10 mmol, 20 equiv.) were added to the solution dropwise at 0 °C. The reaction was then stirred at 90 °C for 24 h. After cooling to room temperature, 94% DMS·BH₃ (0.74 mL, 12.5 mmol, 25 equiv.) was added dropwise and the resulting mixture was then react at room temperature for 1h. The reaction solution was quenched with saturated aqueous NaHCO₃ and then PhMe was evaporated under reduced pressure. Extracted twice with DCM and H₂O, dried over MgSO₄ and evaporated. The crude product was purified by flash column chromatography (eluent: heptane to hept:EA = 1:1) giving the product **39** as a white solid (235 mg, 4.1 mmol, 81%).

IR (neat) ν_{\max} = 3512, 3058, 2924, 2378, 1620, 1597, 1436, 1139, 751. **[α]_D** = -81.05 (1.05, CHCl₃). **³¹P NMR (CDCl₃, 120 MHz)** δ = 19.2, 18.1.

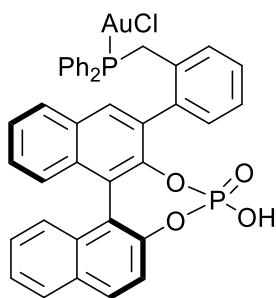
Synthesis of (S)-(2-(2,2'-dihydroxy-[1,1'-binaphthalen]-3-yl)benzyl)diphenylphosphine gold(I) chloride (40)



(S)-(2-(2,2'-dihydroxy-[1,1'-binaphthalen]-3-yl)benzyl)diphenylphosphine borane **39** (690.8 mg, 1.2 mmol, 1.0 equiv.) and DABCO (202.3 mg, 1.8 mmol, 1.5 equiv.) were dissolved in DCM (15 mL), the resulting solution was stirred at room temperature over weekend. The reaction solution was treated with celite and then Me₂S·AuCl (354.2 mg, 1.2 mmol, 1.0 equiv.) was added, and the reaction solution was stirred at room temperature for another 1 h. The solvent was evaporated and the crude product was purified by flash column chromatography, yielding the product **40** as a white solid (496.1 mg, 0.63 mmol, 52%).

IR (neat) ν_{\max} = 3512, 3059, 3007, 2971, 2376, 1739, 1621, 1597, 1436, 1366, 1229, 1217, 750. **[α]_D** = -69.44 (0.90, CHCl₃). **³¹P NMR (CDCl₃, 200 MHz)** δ = 32.2, 32.1.

Synthesis of (S)-(2-(2,2'-dihydroxyphosphate-[1,1'-binaphthalen]-3-yl)benzyl) diphenylphosphine gold(I) chloride (**1c**)

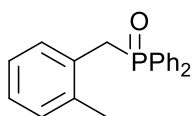


(S)-(2-(2,2'-dihydroxy-[1,1'-binaphthalen]-3-yl)phenyl)diphenylphosphine gold(I) chloride **40** (374.1 mg, 0.43 mmol, 1.0 equiv.) was added to 10 mL pyridine, then POCl₃ (0.05 mL, 0.52 mmol, 1.2 equiv.) was added to the solution dropwise under 0 °C. The resulting solution was stirred at room temperature for 24 h. After completion, it was quenched with water and the solvent were removed under vacuum. 2M·HCl and THF were added, and the reaction mixture was stirred overnight at 50 °C. After cooling to room temperature, the reaction solution was extracted with DCM and H₂O. Crude product was purified by flash column chromatography (eluent: DCM-MeOH-AcOH = 9:1:0.1) giving the product **1c** as a brown solid (361.1 mg, 0.42 mmol, 98%).

IR (neat) ν_{\max} = 3059, 3003, 2926, 2846, 1738, 1509, 1461, 1436, 1216, 1026, 9545, 751. $[\alpha]_D = +69.90$ (0.97, CHCl₃). **³¹P NMR (CDCl₃, 200 MHz)** δ = 31.9, 2.7 (major isomer), 30.5, 3.1 (minor isomer). **HRMS (ESI):** m/z calcd for C₃₉H₂₈AuO₄P₂⁺ 819.1123 [M-Cl]⁺, found, 819.1121; m/z calcd for C₃₉H₂₇AuClO₄P₂⁻ 853.0744 [M-H]⁻, found, 853.0729.

4. Synthesis and Characterization of **1d**

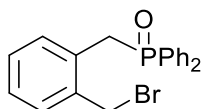
Synthesis of (2-methylbenzyl)diphenylphosphine oxide (**45**)



To a solution of diphenylphosphine (4.04 g, 20 mmol, 1 equiv.) in THF (100 mL) was added 60% NaH (1.68 g, 42 mmol, 2.1 equiv.) slowly under N₂, the suspension was stirred at room temperature for 1.5 h, then 1-(bromomethyl)-2-methylbenzene **44** (4.1 g, 22 mmol, 1.1 equiv.) was added. The resulting solution was stirred at room temperature for another 3 h, and then extracted with DCM and H₂O. Combined organic layers were then dried over MgSO₄ and evaporated. The crude product was used directly for further synthesis without purification (5.43 g, 17.7 mmol, 89%).

¹H NMR (CDCl₃, 500 MHz) δ = 7.67 (dd, $J_1 = 11.0$ Hz, $J_2 = 7.3$ Hz, 4H), 7.47 (t, $J = 7.0$ Hz, 7.41-7.38 (m, 4H), 7.06 (d, $J = 2.7$ Hz, 2H), 6.96-6.95 (m, 2H), 3.65 (d, $J = 14.0$ Hz, 2H), 2.14 (s, 3H). **³¹P NMR (CDCl₃, 200 MHz)** δ = 29.8.

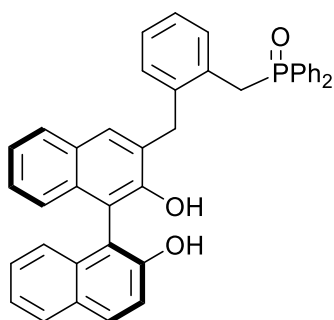
Synthesis of (2-(bromomethyl)benzyl)diphenylphosphine oxide (43)



(2-methylbenzyl)diphenylphosphine oxide **45** (5.43 g, 17.7 mmol, 1 equiv.), NBS (3.14 g, 26.6 mmol, 1.5 equiv.) and AIBN (0.29 g, 1.77 mmol, 10 mol%) were dissolved in CCl₄ (60 mL) under N₂, the resulting solution was allowed to heat to reflux over weekend. After the reaction solution cooling to room temperature, water was added and the solution was extracted with DCM. Organic layers were dried over MgSO₄, filtered and evaporated under vacuum. The crude product was purified by flash column chromatography (Hept to Hept:EA = 1:1), giving product **43** as a white solid (5.8 g, 15.1 mmol, 85%).

¹H NMR (CDCl₃, 500 MHz) δ = 7.70 (dd, J_1 = 11.0 Hz, J_2 = 7.9 Hz, 4H), 7.54 (t, J = 7.3 Hz, 2H), 7.48-7.45 (m, 4H), 7.31 (d, J = 7.3 Hz, 1H), 7.16 (t, J = 7.6 Hz, 1H), 7.04 (t, J = 7.6 Hz, 1H), 4.65 (s, 2H), 3.86 (d, J = 13.1 Hz, 2H). ³¹P NMR (CDCl₃, 200 MHz) δ = 29.7.

Synthesis of (S)-2-((2,2'-dihydroxy-[1,1'-binaphthalen]-3-yl)methyl)benzyl)diphenylphosphine oxide (46)⁴⁸

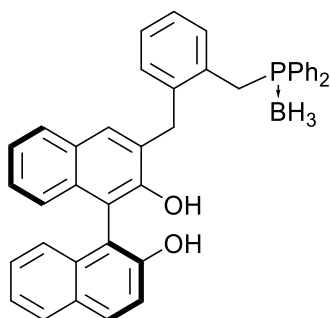


(2-(bromomethyl)benzyl)diphenylphosphine oxide **43** (4.24 g, 11 mmol, 1.1 equiv.) and Pd(PPh₃)₄ (0.58 g, 0.5 mmol, 5 mol%) were added to a flask, followed by anhydrous, degassed THF (100 mL) and H₂O (50 mL). The mixture was stirred at room temperature for 10 min. To this solution were added (S)-2-(2,2'-bis(methoxymethoxy)-[1,1'-binaphthalen]-3-yl)-4,4,5,5-tetramethyl-1,3,2-dioxaborolane **12** (5.0 g, 10 mmol, 1.0 equiv.) and K₂CO₃ (4.15 g, 30 mmol, 3 equiv.), and the solution was stirred at 100 °C for 24 h. After cooling to room temperature, water was added and the reaction mixture was extracted twice with methyl *tert*-butyl ether. The combined organic layers were dried over MgSO₄, filtered and concentrated under vacuum.

The crude product was dissolved in a mixture of THF/MeOH 1:1 (100 mL), then *p*-TsOH·H₂O (1.9 g, 10 mmol, 1 equiv.) was added to this solution and reaction mixture was stirred at 60 °C for 3 hours. After that, it was cooled down to room temperature and solvents were evaporated under reduced pressure. Water was added and the reaction mixture was extracted twice with DCM. The combined organic layers were dried over MgSO₄, filtered and concentrated under vacuum. The crude product was purified by flash column chromatography (eluent: 100% heptane to heptane/ethyl acetate, 30/70) giving the product **46** as a white solid (4.48 g, 7.6 mmol, 76%).

IR (neat) ν_{\max} = 3525, 3060, 1622, 1598, 1437, 1344, 1273, 1175, 1166, 1120, 819, 750. [α]_D = -6 (c 0.99, CHCl₃). ³¹P NMR (CDCl₃, 200 MHz) δ = 32.2.

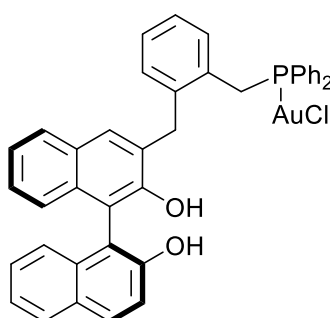
Synthesis of (S)-2-((2,2'-dihydroxy-[1,1'-binaphthalen]-3-yl)methyl)benzyl)diphenylphosphine borane (47)



(S)-2-((2,2'-dihydroxy-[1,1'-binaphthalen]-3-yl)methyl)benzyl)diphenylphosphine oxide **46** (2.36 g, 4 mmol, 1.0 equiv.) was dissolved in toluene (60 mL) at 0 °C, and then Cl₃SiH (8.2 mL, 80 mmol, 20 equiv.) was added to the solution dropwise at 0 °C. The reaction was then stirred at 90 °C for 24 h. After cooling to room temperature, 2M DMS·BH₃ (4 mL, 8 mmol, 2 equiv.) was added dropwise and the resulting mixture was then react at room temperature for 1h. The reaction solution was quenched with saturated aqueous NaOH and then PhMe was evaporated under reduced pressure. Extracted twice with DCM and H₂O, dried over MgSO₄ and evaporated. The crude product was purified by flash column chromatography (eluent: heptane to hept:EA = 1:1) giving the product **47** as a white solid (1.13 g, 2.0 mmol, 48%).

IR (neat) ν_{\max} = 3518, 3058, 3005, 3009, 2924, 2385, 1620, 1597, 1436, 1386, 1214, 1188, 1147, 1060, 751. **[α]_D** = -27 (c 1.42, CHCl₃). **¹H NMR (CDCl₃, 300 MHz)** δ = 7.98 (d, *J* = 8.7 Hz, 1H), 7.90 (d, *J* = 7.9 Hz, 1H), 7.72 (d, *J* = 7.9 Hz, 1H), 7.58 (t, *J* = 8.7 Hz, 4H), 7.50-7.05 (m, 17H), 6.93 (d, *J* = 7.2 Hz, 1H), 5.13 (br, 2H), 3.89 (s, 2H), 3.70 (d, *J* = 12.1 Hz, 1H), 0.86 (br, 3H). **³¹P NMR (CDCl₃, 200 MHz)** δ = 18.5.

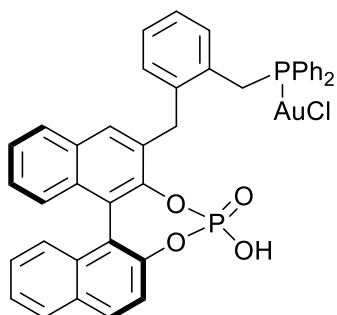
Synthesis of (S)-2-((2,2'-dihydroxy-[1,1'-binaphthalen]-3-yl)methyl)benzyl)diphenylphosphine gold(I) chloride (48)



(S)-2-((2,2'-dihydroxy-[1,1'-binaphthalen]-3-yl)methyl)benzyl)diphenylphosphine borane **47** (119.1 mg, 0.2 mmol, 1.0 equiv.) and DABCO (33.7 mg, 0.3 mmol, 1.5 equiv.) were dissolved in toluene (1 mL), the resulting solution was stirred at room temperature over weekend. The reaction solution was treated with celite and then evaporated, the residue was then dissolved in DCM (1 mL), and Me₂S·AuCl (58.9 mg, 0.2 mmol, 1.0 equiv.) was added, and the reaction solution was stirred at room temperature for another 1 h. The solvent was evaporated and the crude product was purified by flash column chromatography (Heptane:EA = 7:3), yielding the product **48** as a white solid (136.8 mg, 0.17 mmol, 85%).

IR (neat) ν_{\max} = 3518, 3403, 3059, 3006, 2920, 1738, 1620, 1506, 1436, 1384, 1216, 1147, 1104, 750. $[\alpha]_{\text{D}} = -29$ (c 0.99, CHCl_3). $^1\text{H NMR}$ (CDCl_3 , 300 MHz) δ = 7.97 (d, J = 8.9 Hz, 1H), 7.89 (d, J = 7.9 Hz, 1H), 7.75 (d, J = 7.7 Hz, 1H), 7.61-7.53 (m, 5H), 7.51-7.46 (m, 2H), 7.41-7.21 (m, 12H), 7.10-7.05 (m, 3H), 6.96 (d, J = 8.9 Hz, 1H), 5.15 (br, 2H), 4.09 (s, 2H), 3.87 (d, J = 12.4 Hz, 2H). $^{31}\text{P NMR}$ (CDCl_3 , 200 MHz) δ = 31.1.

Synthesis of (S)-(2-((2,2'-diylhydrogenphosphate-[1,1'-binaphthalen]-3-yl)methyl)benzyl)diphenylphosphine gold(I) chloride (1d)

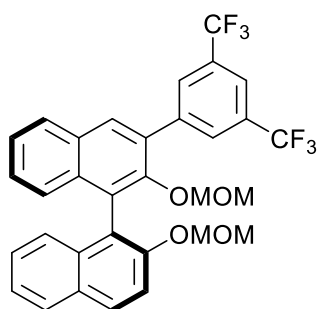


(S)-(2-((2,2'-dihydroxy-[1,1'-binaphthalen]-3-yl)methyl)benzyl)diphenylphosphine gold(I) chloride **48** (1 g, 1.24 mmol, 1.0 equiv.) was added to 30 mL pyridine, then POCl_3 (0.14 mL, 1.49 mmol, 1.2 equiv.) was added to the solution dropwise under 0 °C. The resulting solution was stirred at room temperature for 24 h. After completion, it was quenched with water and the solvent were removed under vacuum. 2M·HCl and THF were added, and the reaction mixture was stirred overnight at 50 °C. After cooling to room temperature, the reaction solution was extracted with DCM and H_2O . Crude product was purified by flash column chromatography (eluent: DCM-MeOH-AcOH = 9:1:0.1) giving the product **1d** as a brown solid (0.85 g, 0.97 mmol, 79%).

IR (neat) ν_{\max} = 3059, 3014, 2923, 1591, 1508, 1437, 1327, 1257, 1229, 1213, 1104, 1024, 956, 899, 751. $[\alpha]_{\text{D}} = +135$ (c 1.06, CHCl_3). $^1\text{H NMR}$ (CDCl_3 , 500 MHz) δ = 11.57 (s, 1H), 7.91 (t, J = 7.0 Hz, 2H), 7.83 (d, J = 8.2 Hz, 1H), 7.57 (s, 1H), 7.49 (t, J = 7.6 Hz, 1H), 7.45-7.15 (m, 16H), 7.07 (t, J = 7.0 Hz, 1H), 7.00 (t, J = 7.3 Hz, 1H), 6.96 (d, J = 7.3 Hz, 1H), 6.87 (d, J = 6.4 Hz, 1H), 4.13 (s, 2H), 3.73 (t, J = 13.1 Hz, 1H), 3.45 (t, J = 13.1 Hz, 1H). $^{31}\text{P NMR}$ (CDCl_3 , 200 MHz) δ = 31.0, 5.3.

5. Synthesis and Characterization of 1e

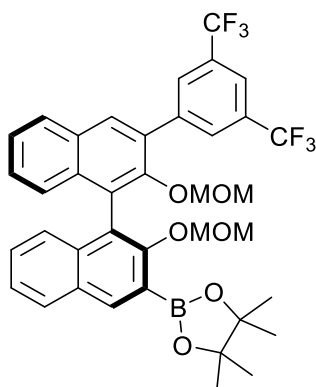
Synthesis of (S)-3-(3,5-bis(trifluoromethyl)phenyl)-2,2'-bis(methoxymethoxy)-1,1'-binaphthalene (53)



A mixture of 1-bromo-3,5-bis(trifluoromethyl)benzene (32.3 mg, 1.1 equiv., 0.11 mmol) and Pd(PPh₃)₄ (5.8 mg, 5 mol%, 0.005 mmol) in degassed THF (2 mL) and H₂O (1 mL) was stirred at room temperature for 10 min, (*S*)-2-(2,2'-bis(methoxymethoxy)-[1,1'-binaphthalen]-3-yl)-4,4,5,5-tetramethyl-1,3,2-dioxaborolane **12** (50 mg, 1 equiv., 0.1 mmol) and K₂CO₃ (41.5 mg, 3 equiv., 0.3 mmol) were then added to the solvent. The resulting mixture was allowed heated to 100 °C and stirred for 24 h. After the reaction completed, the reaction solution was cooling to room temperature and extracted with DCM for 3 times, then the combine organic layers was dried over MgSO₄ and the solvent was removed under vacuum, the residue was purified on silica gel and gave the product **53** as a white solid (54.6 mg, 0.093 mmol, 93% yield).

IR (neat) ν_{\max} = 3060, 2958, 2828, 1738, 1622, 1593, 1377, 1279, 1243, 1171, 1134, 1035, 1010, 965, 924, 893, 845, 810, 752, 682. **¹H NMR (CDCl₃, 300 MHz)** δ = 8.12 (s, 2H), 7.87-7.80 (m, 4H), 7.76 (d, *J* = 8.5 Hz, 1H), 7.50 (t, *J* = 9.0 Hz, 1H), 7.34-7.11 (m, 6H), 5.05(d, *J* = 7.0 Hz, 1H), 5.00 (d, *J* = 7.0 Hz, 1H), 4.29 (d, *J* = 6.0 Hz, 1H), 4.19 (d, *J* = 6.0 Hz, 1H), 3.14 (s, 3H), 2.33 (s, 3H). **¹³C NMR (CDCl₃, 75MHz)** δ = 153.1 (C_q), 151.2 (C_q), 141.6 (C_q), 134.3 (C_q), 134.1 (C_q), 133.6 (C_q), 131.7 (C_q, q, *J*_{C-CF₃} = 33.5 Hz), 131.1 (C_q), 130.6 (CH), 130.3 (CH, m), 129.9 (C_q), 128.4 (CH), 128.2 (CH), 127.2 (CH), 127.1 (CH), 126.2 (CH), 125.9 (CH), 125.6 (CH), 124.4 (CH), 123.7 (C_q, *J*_{CF₃} = 272.8 Hz), 121.0 (CH, m, *J*_{CH-CF₃} = 3.8 Hz), 120.3 (C_q), 116.4 (CH), 99.5 (CH₂), 94.9 (CH₂), 56.4 (CH₃), 56.1 (CH₃). **¹⁹F NMR (CDCl₃, 282 MHz)** δ = -62.66. **HRMS (ESI):** *m/z*: calculated for C₃₂H₂₄F₆NaO₄⁺: 609.1471 [M+Na]⁺, found, 609.1477. [α]_D = -50.3 (c 1.22, CHCl₃).

Synthesis of (*S*)-2-(3'-(3,5-bis(trifluoromethyl)phenyl)-2,2'-bis(methoxymethoxy)-[1,1'-binaphthalen]-3-yl)-4,4,5,5-tetramethyl-1,3,2-dioxaborolane (**54**)

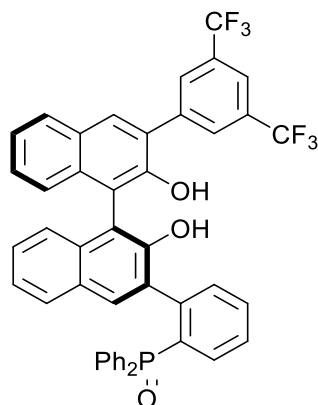


To a solution of (*S*)-3-(3,5-bis(trifluoromethyl)phenyl)-2,2'-bis(methoxymethoxy)-1,1'-binaphthalene **53** (833.5 mg, 1 equiv., 1.42 mmol) in 10 mL anhydrous THF was added n-BuLi (3.6 mL, 4 equiv., 5.68 mmol) dropwise via syringe at -78 °C, the resulting mixture was then stirred at -78 °C for 4 h and then isopropoxypinacolborate (1.16 mL, 4 equiv., 5.68 mmol) was added. The reaction mixture was stirred at room temperature overnight and then quenched with H₂O and extracted with methyl tert-butyl ether (MTBE). Combined organic layers were dried over MgSO₄ and evaporated under vacuum, the crude product was purified on silica gel and gives the product **54** as a white solid (668 mg, 0.94 mmol, 66% yield).

IR (neat) ν_{\max} = 3062, 2979, 2928, 2830, 1739, 1621, 1589, 1448, 1377, 1352, 1279, 1139, 1075, 1033, 975, 923, 844, 753, 707, 682. **¹H NMR (CDCl₃, 300 MHz)** δ = 8.45 (s, 1H), 8.15 (s, 2H), 7.87-7.80 (m, 4H), 7.38-7.29 (m, 2H), 7.25-7.11 (m, 4H), 4.90 (d, *J* = 6.2 Hz, 1H), 4.85 (d, *J* = 6.2 Hz, 1H), 4.22 (s, 2H), 2.35 (s, 3H), 2.29 (s, 3H), 1.33 (s, 6H), 1.32 (s, 6H). **¹³C NMR (CDCl₃, 75MHz)** δ = 157.4 (C_q), 151.4 (C_q), 141.7 (C_q), 140.2 (CH), 135.9 (C_q), 134.8 (C_q), 132.8 (C_q), 131.7 (C_q, q, *J*_{C-CF₃} = 32.9 Hz), 130.8 (C_q), 130.7 (CH), 130.4 (C_q), 130.2 (CH, q,

$J_{CH-CF_3} = 3.3$ Hz), 128.8 (CH), 128.0 (CH), 127.9 (CH), 127.5 (C_q), 127.1 (CH), 127.0 (CH), 126.4 (CH), 125.8 (CH), 125.1 (CH), 125.0 (C_q), 123.7 (C_q, $J_{CF_3} = 272.8$ Hz), 121.0 (CH, m, $J_{CH-CF_3} = 3.8$ Hz), 100.4 (CH₂), 99.1 (CH₂), 84.2 (C_q), 56.3 (CH₃), 55.7 (CH₃), 25.2 (CH₃), 25.0 (CH₃). **¹⁹F NMR (CDCl₃, 282 MHz)** $\delta = -62.59$. **HRMS (ESI):** m/z : calculated for C₃₈H₃₅BF₆NaO₆⁺: 735.2323 [M+Na]⁺, found, .735.2319. **$[\alpha]_D = +12.8$** (c 1.01, CHCl₃).

Synthesis of (S)-2-(3'-(3,5-bis(trifluoromethyl)phenyl)-2,2'-dihydroxy-[1,1'-binaphthalen]-3-yl)phenyl)diphenylphosphine oxide (55)



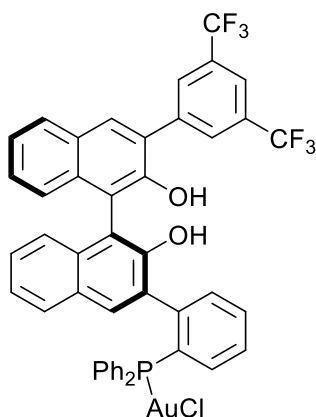
A mixture of (2-bromophenyl)diphenylphosphine oxide **18** (1.71 g, 1.2 equiv., 4.8 mmol) and Pd(PPh₃)₄ (0.23 g, 5 mol%, 0.2 mmol) in degassed THF (60 mL) and H₂O (30 mL) was stirred at room temperature for 10 min, then (S)-2-(3'-(3,5-bis(trifluoromethyl)phenyl)-2,2'-bis(methoxymethoxy)-[1,1'-binaphthalen]-3-yl)-4,4,5,5-tetramethyl-1,3,2-dioxaborolane **54** (2.86 g, 1 equiv., 4 mmol) and K₂CO₃ (1.66 g, 3 equiv., 12 mmol) were added to the mixture. The resulting solution was allowed heated to 100 °C and stirred at 100 °C for 24 h. After completed, the reaction solution was cooling to room temperature and extracted with DCM for 3 times, then the combine organic layers was dried over MgSO₄ and the solvent was removed under vacuum.

The crude product (2.37 g, 2.74 mmol) was dissolved in a mixture solvent of MeOH (30 mL) and THF (30 mL), then TsOH·H₂O (0.52 g, 1 equiv., 2.74 mmol) was added, the mixture was heated at 60 °C and stirred at 60 °C for 3 h. After cooling to room temperature, the solvent was evaporated under vacuum and then extracted with DCM and H₂O. Combined organic layers were dried over MgSO₄ and evaporated under vacuum, the crude product was purified on silica gel and gives the product **55** as a white solide (2.12 g, 2.74 mmol, 69% yield).

IR (neat) $\nu_{max} = 3522, 3059, 1591, 1438, 1377, 1279, 1178, 1132, 1015, 894, 751, 722, 682$. **¹H NMR (CDCl₃, 500 MHz)** $\delta = 8.27-8.23$ (m, 3H), 7.40 (s, 1H), 7.89 (d, $J = 8.2$ Hz, 1H), 7.86 (s, 1H), 7.71-7.64 (m, 4H), 7.50 (t, $J = 7.0$ Hz, 1H), 7.41-7.33 (m, 6H), 7.27-7.17 (m, 10H), 7.16 (s, 1H), 7.07 (d, $J = 7.6$ Hz, 1H), 5.88 (s, 1H). **¹³C NMR (CDCl₃, 125MHz)** $\delta = 151.5$ (C_q), 151.0 (C_q), 143.4 (C_q, d, $J_{C-P} = 7.3$ Hz), 141.4 (C_q), 134.6 (C_q), 133.9 (C_q), 133.6 (CH), 133.5 (CH), 133.3 (C_q), 132.6 (CH), 132.6 (CH), 132.5 (CH), 132.4 (CH), 132.3 (C_q), 132.3 (CH), 132.3 (CH), 132.1 (CH), 132.1 (CH), 131.9 (CH), 131.9 (CH), 131.5 (C_q), 131.4 (CH), 131.4 (CH), 131.4 (CH), 131.2 (CH), 131.2 (C_q), 130.6 (C_q), 130.5 (CH), 130.5 (CH), 130.5 (CH), 129.7 (C_q), 129.0 (C_q), 129.0 (C_q), 128.9 (C_q), 128.7 (CH), 128.6 (CH), 128.5 (CH), 128.4 (CH), 128.4 (CH), 127.5 (CH), 127.4 (CH), 127.4 (CH), 127.2 (CH), 127.0 (CH), 125.4 (CH), 125.2 (CH), 125.0 (C_q), 124.6 (C_q), 124.3 (C_q), 124.1 (CH), 123.9 (CH), 122.8 (C_q), 120.9 (CH, m, $J_{CH-CF_3} = 3.7$ Hz), 115.1 (C_q), 114.9 (C_q). **¹⁹F NMR (CDCl₃, 282 MHz)** $\delta = -62.54, -62.67$. **³¹P NMR (CDCl₃, 120 MHz)** $\delta = 30.1, 30.7$. **HRMS (ESI):** m/z : calculated for C₄₆H₃₀F₆O₃P⁺: 775.1831 [M+Na]⁺, found, 775.1831.

$[\alpha]_D = +23.2$ (c 1.16, CHCl₃).

Synthesis of (S)-(2-(3'-(3,5-bis(trifluoromethyl)phenyl)-2,2'-dihydroxy-[1,1'-binaphthalen]-3-yl)phenyl)diphenylphosphine gold(I) chloride (**57**)

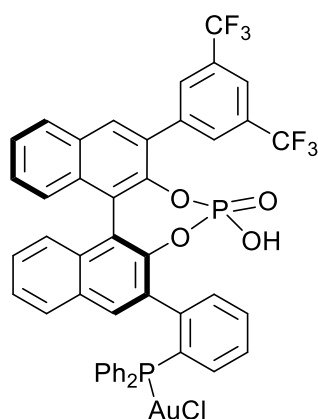


To a solution of (S)-(2-(3'-(3,5-bis(trifluoromethyl)phenyl)-2,2'-dihydroxy-[1,1'-binaphthalen]-3-yl)phenyl)diphenylphosphine oxide **55** (1.7 g, 1 equiv., 2.2 mmol) and Et₃N (2.2 g, 10 equiv., 22.0 mmol) in toluene was added Cl₃SiH (4.5 mL, 20 equiv., 44.0 mmol) dropwise at 0°C. After adding, the reaction solution was allowed heated to 90 °C and stirred at 90 °C for 24 h. After the reaction completed, the reaction solution was cooling to room temperature, then quenched with 2M-NaOH solution, and extract with DCM, then dried over MgSO₄ and evaporated under vacuum.

The residue (1.53 g, 2.0 mmol) was dissolved in DCM and then DMS·AuCl (0.6 g, 1 equiv., 2.0 mmol) was added, the mixture was stirred at room temperature for 1 h and then the solvent was removed under vacuum. The crude product was purified on silica gel and gave the product **57** as a white solid (1.73 g, 1.7 mmol, 72% yield).

IR (neat) ν_{\max} = 3521, 3380, 3016, 2971, 1739, 1621, 1598, 1499, 1437, 1376, 1360, 1279, 1230, 1217, 1178, 1134, 1102, 1014, 976, 895, 845, 750, 710, 694, 682. **¹H NMR (CDCl₃, 500 MHz)** δ = 8.23 (s, 2H), 8.00 (s, 1H), 7.92 (d, J = 8.1 Hz, 1H), 7.89 (s, 1H), 7.71-7.68 (m, 1H), 7.64-7.58 (m, 4H), 7.56-7.43 (m, 8H), 7.40-7.36 (m, 5H), 7.33-7.27 (m, 3H), 7.08 (d, J = 8.4 Hz, 1H), 6.72 (bs, 1H), 4.97 (bs, 1H). **¹³C NMR (CDCl₃, 125MHz)** δ = 151.1 (C_q), 150.3 (C_q), 143.8 (C_q, d, J_{C-P} = 15.9 Hz), 140.5 (C_q), 134.9 (CH), 134.8 (CH), 134.6 (CH), 134.5 (CH), 134.4 (CH), 134.2 (CH), 134.2 (C_q), 133.7 (CH), 133.7 (C_q), 133.7 (CH), 133.4 (CH), 132.2 (CH), 132.1 (CH, d, J_{C-P} = 2.3 Hz), 132.0 (C_q), 131.8 (CH, d, J_{C-P} = 2.3 Hz), 131.7 (C_q), 131.5 (CH, d, J_{C-P} = 2.3 Hz), 131.4 (C_q), 131.2 (C_q), 131.0 (C_q), 130.5 (C_q), 130.3-130.2 (CH, m), 130.1 (CH), 129.8 (C_q), 129.7 (CH), 129.6 (CH), 129.4 (C_q), 129.4 (C_q), 129.2 (CH), 129.1 (C_q), 129.1 (CH), 129.1 (C_q), 128.9 (CH), 128.8 (C_q), 128.8 (CH), 128.5 (C_q), 128.3 (CH), 128.3 (CH), 128.2 (CH), 128.2 (CH), 128.0 (C_q), 125.0 (CH), 124.8 (C_q), 124.7 (CH), 124.7 (CH), 124.3 (CH), 122.7 (C_q), 121.3 (CH, m, J_{C-CF_3} = 3.6 Hz), 113.3 (C_q), 112.5 (C_q). **¹⁹F NMR (CDCl₃, 282 MHz)** δ = -62.58, -62.73. **³¹P NMR (CDCl₃, 202 MHz)** δ = 26.5, 24.5. **[α]_D** = -88.1 (c 1.31, CHCl₃).

Synthesis of (S)-(2-(3'-(3,5-bis(trifluoromethyl)phenyl)-2,2'-dihydroxyphosphato-[1,1'-binaphthalen]-3-yl)phenyl)diphenylphosphine gold(I) chloride (1e)



To a solution of (S)-(2-(3'-(3,5-bis(trifluoromethyl)phenyl)-2,2'-dihydroxy-[1,1'-binaphthalen]-3-yl)phenyl)diphenylphosphine gold(I) chloride **57** (1.57g, 1.0 equiv., 1.58 mmol) in anhydrous pyridine (30 mL) was added POCl₃ (0.17 mL, 1.2 equiv., 1.9 mmol) slowly, the resulting mixture was stirred at room temperature for 24 h. After completion, it was quenched with water and the solvent were removed under vacuum. 2M-HCl and THF were added, and the reaction mixture was stirred overnight at 50 °C. After cooling to room temperature, the reaction solution was extracted with DCM and H₂O. Crude product was purified by flash column chromatography and gave the product **1e** as a white solid (1.38 g, 1.31 mmol, 83%).

IR (neat) ν_{\max} = 3053, 2364, 2219, 1009, 1922, 1714, 1478, 1438, 1323, 1280, 1176, 1138, 1100, 1086, 1022, 975, 964, 899, 849, 751, 691, 681. **[α]_D** = +73.2 (c 0.53, CHCl₃).

-NMR data in *d*⁶-DMSO

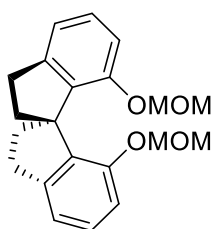
¹H NMR (*d*⁶-DMSO, 500 MHz, 343 K) δ = 11.13 (bs, 1H) 8.48 (s, 2H), 8.31 (m, 1H), 8.14-8.03 (m, 4H), 7.88 (s, 1H), 7.70 (tt, J_1 = 7.6 Hz, J_2 = 1.2 Hz, 1H), 7.59-7.48 (m, 9H), 7.43-7.38 (m, 4H), 7.32 (t, J = 7.6 Hz, 1H), 7.20-7.16 (m, 2H). 7.08 (s, 2H). **³¹P NMR (*d*⁶-DMSO, 202 MHz, 343K)** δ = 26.8, 0.7.

-NMR data in CDCl₃

¹H NMR (CDCl₃, 500 MHz) δ = 10.55 (bs, 1H), 8.40 (s, 1H), 8.09 (m, 5H), 7.70-7.41 (m, 11H), 7.37-7.09 (m, 7H), 6.88 (dd, J_1 = 11.9 Hz, J_2 = 8.2 Hz, 1H), 6.68-6.64 (m, 2H). **¹³C NMR (CDCl₃, 125 MHz)** δ = 143.8 (C_q, d, J_{C-P} = 9.2 Hz), 143.1 (C_q, d, J_{C-P} = 9.2 Hz), 140.8 (C_q, d, J_{C-P} = 15.9 Hz), 139.2 (C_q), 134.9 (CH, d, J_{C-P} = 13.7 Hz), 134.5 (CH, d, J_{C-P} = 14.7 Hz), 133.6 (CH), 133.4 (CH), 133.4 (CH), 133.3 (CH), 133.3 (CH), 133.0 (C_q), 132.7 (C_q), 132.6 (CH), 132.2 (CH), 132.0 (CH), 132.0 (C_q), 131.8 (CH), 131.7 (C_q), 131.7 (CH, d, J_{C-P} = 1.8 Hz), 131.5 (CH), 131.4 (C_q), 131.3 (C_q), 131.2 (C_q), 130.9 (C_q), 130.8 (C_q), 130.7 (C_q), 130.5 (C_q), 130.5 (C_q), 130.5 (C_q), 130.5 (C_q), 130.2 (bs, CH), 129.7 (CH), 129.5 (C_q), 129.4 (CH), 129.3 (CH), 129.0 (C_q), 128.7 (CH), 128.6 (CH), 128.5 (CH), 128.5 (CH), 128.4 (CH), 128.0 (C_q), 127.8 (CH), 127.2 (C_q), 127.0 (C_q), 126.8 (C_q), 126.7 (C_q), 126.7 (C_q), 124.5 (C_q), 123.3 (C_q), 122.7 (C_q), 122.3 (C_q), 121.7 (C_q), 121.4 (CH, m, C_{C-CF₃}), 120.2 (C_q). **¹⁹F NMR (CDCl₃, 282 MHz)** δ = -62.62, -62.69. **³¹P NMR (CDCl₃, 120 MHz)** δ = 27.7, 2.9 (major isomer), 26.3, 4.2 (minor isomer). **HRMS (ESI): *m/z*:** calculated for C₄₈H₃₁AuF₆NO₄P₂⁺: 1058.1293 [M+MeCN-Cl]⁺, found, 1058.1288.

6. Synthesis and Characterization of 1f

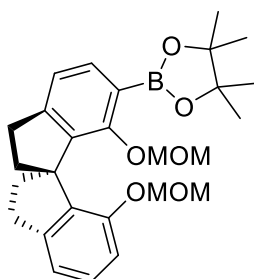
Synthesis of (*R*)-7,7'-bis(methoxymethoxy)-2,2',3,3'-tetrahydro-1,1'-spirobi[indene]^{64a} (**66**)



(*R*)-SPINOL **65a** (757 mg, 3.0 mmol, 1.0 equiv.) was dissolved in 10 mL of anhydrous THF and added dropwise to a suspension of NaH (60% wt in mineral oil, 360 mg, 9 mmol, 3 equiv.) in 5 ml of anhydrous THF at 0 °C. The reaction mixture was stirred for 1 h at room temperature and then MOM-Cl (0.69 mL, 9 mmol, 3 equiv.) was added dropwise at 0 °C. The reaction mixture was stirred for another 3 h at room temperature. When the reaction was completed, it was quenched with saturated aqueous NaHCO₃ and extracted twice with DCM. Combined organic layers were then dried over MgSO₄ and evaporated. The crude product was used directly for further synthesis without purification (885 mg, 2.6 mmol, 87%).

¹H NMR (CDCl₃, 500 MHz) δ = 7.00 (t, *J* = 7.9 Hz, 2H), 6.81 (dd, *J*₁ = 7.5 Hz, *J*₂ = 0.6 Hz, 2H), 6.66 (d, *J* = 8.1 Hz, 2H), 4.80 (d, *J* = 6.4 Hz, 2H), 4.73 (d, *J* = 6.4 Hz, 2H), 3.08-2.89 (m, 10H), 2.45-2.35 (m, 2H), 2.17-2.09 (m, 2H). ¹³C NMR (CDCl₃, 125MHz) δ = 153.7, 146.0, 137.8, 127.9, 117.9, 111.5, 93.7, 59.7, 55.7, 39.4, 32.0. HRMS (ESI): *m/z*: calculated for C₂₁H₂₄NaO₄⁺: 363.1567 [M+Na]⁺, found, 363.1567

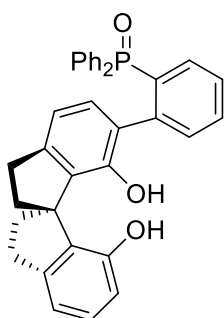
Synthesis of (*R*)-2-(7,7'-bis(methoxymethoxy)-2,2',3,3'-tetrahydro-1,1'-spirobi[inden]-6-yl)-4,4,5,5-tetramethyl-1,3,2-dioxaborolane (**67**)



To a solution of (*R*)-7,7'-bis(methoxymethoxy)-2,2',3,3'-tetrahydro-1,1'-spirobi[indene] **66** (344 mg, 1 mmol, 1.0 equiv.) in 140 mL of anhydrous THF, *n*-BuLi (0.8 mL, 1.2 mmol, 1.2 equiv.) was added dropwise at -78 °C. The reaction mixture was stirred at -78 °C for 6 hours, then isopropoxy-pinacolborate (0.3 mL, 1.2 mmol, 1.2 equiv.) was added to the flask and the resulting solution was allowed to warm to room temperature. It was stirred overnight at room temperature and then quenched with water and extracted with DCM. Combined organic layers were dried over MgSO₄ and evaporated. The crude product was purified by flash column chromatography on silica gel, yielding the product **67** as a white solid (193.9 mg, 0.42 mmol, 42%).

$^1\text{H NMR}$ (CDCl_3 , 500 MHz) δ = 7.62 (d, J = 7.3 Hz, 1H), 7.13 (t, J = 7.6 Hz, 1H), 7.04 (d, J = 7.6 Hz, 1H), 6.91 (d, J = 7.3 Hz, 1H), 6.83 (d, J = 7.9 Hz, 1H), 4.94 (d, J = 6.4 Hz, 1H), 4.89 (d, J = 6.4 Hz, 1H), 4.81 (d, J = 5.5 Hz, 1H), 4.68 (d, J = 5.5 Hz, 1H), 3.17 (s, 3H), 3.10-3.05 (m, 4H), 2.92 (s, 3H), 2.69-2.63 (m, 1H), 2.38-2.32 (m, 1H), 2.26-2.19 (m, 2H), 1.34 (s, 6H), 1.33 (s, 6H). $^{13}\text{C NMR}$ (CDCl_3 , 125 MHz) δ = 159.9, 153.9, 149.9, 145.7, 141.1, 137.8, 136.0, 127.9, 119.6, 117.9, 111.5, 100.5, 93.6, 83.5, 59.6, 56.6, 55.8, 38.9, 38.8, 31.8, 31.6, 24.9, 24.8.

Synthesis of (*R*)-(2-(7,7'-dihydroxy-2,2',3,3'-tetrahydro-1,1'-spirobi[inden]-6-yl)phenyl)diphenylphosphine oxide (**69**)



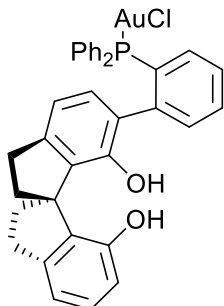
(2-bromophenyl)diphenylphosphine oxide **18** (373.1 mg, 1.05 mmol, 2 equiv.) and $\text{Pd}(\text{PPh}_3)_4$ (45.4 mg, 0.04 mmol, 7.5 mol%) were added to a flask, followed by anhydrous, degassed THF (16 mL) and MeOH (0.68 mL). The mixture was stirred at room temperature for 10 min. To this solution were added (*R*)-2-(7,7'-bis(methoxymethoxy)-2,2',3,3'-tetrahydro-1,1'-spirobi[inden]-6-yl)-4,4,5,5-tetramethyl-1,3,2-dioxaborolane **67** (244.4 mg, 0.52 mmol, 1.0 equiv.) and 1M K_2CO_3 (1.63 mL, 24.9 mmol, 3 equiv.) aqueous solution, the resulting solution was stirred at 100 °C for 22 h. After cooling to room temperature, water was added and the reaction mixture was extracted twice with methyl *tert*-butyl ether. The combined organic layers were dried over MgSO_4 , filtered and concentrated under vacuum.

The crude product was dissolved in a mixture of THF/MeOH 1:1 (10 mL), then *p*-TsOH·H₂O (78.4 mg, 0.412 mmol, 1 equiv.) was added to this solution and reaction mixture was stirred at 60 °C for 3 h. After that, it was cooled down to room temperature and solvents were evaporated under reduced pressure. Water was added and the reaction mixture was extracted twice with DCM. The combined organic layers were dried over MgSO_4 , filtered and concentrated under vacuum. The crude product was purified by flash column chromatography giving the product **69** as a white solid (two rotamers, major/minor = 1/0.6) (218.8 mg, 0.41 mmol, 79%).

$^1\text{H NMR}$ (CDCl_3 , 500 MHz) δ = 8.30 (s, 1H_{minor}, OH), 7.79-7.71 (m, 1H_{major}, 4H_{minor}), 7.60-7.55 (m, m, 3H_{major}, 1H_{minor}), 7.50-7.46 (m, 3H_{major}, 3H_{minor}), 7.43-7.34 (m, 3H_{major}, 6H_{minor}), 7.32-7.26 (m, 4H_{major}), 7.17-7.11 (m, 1H_{major}, 2H_{minor}), 7.05 (t, J = 7.6 Hz, 1H_{minor}), 6.94 (d, J = 7.9 Hz, 2H_{major}), 6.83 (d, J = 7.3 Hz, 1H_{minor}), 6.60 (d, J = 7.6 Hz, 1H_{minor}), 6.45-6.43 (m, 2H_{major}), 6.31 (s, 1H_{major}, OH), 6.28 (d, J = 7.6 Hz, 1H_{major}), 4.65 (s, 1H_{minor}, OH), 3.09-2.86 (m, 4H_{major}, 4H_{minor}), 2.66-2.58 (m, 1H_{minor}), 2.40-2.14 (m, 4H_{major}, 3H_{minor}). $^{13}\text{C NMR}$ (CDCl_3 , 125 MHz) δ = 153.08, 152.58, 152.56, 151.29, 150.58, 145.86, 145.41, 145.08, 144.84, 144.53, 144.47, 144.31, 144.23, 138.72, 137.59, 136.53, 135.21, 135.16, 134.46, 133.20, 133.13, 133.05, 133.03, 132.97, 132.82, 132.77, 132.72, 132.62, 132.54, 132.43, 132.38, 132.29, 132.25, 132.22, 132.11, 132.06, 131.98, 131.95, 131.93, 131.88, 131.82, 131.79, 131.73, 131.66, 131.58, 131.51, 131.43, 131.34, 131.25, 131.22, 131.18, 131.08, 131.00, 130.82, 130.67, 130.61, 130.49, 130.23, 129.86, 129.10, 129.07, 128.94, 128.91, 128.86, 128.78, 128.73, 128.68, 128.63, 128.48, 128.43, 128.38, 128.36, 128.30, 128.27, 128.19, 128.09, 128.00, 126.95, 126.88, 126.85, 126.77, 119.78, 118.74, 117.85, 117.06, 116.97, 113.84, 58.98, 58.61, 37.97, 37.77, 37.58,

31.48, 31.30, 31.23, 31.16. ^{31}P NMR (CDCl_3 , 200 MHz) δ = 32.5, 31.7. HRMS (ESI): m/z : calculated for $\text{C}_{35}\text{H}_{30}\text{O}_3\text{P}^+$: 529.1927 $[\text{M}+\text{Na}]^+$, found, 529.1928.

Synthesis of (*R*)-((2-(7,7'-dihydroxy-2,2',3,3'-tetrahydro-1,1'-spirobi[inden]-6-yl)phenyl)diphenylphosphine)gold(I) chloride (70)

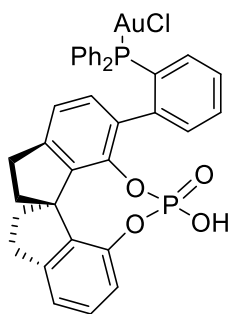


(*R*)-(2-(7,7'-dihydroxy-2,2',3,3'-tetrahydro-1,1'-spirobi[inden]-6-yl)phenyl) diphenylphosphine oxide **69** (100.1 mg, 0.19 mmol, 1.0 equiv.) was dissolved in toluene (7 mL) at 0 °C, and then Cl_3SiH (0.4 mL, 3.79 mmol, 20 equiv.) were added to the solution dropwise at 0 °C. The reaction was then stirred at 90 °C for 24 h. After cooling to room temperature, the reaction solution was quenched with 2M-NaOH and then PhMe was evaporated under reduced pressure. 2M-NaOH was added to dissolve the precipitated solid and then extracted twice with DCM, dried over MgSO_4 and evaporated.

The crude product and $\text{Me}_2\text{S}\cdot\text{AuCl}$ (56 mg, 0.19 mmol, 1.0 equiv.) were dissolved in dry DCM (10 mL), and then the reaction solution was stirred at room temperature for 1 h. The solvent was evaporated and the crude product was purified by flash column chromatography, yielding the product **70** as a white solid (two rotamers, major/minor = 1/0.6) (96 mg, 0.13 mmol, 68%).

^1H NMR (CDCl_3 , 500 MHz) δ = 7.57-7.44 (m, 17.7H), 7.41-7.34 (m, 5.5H), 7.22 (dd, J_1 = 11.0 Hz, J_2 = 8.2 Hz, 1H_{major}), 7.15-7.10 (m, 2.4H), 6.88-6.86 (m, 2.3H), 6.84 (d, J = 7.3 Hz, 0.7H_{minor}), 6.81 (d, J = 7.3 Hz, 1H_{major}), 6.77 (d, J = 7.6 Hz, 1H_{major}), 6.74 (d, J = 8.2 Hz, 1H_{major}), 6.64 (d, J = 7.6 Hz, 0.6H_{minor}), 5.77 (s, 0.8H, OH_{major}), 4.68 (s, 0.6H, OH_{minor}), 4.66 (s, 0.8H, OH_{major}), 4.42 (s, 0.6H, OH), 3.29-3.16 (m, 1.8H), 3.10-2.88 (m, 5.9H), 2.55-2.45 (m, 1.9H) 2.38-2.29 (m, 3.1 H), 2.26-2.20 (m, 1.6H), 2.15-2.09 (m, 1.2H). ^{13}C NMR (CDCl_3 , 125MHz) δ = 177.46, 164.29, 158.23, 153.48, 153.10, 153.06, 150.20, 149.99, 149.95, 147.50, 147.44, 146.39, 146.28, 146.23, 144.33, 144.20, 143.81, 134.86, 134.82, 134.55, 134.48, 134.37, 134.27, 134.17, 134.07, 133.97, 133.86, 133.60, 133.54, 133.25, 133.19, 132.56, 131.76, 131.66, 131.60, 131.55, 131.42, 131.31, 131.21, 130.87, 130.82, 130.69, 130.35, 130.29, 129.99, 129.90, 129.86, 129.80, 129.39, 129.36, 129.29, 129.26, 129.11, 129.00, 128.90, 128.77, 128.43, 128.11, 127.94, 127.91, 127.86, 127.83, 127.76, 127.69, 127.42, 127.37, 125.70, 125.65, 117.75, 117.41, 116.50, 116.48, 115.73, 115.35, 115.34, 114.27, 114.19, 112.61, 100.31, 100.22, 100.16, 93.94, 58.28, 57.85, 38.60, 38.44, 38.13, 37.42, 31.65, 31.49, 31.31, 31.25. ^{31}P NMR (CDCl_3 , 200 MHz) δ = 25.1, 22.9. HRMS (ESI): m/z : calculated for $\text{C}_{35}\text{H}_{29}\text{AuO}_2\text{P}^+$: 709.1565 $[\text{M}-\text{Cl}]^+$, found, 709.1569; m/z : calcd for $\text{C}_{35}\text{H}_{28}\text{AuClO}_2\text{P}^-$ 743.1186 $[\text{M}-\text{H}]^-$, found, 743.1187.

Synthesis of ((2-((5*R*,12*R*)-12-hydroxy-12-oxido-4,5,6,7-tetrahydroindeno[7,1-*de*:1',7'-*fg*][1,3,2]dioxaphosphocin-1-yl)phenyl)diphenylphosphine)gold(I) chloride (**1f**)



(*R*)-((2-(7,7'-dihydroxy-2,2',3,3'-tetrahydro-1,1'-spirobi[indene]-6-yl)phenyl)diphenylphosphine)gold(I) chloride **70** (172.5 mg, 0.23 mmol, 1.0 equiv.) was added to 5 mL pyridine, then POCl₃ (0.026 mL, 0.28 mmol, 1.2 equiv.) was added to the solution dropwise under 0 °C. The resulting solution was stirred at room temperature for 24 h. After completion, H₂O was added and the resulting mixture was stirred at 110 °C overnight. After cooling to room temperature, the solvent were removed under vacuum and the residue was extracted with DCM and H₂O. Crude product was purified by flash column chromatography giving the product **1f** as a brown solid (two rotamers, major/minor = 1/0.3) (90.9 mg, 0.11 mmol, 49%).

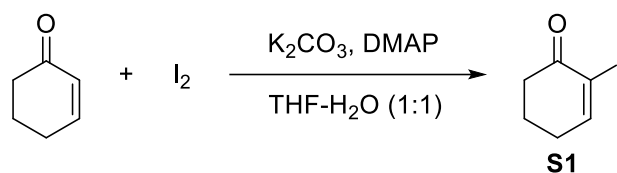
¹H NMR (CDCl₃, 500 MHz) δ = 7.76-7.72 (m, 0.6H_{minor}), 7.63-7.60 (m, 1.5H), 7.57-7.52 (m, 1.7H), 7.48-7.43 (m, 3.4H), 7.39-7.20 (m, 8.9H), 7.18-7.03 (m, 7.7H), 6.95 (d, *J* = 7.6 Hz, 0.3H_{minor}), 6.86 (d, *J* = 7.3 Hz, 0.3H_{minor}), 6.67-6.54 (m, 3.7H), 3.31-3.25 (m, 1H_{major}), 3.17-3.11 (m, 0.3H_{minor}), 3.05-2.98 (m, 1.6H), 2.89-2.83 (m, 1.3H), 2.76 (dd, *J*₁ = 16.2 Hz, *J*₂ = 7.9 Hz, 1H_{major}), 2.55 (dd, *J*₁ = 20.8 Hz, *J*₂ = 10.7 Hz, 0.3H_{minor}), 2.44 (dd, *J*₁ = 12.2 Hz, *J*₂ = 6.1 Hz, 1H_{major}), 2.33 (dd, *J*₁ = 11.9 Hz, *J*₂ = 6.1 Hz, 0.3H_{minor}), 2.30-2.26 (m, 0.3H_{minor}), 2.23 (dd, *J*₁ = 11.6 Hz, *J*₂ = 6.7 Hz, 1H_{major}), 2.15-2.11 (m, 0.3H_{minor}), 2.08-2.02 (m, 1H_{major}), 1.86-1.79 (m, 1H_{major}). ³¹P NMR (CDCl₃, 200 MHz) δ = 25.4, -8.4 (minor isomer), 23.8, -8.6 (major isomer).

Chapter 2. Application of the TCDC strategy in enantioselective catalysis involving 2-alkynyl-ketones

Part 1. Application of the TCDC strategy in cyclization/nucleophilic addition reaction sequences

1.1. Synthesis of enones **71** and indoles **74**

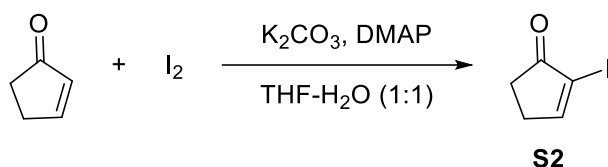
Synthesis of 2-iodocyclohex-2-en-1-one (**S1**)^{67a}



To a stirred solution of cyclohex-2-en-1-one (4.05 mL, 42 mmol, 1.0 equiv.) in a 1:1 mixture of THF-H₂O (200 mL) was added K₂CO₃ (6.9 g, 50 mmol, 1.2 equiv.), I₂ (15.9 g, 63 mmol, 1.5 equiv.) and 4-

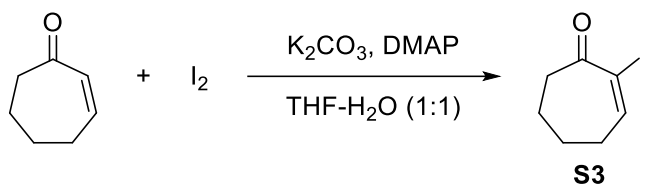
dimethylaminopyridine (DMAP) (1.02 g, 8.3 mmol, 0.2 equiv.) successively. Then the reaction was stirred at room temperature for 2 h. Upon completion, the reaction solution mixture was diluted with ethyl acetate and washed with saturated aqueous $\text{Na}_2\text{S}_2\text{O}_3$ and aqueous 0.1 M HCl successively. The mixture was subsequently extracted with ethyl acetate and dried over MgSO_4 . Crude product was purified by flash column chromatography (heptane to 20% EtOAc-Heptane), giving product **S1** as a white solid (7.17 g, 32 mmol, 77%).

Synthesis of 2-iodocyclopent-2-en-1-one (**S2**)^{67a}



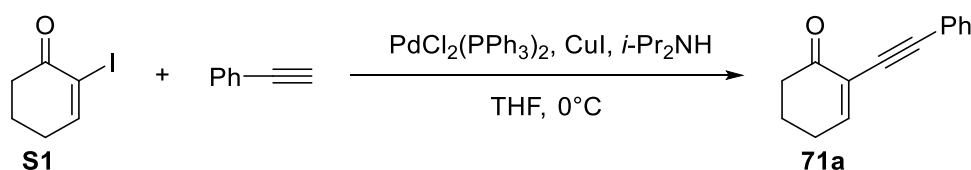
Compound **S2** was prepared by following the general procedure for the synthesis of **S1**. To a stirred solution of cyclopent-2-en-1-one (0.42 mL, 5 mmol, 1.0 equiv.) in a 1:1 mixture of THF- H_2O (30 mL) was added K_2CO_3 (0.83 g, 6 mmol, 1.2 equiv.), I_2 (1.9 g, 7.5 mmol, 1.5 equiv.) and 4-dimethylaminopyridine (DMAP) (0.13 g, 1 mmol, 0.2 equiv.) successively. Then the reaction was stirred at room temperature for 2 h. Upon completion, the reaction solution mixture was diluted with ethyl acetate and washed with saturated aqueous $\text{Na}_2\text{S}_2\text{O}_3$ and aqueous 0.1M-HCl successively. The mixture was subsequently extracted with ethyl acetate and dried over MgSO_4 . Crude product was purified by flash column chromatography (heptane to 20% EtOAc-Heptane), giving product **S2** as a pale yellow solid (0.57 g, 2.7 mmol, 55%).

Synthesis of 2-iodocyclohept-2-en-1-one (**S3**)^{67a}



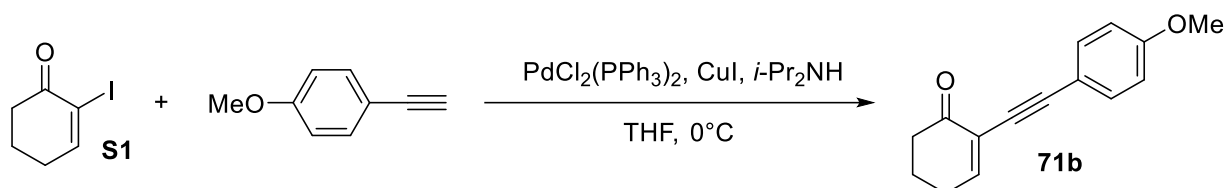
Compound **S3** was prepared by following the general procedure for the synthesis of **S1**. To a stirred solution of cyclohept-2-en-1-one (0.34 mL, 3.0 mmol, 1.0 equiv.) in a 1:1 mixture of THF- H_2O (14 mL) was added K_2CO_3 (0.50 g, 3.6 mmol, 1.2 equiv.), I_2 (1.14 g, 4.5 mmol, 1.5 equiv.) and 4-dimethylaminopyridine (DMAP) (0.08 g, 0.6 mmol, 0.2 equiv.) successively. Then the reaction was stirred at room temperature for 2 h. Upon completion, the reaction solution mixture was diluted with ethyl acetate and washed with saturated aqueous $\text{Na}_2\text{S}_2\text{O}_3$ and aqueous 0.1M-HCl successively. The mixture was subsequently extracted with ethyl acetate and dried over MgSO_4 . Crude product was purified by flash column chromatography (heptane to 20% EtOAc-Heptane), giving product **S3** as a pale yellow oil (0.37 g, 1.6 mmol, 52%).

Synthesis of 2-(phenylethynyl)cyclohex-2-en-1-one (**71a**)^{67a}



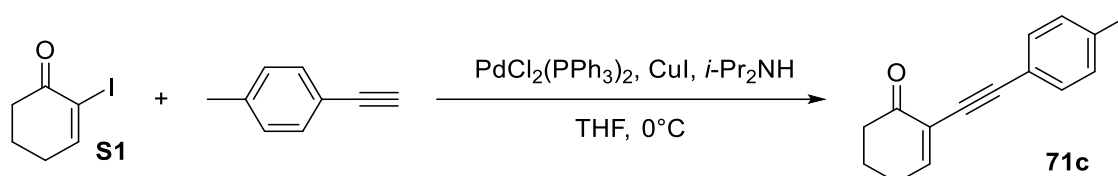
A solution of 2-iodo-cyclohexenone (430.0 mg, 1.94 mmol, 1.0 equiv.) in THF (5.1 mL) was treated with $\text{PdCl}_2(\text{PPh}_3)_2$ (69.0 mg, 0.1 mmol, 5 mol%) and CuI (37.0 mg, 0.19 mmol, 10 mol%) and cooled down to 0 °C under an Ar atmosphere and in the dark. After 10 min of stirring, phenylacetylene (0.44 mL, 409.2 mg, 4.01 mmol) and diisopropyl amine (0.82 mL, 59.0 mg, 5.85 mmol) were added, and the resulting yellow to dark brown solution was stirred at 0 °C. The reaction mixture was partitioned between CH_2Cl_2 and 0.5 N aqueous HCl solution. The aqueous layer was extracted three times with CH_2Cl_2 and the combined organic phases were washed with brine, dried over MgSO_4 , filtered and concentrated under vacuum. The crude product was purified by flash column chromatography to yield alkyne **71a** as a yellow solid (334 mg, 1.75 mmol, 88%).

Synthesis of 2-(phenylethynyl)cyclohex-2-en-1-one (**71b**)⁸¹



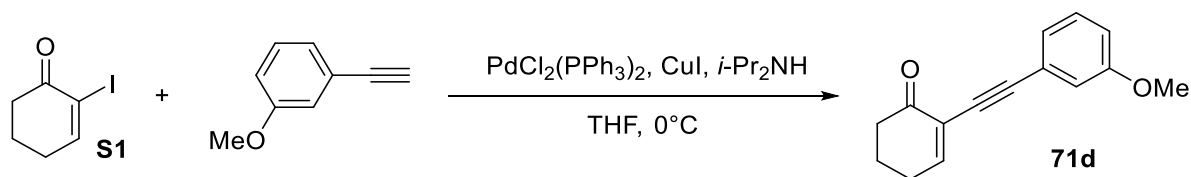
Compound **71b** was prepared by following the general procedure for the synthesis of **71a**. A solution of 2-iodo-cyclohexenone (444.0 mg, 2 mmol, 1.0 equiv.) in THF (5 mL) was treated with $\text{PdCl}_2(\text{PPh}_3)_2$ (70.2 mg, 0.1 mmol, 5 mol%) and CuI (38.1 mg, 0.2 mmol, 10 mol%) and cooled down to 0 °C under an Ar atmosphere. After 10 min of stirring, 1-ethynyl-4-methoxybenzene (528.6 mg, 4 mmol, 2 equiv.) and diisopropyl amine (0.87 mL, 627.4 mg, 6.2 mmol) were added, and the resulting solution was stirred at 0 °C. The reaction mixture was partitioned between CH_2Cl_2 and 0.5 N aqueous HCl solution. The aqueous layer was extracted three times with CH_2Cl_2 and the combined organic phases were washed with brine, dried over MgSO_4 , filtered and concentrated under vacuum. The crude product was purified by flash column chromatography to yield alkyne **71b** as a brown solid (148.7 mg, 0.66 mmol, 33%).

Synthesis of 2-(phenylethynyl)cyclohex-2-en-1-one (**8c**)¹²⁸



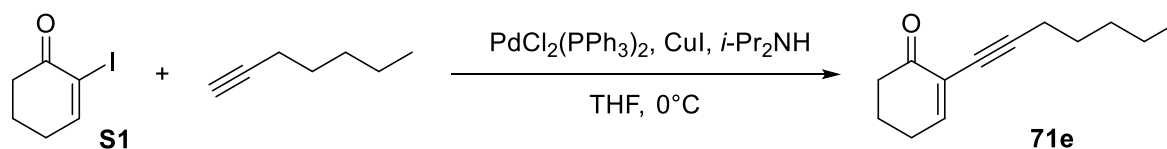
Compound **71c** was prepared by following the general procedure for the synthesis of **71a**. A solution of 2-iodo-cyclohexenone (444.0 mg, 2 mmol, 1.0 equiv.) in THF (5 mL) was treated with $\text{PdCl}_2(\text{PPh}_3)_2$ (70.2 mg, 0.1 mmol, 5 mol%) and CuI (38.1 mg, 0.2 mmol, 10 mol%) and cooled down to 0 °C under an Ar atmosphere. After 10 min of stirring, 1-ethynyl-4-methylbenzene (464.6 mg, 4 mmol, 2 equiv.) and diisopropyl amine (0.87 mL, 627.4 mg, 6.2 mmol) were added, and the resulting solution was stirred at 0 °C. The reaction mixture was partitioned between CH_2Cl_2 and 0.5 N aqueous HCl solution. The aqueous layer was extracted three times with CH_2Cl_2 and the combined organic phases were washed with brine, dried over MgSO_4 , filtered and concentrated under vacuum. The crude product was purified by flash column chromatography to yield alkyne **71c** as a grey solid (313.9 mg, 1.49 mmol, 75%).

Synthesis of 2-(phenylethynyl)cyclohex-2-en-1-one (**71d**)¹²⁹



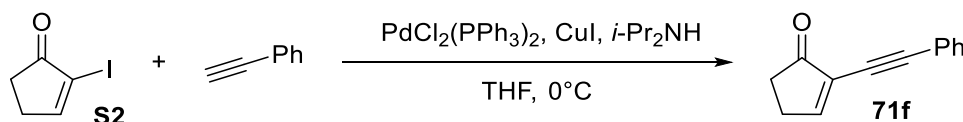
Compound **71d** was prepared by following the general procedure for the synthesis of **71a**. A solution of 2-iodo-cyclohexenone (444.0 mg, 2 mmol, 1.0 equiv.) in THF (5 mL) was treated with $\text{PdCl}_2(\text{PPh}_3)_2$ (70.2 mg, 0.1 mmol, 5 mol%) and CuI (38.1 mg, 0.2 mmol, 10 mol%) and cooled down to 0°C under an Ar atmosphere. After 10 min of stirring, 1-ethynyl-4-methoxybenzene (528.6 mg, 4 mmol, 2 equiv.) and diisopropyl amine (0.87 mL, 627.4 mg, 6.2 mmol) were added, and the resulting solution was stirred at 0°C . The reaction mixture was partitioned between CH_2Cl_2 and 0.5M aqueous HCl solution. The aqueous layer was extracted three times with CH_2Cl_2 and the combined organic phases were washed with brine, dried over MgSO_4 , filtered and concentrated under vacuum. The crude product was purified by flash column chromatography to yield alkyne **71d** as a brown solid (366.6 mg, 1.62 mmol, 53%).

Synthesis of 2-(Heptane-1-yn-1-yl)cyclohex-2-en-1-one (**71e**)¹³⁰



Compound **71e** was prepared by following the general procedure for the synthesis of **71a**. A solution of 2-iodo-cyclohexenone (444 mg, 2 mmol, 1.0 equiv.) in THF (6 mL) was treated with $\text{PdCl}_2(\text{PPh}_3)_2$ (70.2 mg, 0.1 mmol, 5 mol%) and CuI (38.1 mg, 0.2 mmol, 10 mol%) and cooled down to 0°C under Ar atmosphere and in the dark. After 10 min of stirring, Hept-1-yne (0.53 mL, 4.0 mmol, 2 equiv.) and diisopropyl amine (0.83 mL, 6.3 mmol, 3.1 equiv.) were added, and the resulting yellow to dark brown solution was stirred from 0°C . The reaction mixture was partitioned between CH_2Cl_2 and 1.0M aqueous HCl solution. The aqueous layer was extracted three times with CH_2Cl_2 and the combined organic phases were washed with brine, dried over MgSO_4 , filtered and concentrated under vacuum. The crude product was purified by flash column chromatography to yield product **71e** as a white solid (231.9 mg, 1.2 mmol, 59%).

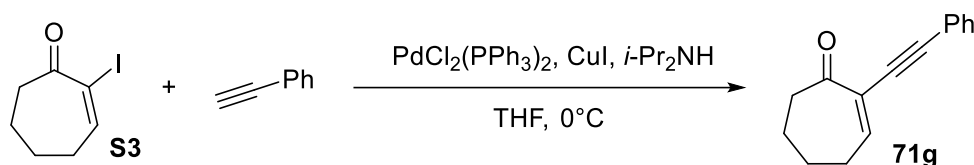
Synthesis of 2-(phenylethynyl)cyclopent-2-en-1-one (**71f**)^{67b}



Compound **71f** was prepared by following the general procedure for the synthesis of **71a**. A solution of 2-iodocyclopent-2-en-1-one (186 mg, 0.89 mmol, 1.0 equiv.) in THF (3 mL) was treated with $\text{PdCl}_2(\text{PPh}_3)_2$ (31.4 mg, 0.04 mmol, 5 mol%) and CuI (17.1 mg, 0.09 mmol, 10 mol%) and cooled down to 0°C under Ar atmosphere and in the dark. After 10 min of stirring, phenylacetylene (0.2 mL, 1.79 mmol, 2 equiv.) and diisopropyl amine (0.39 mL, 2.77 mmol, 3.1 equiv.) were added, and the resulting yellow to dark brown

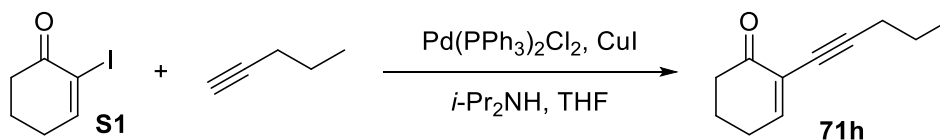
solution was stirred from 0 °C. The reaction mixture was partitioned between CH₂Cl₂ and 1.0M aqueous HCl solution. The aqueous layer was extracted three times with CH₂Cl₂ and the combined organic phases were washed with brine, dried over MgSO₄, filtered and concentrated under vacuum. The crude product was purified by flash column chromatography to yield product **71f** as a pale yellow solid (156.7 mg, 0.86 mmol, 97%).

Synthesis of 2-(phenylethynyl)cyclohept-2-en-1-one (**71g**)^{67b}



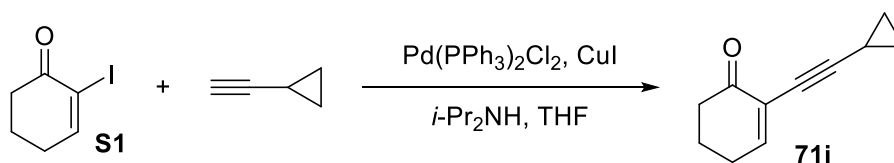
Compound **71g** was prepared by following the general procedure for the synthesis of **71a**. A solution of 2-iodocyclohept-2-en-1-one (219.3 mg, 0.93 mmol, 1.0 equiv.) in THF (3 mL) was treated with PdCl₂(PPh₃)₂ (312.6 mg, 0.05 mmol, 5 mol%) and CuI (17.7 mg, 0.09 mmol, 10 mol%) and cooled down to 0 °C under Ar atmosphere and in the dark. After 10 min of stirring, phenylacetylene (0.21 mL, 1.86 mmol, 2 equiv.) and diisopropyl amine (0.41 mL, 2.88 mmol, 3.1 equiv.) were added, and the resulting yellow to dark brown solution was stirred from 0 °C. The reaction mixture was partitioned between CH₂Cl₂ and 1.0M aqueous HCl solution. The aqueous layer was extracted three times with CH₂Cl₂ and the combined organic phases were washed with brine, dried over MgSO₄, filtered and concentrated under vacuum. The crude product was purified by flash column chromatography to yield product **71g** as a pale yellow oil (188.0 mg, 0.89 mmol, 96%).

Synthesis of 2-(pent-1-yn-1-yl)cyclohex-2-en-1-one (**71h**)¹³⁰



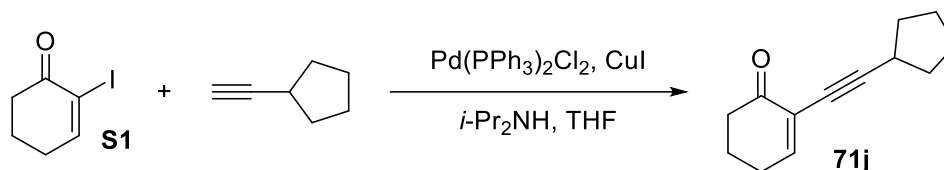
Compound **71h** was prepared by following the general procedure for the synthesis of **71a**. A solution of 2-iodo-cyclohexenone (666 mg, 1 equiv., 3.00 mmol) in THF (6 mL) treated with Pd(PPh₃)₂Cl₂ (105 mg, 5 mol%, 0.15 mmol) and CuI (57 mg, 10 mol%, 0.30 mol) and cooled down to 0°C in the dark, then pent-1-yne (0.6 mL, 2 equiv., 6.00 mmol) and diisopropylamine (**DIPA**, 1.3 mL, 3.1 equiv., 9.30 mmol) were added to the reaction mixture, the resulting mixture was stirred at 0 °C for 1 hours. After the reaction completed, the mixture was extracted with saturated NH₄Cl solution and EtOAc, the combined organic layer was then dry over MgSO₄ and concentrated under vacuum, the crude product was then purified on flash column chromatography and gave the product **71h** as a yellow oil (249.6 mg, 1.54 mmol, 51%).

Synthesis of 2-(cyclopropylethynyl)cyclohex-2-en-1-one (**71i**)^{67b}



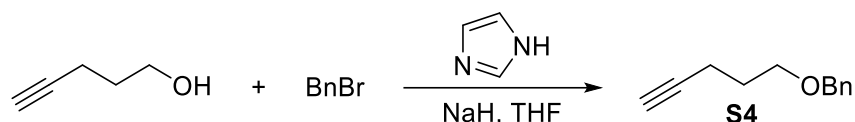
Compound **71i** was prepared by following the general procedure for the synthesis of **71a**. A solution of 2-iodo-cyclohexenone (666 mg, 1.0 equiv., 3.00 mmol) in THF (6 mL) treated with Pd(PPh₃)₂Cl₂ (105 mg, 5 mol%, 0.15 mmol) and CuI (57 mg, 10 mol%, 0.30 mol) and cooled down to 0 °C in the dark, then ethynylcyclopropane (0.6 mL, 2.0 equiv., 6.00 mmol) and diisopropylamine (**DIPA**, 1.3 mL, 3.1 equiv., 9.30 mmol) were added to the reaction mixture, the resulting mixture was stirred at 0 °C for 1 hours. After the reaction completed, the mixture was extracted with saturated NH₄Cl solution and EtOAc, the combined organic layer was then dry over MgSO₄ and concentrated under vacuum, the crude product was then purified on flash column chromatography and gave the product **71i** as a yellow oil (284.9 mg, 1.78 mmol, 59%).

Synthesis of 2-(cyclopentylethynyl)cyclohex-2-en-1-one (**71j**)^{67b}

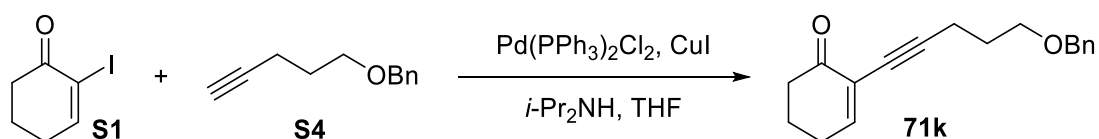


Compound **71j** was prepared by following the general procedure for the synthesis of **71a**. A solution of 2-iodo-cyclohexenone (666 mg, 1.0 equiv., 3.00 mmol) in THF (6 mL) treated with Pd(PPh₃)₂Cl₂ (105 mg, 5 mol%, 0.15 mmol) and CuI (57 mg, 10 mol%, 0.30 mol) and cooled down to 0 °C in the dark, then ethynylcyclopentane (0.7 mL, 2.0 equiv., 6.00 mmol) and diisopropylamine (**DIPA**, 1.3 mL, 3.1 equiv., 9.30 mmol) were added to the reaction mixture, the resulting mixture was stirred at 0 °C for 1 hours. After the reaction completed, the mixture was extracted with saturated NH₄Cl solution and EtOAc, the combined organic layer was then dry over MgSO₄ and concentrated under vacuum, the crude product was then purified on flash column chromatography and gave the product **71j** as a yellow oil (225.0 mg, 1.20 mmol, 40%).

Synthesis of 2-(5-(benzyloxy)pent-1-yn-1-yl)cyclohex-2-en-1-one (**71k**)¹³¹



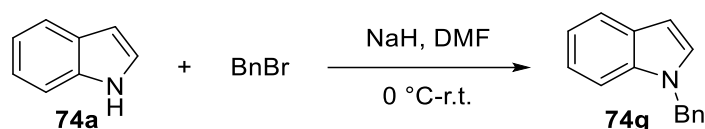
To a stirring flask was added imidazole (1.4 mg, 0.2 mol%, 0.02 mmol) and pent-4-yn-1-ol (841.2 mg, 1.0 equiv., 10 mmol) in anhydrous THF (10 mL), the solution was then cooled to 0 °C and NaH (1.2 g, 3 equiv., 30 mmol) was added at once. After 10 min of stirring, BnBr (2.1 g, 1.2 equiv., 12 mmol) was added dropwise, the suspension was then stirring at room temperature overnight. The reaction solution was then extraction with H₂O, saturated NH₄Cl solution and brine, dried over Mg₂SO₄, filtered and concentrated under vacuum. The crude product was purified by flash column chromatography to yield product **S4** as a pale yellow solid (873.7 mg, 5 mmol, 50%).



Compound **71k** was prepared by following the general procedure for the synthesis of **71a**. A solution of 2-iodo-cyclohexenone **S1** (666 mg, 1.0 equiv., 3.00 mmol) in THF (5 mL) treated with Pd(PPh₃)₂Cl₂ (105 mg, 5 mol%, 0.15 mmol) and CuI (57 mg, 10 mol%, 0.30 mol) and cooled down to 0 °C under N₂ atmosphere in the dark, then ((pent-4-yn-1-yloxy)methyl)benzene **S4** (700 mg, 1.5 equiv., 4.50 mmol) and diisopropylamine(DIPA, 1.3 mL, 3.1 equiv., 9.30 mmol) were added to the reaction mixture, the resulting mixture was stirred at 0 °C for 1 hours. After the reaction completed, the mixture was extracted with saturated NH₄Cl solution and EtOAc, the combined organic layer was then dry over MgSO₄ and concentrated under vacuum, the crude product was then purified on flash column chromatography and gave the product **71k** as a yellow oil (396.2 mg, 1.48 mmol, 49%).

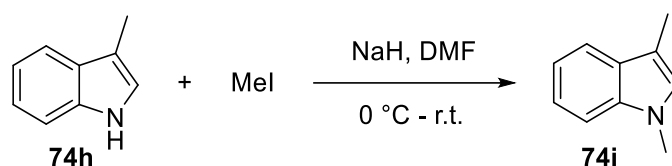
¹H NMR (CDCl₃, 500 MHz) δ = 7.37-7.35 (m, 4H), 7.31-7.29 (m, 1H), 7.17 (t, *J* = 4.6 Hz, 1H), 4.54 (s, 2H), 3.62 (t, *J* = 6.1 Hz, 1H), 2.54-2.48 (m, 4H), 2.45-2.42 (m, 2H), 2.06-2.01 (m, 2H), 1.92-1.87 (m, 2H). ¹³C NMR (CDCl₃, 125MHz) δ = 196.2 (C_q), 153.3 (CH), 138.8 (C_q), 128.5 (CH), 127.8 (CH), 127.6 (CH), 125.7 (C_q), 92.8 (C_q), 75.5 (C_q), 73.1 (CH₂), 69.0 (CH₂), 38.3 (CH₂), 29.0 (CH₂), 26.5 (CH₂), 22.7 (CH₂), 16.5 (CH₂). HRMS (ESI): *m/z*: calculated for C₁₈H₂₁O₂⁺: 269.1536 [M+H]⁺, found, 269.1539.

Synthesis of 1-benzyl-1H-indole (**74g**)¹³²



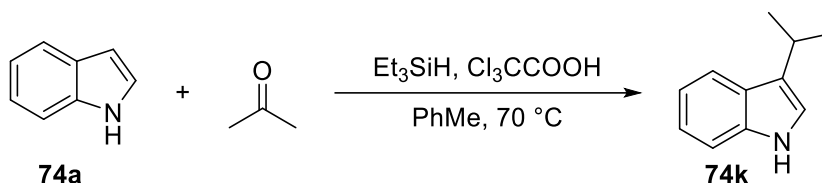
To a stirring solution of indole (352.5 mg, 3 mmol, 1 equiv.) in dry DMF (3 mL), NaH (144.0 mg, 3.6 mmol, 1.2 equiv.) was added portionwise under N₂ at 0 °C. The reaction mixture was then warmed to room temperature and stirred for 30 min. After cooling to 0 °C, BnBr (564.5 mg, 3.3 mmol, 1.1 equiv.) (1.2 mL) was added dropwise to the reaction mixture. The resulting mixture was stirred at room temperature overnight. The reaction was quenched with water and extracted three times with ethyl acetate, the combined organic phases were dried over MgSO₄, filtered and concentrated under vacuum. The crude product was purified by flash column chromatography to yield product **74g** as pale yellow oil (553.4 mg, 2.67 mmol, 89%).

Synthesis of 1,3-dimethyl-1H-indole (**74i**)¹³³



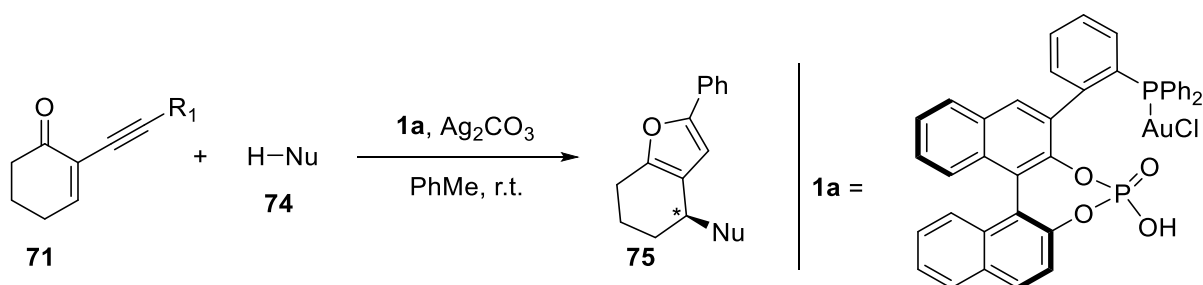
To a stirring solution of 60% NaH (240 mg, 6 mmol, 2 equiv.) in dry DMF (2.4 mL), 3-methylindole (393.5 mg, 3 mmol, 1 equiv.) in DMF (2.4) was added dropwise at 0 °C. The mixture was allowed to warm to room temperature and stirred for 30 min. After cooling to 0 °C, a solution of MeI (0.38 mL, 6 mmol, 2 equiv.) in DMF (1.2 mL) was added dropwise. The resulting mixture was stirred at room temperature overnight. The reaction was quenched with water and extracted three times with ethyl acetate, the combined organic phases were dried over MgSO₄, filtered and concentrated under vacuum. The crude product was purified by flash column chromatography to yield product **74i** as a clear oil (426.9 mg, 2.94 mmol, 98%).

Synthesis of 3-isopropyl-1H-indole (**74k**)¹³⁴



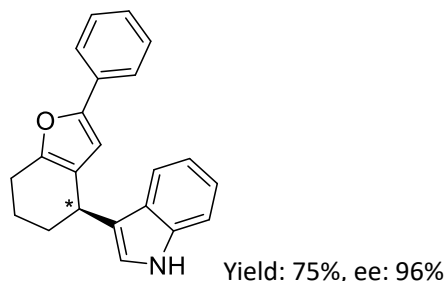
In a oven dried flask, triethylsilane (5.78 mL, 36.0 mmol, 2.4 equiv.) and trichloroacetic acid (2.26 g, 22.5 mmol, 1.5 equiv.) were dissolved in toluene (7.50 mL) and the resulting solution was heated to 70°C . A solution of indole (1.76 g, 15.0 mmol, 1 equiv.) and acetone (1.23 mL, 16.5 mmol, 1.1 equiv.) in toluene (7.50 mL) were then added over 1 h. After an additional 20 min at 70°C the solution was quenched with 10% aqueous solution of sodium carbonate, the organic layer was separated, dried over anhydrous sodium sulfate, concentrated under reduced pressure, and purified by column chromatography to afford indole **74k** (1.61 g, 10.1 mmol, 67%) as a colorless solid.

1.2. Tandem cycloisomerization/nucleophilic addition of ketones and indoles



General procedure 1. To a flask was added 2-(1-alkynyl)-2-alken-1-one **71** (0.55 mmol, 1.1 equiv.), indoles **74** (NuH, 0.5 mmol, 1.0 equiv.), **1a** (0.001 mmol, 0.2 mol%), Ag_2CO_3 (0.5 μmol , 0.1 mol%) and toluene (2.5 mL). The resulting mixture was then stirred overnight at room temperature. The solvent was then removed under vacuum and the residue was purified by flash column chromatography.

Synthesis of (*R*)-3-(2-phenyl-4,5,6,7-tetrahydrobenzofuran-4-yl)-1H-indole (**75a**)

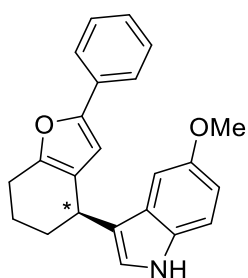


Compound **75a** was prepared according to the **general procedure 1** from **71a** (107.9 mg, 0.55 mmol, 1.1 equiv.), **74a** (58.8 mg, 0.5 mmol, 1.0 equiv.), **1a** (0.8 mg, 0.001 mmol, 0.2 mol%) and Ag_2CO_3 (0.1 mg, 0.5 μmol , 0.1 mol%) in toluene (2.5 mL), yielding product **75a** (116.5 mg, 0.37 mmol, 75%) as a white solid for which the spectroscopical data correspond to those reported in the literature.⁷⁹

75a was alternatively obtained from the same protocol in the absence of Ag_2CO_3 in 80% yield and 92% ee.

m.p.: 158.8-160.3 °C. $[\alpha]_D = +38$ (c 0.89, CHCl_3). ee = 96%, determined on a Chiralpak IA column (heptane:IPA = 95:5, 1 mL/min), retention times: T_R (minor): 19.7 min, T_R (major): 25.6 min. $^1\text{H NMR}$ (CDCl_3 , 500 MHz) δ = 7.89 (s, 1H), 7.62 (d, J = 7.6 Hz, 1H), 7.59 (d, J = 7.6 Hz, 2H), 7.36 (d, J = 7.9 Hz, 1H), 7.33-7.30 (m, 2H), 7.22-7.16 (m, 2H), 7.11 (t, J = 7.3 Hz, 1H), 6.86 (d, J = 1.8 Hz, 1H), 6.44 (s, 1H), 4.25 (br, 1H), 2.76-2.75 (m, 2H), 2.18-2.13 (m, 1H), 1.98-1.93 (m, 2H), 1.88-1.84 (m, 1H). **HRMS (ESI):** m/z : calcd for $\text{C}_{22}\text{H}_{20}\text{NO}^+$ 314.1539 $[\text{M}+\text{H}]^+$, found, 314.1543.

Synthesis of (*R*)-5-methoxy-3-(2-phenyl-4,5,6,7-tetrahydrobenzofuran-4-yl)-1H-indole (**75b**)



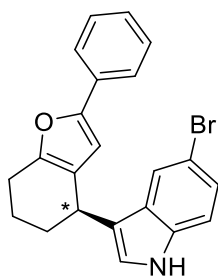
Yield: 81%, ee: 97%.

Compound **75b** was prepared according to the **general procedure 1** from **71a** (107.9 mg, 0.55 mmol, 1.1 equiv.), **74b** (73.6 mg, 0.5 mmol, 1.0 equiv.), **1a** (0.8 mg, 0.001 mmol, 0.2 mol%) and Ag_2CO_3 (0.1 mg, 0.5 μmol , 0.1 mol%) in toluene (2.5 mL), yielding product **75b** (138.2 mg, 0.40 mmol, 81%) as a white solid for which the spectroscopical data correspond to those reported in the literature.⁷⁹

75b was alternatively obtained from the same protocol in the absence of Ag_2CO_3 in 73% yield and 94% ee.

$[\alpha]_D = -7$ (c 0.98, CHCl_3). ee = 97%, determined on a Chiralpak IA column (heptane:IPA = 95:5, 1 mL/min), retention times: T_R (minor): 29.2 min, T_R (major): 41.4 min. $^1\text{H NMR}$ (CDCl_3 , 500 MHz) δ = 7.79 (s, 1H), 7.58 (d, J = 7.6 Hz, 2H), 7.31 (t, J = 7.6 Hz, 2H), 7.23 (d, J = 8.2 Hz, 1H), 7.17 (t, J = 7.3 Hz, 1H), 7.06 (s, 1H), 6.86 (d, J = 8.5 Hz, 1H), 6.81 (s, 1H), 6.44 (s, 1H), 4.20 (t, J = 5.2 Hz, 1H), 3.84 (s, 3H), 2.80-2.71 (m, 2H), 2.16-2.11 (m, 1H), 1.98-1.90 (m, 2H), 1.87-1.82 (m, 1H). **HRMS (ESI):** m/z : calculated for $\text{C}_{23}\text{H}_{22}\text{NO}_2^+$: 344.1645 $[\text{M}+\text{H}]^+$, found, 344.1646.

Synthesis of (*R*)-5-bromo-3-(2-phenyl-4,5,6,7-tetrahydrobenzofuran-4-yl)-1H-indole (**75c**)



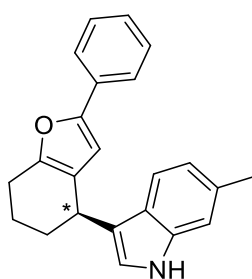
Yield: 77%, ee: 97%.

Compound **75c** was prepared according to the **general procedure 1** from **71a** (107.9 mg, 0.55 mmol, 1.1 equiv.), **74c** (98.0 mg, 0.5 mmol, 1.0 equiv.), **1a** (0.8 mg, 0.001 mmol, 0.2 mol%) and Ag₂CO₃ (0.1 mg, 0.5 μmol, 0.1 mol%) in toluene (2.5 mL), yielding product **75c** (150.9 mg, 0.39 mmol, 77%) as a white solid for which the spectroscopical data correspond to those reported in the literature.⁷⁹

75c was alternatively obtained from the same protocol in the absence of Ag₂CO₃ in 30% yield and 75% ee.

[α]_D = -10 (c 1.02, CHCl₃). ee = 97%, determined on a Chiralpak IA column (heptane:IPA = 95:5, 1 mL/min), retention times: T_R (minor): 19.4 min, T_R (major): 26.7 min. ¹H NMR (CDCl₃, 300 MHz) δ = 7.93 (s, 1H), 7.74 (d, J = 1.3 Hz, 1H), 7.60-7.57 (m, 2H), 7.34-7.16 (m, 5H), 6.83 (d, J = 2.3 Hz, 1H), 6.40 (s, 1H), 4.17 (t, J = 5.5 Hz, 1H), 2.76-2.73 (m, 2H), 2.19-2.07 (m, 1H), 1.96-1.79 (m, 3H). HRMS (ESI): m/z: calculated for C₂₂H₁₉BrNO⁺: 392.0645 [M+H]⁺, found, 392.0638.

Synthesis of (*R*)-6-methyl-3-(2-phenyl-4,5,6,7-tetrahydrobenzofuran-4-yl)-1H-indole (**75d**)

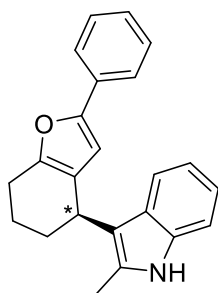


Yield: 44%, ee: 96%

Compound **75d** was prepared according to the **general procedure 1** from **71a** (21.6 mg, 0.11 mmol, 1.1 equiv.), **74d** (13.1 mg, 0.1 mmol, 1.0 equiv.), **1a** (0.2 mg, 0.2 μmol, 0.2 mol%) and Ag₂CO₃ (0.1 mg, 0.0001 mmol, 0.1 mol%) in toluene (2.5 mL), yielding product **75d** (14.4 mg, 0.04 mmol, 44%) as a white solid for which the spectroscopical data correspond to those reported in the literature.⁷⁹

[α]_D = +28 (c 1.21, CHCl₃). ee = 96%, determined on a Chiralpak IA column (heptane:IPA = 95:5, 1 mL/min), retention times: T_R (minor): 19.5 min, T_R (major): 22.4 min. ¹H NMR (CDCl₃, 500 MHz) δ = 7.71 (s, 1H), 7.57 (d, J = 7.9 Hz, 2H), 7.48 (d, J = 7.9 Hz, 1H), 7.30 (t, J = 7.6 Hz, 2H), 7.18-7.12 (m, 2H), 6.93 (d, J = 7.9 Hz, 1H), 6.75 (s, 1H), 6.42 (s, 1H), 4.20 (br, 1H), 2.76-2.73 (m, 2H), 2.45 (s, 3H), 2.15-2.10 (m, 1H), 1.98-1.90 (m, 2H), 1.86-1.83 (m, 1H). HRMS (ESI): m/z: calculated for C₂₃H₂₂NO⁺: 328.1696 [M+H]⁺, found, 328.1696.

Synthesis of (*R*)-2-methyl-3-(2-phenyl-4,5,6,7-tetrahydrobenzofuran-4-yl)-1H-indole (**75e**)

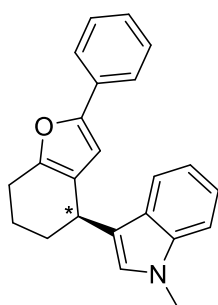


Yield: 49%, ee: 82%.

Compound **75e** was prepared according to the **general procedure 1** from **71a** (107.9 mg, 0.55 mmol, 1.1 equiv.), **74e** (65.6 mg, 0.5 mmol, 1.0 equiv.), **1a** (0.8 mg, 0.001 mmol, 0.2 mol%) and Ag₂CO₃ (0.1 mg, 0.5 μmol, 0.1 mol%) in toluene (2.5 mL), yielding product **75e** (80.0 mg, 0.24 mmol, 49%) as a white solid for which the spectroscopical data correspond to those reported in the literature.⁷⁹

[α]_D = +26 (c 1.20, CHCl₃). ee = 82%, determined on a Chiralpak AD-H column (heptane:IPA = 90:10, 1 mL/min), retention times: T_R (minor): 4.3 min, T_R (major): 5.3 min. ¹H NMR (CDCl₃, 500 MHz) δ = 7.69 (s, 1H), 7.54 (d, J = 7.9 Hz, 2H), 7.30-7.24 (m, 4H), 7.15 (t, J = 7.3 Hz, 1H), 7.06 (t, J = 7.3 Hz, 1H), 6.94 (t, J = 7.6 Hz, 1H), 6.28 (s, 1H), 4.14 (br, 1H), 2.82 (br, 2H), 2.31 (s, 3H), 2.11-2.04 (m, 2H), 1.96-1.88 (m, 2H). HRMS (ESI): m/z: calculated for C₂₃H₂₂NO⁺: 328.1696 [M+H]⁺, found, 328.1691.

Synthesis of (R)-1-methyl-3-(2-phenyl-4,5,6,7-tetrahydrobenzofuran-4-yl)-1H-indole (75f)

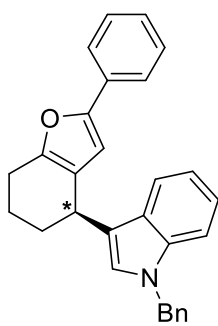


Yield: 92%, ee: 94%.

Compound **75f** was prepared according to the **general procedure 1** from **71a** (107.9 mg, 0.55 mmol, 1.1 equiv.), **74f** (65.6 mg, 0.5 mmol, 1.0 equiv.), **1a** (0.8 mg, 0.001 mmol, 0.2 mol%) and Ag₂CO₃ (0.1 mg, 0.5 μmol, 0.1 mol%) in toluene (2.5 mL), yielding product **75f** (150.2 mg, 0.46 mmol, 92%) as a white solid for which the spectroscopical data correspond to those reported in the literature.⁷⁹

[α]_D = -5 (c 0.78, CHCl₃). ee: 94%, determined on a Chiralpak IC column (heptane:IPA = 95:05, 1 mL/min), retention times: T_R (minor): 4.7 min, T_R (major): 5.1 min. ¹H NMR (CDCl₃, 500 MHz) δ = 7.60 (t, J = 7.6 Hz, 3H), 7.33-7.29 (m, 3H), 7.24-7.21 (m, 1H), 7.18 (t, J = 7.3 Hz, 1H), 7.10 (t, J = 7.3 Hz, 1H), 6.72 (s, 1H), 6.44 (s, 1H), 4.24 (t, J = 5.5 Hz, 1H), 3.71 (s, 3H), 2.76-2.75 (m, 2H), 2.16-2.12 (m, 1H), 1.97-1.91 (m, 2H), 1.87-1.84 (m, 1H). HRMS (ESI): m/z: calcd for C₂₃H₂₂NO⁺ 328.1696 [M+H]⁺, found, 328.1696.

Synthesis of (R)-1-benzyl-3-(2-phenyl-4,5,6,7-tetrahydrobenzofuran-4-yl)-1H-indole (75g)

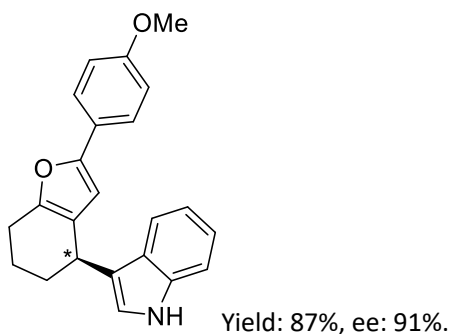


Yield: 83%, ee: 92%.

Compound **75g** was prepared according to the **general procedure 1** from **71a** (21.6 mg, 0.11 mmol, 1.1 equiv.), **74g** (20.7 mg, 0.1 mmol, 1.0 equiv.), **1a** (0.2 mg, 0.2 μmol, 0.2 mol%) and Ag₂CO₃ (0.1 mg, 0.0001 mmol, 0.1 mol%) in toluene (0.5 mL), yielding product **75g** (33.3 mg, 0.08 mmol, 83%) as a pale yellow solid.

$[\alpha]_D^{25} = +34$ (c 1.00, CHCl₃). ee: 92%, determined on a Chiralpak IA column (heptane:IPA = 95:05, 1 mL/min), retention times: T_R (major): 6.5 min, T_R (minor): 11.3 min. **¹H NMR (CDCl₃, 500 MHz)** δ = 7.54 (d, J = 7.6 Hz, 1H), 7.49 (d, J = 7.9 Hz, 2H), 7.23-7.13 (m, 6H), 7.08 (t, J = 7.6 Hz, 2H), 7.02-7.97 (m, 3H), 6.73 (s, 1H), 6.35 (s, 1H), 5.14 (dd, J_1 = 21.3 Hz, J_2 = 16.2 Hz, 2H), 4.17 (t, J = 6.1 Hz, 1H), 2.68-2.64 (m, 2H), 2.10-2.05 (m, 1H), 1.90-1.84 (m, 2H), 1.80-1.73 (m, 1H). **¹³C NMR (CDCl₃, 125 MHz)** δ = 151.9, 151.4, 138.0, 137.2, 131.6, 128.9, 128.7, 127.7, 127.6, 126.9, 126.8, 126.6, 123.5, 122.4, 121.9, 119.6, 119.6, 119.2, 110.0, 106.3, 50.2, 31.6, 31.1, 23.6, 21.4. **HRMS (ESI):** m/z : calcd for C₂₉H₂₄NO⁺ 402.1852 [M+H-H₂]⁺, found, 402.1858.

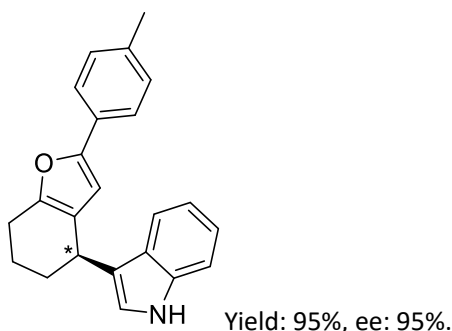
Synthesis of (R)-3-(2-(4-methoxyphenyl)-4,5,6,7-tetrahydrobenzofuran-4-yl)-1H-indole (75h)



Compound **75h** was prepared according to the **general procedure 1** from **71b** (24.9 mg, 0.11 mmol, 1.1 equiv.), **74a** (11.7 mg, 0.1 mmol, 1.0 equiv.), **1a** (0.2 mg, 0.2 μ mol, 0.2 mol%) and Ag₂CO₃ (0.1 mg, 0.0001 mmol, 0.1 mol%) in toluene (0.5 mL), yielding product **75h** (29.8 mg, 0.09 mmol, 87%) as a pale yellow solid for which the spectroscopical data correspond to those reported in the literature.⁷⁹

$[\alpha]_D^{25} = +11$ (c 1.90, CHCl₃). ee = 91%, determined on a Chiralpak IC column (heptane:IPA = 95:5, 1 mL/min), retention times: T_R (minor): 9.5 min, T_R (major): 10.5 min. **¹H NMR (CDCl₃, 500 MHz)** δ = 7.89 (s, 1H), 7.62 (d, J = 7.9 Hz, 1H), 7.51 (d, J = 8.5 Hz, 2H), 7.34 (d, J = 7.9 Hz, 1H), 7.19 (t, J = 7.6 Hz, 1H), 7.10 (t, J = 7.6 Hz, 1H), 6.86-6.84 (m, 3H), 6.29 (s, 1H), 4.24-4.22 (m, 1H), 3.79 (s, 3H), 2.75-2.72 (m, 2H), 2.61-2.11 (m, 1H), 1.98-1.91 (m, 2H), 1.86-1.81 (m, 1H). **HRMS (ESI):** m/z : calculated for C₂₃H₂₂NO₂⁺: 344.1645 [M+H]⁺, found, 344.1645.

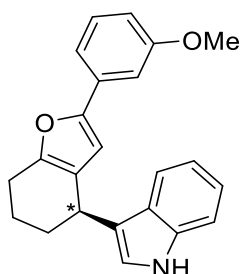
Synthesis of (R)-3-(2-(p-tolyl)-4,5,6,7-tetrahydrobenzofuran-4-yl)-1H-indole (75i)



Compound **75i** was prepared according to the **general procedure 1** from **71c** (23.1 mg, 0.11 mmol, 1.1 equiv.), **74a** (11.7 mg, 0.1 mmol, 1.0 equiv.), **1a** (0.2 mg, 0.2 μ mol, 0.2 mol%) and Ag₂CO₃ (0.1 mg, 0.0001 mmol, 0.1 mol%) in toluene (0.5 mL), yielding product **75i** (31.0 mg, 0.09 mmol, 95%) as a pale yellow solid for which the spectroscopical data correspond to those reported in the literature.⁷⁹

$[\alpha]_D^{25} = +68$ (c 1.01, CHCl₃). ee = 95%, determined on a Chiralpak IC column (heptane:IPA = 95:5, 1 mL/min), retention times: T_R (minor): 6.3 min, T_R (major): 7.2 min. ¹H NMR (CDCl₃, 500 MHz) δ = 7.71 (s, 1H), 7.52 (d, J = 7.9 Hz, 1H), 7.38 (d, J = 7.9 Hz, 2H), 7.21 (d, J = 8.2 Hz, 1H), 7.09 (t, J = 7.6 Hz, 1H), 7.03-7.00 (m, 3H), 6.70-6.69 (m, 1H), 6.27 (s, 1H), 4.13 (t, J = 5.5 Hz, 1H), 2.66-2.63 (m, 2H), 2.22 (s, 3H), 2.06-2.01 (m, 1H), 1.86-1.81 (m, 2H), 1.76-1.71 (m, 1H). HRMS (ESI): m/z : calculated for C₂₃H₂₀NO⁺: 326.1539 [M+H₂]⁺, found, 326.1537.

Synthesis of (*R*)-3-(2-(3-methoxyphenyl)-4,5,6,7-tetrahydrobenzofuran-4-yl)-1H-indole (75j)

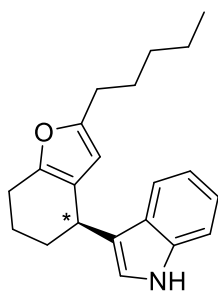


Yield : 77%, ee : 84%.

Compound **75j** was prepared according to the **general procedure 1** from **71d** (24.9 mg, 0.11 mmol, 1.1 equiv.), **74a** (11.7 mg, 0.1 mmol, 1.0 equiv.), **1a** (0.2 mg, 0.2 μ mol, 0.2 mol%) and Ag₂CO₃ (0.1 mg, 0.0001 mmol, 0.1 mol%) in toluene (0.5 mL), yielding product **75j** (26.4 mg, 0.08 mmol, 77%) as a pale yellow solid.

$[\alpha]_D^{25} = +15$ (c 1.29, CHCl₃). ee = 84%, determined on a Chiralpak IA column (heptane:IPA = 90:10, 1 mL/min), retention times: T_R (minor): 12.1 min, T_R (major): 23.7 min. ¹H NMR (CDCl₃, 500 MHz) δ = 7.92 (s, 1H), 7.61 (d, J = 7.9 Hz, 1H), 7.36 (d, J = 8.2 Hz, 1H), 7.24-7.09 (m, 5H), 6.86 (d, J = 1.8 Hz, 1H), 6.74 (dd, J_1 = 7.9 Hz, J_2 = 1.8 Hz, 1H), 6.43 (s, 1H), 4.25 (t, J = 5.5 Hz, 1H), 3.82 (s, 3H), 2.78-2.74 (m, 2H), 2.18-2.13 (m, 1H), 1.98-1.92 (m, 2H), 1.88-1.82 (m, 1H). ¹³C NMR (CDCl₃, 125 MHz) δ = 136.8, 132.9, 129.8, 126.9, 122.4, 122.3, 122.2, 120.5, 119.5, 119.4, 116.1, 112.9, 111.4, 108.6, 106.6, 160.1, 151.7, 151.5, 55.5, 31.4, 31.1, 23.6, 21.4. HRMS (ESI): m/z : calculated for C₂₃H₂₂NO₂⁺: 344.1645 [M+H]⁺, found, 344.1641.

Synthesis of (*R*)-3-(2-pentyl-4,5,6,7-tetrahydrobenzofuran-4-yl)-1H-indole (75k)



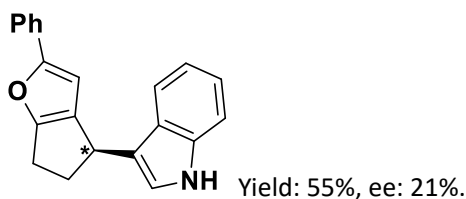
Yield: 46%, ee: 87%.

Compound **75k** was prepared according to the **general procedure 1** from **71e** (20.9 mg, 0.11 mmol, 1.1 equiv.), **74a** (11.7 mg, 0.1 mmol, 1.0 equiv.), **1a** (0.8 mg, 0.001 mmol, 1 mol%) and Ag₂CO₃ (0.1 mg, 0.5 μ mol, 0.5 mol%) in toluene (0.5 mL), yielding product **75k** (14 mg, 0.05 mmol, 46%) as a white solid.

$[\alpha]_D^{25} = +2$ (c 0.14, CHCl₃). ee = 87%, determined on a Chiralpak IA column (heptane:IPA = 95:5, 1 mL/min), retention times: T_R (minor): 8.7 min, T_R (major): 10.5 min. ¹H NMR (CDCl₃, 500 MHz) δ = 7.88 (bs, 1H), 7.59 (d, J = 7.9 Hz, 1H), 7.34 (d, J = 7.9 Hz, 1H), 7.18 (t, J = 7.6 Hz, 1H), 7.09 (t, J = 7.6 Hz, 1H), 6.83 (s, 1H), 5.74 (s, 1H), 4.17 (t, J = 5.5 Hz, 1H), 2.67-2.60 (m, 2H), 2.54 (t, J = 7.6 Hz, 2H), 2.14-2.09 (m, 1H), 1.94-1.86 (m, 2H), 1.82-1.76 (m, 1H), 1.62-1.57 (m, 2H), 1.32-1.28 (m, 4H), 0.88 (t, J = 6.7 Hz, 3H). ¹³C NMR (CDCl₃, 125 MHz) δ

= 154.4, 149.2, 136.8, 127.0, 122.2, 122.1, 120.8, 120.4, 119.5, 119.3, 111.3, 105.6, 31.7, 31.5, 31.1, 28.4, 28.2, 23.5, 22.6, 21.5, 14.2. **HRMS (ESI):** m/z : calculated for $C_{21}H_{24}NO^+$: 306.1852 $[M+H-H_2]^+$, found, 306.1857.

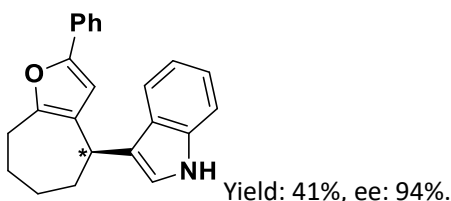
Synthesis of (*R*)-3-(2-phenyl-5,6-dihydro-4H-cyclopenta[b]furan-4-yl)-1H-indole (**75l**)



Compound **75l** was prepared according to the **general procedure 1** from **71f** (20.1 mg, 0.11 mmol, 1.1 equiv.), **74a** (11.7 mg, 0.1 mmol, 1.0 equiv.), **1a** (1.7 mg, 0.002 mmol, 2 mol%) and Ag_2CO_3 (0.3 mg, 0.001 mmol, 1 mol%) in toluene (0.5 mL), yielding product **75l** (16.4 mg, 0.06 mmol, 55%) as a white solid.

$[\alpha]_D = -18$ (c 0.75, $CHCl_3$). ee = 21%, determined on a Chiralpak IA column (heptane:IPA = 95:05, 1 mL/min), retention times: T_R (major): 26.1 min, T_R (minor): 29.9 min. 1H NMR ($CDCl_3$, 500 MHz) δ = 7.88 (bs, 1H), 7.61 (d, J = 7.3 Hz, 2H), 7.58 (d, J = 7.9 Hz, 1H), 7.36-7.32 (m, 3H), 7.19 (t, J = 7.6 Hz, 2H), 7.09 (t, J = 7.6 Hz, 1H), 6.93 (d, J = 1.9 Hz, 1H), 6.57 (s, 1H), 4.47 (t, J = 6.6 Hz, 1H), 3.07-3.00 (m, 1H), 2.96-2.83 (m, 2H), 2.52-2.46 (m, 1H). ^{13}C NMR ($CDCl_3$, 125 MHz) δ = 159.6, 158.0, 137.0, 132.1, 130.3, 128.8, 126.9, 126.9, 123.3, 122.3, 120.9, 120.7, 119.5 (2C), 111.4, 103.8, 37.7, 34.2, 25.0. **HRMS (ESI):** m/z : calculated for $C_{21}H_{16}NO^+$: 298.1226 $[M+H-H_2]^+$, found, 298.1227.

Synthesis of (*R*)-3-(2-phenyl-5,6,7,8-tetrahydro-4H-cyclohepta[b]furan-4-yl)-1H-indole (**75m**)

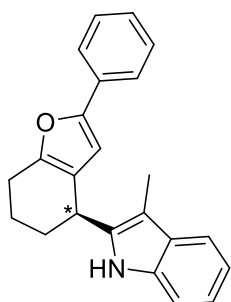


Compound **75m** was prepared according to the **general procedure 1** from **71g** (23.1 mg, 0.11 mmol, 1.1 equiv.), **74a** (11.7 mg, 0.1 mmol, 1.0 equiv.), **1a** (0.17 mg, 0.2 μ mol, 0.2 mol%) and Ag_2CO_3 (0.1 mg, 0.0001 mmol, 0.1 mol%) in toluene (0.5 mL), yielding product **75m** (13.5 mg, 0.04 mmol, 41%) as a white solid.

75m was alternatively obtained from the same protocol in the absence of Ag_2CO_3 in 55% yield and 95% ee.

$[\alpha]_D = +107$ (c 0.59, $CHCl_3$). ee = 94%, determined on a Chiralpak IA column (heptane:IPA = 95:05, 1 mL/min), retention times: T_R (minor): 8.7 min, T_R (major): 10.5 min. 1H NMR ($CDCl_3$, 500 MHz) δ = 7.92 (bs, 1H), 7.61 (d, J = 7.9 Hz, 1H), 7.51 (d, J = 7.3 Hz, 2H), 7.36 (d, J = 8.2 Hz, 1H), 7.28 (t, J = 7.9 Hz, 2H), 7.19 (t, J = 7.6 Hz, 1H), 7.14 (t, J = 7.6 Hz, 1H), 7.10 (t, J = 7.6 Hz, 1H), 6.81 (d, J = 1.9 Hz, 1H), 6.25 (s, 1H), 4.27 (dd, J_1 = 7.6 Hz, J_2 = 3.2 Hz, 1H), 2.95 (t, J = 5.7 Hz, 2H), 2.33-2.28 (m, 1H), 2.09-2.04 (m, 1H), 1.83-1.76 (m, 3H), 1.74-1.69 (m, 1H). ^{13}C NMR ($CDCl_3$, 125 MHz) δ = 153.0, 150.0, 136.9, 131.4, 128.7, 126.8, 126.6, 126.2, 123.4, 122.6, 122.1, 120.0, 119.8, 119.4, 111.4, 109.1, 35.5, 34.6, 29.3, 27.6, 26.9. **HRMS (ESI):** m/z : calculated for $C_{23}H_{22}NO^+$: 328.1696 $[M+H]^+$, found, 328.1696.

Synthesis of (S)-3-methyl-2-(2-phenyl-4,5,6,7-tetrahydrobenzofuran-4-yl)-1H-indole (75n)

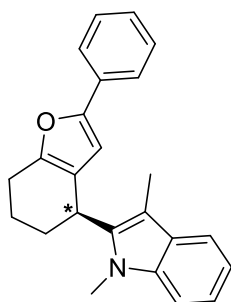


Yield: 83%, ee: 93%.

Compound **75n** was prepared according to the **general procedure 1** from **71a** (21.6 mg, 0.11 mmol, 1.1 equiv.), **74h** (13.1 mg, 0.1 mmol, 1.0 equiv.), **1a** (0.2 mg, 0.2 μ mol, 0.2 mol%) and Ag_2CO_3 (0.1 mg, 0.0001 mmol, 0.1 mol%) in toluene (0.5 mL), yielding product **75n** (27.1 mg, 0.08 mmol, 83%) as a pale yellow solid.

$[\alpha]_D^{25} = +68$ (c 1.01, CHCl_3). ee = 95%, determined on a Chiralpak IA column (heptane:IPA = 95:5, 1 mL/min), retention times: T_R (minor): 7.1 min, T_R (major): 10.3 min. $^1\text{H NMR}$ (CDCl_3 , 500 MHz) $\delta = 7.63$ (s, 1H), 7.58 (d, $J = 7.6$ Hz, 2H), 7.54-7.52 (m, 1H), 7.33 (t, $J = 7.6$ Hz, 2H), 7.22-7.19 (m, 2H), 7.12-7.07 (m, 2H), 6.35 (s, 1H), 4.25 (dd, $J_1 = 7.3$ Hz, $J_2 = 5.8$ Hz, 1H), 2.78 (t, $J = 6.1$ Hz, 2H), 2.33 (s, 3H), 2.17-2.11 (m, 1H), 2.05-1.98 (m, 1H), 1.93-1.85 (m, 1H), 1.83-1.76 (m, 1H). $^{13}\text{C NMR}$ (CDCl_3 , 125 MHz) $\delta = 152.6, 152.2, 137.2, 135.1, 131.2, 129.7, 129.0, 128.9, 128.7, 127.2, 123.5, 121.3, 120.1, 119.2, 118.3, 110.7, 107.0, 105.7, 31.8, 31.4, 23.4, 22.0, 8.7$. **HRMS (ESI)**: m/z : calculated for $\text{C}_{23}\text{H}_{20}\text{NO}^+$: 326.1539 $[\text{M}+\text{H}-\text{H}_2]^+$, found, 326.1541.

Synthesis of (S)-1,3-dimethyl-2-(2-phenyl-4,5,6,7-tetrahydrobenzofuran-4-yl)-1H-indole (75o)

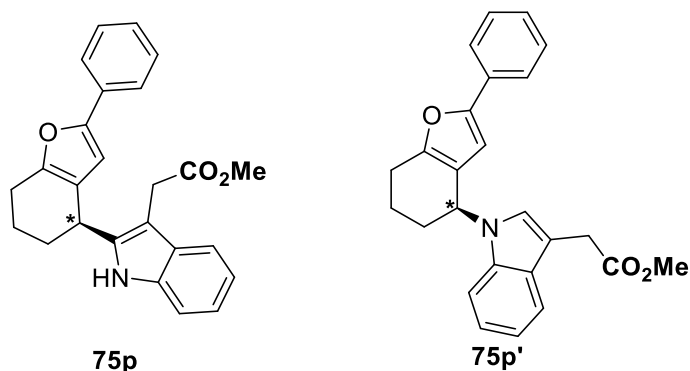


Yield: 65%, ee: 97%.

Compound **75o** was prepared according to the **general procedure 1** from **71a** (21.6 mg, 0.11 mmol, 1.1 equiv.), **74i** (14.5 mg, 0.1 mmol, 1.0 equiv.), **1a** (0.2 mg, 0.2 μ mol, 0.2 mol%) and Ag_2CO_3 (0.1 mg, 0.0001 mmol, 0.1 mol%) in toluene (0.5 mL), yielding product **75o** (20.5 mg, 0.07 mmol, 65%) as a white solid.

$[\alpha]_D^{25} = +28$ (c 0.94, CHCl_3). ee = 97%, determined on a Chiralpak IC column (heptane:IPA = 95:5, 1 mL/min), retention times: T_R (major): 4.4 min, T_R (minor): 4.9 min. $^1\text{H NMR}$ (CDCl_3 , 500 MHz) $\delta = 7.58$ (d, $J = 7.6$ Hz, 2H), 7.55 (d, $J = 7.9$ Hz, 1H), 7.33 (t, $J = 7.6$ Hz, 2H), 7.26 (d, $J = 8.2$ Hz, 1H), 7.20 (td, $J_1 = 7.3$ Hz, $J_2 = 3.1$ Hz, 2H), 7.13 (t, $J = 7.3$ Hz, 1H), 6.32 (s, 1H), 4.37-4.35 (m, 1H), 3.58 (s, 3H), 2.84-2.81 (m, 2H), 2.23 (s, 3H), 2.20-2.11 (m, 2H), 2.00-1.87 (m, 2H). $^{13}\text{C NMR}$ (CDCl_3 , 125 MHz) $\delta = 152.5, 150.8, 137.4, 137.2, 131.3, 128.8, 128.7, 127.0, 123.5, 121.2, 118.9, 118.4, 108.8, 107.8, 105.6, 105.3, 32.0, 30.5, 23.4, 23.2, 9.2$. **HRMS (ESI)**: m/z : calculated for $\text{C}_{24}\text{H}_{24}\text{NO}^+$: 342.1852 $[\text{M}+\text{H}]^+$, found, 342.1853.

Synthesis of methyl (S)-2-(2-(2-phenyl-4,5,6,7-tetrahydrobenzofuran-4-yl)-1H-indol-3-yl)acetate (75p) and methyl (S)-2-(1-(2-phenyl-4,5,6,7-tetrahydrobenzofuran-4-yl)-1H-indol-3-yl)acetate (75p')



Compound **75p** and **75p'** were prepared according to the **general procedure 1** from **71a** (23.1 mg, 0.11 mmol, 1.1 equiv.), **74j** (18.9 mg, 0.1 mmol, 1.0 equiv.), **1a** (0.2 mg, 0.2 μ mol, 0.2 mol%) and Ag_2CO_3 (0.1 mg, 0.0001 mmol, 0.1 mol%) in toluene (0.5 mL), yielding product **75p** (20 mg, 0.05 mmol, 52%) as a white solid and **75p'** (16.7 mg, 0.05 mmol, 46%) as a white solid.

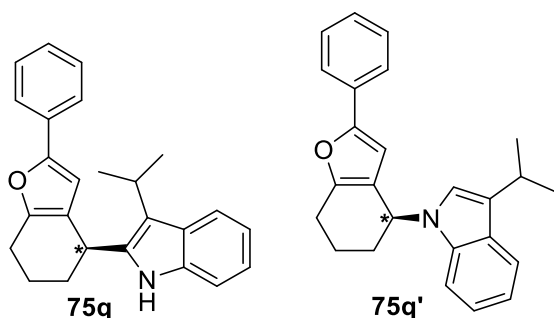
Data for 75p

$[\alpha]_D = +59$ (c 1.08, CHCl_3). ee = 91%, determined on a Chiralpak IC column (heptane:IPA = 98:2, 1 mL/min), retention times: T_R (minor): 31.8 min, T_R (major): 35.8 min. $^1\text{H NMR}$ (CDCl_3 , 500 MHz) δ = 7.73 (bs, 1H), 7.54-7.50 (m, 3H), 7.26 (t, J = 7.9 Hz, 2H), 7.17-7.12 (m, 2H), 7.07-7.03 (m, 2H), 6.26 (s, 1H), 4.22 (dd, J_1 = 7.3 Hz, J_2 = 6.0 Hz, 1H), 3.73 (dd, J_1 = 22.8 Hz, J_2 = 15.4 Hz, 2H), 3.61 (s, 3H), 2.72 (t, J = 6.0 Hz, 2H), 2.16-2.11 (m, 1H), 1.99-1.96 (m, 1H), 1.88-1.80 (m, 1H), 1.78-1.71 (m, 1H). $^{13}\text{C NMR}$ (CDCl_3 , 125 MHz) δ = 172.6, 152.7, 152.3, 139.2, 135.1, 131.1, 128.9, 128.7, 128.7, 127.3, 123.5, 121.8, 119.9, 118.6, 110.9, 105.6, 104.5, 52.2, 31.9, 31.7, 30.4, 23.4, 22.1. **HRMS (ESI)**: m/z : calculated for $\text{C}_{25}\text{H}_{24}\text{NO}_3^+$: 386.1751 $[\text{M}+\text{H}]^+$, found, 386.1751.

Data for 75p'

$[\alpha]_D = -4$ (c 0.94, CHCl_3). ee = 95%, determined on a Chiralpak IC column (heptane:IPA = 98:2, 1 mL/min), retention times: T_R (major): 23.1 min, T_R (minor): 25.9 min. $^1\text{H NMR}$ (CDCl_3 , 500 MHz) δ = 7.63 (d, J = 7.9 Hz, 1H), 7.59 (d, J = 7.6 Hz, 2H), 7.39 (d, J = 8.5 Hz, 1H), 7.34 (t, J = 7.9 Hz, 2H), 7.23-7.20 (m, 2H), 7.14 (t, J = 7.6 Hz, 1H), 6.99 (s, 1H), 6.40 (s, 1H), 5.53 (d, J = 5.4 Hz, 1H), 3.72 (dd, J_1 = 18.6 Hz, J_2 = 16.1 Hz, 2H), 3.66 (s, 3H), 2.85 (dt, J_1 = 16.7 Hz, J_2 = 6.3 Hz, 1H), 2.74 (dt, J_1 = 16.7 Hz, J_2 = 6.3 Hz, 1H), 2.19-2.13 (m, 1H), 2.09-2.03 (m, 1H), 1.98-1.85 (m, 2H). $^{13}\text{C NMR}$ (CDCl_3 , 125 MHz) δ = 172.5, 153.2, 153.0, 135.9, 130.8, 128.7, 128.4, 127.2, 125.4, 123.5, 121.6, 119.4, 119.3, 118.5, 109.7, 106.8, 104.8, 77.3, 77.0, 76.8, 51.9, 50.0, 31.3, 30.6, 23.1, 20.3. **HRMS (ESI)**: m/z : calculated for $\text{C}_{25}\text{H}_{24}\text{NO}_3^+$: 386.1751 $[\text{M}+\text{H}]^+$, found, 386.1747.

Synthesis of (S)-3-isopropyl-2-(2-phenyl-4,5,6,7-tetrahydrobenzofuran-4-yl)-1H-indole (75q) and (S)-3-isopropyl-1-(2-phenyl-4,5,6,7-tetrahydrobenzofuran-4-yl)-1H-indole (75q')



Compound **75q** and **75q'** were prepared according to the **general procedure 1** from **71a** (23.1 mg, 0.11 mmol, 1.1 equiv.), **75k** (15.9 mg, 0.1 mmol, 1.0 equiv.), **1a** (0.2 mg, 0.2 μ mol, 0.2 mol%) and Ag_2CO_3 (0.1 mg, 0.0001 mmol, 0.1 mol%) in toluene (0.5 mL), yielding product **75q** (7.4 mg, 0.06 mmol, 21%) as a pale yellow solid and **75q'** (20.7 mg, 0.02 mmol, 59%) as a pale yellow solid.

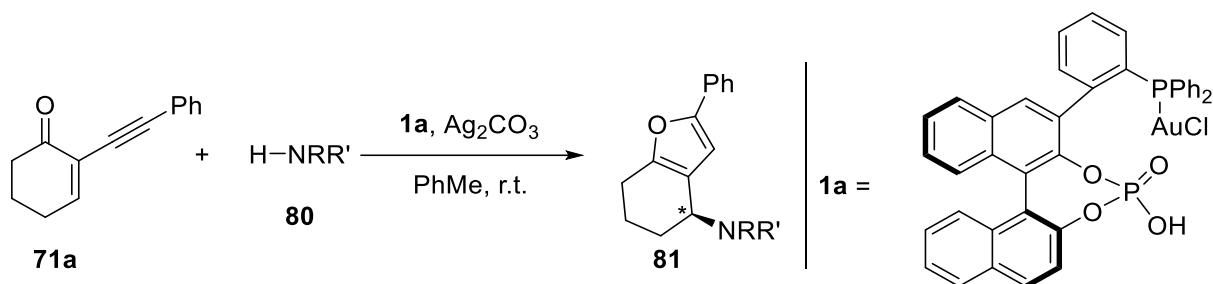
Data for 75q

$[\alpha]_D = -14$ (c 1.00, CHCl_3). ee = 49%, determined on a Chiralpak IA column (heptane:IPA = 95:5, 1 mL/min), retention times: T_R (minor): 5.2 min, T_R (major): 6.9 min. $^1\text{H NMR}$ (CDCl_3 , 500 MHz) δ = 7.66 (d, J = 7.0 Hz, 1H), 7.51 (d, J = 7.2 Hz, 2H), 7.26 (t, J = 7.7 Hz, 2H), 7.18-7.11 (m, 2H), 7.05-7.6.96 (m, 2H), 6.27 (s, 1H), 4.22 (dd, J_1 = 7.5 Hz, J_2 = 5.6 Hz, 1H), 3.22 (m, J = 7.1 Hz, 1H), 2.73-2.70 (m, 2H), 2.12-2.02 (m, 1H), 2.02-1.92 (m, 1H), 1.89-1.79 (m, 1H), 1.76-1.65 (m, 1H), 1.43 (t, J = 7.3 Hz, 6H). $^{13}\text{C NMR}$ (CDCl_3 , 125 MHz) δ = 152.6, 152.3, 135.9, 135.6, 131.1, 128.9, 127.4, 127.2, 123.5, 121.0, 120.3, 120.2, 118.9, 118.1, 111.0, 105.7, 32.3, 31.9, 26.1, 23.7, 23.6, 23.5, 22.1. **HRMS (ESI)**: m/z : calculated for $\text{C}_{25}\text{H}_{26}\text{NO}^+$: 356.2009 $[\text{M}+\text{H}]^+$, found, 356.2009.

Data for 75q'

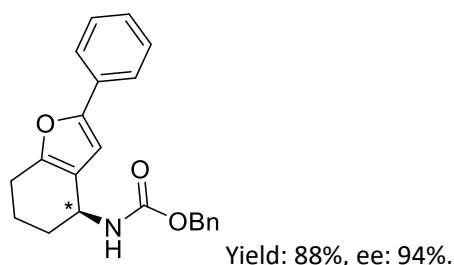
$[\alpha]_D = +16$ (c 0.50, CHCl_3). ee = 92%, determined on a Chiralpak IA column (heptane:IPA = 95:5, 1 mL/min), retention times: T_R (minor): 4.2 min, T_R (major): 4.6 min. $^1\text{H NMR}$ (CDCl_3 , 500 MHz) δ = 7.71 (d, J = 7.9 Hz, 1H), 7.65 (d, J = 7.9 Hz, 2H), 7.42 (d, J = 8.2 Hz, 1H), 7.39 (t, J = 7.6 Hz, 2H), 7.28-7.22 (m, 2H), 7.15 (d, J = 7.6 Hz, 1H), 6.81 (s, 1H), 6.45 (s, 1H), 5.56 (t, J = 5.5, 1H), 3.21 (m, J = 6.7 Hz, 1H), 2.93-2.88 (m, 1H), 2.82-2.77 (m, 1H), 2.23-2.17 (m, 1H), 2.12-2.06 (m, 1H), 2.03-1.92 (m, 2H), 1.35 (dd, J_1 = 6.7 Hz, J_2 = 4.6 Hz, 6H). $^{13}\text{C NMR}$ (CDCl_3 , 125 MHz) δ = 153.2, 153.0, 136.5, 131.1, 128.9, 128.0, 127.3, 123.7, 122.6, 121.7, 121.4, 119.9, 119.2, 118.8, 109.8, 105.1, 50.1, 30.9, 25.8, 23.7, 23.6, 23.3, 20.7. **HRMS (ESI)**: m/z : calculated for $\text{C}_{25}\text{H}_{26}\text{NO}^+$: 356.2009 $[\text{M}+\text{H}]^+$, found, 356.2010.

1.3. Tandem cycloisomerization/nucleophilic addition of ketones and amines



General Procedure 2: To a flask was added 2-(1-alkynyl)-2-alken-1-one **71a** (107.9 mg, 0.55 mmol, 1.1 equiv.), amines **80** (0.5 mmol, 1.0 equiv.), **1a** (0.001 mmol, 0.2 mol%), Ag_2CO_3 (0.5 μmol , 0.1 mol%) and toluene (2.5 mL). The resulting mixture was then stirred overnight at room temperature. The solvent was then removed under vacuum and the residue was purified by flash column chromatography.

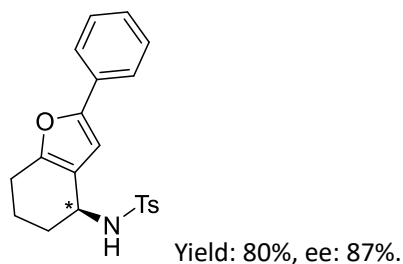
Synthesis of benzyl (S)-(2-phenyl-4,5,6,7-tetrahydrobenzofuran-4-yl)carbamate (**81a**)



Compound **81a** was prepared according to a modified **general procedure 2** from **71a** (107.9 mg, 0.55 mmol, 1.1 equiv.), benzyl carbamate **80a** (75.6 mg, 0.5 mmol, 1.0 equiv.), **1a** (8.4 mg, 0.01 mmol, 2 mol%) and Ag_2CO_3 (1.4 mg, 0.005 mmol, 1 mol%) in toluene (2.5 mL), yielding product **81a** (151.7 mg, 0.44 mmol, 88%) as a white solid for which the spectroscopical data correspond to those reported in the literature.⁷⁹

$[\alpha]_{\text{D}}^{25} = -3$ (c 1.15, CHCl_3). ee = 94%, determined on a Chiralpak IB column (heptane:IPA = 97:3, 1 mL/min), retention times: T_{R} (minor): 17.7 min, T_{R} (major): 22.5 min. $^1\text{H NMR}$ (CDCl_3 , 500 MHz) δ = 7.56 (d, J = 7.6 Hz, 2H), 7.33-7.29 (m, 7H), 7.18 (t, J = 7.3 Hz, 1H), 6.53 (s, 1H), 5.11 (s, 2H), 5.03 (d, J = 7.9 Hz, 1H), 4.75-4.74 (m, 1H), 2.63-2.54 (m, 2H), 2.00-1.96 (m, 1H), 1.88-1.80 (m, 2H), 1.69-1.66 (m, 1H). **HRMS (ESI):** m/z : calculated for $\text{C}_{22}\text{H}_{22}\text{NO}_3^+$: 348.1594 $[\text{M}+\text{H}]^+$, found, 348.1597.

Synthesis of (S)-4-methyl-N-(2-phenyl-4,5,6,7-tetrahydrobenzofuran-4-yl)benzenesulfonamide (**81b**)



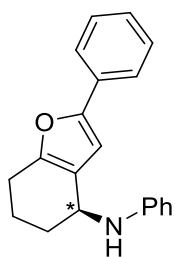
Compound **81b** was prepared according to the **general procedure 2** from **71a** (107.9 mg, 0.55 mmol, 1.1 equiv.), tosylamide **80b** (85.6 mg, 0.5 mmol, 1.0 equiv.), **1a** (0.8 mg, 0.001 mmol, 0.2 mol%) and Ag_2CO_3 (0.1 mg, 0.5 μmol , 0.1 mol%) in toluene (2.5 mL), yielding product **81b** (146.4 mg, 0.40 mmol, 80%) as a white solid for which the spectroscopical data correspond to those reported in the literature.⁷⁹

When the reaction was performed with 0.2 mol% of catalyst **1a**, the obtained ee was 94% but with a decrease of the yield to 17%.

81b was alternatively obtained from the same protocol in the absence of Ag_2CO_3 in 41% yield and 88% ee.

$[\alpha]_D = -99$ (c 1.14, CHCl_3). ee = 87%, determined on a Chiralpak IC column (heptane:IPA = 90:10, 1 mL/min), retention times: T_R (major): 35.7 min, T_R (minor): 41.7 min. $^1\text{H NMR}$ (CDCl_3 , 500 MHz) δ = 7.84 (d, J = 8.2 Hz, 2H), 7.46 (d, J = 7.3 Hz, 2H), 7.37 (d, J = 8.2 Hz, 2H), 7.33 (t, J = 7.6 Hz, 2H), 7.21 (t, J = 7.3 Hz, 1H), 5.86-5.85 (m, 1H), 4.59 (d, J = 8.2 Hz, 1H), 4.38-4.36 (m, 1H), 2.66-2.61 (m, 1H), 2.58-2.52 (1H), 2.48 (s, 3H), 1.90-1.73 (m, 4H). **HRMS (ESI)**: m/z : calculated for $\text{C}_{21}\text{H}_{20}\text{NO}_3\text{S}^-$: 366.1169 [M-H]⁻, found, 366.1172.

Synthesis of (S)-N,2-diphenyl-4,5,6,7-tetrahydrobenzofuran-4-amine (**81c**)

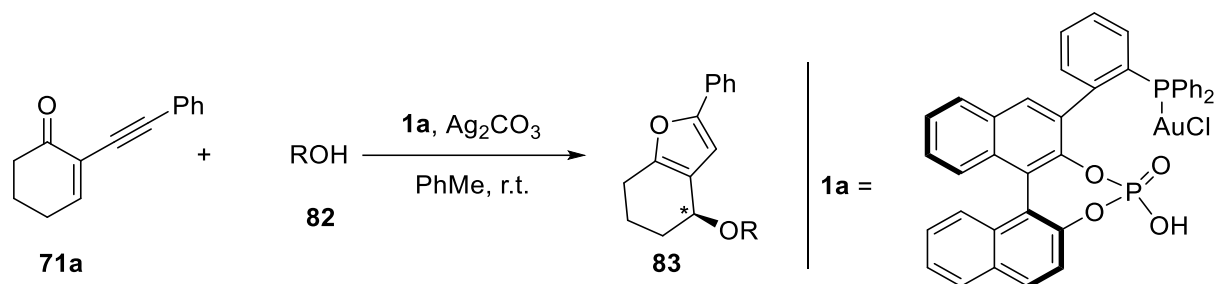


Yield: 89%, ee: 65%.

Compound **81c** was prepared according to the **general procedure 2** from **71a** (21.6 mg, 0.11 mmol, 1.1 equiv.), aniline **80c** (0.009 mL, 0.1 mmol, 1.0 equiv.), **1a** (8.4 mg, 0.01 mmol, 2 mol%) and Ag_2CO_3 (1.4 mg, 0.005 mmol, 1 mol%) in toluene (1 mL), yielding product **81c** (25.6 mg, 0.09 mmol, 89%) as a white solid for which the spectroscopical data correspond to those reported in the literature.⁷⁹

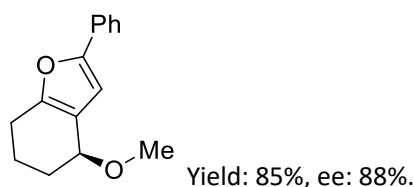
$[\alpha]_D = +4$ (c 0.95, CHCl_3). ee = 65%, determined on a Chiralpak IB column (heptane:IPA = 98:02, 1 mL/min), retention times: T_R (major): 10.5 min, T_R (minor): 14.0 min. $^1\text{H NMR}$ (CDCl_3 , 500 MHz) δ = 7.59 (t, J = 7.3 Hz, 2H), 7.33 (t, J = 7.6 Hz, 2H), 7.24-7.19 (m, 3H), 6.74-6.68 (m, 3H), 6.58 (s, 1H), 4.56 (br, 1H), 3.79 (bs, 1H), 2.75-2.62 (m, 2H), 2.02-1.95 (m, 2H), 1.88-1.80 (m, 2H). **HRMS (ESI)**: m/z : calculated for $\text{C}_{20}\text{H}_{18}\text{NO}^+$: 288.1383 [M-H₂+H]⁺, found, 288.1393.

1.4. Tandem cycloisomerization/nucleophilic addition of ketones and alcohols



General procedure 3: To a flask was added 2-(1-alkynyl)-2-alken-1-one **71a** (0.55 mmol, 1.1 equiv.), alcohol **82** (0.5 mmol, 1.0 equiv.), **1a** (0.001 mmol, 0.2 mol%), Ag_2CO_3 (0.5 μmol , 0.1 mol%) and toluene (2.5 mL). The resulting mixture was then stirred overnight at room temperature. The solvent was then removed under vacuum and the residue was purified by flash column chromatography.

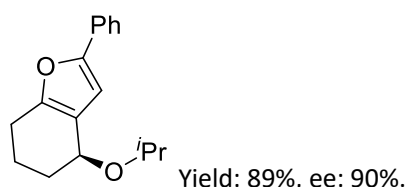
Synthesis of (S)-4-methoxy-2-phenyl-4,5,6,7-tetrahydrobenzofuran (**83a**)



Compound **83a** was prepared according to the **general procedure 3** in the absence of silver carbonate from **71a** (58.9 mg, 0.3 mmol, 1 equiv.), MeOH **82a** (3 mL, 0.3 M in DCM, 3 equiv.), **1a** (0.5 mg, 0.6 μmol , 0.2 mol %), yielding product **83a** (58.3 mg, 0.26 mmol, 85 %) as a colorless oil.^{67a}

ee: 88 %, determined on a Chiralpak IB column (heptane:IPA = 98:02, 1 mL/min), retention times: T_R (major): 5.9 min, T_R (minor): 6.6 min. $^1\text{H NMR}$ (CDCl_3 , 500 MHz) δ = 7.62 (d, J = 7.3 Hz, 2H), 7.34 (t, J = 7.6 Hz, 2H), 7.21 (t, J = 7.3 Hz, 1H), 6.64 (s, 1H), 4.30 (t, J = 4.0 Hz, 1H), 3.44 (s, 3H), 2.72 (dt, J_1 = 16.8 Hz, J_2 = 4.9 Hz, 1H), 2.64-2.57 (m, 1H), 2.09-2.00 (m, 1H), 1.98-1.93 (m, 1H), 1.86-1.78 (m, 2H). $^{13}\text{C NMR}$ (CDCl_3 , 125 MHz) δ = 153.1 (C_q), 152.5 (C_q), 131.4 (C_q), 128.8 (CH), 123.7 (CH), 120.2 (CH), 105.5 (C_q), 72.6 (CH), 56.3 (CH_3), 28.6 (CH_2), 23.5 (CH_2), 19.1 (CH_2).

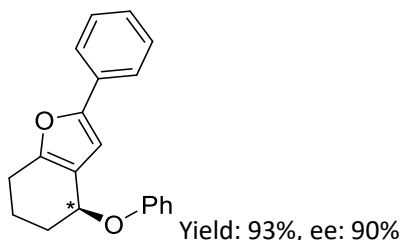
Synthesis of (S)-4-isopropoxy-2-phenyl-4,5,6,7-tetrahydrobenzofuran (**83b**)



Compound **83b** was prepared according to the **general procedure 3** in the absence of silver carbonate from **71a** (58.9 mg, 0.3 mmol, 1 equiv.), $i\text{-PrOH}$ **82c** (3 mL, 0.3 M in DCM, 3 equiv.), **1a** (0.5 mg, 0.6 μmol , 0.2 mol %), yielding product **83b** (68.5 mg, 0.27 mmol, 89 %) as a colorless oil.

ee: 90 %, determined on a Chiralpak IB column (heptane:IPA = 99:01, 1 mL/min), retention times: T_R (major): 4.2 min, T_R (minor): 4.7 min. $^1\text{H NMR}$ (CDCl_3 , 500 MHz) δ = 7.61 (d, J = 7.6 Hz, 2H), 7.33 (t, J = 7.6 Hz, 2H), 7.20 (t, J = 7.3 Hz, 1H), 6.58 (s, 1H), 4.45 (t, J = 4.3 Hz, 1H), 3.82 (m, J = 6.1 Hz, 1H), 2.71 (dt, J_1 = 16.5 Hz, J_2 = 5.5 Hz, 1H), 2.61-2.55 (m, 1H), 2.10-2.02 (m, 1H), 1.88-1.77 (m, 3H), 1.23 (t, J = 5.8 Hz, 6H). $^{13}\text{C NMR}$ (CDCl_3 , 125 MHz) δ = 152.8 (C_q), 152.5 (C_q), 131.5 (C_q), 128.7 (CH), 127.0 (CH), 123.7 (CH), 121.2 (C_q), 105.3 (CH), 69.6 (CH), 68.7 (CH), 30.0 (CH_2), 23.5 (CH_2), 23.4 (CH_3), 22.9 (CH_3), 19.2 (CH_2).

Synthesis of (S)-4-phenoxy-2-phenyl-4,5,6,7-tetrahydrobenzofuran (83c)

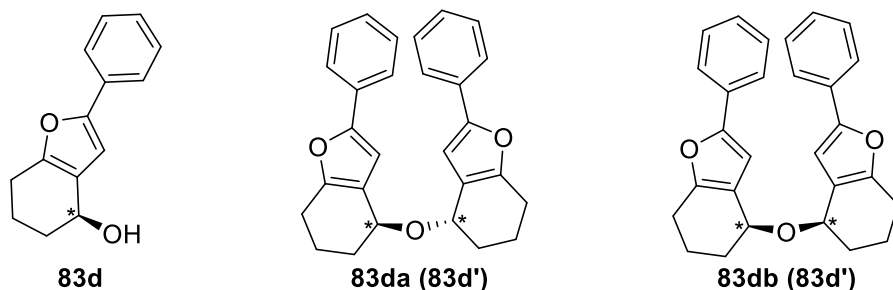


Compound **83c** was prepared according to the **general procedure 3** from **71a** (107.9 mg, 0.55 mmol, 1.1 equiv.), phenol **82c** (47.1 mg, 0.5 mmol, 1.0 equiv.), **1a** (0.8 mg, 0.001 mmol, 0.2 mol%) and Ag_2CO_3 (0.1 mg, 0.5 μmol , 0.1 mol%) in toluene (2.5 mL), yielding product **83c** (133.9 mg, 0.46 mmol, 93%) as a white solid for which the spectroscopical data correspond to those reported in the literature.⁷⁹

83c was alternatively obtained from the same protocol in the absence of Ag_2CO_3 in 36% yield and 63% ee.

$[\alpha]_D = -21$ (c 0.99, CHCl_3). ee = 90%, determined on a Chiralpak IB column (heptane:IPA = 98:02, 1 mL/min), retention times: T_R (major): 6.1 min, T_R (minor): 9.2 min. $^1\text{H NMR}$ (CDCl_3 , 500 MHz) δ = 7.60 (d, J = 7.3 Hz, 2H), 7.35-7.30 (m, 4H), 7.21 (t, J = 7.3 Hz, 1H), 7.03 (d, J = 7.9 Hz, 2H), 6.98 (t, J = 7.3 Hz, 1H), 6.58 (s, 1H), 5.36 (t, J = 4.3 Hz, 1H), 2.80 (dt, J_1 = 16.8, J_2 = 5.2 Hz, 1H), 2.69-2.63 (m, 1H), 2.16-2.08 (m, 2H), 2.00-1.93 (m, 1H), 1.92-1.85 (m, 1H). **HRMS (ESI)**: m/z : calculated for $\text{C}_{20}\text{H}_{17}\text{O}_2^+$: 289.1223 $[\text{M}-\text{H}_2+\text{H}]^+$, found, 289.1224.

Synthesis of (S)-2-phenyl-4,5,6,7-tetrahydrobenzofuran-4-ol (83d), (4S,4'S)-4,4'-oxybis(2-phenyl-4,5,6,7-tetrahydrobenzofuran) (83da) and (S)-2-phenyl-4-(((R)-2-phenyl-4,5,6,7-tetrahydrobenzofuran-4-yl)oxy)-4,5,6,7-tetrahydrobenzofuran (83db)



Compound **83d** and **83d'** were prepared according to the **general procedure 3** from **71a** (98.1 mg, 0.5 mmol, 1.0 equiv.), water (0.03 mL, 1.5 mmol, 3.0 equiv.), **1a** (0.8 mg, 0.001 mmol, 0.2 mol%) and Ag_2CO_3 (0.1 mg, 0.5 μmol , 0.1 mol%) in toluene (2.5 mL), yielding products **83d** (34.3 mg, 0.16 mmol, 32%), **83da** (50.9 mg, 0.25 mmol, 50%) and **83db** (18.1 mg, 0.09 mmol, 18%) as white solids.

Data for 83d:⁷⁹

$[\alpha]_D = +12$ (c 1.44, CHCl₃). ee = 97%, determined on a Chiralpak IB column (heptane:IPA = 98:2, 1 mL/min), retention times: T_R (major): 28.3 min, T_R (minor): 34.5 min. ¹H NMR (CDCl₃, 500 MHz) δ = 7.62 (d, *J* = 7.3 Hz, 2H), 7.35 (t, *J* = 7.6 Hz, 2H), 7.22 (t, *J* = 7.6 Hz, 1H), 6.66 (s, 1H), 4.77-4.75 (m, 1H), 2.75-2.69 (m, 1H), 2.64-2.58 (m, 1H), 2.08-2.00 (m, 1H), 1.98-1.92 (m, 1H), 1.89-1.78 (m, 2H), 1.62 (s, 1H). HRMS (ESI): *m/z*: calculated for C₁₄H₁₃O₂⁺: 213.0910 [M-H₂+H]⁺, found, 213.0912.

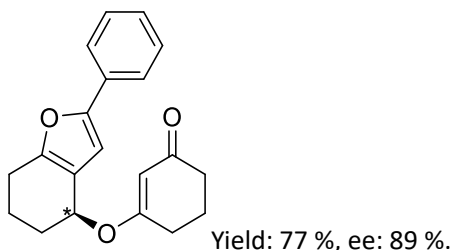
Data for 83da:

$[\alpha]_D = +75$ (c 0.95, CHCl₃). ¹H NMR (CDCl₃, 500 MHz) δ = 7.61 (d, *J* = 7.9 Hz, 4H), 7.34 (t, *J* = 7.9 Hz, 4H), 7.20 (t, *J* = 7.3 Hz, 2H), 6.61 (s, 2H), 4.62 (t, *J* = 3.8 Hz, 2H), 2.74 (dt, *J*₁ = 16.4 Hz, *J*₂ = 5.0 Hz, 2H), 2.64-2.58 (m, 2H), 2.16-2.11 (m, 2H), 2.03-1.99 (m, 2H), 1.92-1.87 (m, 4H). ¹³C NMR (CDCl₃, 125 MHz) δ = 153.0, 131.4, 128.9, 128.8, 127.1, 123.7, 120.9, 105.3, 69.2, 29.8, 23.5, 19.2. HRMS (ESI): *m/z*: calculated for C₂₈H₂₇O₃⁺: 411.1955 [M+H]⁺, found, 411.1956.

Data for 83db:

¹H NMR (CDCl₃, 500 MHz) δ = 7.62 (d, *J* = 7.9 Hz, 4H), 7.34 (t, *J* = 7.6 Hz, 4H), 7.20 (t, *J* = 7.3 Hz, 2H), 6.61 (s, 2H), 4.70 (t, *J* = 4.1 Hz, 2H), 2.75 (dt, *J*₁ = 16.4 Hz, *J*₂ = 5.3 Hz, 2H), 2.66-2.60 (m, 2H), 2.16-2.10 (m, 2H), 1.96-1.93 (m, 4H), 1.88-1.84 (m, 2H). ¹³C NMR (CDCl₃, 125 MHz) δ = 152.9, 131.4, 128.8, 127.1, 123.8, 123.7, 121.1, 105.3, 69.3, 30.2, 23.5, 19.5. HRMS (ESI): *m/z*: calculated for C₂₈H₂₇O₃⁺: 411.1955 [M+H]⁺, found, 411.1953.

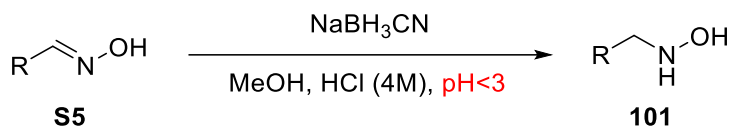
Synthesis of (S)-3-((2-phenyl-4,5,6,7-tetrahydrobenzofuran-4-yl)oxy)cyclohex-2-en-1-one (83e)



Compound **83e** was prepared according to the **general procedure 3** from **71a** (98 mg, 0.5 mmol, 1 equiv.), **82e** (11.2 mg, 0.1 mmol, 1.0 equiv.), **1a** (0.2 mg, 0.2 μ mol, 0.2 mol %) and Ag₂CO₃ (0.1 mg, 0.0001 mmol, 0.1 mol %) in toluene (0.5 mL), yielding product **83e** (23.6 mg, 0.77 mmol, 77 %) as a white solid for which the spectroscopical data correspond to those reported in the literature.⁷⁹

$[\alpha]_D = -150$ (c 0.92, CHCl₃). ee: 89 %, determined on a Chiralpak IA column (heptane:IPA = 98:02, 1 mL/min), retention times: T_R (major): 22.8 min, T_R (minor): 27.1 min. ¹H NMR (CDCl₃, 300 MHz) δ = 7.54 (d, *J* = 7.3 Hz, 2H), 7.28 (t, *J* = 7.5 Hz, 2H), 7.16 (t, *J* = 7.7 Hz, 1H), 6.53 (s, 1H), 5.54 (s, 1H), 5.19 (t, *J* = 3.6 Hz, 1H), 2.72 (dt, *J*₁ = 16.8 Hz, *J*₂ = 4.7 Hz, 1H), 2.63-2.53 (m, 1H), 2.37-2.29 (m, 4H), 2.05-1.79 (m, 6H). HRMS (ESI): *m/z*: calcd for C₄₀H₄₀NaO₆⁺ 639.2723 [2M+Na]⁺, found, 639.2717.

A solution of $\text{NH}_2\text{OH}\cdot\text{HCl}$ (280 mg, 4 mmol, 1 equiv.) and $\text{NaOAc}\cdot 3\text{H}_2\text{O}$ (554.3 mg, 4 mmol, 1 equiv.) in H_2O (2.5 mL) was added to a solution of aldehyde (4 mmol, 1 equiv.) in EtOH (10 mL). The mixture was then stirred at room temperature for 3 h, then the reaction mixture was concentrated to dryness under vacuum. The residue was diluted with H_2O and extracted with EtOAc, the combined organic phases dried over MgSO_4 , filtered and concentrated under vacuum. The crude product was then crystallized from dichloromethane and petroleum ether, to give the products as white solid that was directly engaged in the next step.



Oxime (4 mmol, 1 equiv) was dissolved in MeOH (10 mL), and then NaBH_3CN (252 mg, 4 mmol, 1 equiv.) was added slowly, then HCl (4M) was added to the mixture carefully and keep the $\text{pH}<3$ during the process. 15 min later, the reaction mixture was concentrated under vacuum. The residue was diluted with 1M-NaOH and extracted with EtOAc. The combined organic phases were dried over MgSO_4 , filtered and concentrated under vacuum. The crude product was then crystallized from dichloromethane and petroleum ether to give the products as white solid.

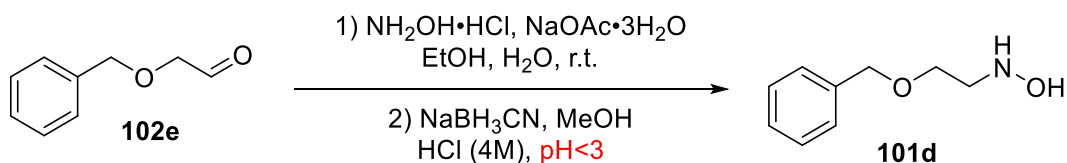
Synthesis of *N*-(3-phenylpropyl)hydroxylamine (101c)



Compound **101c** was prepared according to the general procedure for the synthesis of hydroxylamines. A solution of $\text{NH}_2\text{OH}\cdot\text{HCl}$ (280 mg, 4 mmol, 1 equiv.) and $\text{NaOAc}\cdot 3\text{H}_2\text{O}$ (554.3 mg, 4 mmol, 1 equiv.) in H_2O (2.5 mL) was added to a solution of aldehyde (0.53 mL, 4 mmol, 1 equiv.) in EtOH (10 mL). The mixture was then stirred at room temperature for 3 h, then the reaction mixture was concentrated to dryness under vacuum. The residue was diluted with H_2O and extracted with EtOAc, the combined organic phases were dried over MgSO_4 , filtered and concentrated under vacuum.

The crude product was then dissolved in MeOH (10 mL), and then NaBH_3CN (252 mg, 4 mmol, 1 equiv.) was added slowly, then HCl (4 M) was added to the mixture carefully to keep the $\text{pH}<3$ during the process. 15 min later, the reaction mixture was concentrated under vacuum. The residue was diluted with 1 M-NaOH and extracted with EtOAc. The combined organic layers were dried over MgSO_4 , filtered and concentrated under vacuum. The crude product was then crystallized from dichloromethane and petroleum ether to give the product **101c** (424 mg, 2.8 mmol, 70 %) as white solid.

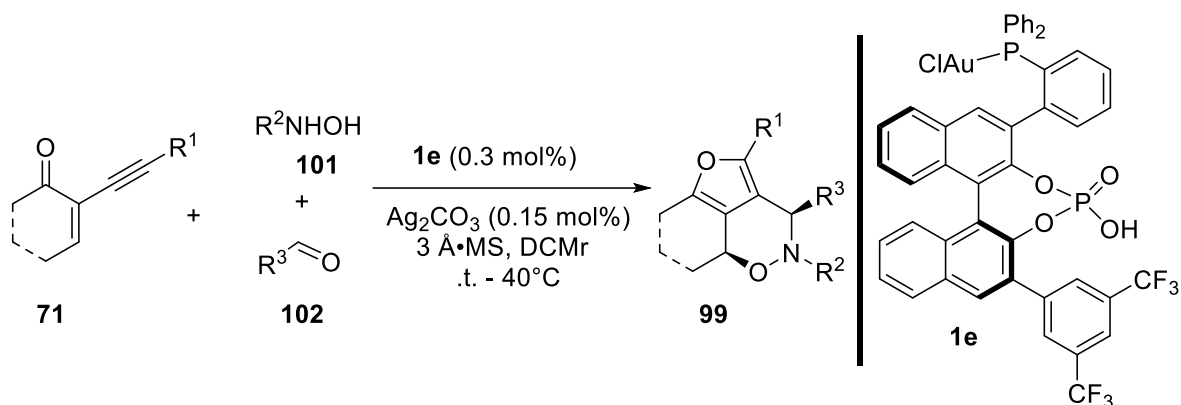
Synthesis of *N*-(2-(benzyloxy)ethyl)hydroxylamine (101d)



Compound **101d** was prepared according to the general procedure for the synthesis of hydroxyamines. A solution of $\text{NH}_2\text{OH}\cdot\text{HCl}$ (280 mg, 4 mmol, 1 equiv.) and $\text{NaOAc}\cdot 3\text{H}_2\text{O}$ (554.3 mg, 4 mmol, 1 equiv.) in H_2O (2.5 mL) was added to a solution of aldehyde (600 mg, 4 mmol, 1 equiv.) in EtOH (10 mL). The mixture was then stirred at room temperature for 3 h, then the reaction mixture was concentrated to dryness under vacuum. The residue was diluted with H_2O and extracted with EtOAc. The combined organic layers were dried over MgSO_4 , filtered and concentrated under vacuum.

The crude product was then dissolved in MeOH (10 mL), and then NaBH_3CN (252 mg, 4 mmol, 1 equiv.) was added slowly, then HCl (4M) was added to the mixture carefully to keep the $\text{pH} < 3$ during the process. 15 min later, the reaction mixture was concentrated under vacuum. The residue was diluted with 1 M-NaOH and extracted with EtOAc, the combined organic phases dried over MgSO_4 , filtered and concentrated under vacuum. The crude product was then crystallized from dichloromethane and petroleum ether to give the products **101d** (555 mg, 3.3 mmol, 83 %) as white solid.

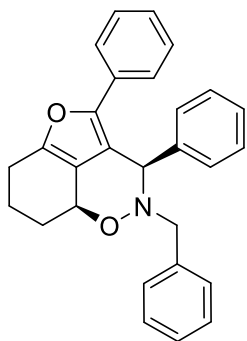
2.2. Reactions from ketones **71**



General procedure 4: To a stirring schlenk tube were added 2-(1-alkynyl)-2-alken-1-one **71** (1.5 equiv., 4.5 mmol), hydroxylamine **101** (1.0 equiv., 3 mmol), aldehyde **102** (1.0 equiv., 3 mmol), 3 Å-MS (300 mg), catalyst **1e** (1 mg, 0.9 μmol , 0.3 mol%), Ag_2CO_3 (0.1 mg, 0.45 μmol , 0.15 mol%) and DCM (3 mL), the resulting mixture was then stirred at room temperature for 24 h. After the reaction completed, DCM was removed under vacuum and the crude mixture was purified by flash column chromatography.

General procedure 5: To a stirring schlenk tube were added hydroxylamine **101** (1.0 equiv., 3 mmol), aldehyde **102** (1.0 equiv., 3 mmol) and DCM (3 mL), the solution was stirred at room temperature for 30 min and then 2-(1-alkynyl)-2-alken-1-one **71** (1.5 equiv., 4.5 mmol), 3 Å-MS (300 mg), catalyst **1e** (1 mg, 0.9 μmol , 0.3 mol%) and Ag_2CO_3 (0.1 mg, 0.45 μmol , 0.15 mol%) were added, the resulting mixture was stirred at room temperature for 24 h. After the reaction completed, the DCM was removed under vacuum and the crude mixture was purified by flash column chromatography.

Synthesis of (3*R*,8*aS*)-2-benzyl-3,4-diphenyl-2,3,6,7,8,8*a*-hexahydrobenzofuro[3,4-*de*][1,2]oxazine (99ab)

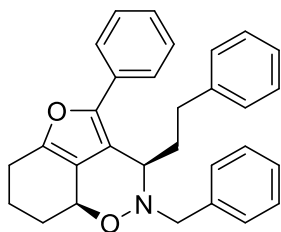


yield: 83%, ee: 98%

Compound **99ab** was prepared according to the **general procedure 4** from 2-(phenylethynyl)cyclohex-2-en-1-one **71a** (88.3 mg, 4.5 mmol, 1.5 equiv.), *N*-benzylhydroxylamine **101b** (37.0 mg, 3 mmol, 1 equiv.), benzaldehyde **102a** (31 μ L, 3 mmol, 1 equiv.), 3 \AA -MS (300 mg), catalyst **1e** (1.6 mg, 0.5 mol%, 1.5 μ mol), Ag_2CO_3 (0.2 mg, 0.25 mol%, 0.75 μ mol) and DCM (3 mL). The resulting mixture was then stirred at 40 $^\circ\text{C}$ for 24 hours, the DCM was removed under vacuum and the crude mixture was purified by flash column chromatography to give the product **99ab** as a white solid (101.4 mg, 0.25 mmol, 83%).

$[\alpha]_D = +185.9$ (c 0.83, CHCl_3). ee = 98%, determined on a Chiralpak IA column (heptane:IPA = 80:20, 1 mL/min), retention times: T_R (minor): 4.5 min, T_R (major): 5.0 min. $^1\text{H NMR}$ (CDCl_3 , 500 MHz) δ = 7.38 (d, J = 7.3 Hz, 2H), 7.34-7.30 (m, 4H), 7.27-7.13 (m, 8H), 7.03 (t, J = 7.3 Hz, 1H), 5.27 (s, 1H), 4.98-4.95 (m, 1H), 3.73 (d, J = 14.3 Hz, 1H), 3.53 (d, J = 14.3 Hz, 1H), 2.82-2.68 (m, 2H), 2.17-2.14 (m, 1H), 2.11-2.08 (m, 1H), 1.90-1.80 (m, 1H), 1.41-1.34 (m, 1H). $^{13}\text{C NMR}$ (CDCl_3 , 125 MHz) δ = 147.0 (C_q), 146.7 (C_q), 138.3 (C_q), 137.3 (C_q), 131.2 (C_q), 130.4 (CH), 128.8 (CH), 128.4 (CH), 128.4 (CH), 128.0 (CH), 128.0 (CH), 127.2 (CH), 126.4 (CH), 124.1 (CH), 123.3 (C_q), 119.3 (C_q), 75.4 (CH), 65.1 (CH), 58.9 (CH_2), 28.2 (CH_2), 23.3 (CH_2), 20.6 (CH_2). **HRMS (ESI)**: m/z : calculated for $\text{C}_{28}\text{H}_{26}\text{NO}_2^+$: 408.1958 $[\text{M}+\text{H}]^+$, found, 408.1966.

Synthesis of (3*R*,8*aS*)-2-benzyl-3-phenethyl-4-phenyl-2,3,6,7,8,8*a*-hexahydrobenzofuro[3,4-*de*][1,2]oxazine (99ac)



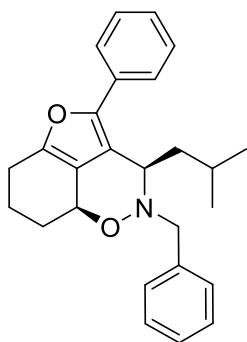
yield: 96%, ee: 99%

Compound **99ac** was prepared according to the **general procedure 4** from 2-(phenylethynyl)cyclohex-2-en-1-one **71a** (88.3 mg, 4.5 mmol, 1.5 equiv.), *N*-benzylhydroxylamine **101b** (37.0 mg, 3 mmol, 1 equiv.), 3-phenylpropanal **102b** (40.3 mg, 3 mmol, 1 equiv.), 3 \AA -MS (300 mg), catalyst **1e** (1 mg, 0.9 μ mol, 0.3 mol%), Ag_2CO_3 (0.1 mg, 0.45 μ mol, 0.15 mol%) and DCM (3 mL). The resulting mixture was then stirred at room temperature overnight, the DCM was removed under vacuum and the crude mixture was purified by flash column chromatography to give the product **99ac** as a white solid (125.3 mg, 0.29 mmol, 96%).

$[\alpha]_D = +100.6$ (c 1.25, CHCl_3). ee = 99%, determined on a Chiralpak IC column (heptane:IPA = 95:5, 1 mL/min), retention times: T_R (minor): 4.2 min, T_R (major): 4.6 min. $^1\text{H NMR}$ (CDCl_3 , 500 MHz) δ = 7.52 (d, J =

7.3 Hz, 2H), 7.39 (t, $J = 7.3$ Hz, 2H), 7.32 (t, $J = 7.3$ Hz, 1H), 7.26 (d, $J = 7.3$ Hz, 2H), 7.20 (t, $J = 7.6$ Hz, 2H), 7.15-7.09 (m, 4H), 6.79 (d, $J = 6.7$ Hz, 2H), 4.85-4.82 (m, 1H), 4.34 (d, $J = 13.1$ Hz, 1H), 4.19-4.15 (m, 2H), 2.77-2.71 (m, 2H), 2.66-2.59 (m, 2H), 2.18-2.08 (m, 2H), 2.01-1.98 (m, 1H), 1.82-1.75 (m, 2H), 1.30-1.23 (m, 1H). ^{13}C NMR (CDCl_3 , 125MHz) $\delta = 147.4$ (C_q), 146.9 (C_q), 142.3 (C_q), 137.9 (C_q), 131.5 (C_q), 129.3 (CH), 128.8 (CH), 128.8 (CH), 128.7 (CH), 128.4 (CH), 127.6 (CH), 126.5 (CH), 125.8 (CH), 124.2 (CH), 121.1 (C_q), 116.7 (C_q), 68.6 (CH), 58.7 (CH_2), 57.5 (CH), 34.4 (CH_2), 32.9 (CH_2), 27.9 (CH_2), 23.2 (CH_2), 20.4 (CH_2). HRMS (ESI): m/z : calculated for $\text{C}_{30}\text{H}_{30}\text{NO}_2^+$: 436.2271 [$\text{M}+\text{H}$] $^+$, found, 436.2265.

Synthesis of (3*R*,8*aS*)-2-benzyl-3-isobutyl-4-phenyl-2,3,6,7,8,8*a*-hexahydrobenzofuro[3,4-*de*][1,2]oxazine (99ad)

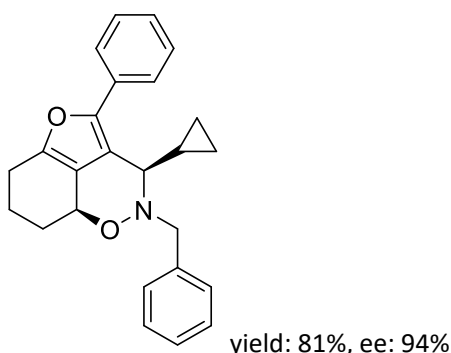


yield: 81%, ee: 98%

Compound **99ad** was prepared according to the **general procedure 4** from 2-(phenylethynyl)cyclohex-2-en-1-one **71a** (88.3 mg, 4.5 mmol, 1.5 equiv.), *N*-benzylhydroxylamine **101b** (37.0 mg, 3 mmol, 1 equiv.), 3-methylbutanal **102c** (33 μL , 3 mmol, 1 equiv.), 3 Å-MS (300 mg), catalyst **1e** (1 mg, 0.9 μmol , 0.3 mol%), Ag_2CO_3 (0.1 mg, 0.45 μmol , 0.15 mol%) and DCM (3 mL). The resulting mixture was then stirred at room temperature for 60 hours, the DCM was removed under vacuum and the crude mixture was purified by flash column chromatography to give the product **99ad** as a white solid (94.1 mg, 0.24 mmol, 81%).

$[\alpha]_D = +100.2$ (c 1.63, CHCl_3). ee = 98%, determined on a Chiralpak IB column (heptane:IPA = 80:20, 1 mL/min), retention times: T_R (minor): 4.0 min, T_R (major): 5.4 min. ^1H NMR (CDCl_3 , 500 MHz) $\delta = 7.49$ -7.47 (m, 4H), 7.40-7.30 (m, 5H), 7.19 (t, $J = 7.5$ Hz, 1H), 4.88-4.83 (m, 1H), 4.39 (d, $J = 12.8$ Hz, 1H), 4.20-4.16 (m, 2H), 2.83-2.61 (m, 2H), 2.20-2.12 (m, 1H), 2.06-1.76 (m, 4H), 1.37-1.24 (m, 1H), 1.14-1.05 (m, 1H), 0.76 (d, $J = 6.8$ Hz, 3H), 0.63 (d, $J = 6.4$ Hz, 3H). ^{13}C NMR (CDCl_3 , 125MHz) $\delta = 147.5$ (C_q), 146.9 (C_q), 137.8 (C_q), 131.7 (C_q), 129.3 (CH), 128.7 (CH), 128.6 (CH), 127.6 (CH), 126.6 (CH), 124.4 (CH), 120.7 (C_q), 117.0 (C_q), 67.5 (CH), 58.9 (CH_2), 56.3 (CH), 42.6 (CH_2), 27.9 (CH_2), 24.9 (CH), 23.7 (CH_3), 23.3 (CH_2), 21.1 (CH_3), 20.5 (CH_2). HRMS (ESI): m/z : calculated for $\text{C}_{26}\text{H}_{30}\text{NO}_2^+$: 388.2271 [$\text{M}+\text{H}$] $^+$, found, 388.2264.

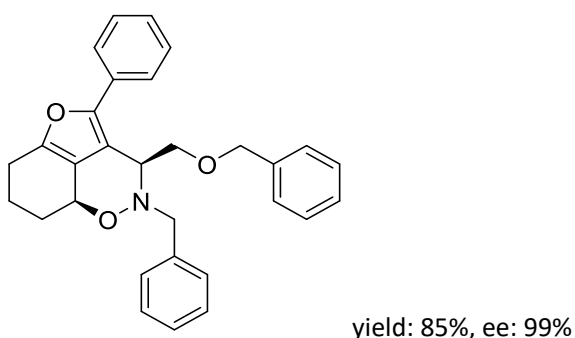
Synthesis of (3*R*,8*aS*)-2-benzyl-3-cyclopropyl-4-phenyl-2,3,6,7,8,8*a*-hexahydrobenzofuro[3,4-*de*][1,2]oxazine (99ae)



Compound **99ae** was prepared according to the **general procedure 4** from 2-(phenylethynyl)cyclohex-2-en-1-one **71a** (88.3 mg, 4.5 mmol, 1.5 equiv.), *N*-benzylhydroxylamine **101b** (37.0 mg, 3 mmol, 1 equiv.), cyclopropanecarbaldehyde **102d** (23 μ L, 3 mmol, 1 equiv.), 3 Å-MS (300 mg), catalyst **1e** (1 mg, 0.9 μ mol, 0.3 mol%), Ag₂CO₃ (0.1 mg, 0.45 μ mol, 0.15 mol%) and DCM (3 mL). The resulting mixture was then stirred at room temperature for 24 h, the DCM was removed under vacuum and the crude mixture was purified by flash column chromatography to give the product **99ae** as a white solid (90 mg, 0.24 mmol, 81%).

[α]_D = +100.0 (*c* 1.05, CHCl₃). ee = 94%, determined on a Chiralpak IA column (heptane:IPA = 80:20, 1 mL/min), retention times: T_R (major): 4.0 min, T_R (minor): 4.7 min. ¹H NMR (CDCl₃, 500 MHz) δ = 7.58-7.55 (m, 2H), 7.50 (d, *J* = 7.5 Hz, 2H), 7.39-7.19 (m, 6H), 4.81-4.76 (m, 1H), 4.41 (d, *J* = 14.3 Hz, 1H), 4.15-4.10 (m, 2H), 2.76-2.56 (m, 2H), 2.13-1.96 (m, 2H), 1.86-1.71 (m, 1H), 1.37-1.21 (m, 2H), 0.52-0.43 (m, 1H), 0.32-0.15 (m, 3H). ¹³C NMR (CDCl₃, 125MHz) δ = 146.9 (C_q), 146.3 (C_q), 138.8 (C_q), 132.5 (C_q), 128.7 (CH), 128.6 (CH), 128.4 (CH), 127.2 (CH), 127.1 (CH), 125.7 (CH), 122.6 (C_q), 118.2 (C_q), 74.4 (CH), 63.3 (CH), 59.0 (CH₂), 27.9 (CH₂), 23.1 (CH₂), 20.8 (CH₂), 11.9 (CH), 4.8 (CH₂), 1.1 (CH₂). HRMS (ESI): *m/z*: calculated for C₂₅H₂₆NO₂⁺: 372.1958 [M+H]⁺, found, 372.1952.

Synthesis of (3*S*,8*aS*)-2-benzyl-3-((benzyloxy)methyl)-4-phenyl-2,3,6,7,8,8*a*-hexahydrobenzofuro[3,4-*de*][1,2]oxazine (99af)

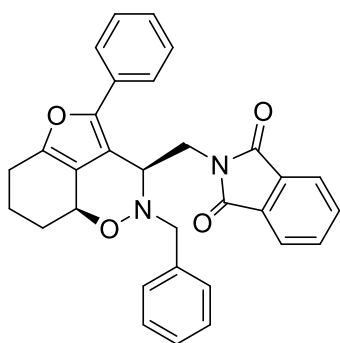


Compound **99af** was prepared according to the **general procedure 4** from 2-(phenylethynyl)cyclohex-2-en-1-one **71a** (88.3 mg, 4.5 mmol, 1.5 equiv.), *N*-benzylhydroxylamine **101b** (37.0 mg, 3 mmol, 1 equiv.), 2-(benzyloxy)acetaldehyde **102e** (45.1 mg, 3 mmol, 1 equiv.), 3 Å-MS (300 mg), catalyst **1e** (1 mg, 0.9 μ mol, 0.3 mol%), Ag₂CO₃ (0.1 mg, 0.45 μ mol, 0.15 mol%) and DCM (3 mL). The resulting mixture was then stirred at

room temperature for 24 hours, the DCM was removed under vacuum and the crude mixture was purified by flash column chromatography to give the product **99af** as a white solid (115.0 mg, 0.26 mmol, 85%).

$[\alpha]_D = +136.3$ (c 2.63, CHCl_3). ee = 99%, determined on a Chiralpak IB column (heptane:IPA = 98:02, 1 mL/min), retention times: T_R (minor): 5.2 min, T_R (major): 5.7 min. $^1\text{H NMR}$ (CDCl_3 , 500 MHz) δ = 7.56 (d, J = 7.6 Hz, 2H), 7.48 (d, J = 7.6 Hz, 2H), 7.38-7.25 (m, 10H), 7.21 (t, J = 7.3 Hz, 1H), 4.78-4.74 (m, 2H), 4.52 (d, J = 11.9 Hz, 1H), 4.45 (d, J = 11.9 Hz, 1H), 4.33 (d, J = 15.0 Hz, 1H), 4.26 (d, J = 15.0 Hz, 1H), 4.09 (dd, J_1 = 11.0 Hz, J_2 = 8.3 Hz, 1H), 3.43 (dd, J_1 = 10.7 Hz, J_2 = 1.2 Hz, 1H), 2.74-2.69 (m, 1H), 2.61-2.54 (m, 1H), 2.09-2.05 (m, 1H), 1.99-1.94 (m, 1H), 1.80-1.71 (m, 1H), 1.20-1.12 (m, 1H) $^{13}\text{C NMR}$ (CDCl_3 , 125MHz) δ = 147.0 (C_q), 146.7 (C_q), 139.3 (C_q), 138.4 (C_q), 131.4 (C_q), 129.0 (CH), 128.7 (CH), 128.6 (CH), 128.3 (CH), 127.8 (CH), 127.8 (CH), 127.1 (CH), 126.8 (CH), 124.2 (CH), 123.2 (C_q), 116.6 (C_q), 74.7 (CH), 73.3 (CH_2), 70.0 (CH_2), 62.1 (CH), 59.5 (CH_2), 27.7 (CH_2), 23.2 (CH_2), 20.5 (CH_2). **HRMS (ESI)**: m/z : calculated for $\text{C}_{30}\text{H}_{30}\text{NO}_3^+$: 452.2220 $[\text{M}+\text{H}]^+$, found, 452.2214.

Synthesis of 2-(((3*S*,8*aS*)-2-benzyl-4-phenyl-2,3,6,7,8,8*a*-hexahydrobenzofuro[3,4-*de*][1,2]oxazin-3-yl)methyl)isoindoline-1,3-dione (**99ag**)

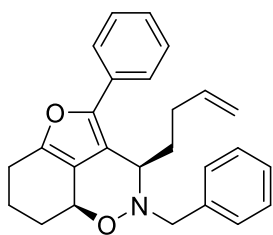


yield: 97%, ee: 99%

Compound **99ag** was prepared according to the **general procedure 5** from 2-(phenylethynyl)cyclohex-2-en-1-one **71a** (88.3 mg, 4.5 mmol, 1.5 equiv.), *N*-benzylhydroxylamine **101b** (37.0 mg, 3 mmol, 1 equiv.), 2-(1,3-dioxoisindolin-2-yl)acetaldehyde **102f** (56.8 mg, 3 mmol, 1 equiv.), 3 Å-MS (300 mg), catalyst **1e** (1 mg, 0.9 μmol , 0.3 mol%), Ag_2CO_3 (0.1 mg, 0.45 μmol , 0.15 mol%) and DCM (3 mL). The resulting mixture was then stirred at room temperature for 24 h, the DCM was removed under vacuum and the crude mixture was purified by flash column chromatography to give the product **99ag** as a white solid (142.6 mg, 0.29 mmol, 97%).

$[\alpha]_D = -41.3$ (c 1.02, CHCl_3). ee = 99%, determined on a Chiralpak IA column (heptane:IPA = 80:20, 1 mL/min), retention times: T_R (minor): 6.5 min, T_R (major): 8.7 min. $^1\text{H NMR}$ (CDCl_3 , 500 MHz) δ = 7.63-7.60 (m, 4H), 7.55 (d, J = 7.6 Hz, 2H), 7.26 (d, J = 7.0 Hz, 2H), 7.16 (t, J = 7.6 Hz, 3H), 7.08 (d, J = 7.3 Hz, 2H), 6.95 (d, J = 7.3 Hz, 1H), 4.90-4.87 (m, 1H), 4.74 (dd, J_1 = 7.6 Hz, J_2 = 6.1 Hz, 1H), 4.30 (d, J = 12.8 Hz, 1H), 4.20 (d, J = 12.8 Hz, 1H), 4.08 (dd, J_1 = 13.7 Hz, J_2 = 8.3 Hz, 1H), 3.75 (dd, J_1 = 13.4 Hz, J_2 = 5.8 Hz, 1H), 2.79-2.66 (m, 2H), 2.19-2.16 (m, 1H), 2.12-2.08 (m, 1H), 1.89-1.79 (m, 1H), 1.48-1.40 (m, 1H). $^{13}\text{C NMR}$ (CDCl_3 , 125MHz) δ = 168.3 (C_q), 148.4 (C_q), 147.6 (C_q), 137.4 (C_q), 133.6 (CH), 132.3 (C_q), 131.2 (C_q), 128.9 (CH), 128.8 (CH), 128.5 (CH), 127.5 (CH), 126.8 (CH), 124.8 (CH), 123.2 (CH), 120.8 (C_q), 113.1 (C_q), 69.9 (CH), 58.6 (CH_2), 55.9 (CH), 38.6 (CH_2), 27.8 (CH_2), 23.2 (CH_2), 20.5 (CH_2). **HRMS (ESI)**: m/z : calculated for $\text{C}_{31}\text{H}_{27}\text{N}_2\text{O}_4^+$: 491.1965 $[\text{M}+\text{H}]^+$, found, 491.1964.

Synthesis of (3R,8aS)-2-benzyl-3-(but-3-en-1-yl)-4-phenyl-2,3,6,7,8,8a-hexahydrobenzofuro[3,4-de][1,2]oxazine (99ai)

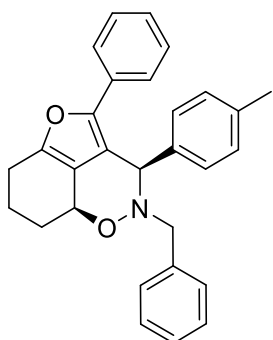


yield: 61%, ee: 97%

Compound **99ai** was prepared according to the **general procedure 5** from 2-(phenylethynyl)cyclohex-2-en-1-one **71a** (88.3 mg, 4.5 mmol, 1.5 equiv.), *N*-benzylhydroxylamine **101b** (37.0 mg, 3 mmol, 1 equiv.), pent-4-enal **102h** (29.7 μ L, 3 mmol, 1 equiv.), 3 Å-MS (300 mg), catalyst **1e** (1 mg, 0.9 μ mol, 0.3 mol%), Ag₂CO₃ (0.1 mg, 0.45 μ mol, 0.15 mol%) and DCM (3 mL). The resulting mixture was then stirred at room temperature for 24 h, the DCM was removed under vacuum and the crude mixture was purified by flash column chromatography to give the product **99ai** as a white solid (71.2 mg, 0.18 mmol, 61%).

$[\alpha]_D^{25} = +62.3$ (c 1.81, CHCl₃). ee = 97%, determined on a Chiralpak IB column (heptane:IPA = 95:05, 1 mL/min), retention times: T_R (minor): 4.4 min, T_R (major): 11.4 min. ¹H NMR (CDCl₃, 500 MHz) δ = 7.48 (d, *J* = 7.6 Hz, 4H), 7.38-7.28 (m, 5H), 7.18 (t, *J* = 7.3 Hz, 1H), 5.65-5.57 (m, 1H), 4.83 (d, *J* = 10.1 Hz, 2H), 4.76 (d, *J* = 17.1 Hz, 1H), 4.28 (d, *J* = 13.4 Hz, 1H), 4.24 (dd, *J*₁ = 7.9 Hz, *J*₂ = 2.4 Hz, 1H), 4.18 (d, *J* = 13.4 Hz, 1H), 2.78-2.74 (m, 1H), 2.68-2.62 (m, 1H), 2.21-2.06 (m, 3H), 2.02-1.89 (m, 2H), 1.87-1.77 (m, 1H), 1.66-1.59 (m, 1H), 1.30-1.23 (m, 1H). ¹³C NMR (CDCl₃, 125 MHz) δ = 147.3 (C_q), 146.9 (C_q), 138.6 (CH), 138.0 (C_q), 131.7 (C_q), 129.1 (CH), 128.8 (CH), 128.6 (CH), 127.5 (CH), 126.7 (CH), 124.5 (CH), 121.4 (C_q), 117.3 (C_q), 115.0 (CH₂), 69.6 (CH), 58.7 (CH₂), 58.1 (CH), 31.5 (CH₂), 31.1 (CH₂), 27.9 (CH₂), 23.3 (CH₂), 20.5 (CH₂). HRMS (ESI): *m/z*: calculated for C₂₆H₂₈NO₂⁺: 386.2115 [M+H]⁺, found, 386.2110.

Synthesis of (3R,8aS)-2-benzyl-4-phenyl-3-(p-tolyl)-2,3,6,7,8,8a-hexahydrobenzofuro[3,4-de][1,2]oxazine (99ap)

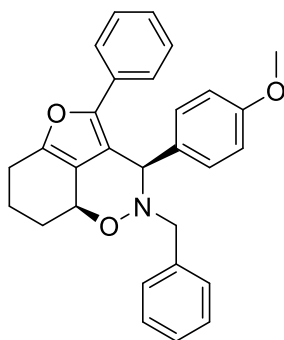


yield: 48%, ee: 95%

Compound **99ap** was prepared according to the **general procedure 4** from 2-(phenylethynyl)cyclohex-2-en-1-one **71a** (88.3 mg, 4.5 mmol, 1.5 equiv.), *N*-benzylhydroxylamine **101b** (37.0 mg, 3 mmol, 1 equiv.), 4-methylbenzaldehyde **102o** (35 μ L, 3 mmol, 1 equiv.), 3 Å-MS (300 mg), catalyst **1e** (1.6 mg, 0.5 mol%, 1.5 μ mol), Ag₂CO₃ (0.2 mg, 0.25 mol%, 0.75 μ mol) and DCM (3 mL). The resulting mixture was then stirred at 40 °C for 24 hours, the DCM was removed under vacuum and the crude mixture was purified by flash column chromatography to give the product **99ap** as a pale yellow solid (60.5 mg, 0.14 mmol, 48%).

$[\alpha]_D = +19.7$ (c 1.47, CHCl_3). ee = 95%, determined on a Chiralpak IA column (heptane:IPA = 95:05, 1 mL/min), retention times: T_R (minor): 5.0 min, T_R (major): 5.7 min. $^1\text{H NMR}$ (CDCl_3 , 500 MHz) δ = 7.38 (d, J = 7.3 Hz, 2H), 7.35-7.28 (m, 4H), 7.25 (t, J = 7.0 Hz, 1H), 7.16 (t, J = 7.6 Hz, 2H), 7.07-7.02 (m, 5H), 5.23 (s, 1H), 4.97-4.94 (m, 1H), 3.72 (d, J = 14.3 Hz, 1H), 3.53 (d, J = 14.3 Hz, 1H), 2.82-2.68 (m, 2H), 2.27 (s, 3H), 2.17-2.14 (m, 1H), 2.09-2.06 (m, 1H), 1.89-1.80 (m, 1H), 1.41-1.33 (m, 1H). $^{13}\text{C NMR}$ (CDCl_3 , 125MHz) δ = 146.9 (C_q), 146.6 (C_q), 138.4 (C_q), 137.6 (C_q), 134.2 (C_q), 131.3 (C_q), 130.3 (CH), 128.8 (CH), 128.8 (CH), 128.4 (CH), 128.4 (CH), 127.1 (CH), 126.3 (CH), 124.1 (CH), 123.3 (C_q), 119.5 (C_q), 75.4 (CH), 64.8 (CH), 58.9 (CH_2), 28.2 (CH_2), 23.4 (CH_2), 21.4 (CH_3), 20.6 (CH_2). **HRMS (ESI):** m/z : calculated for $\text{C}_{29}\text{H}_{28}\text{NO}_2^+$: 422.2115 $[\text{M}+\text{H}]^+$, found, 422.2111.

Synthesis of (3*R*,8*aS*)-2-benzyl-3-(4-methoxyphenyl)-4-phenyl-2,3,6,7,8*a*-hexahydrobenzofuro[3,4-*de*][1,2]oxazine (99aq)

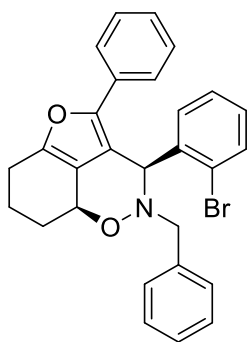


yield: 46%, ee: 99%

Compound **99aq** was prepared according to the **general procedure 5** from 2-(phenylethynyl)cyclohex-2-en-1-one **71a** (88.3 mg, 4.5 mmol, 1.5 equiv.), *N*-benzylhydroxylamine **101b** (37.0 mg, 3 mmol, 1 equiv.), 4-methoxybenzaldehyde **102p** (37 μL , 3 mmol, 1 equiv.), 3 Å-MS (300 mg), catalyst **1e** (1.6 mg, 0.5 mol%, 1.5 μmol), Ag_2CO_3 (0.2 mg, 0.25 mol%, 0.75 μmol) and DCM (3 mL). The resulting mixture was then stirred at 40 °C for 5 days, the DCM was removed under vacuum and the crude mixture was purified by flash column chromatography to give the product **99aq** as a pale yellow solid (60.0 mg, 0.14 mmol, 46%).

$[\alpha]_D = +83.9$ (c 1.17, CHCl_3). ee = 99%, determined on a Chiralpak IA column (heptane:IPA = 95:05, 1 mL/min), retention times: T_R (minor): 6.3 min, T_R (major): 6.9 min. $^1\text{H NMR}$ (CDCl_3 , 500 MHz) δ = 7.38 (d, J = 7.3 Hz, 2H), 7.34-7.25 (m, 5H), 7.16 (t, J = 7.6 Hz, 2H), 7.10 (d, J = 8.5 Hz, 2H), 7.04 (t, J = 7.3 Hz, 1H), 6.78 (d, J = 8.5 Hz, 2H), 5.23 (s, 1H), 4.97-4.94 (m, 1H), 3.75 (s, 3H), 3.71 (d, J = 14.3 Hz, 1H), 3.54 (d, J = 14.3 Hz, 1H), 2.82-2.78 (m, 1H), 2.74-2.68 (m, 1H), 2.18-2.15 (m, 1H), 2.11-2.08 (m, 1H), 1.90-1.81 (m, 1H), 1.40-1.32 (m, 1H). $^{13}\text{C NMR}$ (CDCl_3 , 125MHz) δ = 159.3 (C_q), 146.9 (C_q), 146.6 (C_q), 138.4 (C_q), 131.5 (CH), 131.3 (C_q), 129.5 (C_q), 128.8 (CH), 128.4 (CH), 128.4 (CH), 127.2 (CH), 126.3 (CH), 124.1 (CH), 123.3 (C_q), 119.6 (C_q), 113.4 (CH), 75.4 (CH), 64.4 (CH), 58.9 (CH_2), 55.3 (CH_3), 28.2 (CH_2), 23.4 (CH_2), 20.6 (CH_2). **HRMS (ESI):** m/z : calculated for $\text{C}_{29}\text{H}_{28}\text{NO}_3^+$: 438.2064 $[\text{M}+\text{H}]^+$, found, 438.2055.

Synthesis of (3*S*,8*aS*)-2-benzyl-3-(2-bromophenyl)-4-phenyl-2,3,6,7,8,8*a*-hexahydrobenzofuro[3,4-*de*][1,2]oxazine (**99ar**)

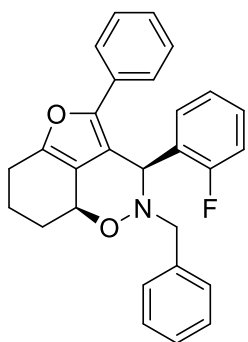


yield: 48%, ee: 99%

Compound **99ar** was prepared according to the **general procedure 4** from 2-(phenylethynyl)cyclohex-2-en-1-one **71a** (88.3 mg, 4.5 mmol, 1.5 equiv.), *N*-benzylhydroxylamine **101b** (37.0 mg, 3 mmol, 1 equiv.), 2-bromobenzaldehyde **102aq** (35 μ L, 3 mmol, 1 equiv.), 3 \AA -MS (300 mg), catalyst **1e** (1.6 mg, 0.5 mol%, 1.5 μ mol), Ag_2CO_3 (0.2 mg, 0.25 mol%, 0.75 μ mol) and DCM (3 mL). The resulting mixture was then stirred at 40 $^\circ\text{C}$ for 48 h, the DCM was removed under vacuum and the crude mixture was purified by flash column chromatography to give the product **99ar** as a white solid (70.0 mg, 0.14 mmol, 48%).

$[\alpha]_D^{25} = +99.8$ (c 1.73, CHCl_3). ee = 99%, determined on a Chiralpak IA column (heptane:IPA = 98:02, 1 mL/min), retention times: T_R (major): 5.2 min, T_R (minor): 6.1 min. $^1\text{H NMR}$ (CDCl_3 , 500 MHz) δ = 7.53 (d, J = 7.9 Hz, 1H), 7.44 (d, J = 7.3 Hz, 2H), 7.39 (d, J = 7.3 Hz, 2H), 7.30 (t, J = 7.3 Hz, 2H), 7.25-7.21 (m, 3H), 7.12-7.02 (m, 4H), 6.10 (s, 1H), 4.90-4.87 (m, 1H), 4.19 (d, J = 15.0 Hz, 1H), 3.27 (d, J = 14.6 Hz, 1H), 2.82-2.67 (m, 2H), 2.15-2.12 (m, 1H), 2.07-2.02 (m, 1H), 1.87-1.77 (m, 1H), 1.36-1.28 (m, 1H). $^{13}\text{C NMR}$ (CDCl_3 , 125 MHz) δ = 147.3 (C_q), 146.8 (C_q), 138.8 (C_q), 137.0 (C_q), 132.3 (CH), 132.3 (CH), 130.9 (C_q), 129.5 (CH), 128.5 (CH), 128.4 (CH), 128.3 (CH), 127.7 (CH), 127.0 (CH), 126.6 (CH), 125.8 (C_q), 124.2 (CH), 123.1 (C_q), 118.9 (C_q), 75.2 (CH), 63.3 (CH), 58.2 (CH_2), 28.1 (CH_2), 23.3 (CH_2), 20.4 (CH_2). **HRMS (ESI)**: m/z : calculated for $\text{C}_{28}\text{H}_{25}\text{BrNO}_2^+$: 486.1063 $[\text{M}+\text{H}]^+$, found, 486.1071.

Synthesis of (3*S*,8*aS*)-2-benzyl-3-(2-fluorophenyl)-4-phenyl-2,3,6,7,8,8*a*-hexahydrobenzofuro[3,4-*de*][1,2]oxazine (**99as**)



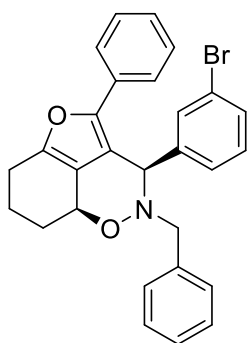
yield: 70%, ee: 97%

Compound **99as** was prepared according to the **general procedure 4** from 2-(phenylethynyl)cyclohex-2-en-1-one **71a** (88.3 mg, 4.5 mmol, 1.5 equiv.), *N*-benzylhydroxylamine **101b** (37.0 mg, 3 mmol, 1 equiv.), 2-fluorobenzaldehyde **102r** (32 μ L, 3 mmol, 1 equiv.), 3 \AA -MS (300 mg), catalyst **1e** (1.6 mg, 0.5 mol%, 1.5 μ mol), Ag_2CO_3 (0.2 mg, 0.25 mol%, 0.75 μ mol) and DCM (3 mL). The resulting mixture was then stirred at 40 $^\circ\text{C}$ for

48 h, the DCM was removed under vacuum and the crude mixture was purified by flash column chromatography to give the product **99as** as a pale yellow solid (89.5 mg, 0.21 mmol, 70%).

$[\alpha]_D = +94.9$ (c 1.01, CHCl₃). ee = 97%, determined on a Chiralpak ID column (heptane:IPA = 80:20, 1 mL/min), retention times: T_R (major): 4.1min, T_R (minor): 4.3 min. ¹H NMR (CDCl₃, 500 MHz) δ = 7.40-7.37 (m, 4H), 7.31 (t, J = 7.3 Hz, 2H), 7.26-7.25 (m, 1H), 7.22-7.17 (m, 3H), 7.08-7.02 (m, 3H), 6.97 (d, J = 7.3 Hz, 1H), 5.89 (s, 1H), 4.93-4.90 (m, 1H), 3.92 (d, J = 14.3 Hz, 1H), 3.43 (d, J = 14.6 Hz, 1H), 2.83-2.68 (m, 2H), 2.17-2.14 (m, 1H), 2.09-2.06 (m, 1H), 1.89-1.80 (m, 1H), 1.37-1.29 (m, 1H). ¹³C NMR (CDCl₃, 125MHz) δ = 161.3 (C_q, d, J_{C-F} = 224.7 Hz), 146.9 (C_q, d, J_{C-F} = 8.2 Hz), 138.5 (C_q), 132.0 (CH, d, J_{C-F} = 3.7 Hz), 131.1 (C_q), 129.7 (CH, d, J_{C-F} = 8.2 Hz), 128.7 (CH), 128.5 (CH), 128.3 (CH), 127.1 (CH), 126.5 (CH), 124.6 (C_q), 124.4 (CH, d, J_{C-F} = 2.7 Hz), 123.8 (CH), 123.4 (C_q), 118.6 (C_q), 114.6 (CH), 114.4 (CH), 75.4 (CH), 58.4 (CH₂), 56.9 (CH), 28.2 (CH₂), 23.4 (CH₂), 20.5 (CH₂). ¹⁹F NMR (CDCl₃, 282MHz) δ = -119.37. HRMS (ESI): m/z: calculated for C₂₈H₂₅FNO₂⁺: 426.1864 [M+H]⁺, found, 426.1856.

Synthesis of (3*S*,8*aS*)-2-benzyl-3-(3-bromophenyl)-4-phenyl-2,3,6,7,8,8*a*-hexahydrobenzofuro[3,4-*de*][1,2]oxazine (**99at**)

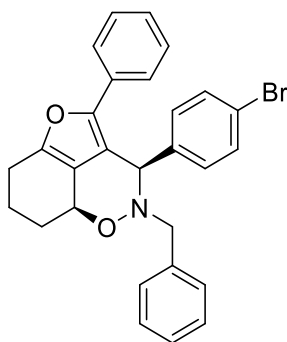


yield: 87%, ee: 92%

Compound **99at** was prepared according to the **general procedure 4** from 2-(phenylethynyl)cyclohex-2-en-1-one **71a** (88.3 mg, 4.5 mmol, 1.5 equiv.), *N*-benzylhydroxylamine **101b** (37.0 mg, 3 mmol, 1 equiv.), 3-bromobenzaldehyde **102s** (35 μL, 3 mmol, 1 equiv.), 3 Å-MS (300 mg), catalyst **1e** (1.6 mg, 0.9 μmol, 0.3 mol%), Ag₂CO₃ (0.1 mg, 0.45 μmol, 0.15 mol%) and DCM (3 mL). The resulting mixture was then stirred at 40 °C for 48 h, the DCM was removed under vacuum and the crude mixture was purified by flash column chromatography to give the product **99at** as a white solid (126.6 mg, 0.26 mmol, 87%).

$[\alpha]_D = +143.7$ (c 1.00, CHCl₃). ee = 92%, determined on a Chiralpak IA column (heptane:IPA = 80:20, 1 mL/min), retention times: T_R (minor): 4.6 min, T_R (major): 5.4 min. ¹H NMR (CDCl₃, 500 MHz) δ = 7.39-7.32 (m, 8H), 7.27 (t, J = 7.3 Hz, 1H), 7.18 (t, J = 7.6 Hz, 2H), 7.11-7.10 (m, 2H), 7.06 (t, J = 7.3 Hz, 1H), 5.22 (s, 1H), 4.98-4.95 (m, 1H), 3.68 (d, J = 14.3 Hz, 1H), 3.59 (d, J = 14.0 Hz, 1H), 2.82-2.69 (m, 2H), 2.17-2.15 (m, 1H), 2.11-2.08 (m, 1H), 1.89-1.80 (m, 1H), 1.40-1.32 (m, 1H). ¹³C NMR (CDCl₃, 125MHz) δ = 147.2 (C_q), 146.9 (C_q), 139.7 (C_q), 137.8 (C_q), 133.2 (CH), 131.2 (CH), 131.0 (C_q), 129.6 (CH), 129.0 (CH), 128.8 (CH), 128.5 (CH), 127.4 (CH), 126.6 (CH), 124.2 (CH), 123.0 (C_q), 122.2 (C_q), 118.5 (C_q), 75.4 (CH), 64.4 (CH), 58.9 (CH₂), 28.1 (CH₂), 23.3 (CH₂), 20.5 (CH₂). HRMS (ESI): m/z: calculated for C₂₈H₂₅BrNO₂⁺: 486.1063 [M+H]⁺, found, 486.1064.

Synthesis of (3*R*,8*aS*)-2-benzyl-3-(4-bromophenyl)-4-phenyl-2,3,6,7,8,8*a*-hexahydrobenzofuro[3,4-*de*][1,2]oxazine (99au)

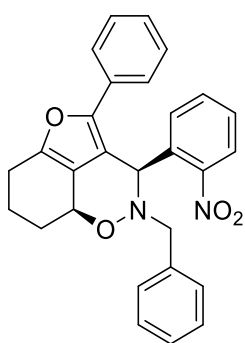


yield: 75%, ee: 99%

Compound **99au** was prepared according to the **general procedure 4** from 2-(phenylethynyl)cyclohex-2-en-1-one **71a** (88.3 mg, 4.5 mmol, 1.5 equiv.), *N*-benzylhydroxylamine **101b** (37.0 mg, 3 mmol, 1 equiv.), 4-bromobenzaldehyde **99t** (35 μ L, 3 mmol, 1 equiv.), 3 Å-MS (300 mg), catalyst **1e** (1.6 mg, 0.9 μ mol, 0.3 mol%), Ag₂CO₃ (0.1 mg, 0.45 μ mol, 0.15 mol%) and DCM (3 mL). The resulting mixture was then stirred at 40 °C for 48 h, the DCM was removed under vacuum and the crude mixture was purified by flash column chromatography to give the product **99au** as a pale yellow solid (110.3 mg, 0.23 mmol, 75%).

[α]_D = +61.2 (c 1.15, CHCl₃). ee = 99%, determined on a Chiralpak IA column (heptane:IPA = 95:05, 1 mL/min), retention times: T_R (minor): 5.9 min, T_R (major): 6.9 min. ¹H NMR (CDCl₃, 500 MHz) δ = 7.37 (d, *J* = 8.2 Hz, 4H), 7.34-7.31 (m, 4H), 7.28 (d, *J* = 7.0 Hz, 1H), 7.18 (t, *J* = 7.6 Hz, 2H), 7.08-7.04 (m, 3H), 5.24 (s, 1H), 4.98-4.95 (m, 1H), 3.68 (d, *J* = 14.3 Hz, 1H), 3.56 (d, *J* = 14.3 Hz, 1H), 2.83-2.68 (m, 2H), 2.18-2.16 (m, 1H), 2.11-2.08 (m, 1H), 1.90-1.81 (m, 1H), 1.39-1.31 (m, 1H). ¹³C NMR (CDCl₃, 125MHz) δ = 147.1 (C_q), 146.9 (C_q), 137.9 (C_q), 136.3 (C_q), 132.0 (CH), 131.2 (CH), 131.1 (C_q), 128.8 (CH), 128.5 (CH), 128.5 (CH), 127.3 (CH), 126.6 (CH), 124.1 (CH), 123.1 (C_q), 122.2 (C_q), 118.7 (C_q), 75.4 (CH), 64.3 (CH), 58.9 (CH₂), 28.2 (CH₂), 23.3 (CH₂), 20.5 (CH₂). HRMS (ESI): *m/z*: calculated for C₂₈H₂₅BrNO₂⁺: 486.1063 [M+H]⁺, found, 486.1069.

Synthesis of (3*R*,8*aS*)-2-benzyl-3-(2-nitrophenyl)-4-phenyl-2,3,6,7,8,8*a*-hexahydrobenzofuro[3,4-*de*][1,2]oxazine (99av)



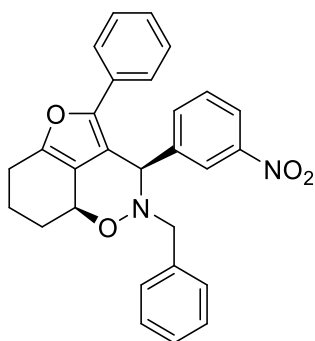
yield: 41%, ee: 99%

Compound **99av** was prepared according to the **general procedure 4** from 2-(phenylethynyl)cyclohex-2-en-1-one **71a** (88.3 mg, 4.5 mmol, 1.5 equiv.), *N*-benzylhydroxylamine **101b** (37.0 mg, 3 mmol, 1 equiv.), 2-nitrobenzaldehyde **102u** (45.4 mg, 3 mmol, 1 equiv.), 3 Å-MS (300 mg), catalyst **1e** (1.6 mg, 0.5 mol%, 1.5 μ mol), Ag₂CO₃ (0.2 mg, 0.25 mol%, 0.75 μ mol) and DCM (3 mL). The resulting mixture was then stirred at

40 °C for 48 h, the DCM was removed under vacuum and the crude mixture was purified by flash column chromatography to give the product **99av** as a yellow solid (55.8 mg, 0.12 mmol, 41%).

$[\alpha]_D = +215.9$ (c 1.21, CHCl_3). ee = 99%, determined on a Chiralpak IC column (heptane:IPA = 80:20, 1 mL/min), retention times: T_R (major): 4.5 min, T_R (minor): 5.5 min. $^1\text{H NMR}$ (CDCl_3 , 500 MHz) δ = 7.83 (dd, $J_1 = 8.2$ Hz, $J_2 = 1.2$ Hz, 1H), 7.46 (d, $J = 7.6$ Hz, 2H), 7.40 (td, $J_1 = 7.6$ Hz, $J_2 = 0.9$ Hz, 1H), 7.35-7.28 (m, 5H), 7.26-7.19 (m, 4H), 7.09 (t, $J = 7.3$ Hz, 1H), 6.52 (s, 1H), 4.89-4.86 (m, 1H), 3.98 (d, $J = 14.0$ Hz, 1H), 3.29 (d, $J = 14.3$ Hz, 1H), 2.83-2.69 (m, 2H), 2.16-2.13 (m, 1H), 2.07-2.02 (m, 1H), 1.88-1.79 (m, 1H), 1.35-1.27 (m, 1H). $^{13}\text{C NMR}$ (CDCl_3 , 125MHz) δ = 150.8 (C_q), 147.7 (C_q), 147.1 (C_q), 138.1 (C_q), 132.8 (CH), 132.6 (CH), 132.4 (C_q), 130.7 (C_q), 128.8 (CH), 128.7 (CH), 128.5 (CH), 128.3 (CH), 127.2 (CH), 126.9 (CH), 124.1 (CH), 124.0 (CH), 122.9 (C_q), 117.8 (C_q), 75.1 (CH), 58.3 (CH_2), 58.2 (CH), 28.1 (CH_2), 23.3 (CH_2), 20.4 (CH_2). HRMS (ESI): m/z : calculated for $\text{C}_{28}\text{H}_{25}\text{N}_2\text{O}_4^+$: 453.1809 $[\text{M}+\text{H}]^+$, found, 453.1807.

Synthesis of (3*R*,8*aS*)-2-benzyl-3-(3-nitrophenyl)-4-phenyl-2,3,6,7,8,8*a*-hexahydrobenzofuro[3,4-*de*][1,2]oxazine (**99aw**)

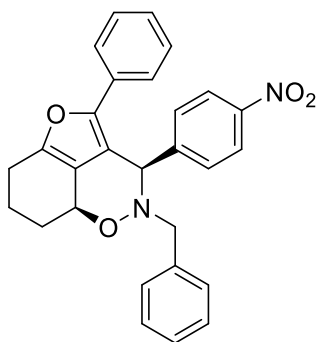


yield: 78%, ee: 96%

Compound **99aw** was prepared according to the **general procedure 4** from 2-(phenylethynyl)cyclohex-2-en-1-one **71a** (88.3 mg, 4.5 mmol, 1.5 equiv.), *N*-benzylhydroxylamine **101b** (37.0 mg, 3 mmol, 1 equiv.), 3-nitrobenzaldehyde **102v** (45.4 mg, 3 mmol, 1 equiv.), 3 Å-MS (300 mg), catalyst **1e** (1.6 mg, 0.5 mol%, 1.5 μmol), Ag_2CO_3 (0.2 mg, 0.25 mol%, 0.75 μmol) and DCM (3 mL). The resulting mixture was then stirred at 40 °C for 48 h, the DCM was removed under vacuum and the crude mixture was purified by flash column chromatography to give the product **99aw** as a yellow solid (106.2 mg, 0.23 mmol, 78%).

$[\alpha]_D = +98.5$ (c 0.93, CHCl_3). ee = 96%, determined on a Chiralpak IA column (heptane:IPA = 80:20, 1 mL/min), retention times: T_R (minor): 5.5 min, T_R (major): 8.8 min. $^1\text{H NMR}$ (CDCl_3 , 500 MHz) δ = 8.08 (d, $J = 8.2$ Hz, 1H), 8.04 (t, $J = 1.8$ Hz, 1H), 7.50 (d, $J = 7.9$ Hz, 1H), 7.41 (t, $J = 7.9$ Hz, 1H), 7.36-7.30 (m, 7H), 7.17 (t, $J = 7.9$ Hz, 2H), 7.06 (t, $J = 7.3$ Hz, 1H), 5.39 (s, 1H), 5.03-4.99 (m, 1H), 3.67 (d, $J = 14.0$ Hz, 1H), 3.59 (d, $J = 14.0$ Hz, 1H), 2.84-2.71 (m, 2H), 2.21-2.17 (m, 1H), 2.15-2.10 (m, 1H), 1.92-1.82 (m, 1H), 1.44-1.36 (m, 1H). $^{13}\text{C NMR}$ (CDCl_3 , 125MHz) δ = 418.0 (C_q), 147.4 (C_q), 147.3 (C_q), 139.5 (C_q), 137.3 (C_q), 136.2 (CH), 130.8 (C_q), 129.0 (CH), 128.8 (CH), 128.6 (CH), 128.6 (CH), 127.6 (CH), 126.9 (CH), 125.0 (CH), 124.1 (CH), 123.1 (CH), 122.9 (C_q), 118.1 (C_q), 75.5 (CH), 64.0 (CH), 58.9 (CH_2), 28.1 (CH_2), 23.3 (CH_2), 20.5 (CH_2). HRMS (ESI): m/z : calculated for $\text{C}_{28}\text{H}_{25}\text{N}_2\text{O}_4^+$: 453.1809 $[\text{M}+\text{H}]^+$, found, 453.1812.

Synthesis of (3*R*,8*aS*)-2-benzyl-3-(4-nitrophenyl)-4-phenyl-2,3,6,7,8,8*a*-hexahydrobenzofuro[3,4-*de*][1,2]oxazine (99ax)

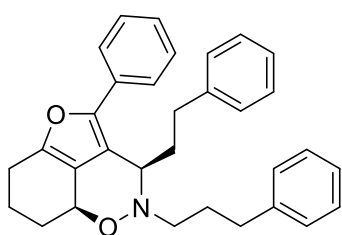


yield: 62%, ee: 84%

Compound **99ax** was prepared according to the **general procedure 4** from 2-(phenylethynyl)cyclohex-2-en-1-one **71a** (88.3 mg, 4.5 mmol, 1.5 equiv.), *N*-benzylhydroxylamine **101b** (37.0 mg, 3 mmol, 1 equiv.), 4-nitrobenzaldehyde **102w** (45.4 mg, 3 mmol, 1 equiv.), 3 Å-MS (300 mg), catalyst **1e** (1.6 mg, 0.5 mol%, 1.5 μmol), Ag₂CO₃ (0.2 mg, 0.25 mol%, 0.75 μmol) and DCM (3 mL). The resulting mixture was then stirred at 40 °C for 48 h, the DCM was removed under vacuum and the crude mixture was purified by flash column chromatography to give the product **99ax** as a yellow solid (84.5 mg, 0.19 mmol, 62%).

[α]_D = +133.2 (c 1.98, CHCl₃). ee = 84%, determined on a Chiralpak IA column (heptane:IPA = 80:20, 1 mL/min), retention times: T_R (minor): 6.4 min, T_R (major): 7.4 min. ¹H NMR (CDCl₃, 500 MHz) δ = 8.09 (d, *J* = 8.9 Hz, 2H), 7.35-7.29 (m, 9H), 7.17 (t, *J* = 7.6 Hz, 2H), 7.07 (t, *J* = 7.3 Hz, 1H), 5.38 (s, 1H), 5.01-4.98 (m, 1H), 3.67 (d, *J* = 14.0 Hz, 1H), 3.58 (d, *J* = 14.0 Hz, 1H), 2.84-2.70 (m, 2H), 2.21-2.18 (m, 1H), 2.14-2.10 (m, 1H), 1.92-1.82 (m, 1H), 1.41-1.33 (m, 1H). ¹³C NMR (CDCl₃, 125MHz) δ = 147.7 (C_q), 147.5 (C_q), 147.3 (C_q), 144.8 (C_q), 137.4 (C_q), 131.1 (CH), 130.7 (C_q), 128.7 (CH), 128.6 (CH), 127.6 (CH), 126.9 (CH), 124.1 (CH), 123.2 (CH), 122.8 (C_q), 117.9 (C_q), 75.4 (CH), 64.0 (CH), 58.9 (CH₂), 28.1 (CH₂), 23.3 (CH₂), 20.5 (CH₂). HRMS (ESI): *m/z*: calculated for C₂₈H₂₅N₂O₄⁺: 453.1809 [M+H]⁺, found, 453.1809.

Synthesis of (3*R*,8*aS*)-3-phenethyl-4-phenyl-2-(3-phenylpropyl)-2,3,6,7,8,8*a*-hexahydrobenzofuro[3,4-*de*][1,2]oxazine (99bf)

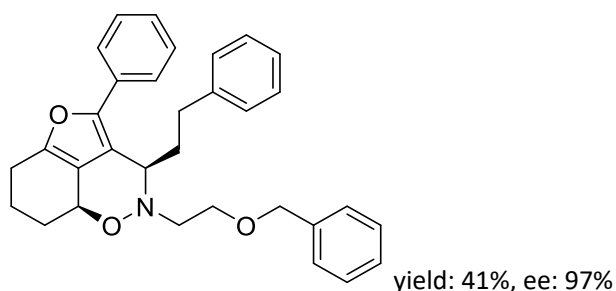


yield: 86%, ee: 99%

Compound **99bf** was prepared according to the **general procedure 4** from 2-(phenylethynyl)cyclohex-2-en-1-one **71a** (88.3 mg, 4.5 mmol, 1.5 equiv.), *N*-(3-phenylpropyl)hydroxylamine **101b** (45.4 mg, 3 mmol, 1 equiv.), 3-phenylpropanal **102b** (40.3 mg, 3 mmol, 1 equiv.), 3 Å-MS (300 mg), catalyst **1e** (1 mg, 0.9 μmol, 0.3 mol%), Ag₂CO₃ (0.1 mg, 0.45 μmol, 0.15 mol%) and DCM (3 mL). The resulting mixture was then stirred at room temperature for 24 h, the DCM was removed under vacuum and the crude mixture was purified by flash column chromatography to give the product **99bf** as a colorless oil (119.5 mg, 0.26 mmol, 86%).

$[\alpha]_D^{25} = +91.4$ (*c* 2.04, CHCl₃). ee = 99%, determined on a Chiralpak IB column (heptane:IPA = 98:02, 1 mL/min), retention times: *T_R* (minor): 5.3 min, *T_R* (major): 6.1 min. ¹H NMR (CDCl₃, 500 MHz) δ = 7.38 (d, *J* = 7.9 Hz, 2H), 7.33-7.26 (m, 6H), 7.23-7.17 (m, 4H), 7.13 (t, *J* = 7.3 Hz, 1H), 6.97 (d, *J* = 7.3 Hz, 2H), 4.79-4.76 (m, 1H), 4.14-4.12 (m, 1H), 3.09-3.04 (m, 1H), 3.02-2.95 (m, 1H), 2.89-2.72 (m, 4H), 2.67-2.56 (m, 2H), 2.16-2.03 (m, 5H), 1.89-1.78 (m, 2H), 1.32-1.25 (m, 1H). ¹³C NMR (CDCl₃, 125 MHz) δ = 147.1 (C_q), 146.8 (C_q), 142.5 (C_q), 142.4 (C_q), 131.7 (C_q), 128.8 (CH), 128.8 (CH), 128.8 (CH), 128.6 (CH), 128.4 (CH), 126.6 (CH), 126.0 (CH), 125.9 (CH), 124.5 (CH), 121.8 (C_q), 117.6 (C_q), 69.6 (CH), 59.6 (CH), 53.7 (CH₂), 33.7 (CH₂), 33.5 (CH₂), 33.3 (CH₂), 29.6 (CH₂), 27.9 (CH₂), 23.3 (CH₂), 20.5 (CH₂). HRMS (ESI): *m/z*: calculated for C₃₂H₃₄NO₂⁺: 464.2584 [M+H]⁺, found, 464.2578.

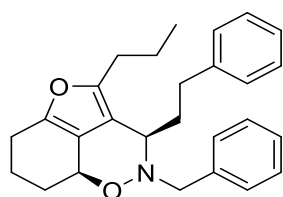
Synthesis of (3*R*,8*aS*)-2-(2-(benzyloxy)ethyl)-3-phenethyl-4-phenyl-2,3,6,7,8,8*a*-hexahydrobenzofuro[3,4-*de*][1,2]oxazine (99bg)



Compound **99bg** was prepared according to the **general procedure 4** from 2-(phenylethynyl)cyclohex-2-en-1-one **71a** (88.3 mg, 4.5 mmol, 1.5 equiv.), *N*-(2-(benzyloxy)ethyl)hydroxylamine **101c** (51.2 mg, 3 mmol, 1 equiv.), 3-phenylpropanal **102b** (40.3 mg, 3 mmol, 1 equiv.), 3 Å-MS (300 mg), catalyst **1e** (1 mg, 0.9 μmol, 0.3 mol%), Ag₂CO₃ (0.1 mg, 0.45 μmol, 0.15 mol%) and DCM (3 mL). The resulting mixture was then stirred at room temperature for 24 h, the DCM was removed under vacuum and the crude mixture was purified by flash column chromatography to give the product **99bg** as a colorless oil (59.1 mg, 0.12 mmol, 41%).

$[\alpha]_D^{25} = +99.6$ (*c* 2.30, CHCl₃). ee = 97%, determined on a Chiralpak IB column (heptane:IPA = 98:02, 1 mL/min), retention times: *T_R* (minor): 7.8 min, *T_R* (major): 9.2 min. ¹H NMR (CDCl₃, 500 MHz) δ = 7.42 (d, *J* = 7.6 Hz, 2H), 7.39-7.26 (m, 7H), 7.19-7.16 (m, 3H), 7.10 (t, *J* = 7.3 Hz, 1H), 6.97 (d, *J* = 7.3 Hz, 2H), 4.81-4.78 (m, 1H), 4.63 (d, *J* = 11.9 Hz, 1H), 4.60 (d, *J* = 11.9 Hz, 1H), 4.33 (dd, *J*₁ = 7.0 Hz, *J*₂ = 3.1 Hz, 1H), 3.88-3.80 (m, 2H), 3.32-3.24 (m, 2H), 2.80-2.71 (m, 2H), 2.65-2.51 (m, 2H), 2.14-2.02 (m, 3H), 1.94-1.76 (m, 2H), 1.29-1.21 (m, 1H). ¹³C NMR (CDCl₃, 125 MHz) δ = 146.9 (C_q), 146.8 (C_q), 142.5 (C_q), 138.6 (C_q), 131.7 (C_q), 128.8 (CH), 128.6 (CH), 128.6 (CH), 128.4 (CH), 127.9 (CH), 127.8 (CH), 126.7 (CH), 125.8 (CH), 124.5 (CH), 121.9 (C_q), 117.7 (C_q), 73.5 (CH₂), 70.8 (CH), 68.5 (CH₂), 60.1 (CH), 54.4 (CH₂), 33.2 (CH₂), 33.2 (CH₂), 27.9 (CH₂), 23.2 (CH₂), 20.5 (CH₂). HRMS (ESI): *m/z*: calculated for C₃₂H₃₄NO₃⁺: 480.2533 [M+H]⁺, found, 480.2536.

Synthesis of (3*R*,8*aS*)-2-benzyl-3-phenethyl-4-propyl-2,3,6,7,8,8*a*-hexahydrobenzofuro[3,4-*de*][1,2]oxazine (99bm)



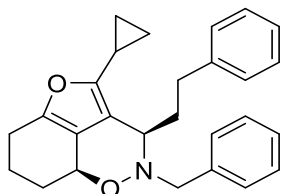
Compound **99bm** was prepared according to the **general procedure 4** from 2-(pent-1-yn-1-yl)cyclohex-2-en-1-one **71h** (73.0 mg, 4.5 mmol, 1.5 equiv.), *N*-benzylhydroxylamine **101b** (37.0 mg, 3 mmol, 1 equiv.), 3-phenylpropanal **102b** (40.3 mg, 3 mmol, 1 equiv.), 3 Å-MS (300 mg), catalyst **1e**, Ag₂CO₃ and DCM (3 mL). The resulting mixture was then stirred at room temperature overnight, the DCM was removed under vacuum and the crude mixture was purified by flash column chromatography to give the product **99bm** as a pale yellow oil in 44% (53.2 mg, 0.13 mmol) yield and 89% ee.

99bm was alternatively obtained from the same protocol in the presence of 0.6 mol% **1e** in 49% yield and 92% ee.

99bm was alternatively obtained from the same protocol in the absence of Ag₂CO₃ in 44% yield and 88% ee.

[α]_D = +42.3 (c 2.10, CHCl₃). ee = 92%, determined on a Chiralpak IB column (heptane:IPA = 80:20, 1 mL/min), retention times: T_R (minor): 3.8 min, T_R (major): 7.5 min. ¹H NMR (CDCl₃, 500 MHz) δ = 7.47 (d, *J* = 7.3 Hz, 2H), 7.35 (t, *J* = 7.3 Hz, 2H), 7.29 (t, *J* = 7.3 Hz, 1H), 7.23 (t, *J* = 7.3 Hz, 2H), 7.14 (t, *J* = 7.3 Hz, 1H), 7.05 (d, *J* = 7.3 Hz, 2H), 4.80-4.77 (m, 1H), 4.19 (s, 2H), 3.93 (dd, *J*₁ = 6.7 Hz, *J*₂ = 3.7 Hz, 1H), 2.76-2.70 (m, 1H), 2.67-2.58 (m, 2H), 2.57-2.49 (m, 2H), 2.44-2.38 (m, 1H), 2.12-2.04 (m, 2H), 1.99-1.89 (m, 2H), 1.82-1.72 (m, 1H), 1.63-1.56 (m, 2H), 1.24-1.16 (m, 1H), 0.91 (t, *J* = 7.3 Hz, 3H). ¹³C NMR (CDCl₃, 125 MHz) δ = 149.4 (C_q), 145.2 (C_q), 142.9 (C_q), 138.2 (C_q), 129.0 (CH), 128.6 (CH), 128.5 (CH), 128.5 (CH), 127.4 (CH), 125.8 (CH), 120.2 (C_q), 115.2 (C_q), 71.1 (CH), 58.5 (CH₂), 57.1 (CH), 35.3 (CH₂), 32.8 (CH₂), 29.9 (CH₂), 28.0 (CH₂), 23.3 (CH₂), 22.0 (CH₂), 20.7 (CH₂), 14.1 (CH₂). HRMS (ESI): *m/z*: calculated for C₂₇H₃₂NO₂⁺: 402.2428 [M+H]⁺, found, 402.2428.

Synthesis of (3*R*,8*a*S)-2-benzyl-4-cyclopropyl-3-phenethyl-2,3,6,7,8,8*a*-hexahydrobenzofuro[3,4-*de*][1,2]oxazine (**99bn**)



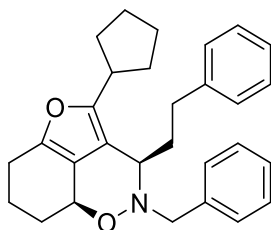
Compound **99bn** was prepared according to the **general procedure 4** from 2-(cyclopropylethynyl)cyclohex-2-en-1-one **71i** (72.1 mg, 4.5 mmol, 1.5 equiv.), *N*-benzylhydroxylamine **101b** (37.0 mg, 3 mmol, 1 equiv.), 3-phenylpropanal **102b** (40.3 mg, 3 mmol, 1 equiv.), 3 Å-MS (300 mg), catalyst **1e**, Ag₂CO₃ and DCM (3 mL). The resulting mixture was then stirred at room temperature overnight, the DCM was removed under vacuum and the crude mixture was purified by flash column chromatography to give the product **99bn** as a pale yellow oil in 58% (69.5 mg, 0.17 mmol) yield and 92% ee.

99bn was alternatively obtained from the same protocol in the presence of 0.6 mol% **1e** in 62% yield and 95% ee.

99bn was alternatively obtained from the same protocol in the absence of Ag₂CO₃ in 57% yield and 93% ee.

$[\alpha]_D = +31.6$ (c 2.03, CHCl₃). ee = 95%, determined on a Chiralpak IB column (heptane:IPA = 80:20, 1 mL/min), retention times: T_R (minor): 4.0 min, T_R (major): 7.6 min. $^1\text{H NMR}$ (CDCl₃, 500 MHz) δ = 7.47 (d, J = 7.3 Hz, 2H), 7.35 (t, J = 7.3 Hz, 2H), 7.28 (t, J = 7.3 Hz, 1H), 7.23 (t, J = 7.3 Hz, 2H), 7.14 (t, J = 7.3 Hz, 1H), 7.10 (d, J = 7.3 Hz, 2H), 4.77-4.74 (m, 1H), 4.19 (d, J_1 = 13.7 Hz, 1H), 4.15 (d, J_1 = 13.7 Hz, 1H), 3.97 (t, J = 5.5 Hz, 1H), 2.84-2.77 (m, 1H), 2.66-2.58 (m, 2H), 2.53-2.46 (m, 1H), 2.20-2.13 (m, 1H), 2.08-2.01 (m, 2H), 1.97-1.93 (m, 1H), 1.79-1.69 (m, 2H), 1.23-1.15 (m, 1H), 0.86-0.69 (m, 4H). $^{13}\text{C NMR}$ (CDCl₃, 125MHz) δ = 149.5 (C_q), 144.6 (C_q), 142.8 (C_q), 138.1 (C_q), 128.7 (CH), 128.4 (CH), 128.3 (CH), 128.3 (CH), 127.2 (CH), 125.6 (CH), 120.3 (C_q), 115.5 (C_q), 71.2 (CH), 58.3 (CH₂), 57.5 (CH), 34.7 (CH₂), 32.6 (CH₂), 27.7 (CH₂), 23.0 (CH₂), 20.4 (CH₂), 8.6 (CH₂), 7.1 (CH₂), 5.4 (CH₂). **HRMS (ESI)**: m/z : calculated for C₂₇H₃₀NO₂⁺: 400.2271 [M+H]⁺, found, 400.2267.

Synthesis of (3*R*,8*aS*)-2-benzyl-4-cyclopentyl-3-phenethyl-2,3,6,7,8,8*a*-hexahydrobenzofuro[3,4-*de*][1,2]oxazine (99*bo*)



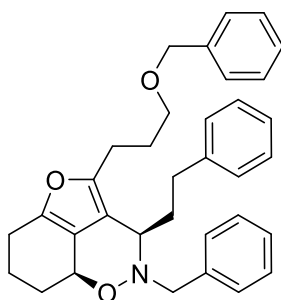
Compound **99bo** was prepared according to the **general procedure 4** from 2-(cyclopentylethynyl)cyclohex-2-en-1-one **71j** (84.7 mg, 4.5 mmol, 1.5 equiv.), *N*-benzylhydroxylamine **101b** (37.0 mg, 3 mmol, 1 equiv.), 3-phenylpropanal **102b** (40.3 mg, 3 mmol, 1 equiv.), 3 Å-MS (300 mg), catalyst **1e**, Ag₂CO₃ and DCM (3 mL). The resulting mixture was then stirred at room temperature overnight, the DCM was removed under vacuum and the crude mixture was purified by flash column chromatography to give the product **99bo** as a white solid in 63% (80.9 mg, 0.19 mmol) yield and 90% ee.

99bo was alternatively obtained from the same protocol in the presence of 0.6 mol% **1e** in 62% yield and 93% ee.

99bo was alternatively obtained from the same protocol in the absence of Ag₂CO₃ in 53% yield and 92% ee.

$[\alpha]_D = +42.9$ (c 2.56, CHCl₃). ee = 93%, determined on a Chiralpak IB column (heptane:IPA = 80:20, 1 mL/min), retention times: T_R (minor): 3.8 min, T_R (major): 7.7 min. $^1\text{H NMR}$ (CDCl₃, 500 MHz) δ = 7.47 (d, J = 7.3 Hz, 2H), 7.34 (t, J = 7.3 Hz, 2H), 7.28 (t, J = 7.3 Hz, 1H), 7.22 (t, J = 7.3 Hz, 2H), 7.14 (t, J = 7.3 Hz, 1H), 7.06 (d, J = 7.3 Hz, 2H), 4.79-4.76 (m, 1H), 4.21 (d, J = 14.0 Hz, 1H), 4.18 (d, J = 14.0 Hz, 1H), 3.95 (dd, J_1 = 6.4 Hz, J_2 = 3.7 Hz, 1H), 2.90-2.84 (m, 1H), 2.79-2.73 (m, 1H), 2.66-2.49 (m, 3H), 2.14-2.03 (m, 2H), 1.97-1.89 (m, 3H), 1.85-1.71 (m, 5H), 1.68-1.53 (m, 3H), 1.26-1.17 (m, 1H). $^{13}\text{C NMR}$ (CDCl₃, 125MHz) δ = 152.0 (C_q), 145.0 (C_q), 143.0 (C_q), 138.2 (C_q), 129.0 (CH), 128.6 (CH), 128.5 (CH), 128.5 (CH), 127.4 (CH), 125.8 (CH), 120.0 (C_q), 114.5 (C_q), 71.2 (CH), 58.5 (CH₂), 57.3 (CH), 38.8 (CH), 35.7 (CH₂), 32.9 (CH₂), 32.3 (CH₂), 31.9 (CH₂), 28.0 (CH₂), 25.8 (CH₂), 25.7 (CH₂), 23.2 (CH₂), 20.7 (CH₂). **HRMS (ESI)**: m/z : calculated for C₂₉H₃₄NO₂⁺: 428.2584 [M+H]⁺, found, 428.2584.

Synthesis of (3*R*,8*aS*)-2-benzyl-4-(3-(benzyloxy)propyl)-3-phenethyl-2,3,6,7,8,8*a*-hexahydrobenzofuro[3,4-*de*][1,2]oxazine (99bp)



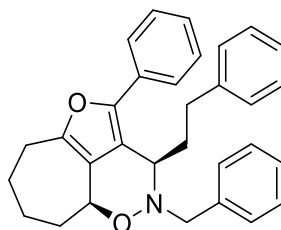
Compound **99bp** was prepared according to the **general procedure 4** from 2-(5-(benzyloxy)pent-1-yn-1-yl)cyclohex-2-en-1-one **71k** (120.8 mg, 4.5 mmol, 1.5 equiv.), *N*-benzylhydroxylamine **101b** (37.0 mg, 3 mmol, 1 equiv.), 3-phenylpropanal **5a** (40.3 mg, 3 mmol, 1 equiv.), 3 Å·MS (300 mg), catalyst **1e**, Ag₂CO₃ and DCM (3 mL). The resulting mixture was then stirred at room temperature overnight, the DCM was removed under vacuum and the crude mixture was purified by flash column chromatography to give the product **99bp** as a colorless oil in 37% (56.4 mg, 0.11 mmol) yield and 91% ee.

99bp was alternatively obtained from the same protocol in the presence of 0.6 mol% **1e** in 71% yield and 93% ee.

99bp was alternatively obtained from the same protocol in the absence of Ag₂CO₃ in 54% yield and 92% ee.

[α]_D = -16.3 (c 1.32, CHCl₃). ee = 93%, determined on a Chiralpak IB column (heptane:IPA = 80:20, 1 mL/min), retention times: T_R (minor): 4.8 min, T_R (major): 11.3 min. ¹H NMR (CDCl₃, 500 MHz) δ = 7.46 (d, *J* = 7.3 Hz, 2H), 7.36-7.24 (m, 8H), 7.21 (t, *J* = 7.3 Hz, 2H), 7.13 (t, *J* = 7.3 Hz, 1H), 7.06 (d, *J* = 7.6 Hz, 2H), 4.79-4.76 (m, 1H), 4.46 (d, *J* = 11.9 Hz, 1H), 4.43 (d, *J* = 11.9 Hz, 1H), 4.18 (d, *J* = 13.7 Hz, 1H), 4.15 (d, *J* = 13.7 Hz, 1H), 3.92 (dd, *J*₁ = 5.8 Hz, *J*₂ = 4.6 Hz, 1H), 3.50-3.42 (m, 2H), 2.75-2.49 (m, 6H), 2.09-2.03 (m, 2H), 1.97-1.85 (m, 4H), 1.81-1.72 (m, 1H), 1.24-1.16 (m, 1H). ¹³C NMR (CDCl₃, 125 MHz) δ = 148.6 (C_q), 145.4 (C_q), 142.9 (C_q), 138.8 (C_q), 138.2 (C_q), 129.0 (CH), 128.6 (CH), 128.6 (CH), 128.5 (CH), 128.5 (CH), 127.8 (CH), 127.7 (CH), 127.4 (CH), 125.8 (CH), 120.3 (C_q), 115.6 (C_q), 73.0 (CH₂), 71.2 (CH), 69.6 (CH₂), 58.5 (CH₂), 57.2 (CH), 35.1 (CH₂), 32.8 (CH₂), 28.7 (CH₂), 28.0 (CH₂), 24.6 (CH₂), 23.2 (CH₂), 20.7 (CH₂). HRMS (ESI): *m/z*: calculated for C₃₄H₃₈NO₃⁺: 508.2846 [M+H]⁺, found, 508.2841.

Synthesis of (3*R*,5*aS*)-4-benzyl-3-phenethyl-2-phenyl-3,4,5*a*,7,8,9-hexahydro-6*H*-1,5-dioxo-4-azabenzo[*cd*]azulene (99bq)



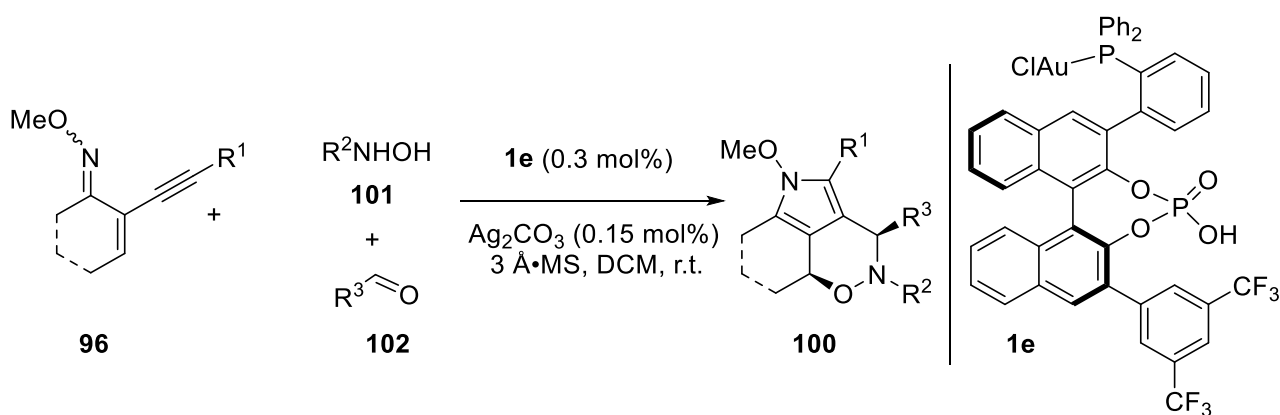
Compound **99bq** was prepared according to the **general procedure 4** from 2-(phenylethynyl)cyclohept-2-en-1-one **71g** (95.0 mg, 4.5 mmol, 1.5 equiv.), *N*-benzylhydroxylamine **101b** (37.0 mg, 3 mmol, 1 equiv.), 3-phenylpropanal **102b** (40.3 mg, 3 mmol, 1 equiv.), 3 Å-MS (300 mg), catalyst **1e**, Ag₂CO₃ and DCM (3 mL). The resulting mixture was then stirred at room temperature overnight, the DCM was removed under vacuum and the crude mixture was purified by flash column chromatography to give the product **99bq** (52.6 mg, 0.12 mmol, 39%) as a white solid.

99bq was alternatively obtained from the same protocol in the presence of 0.6 mol% **1e** in 35% yield and 97% ee.

99bq was alternatively obtained from the same protocol in the absence of Ag₂CO₃ in 15% yield and 95% ee.

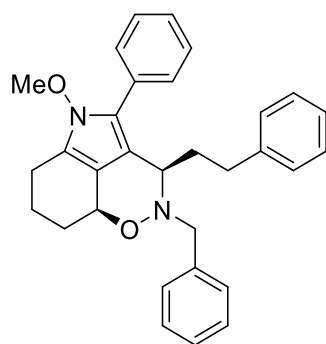
[α]_D = +7.5 (*c* 1.47, CHCl₃). ee = 97%, determined on a Chiralpak IC column (heptane:IPA = 95:05, 1 mL/min), retention times: T_R (minor): 4.2 min, T_R (major): 4.7 min. ¹H NMR (CDCl₃, 500 MHz) δ = 7.46 (d, *J* = 7.0 Hz, 2H), 7.40-7.33 (m, 3H), 7.18-7.10 (m, 8H), 6.84 (d, *J* = 7.3 Hz, 2H), 4.80-4.78 (m, 1H), 4.27 (d, *J* = 12.8 Hz, 1H), 4.01 (d, *J* = 12.8 Hz, 1H), 3.97 (dd, *J*₁ = 9.5 Hz, *J*₂ = 2.4 Hz, 1H), 2.94-2.90 (m, 1H), 2.81-2.71 (m, 3H), 2.36-2.31 (m, 1H), 2.20-2.15 (m, 1H), 2.04-1.96 (m, 2H), 1.79-1.73 (m, 1H), 1.62-1.51 (m, 3H). ¹³C NMR (CDCl₃, 125 MHz) δ = 149.1 (C_q), 142.4 (C_q), 137.6 (C_q), 131.5 (C_q), 129.6 (CH), 129.3 (C_q), 129.0 (CH), 128.8 (CH), 128.8 (CH), 128.5 (CH), 127.7 (CH), 126.3 (CH), 125.8 (CH), 123.9 (C_q), 123.8 (CH), 119.5 (C_q), 69.7 (CH), 58.2 (CH₂), 55.1 (CH), 34.9 (CH₂), 33.4 (CH₂), 32.7 (CH₂), 28.9 (CH₂), 27.0 (CH₂), 26.6 (CH₂). HRMS (ESI): *m/z*: calculated for C₃₁H₃₂NO₂⁺: 450.2428 [M+H]⁺, found, 450.2424.

2.3. Reactions from oximes 96



General procedure 6: To a stirring schlenk tube were added oxime **96** (4.5 mmol, 1.5 equiv.), hydroxylamine **101** (3 mmol, 1.0 equiv.), aldehyde **102** (3 mmol, 1.0 equiv.), 3 Å-MS (300 mg), catalyst **1e** (1 mg, 0.9 μmol, 0.3 mol%), Ag₂CO₃ (0.1 mg, 0.45 μmol, 0.15 mol%), DCM (3 mL) and the resulting mixture was stirred at room temperature for 24 h. After the reaction completed, DCM was removed under vacuum and the crude mixture was purified by flash column chromatography.

(3*R*,8*aS*)-2-benzyl-5-methoxy-3-phenethyl-4-phenyl-3,5,6,7,8,8*a*-hexahydro-2*H*-[1,2]oxazino[4,5,6-*cd*]indole (100b**)**

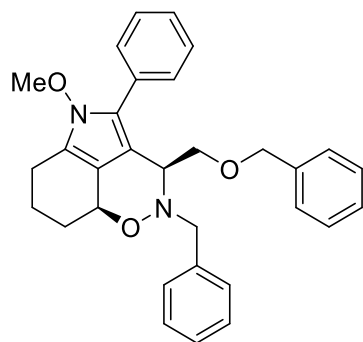


yield: 85 %, ee: 97 %

Compound **100b** was prepared according to the **general procedure 6** from 2-(phenylethynyl)cyclohex-2-en-1-one *O*-methyl oxime (**96a**, 44.7 mg, 1.5 equiv., 0.20 mmol), *N*-benzylhydroxylamine (**101b**, 16.0 mg, 1 equiv., 0.13 mmol), 3-phenylpropanal (**102b**, 17.4 mg, 1 equiv., 0.13 mmol), 3 Å-MS (130 mg), catalyst **1e** (0.41 mg, 0.3 mol%, 0.4 μmol), Ag₂CO₃ (0.06 mg, 0.15 mol%, 0.2 μmol) and DCM (2 mL). The resulting mixture was then stirred at room temperature for 24 h, the DCM was removed under vacuum and the crude mixture was purified by flash column chromatography to give the product **100b** as a white solid (51.3 mg, 0.11 mmol, 85%).

[α]_D = +30.0 (c 1.0, CHCl₃). ee = 97 %, determined on a Chiralpak IA column (heptane:IPA = 95:05, 1 mL/min), retention times: T_R (minor): 4.8 min, T_R (major): 4.2 min. IR (neat) ν_{max}: 2935, 1528, 1446, 1334, 1261, 1105, 1028, 915, 752, 698 cm⁻¹. ¹H NMR (Benzene-d₆, 500 MHz): δ = 7.65 (t, *J* = 6.6 Hz, 4H), 7.30 (t, *J* = 7.8 Hz, 2H), 7.19-7.16 (m, 3H), 7.04 (t, *J* = 7.2 Hz, 3H), 6.98 (t, *J* = 7.2 Hz, 1H), 6.85 (d, *J* = 7.2 Hz, 2H), 5.00 (dd, *J* = 10.4 and 4.6 Hz, 1H), 4.43-4.41 (m, 1H), 4.31 (d, *J*_{AB} = 13.7 Hz, 1H), 4.15 (d, *J*_{AB} = 13.7 Hz, 1H), 3.21 (s, 3H), 2.91-2.85 (m, 1H), 2.51-2.44 (m, 2H), 2.39-2.35 (m, 1H), 2.11-2.05 (m, 1H), 2.00-1.92 (m, 1H), 1.79-1.76 (m, 1H), 1.60-1.56 (m, 1H), 1.45-1.40 (m, 1H), 1.19-1.11 (m, 1H). ¹³C NMR (Benzene-d₆, 125 MHz): δ = 143.8 (C_q), 140.0 (C_q), 132.3 (C_q), 129.5 (2xCH), 129.2 (2xCH), 129.1 (2xCH), 129.0 (3xCH), 128.8 (2xCH), 128.7 (CH), 127.7 (CH), 126.9 (CH), 126.0 (CH), 124.0 (C_q), 121.2 (C_q), 118.0 (C_q), 113.8 (C_q), 72.4 (CH), 65.7 (CH₃), 60.0 (CH), 59.2 (CH₂), 34.7 (CH₂), 33.8 (CH₂), 29.0 (CH₂), 21.8 (CH₂), 20.9 (CH₂). HRMS (ESI): calcd for C₃₁H₃₃N₂O₂ [M+H]⁺ 465.2542; found 465.2533.

(3*S*,8*aS*)-2-benzyl-3-((benzyloxy)methyl)-5-methoxy-4-phenyl-3,5,6,7,8,8*a*-hexahydro-2*H*-[1,2]oxazino[4,5,6-*cd*]indole (100c)

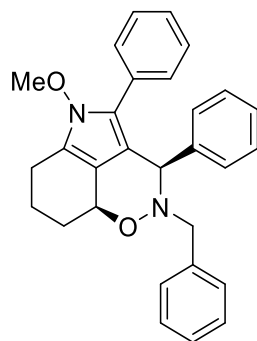


yield: 74 %, ee: 97 %

Compound **100c** was prepared according to the **general procedure 6** from 2-(phenylethynyl)cyclohex-2-en-1-one *O*-methyl oxime (**96a**, 44.7 mg, 1.5 equiv., 0.20 mmol), *N*-benzylhydroxylamine (**101b**, 16.0 mg, 1 equiv., 0.13 mmol), 2-(benzyloxy)acetaldehyde (**102c**, 19.5 mg, 1 equiv., 0.13 mmol), 3Å-MS (130 mg), catalyst **1e** (0.41 mg, 0.3 mol%, 0.4 μmol), Ag₂CO₃ (0.06 mg, 0.15 mol%, 0.2 μmol) and DCM (2 mL). The resulting mixture was then stirred at room temperature for 24 h, the DCM was removed under vacuum and the crude mixture was purified by flash column chromatography to give the product **100c** as a white solid (46.0 mg, 0.1 mmol, 74%).

[α]_D = +11.0 (c 1.2, CHCl₃). ee = 97 %, determined on a Chiralpak IA column (heptane:IPA = 95:05, 1 mL/min), retention times: T_R (minor): 5.2 min, T_R (major): 4.7 min. IR (neat) ν_{max}: 2935, 1528, 1495, , 1446, 1335, 1217, 1105, 1028, 915, 752, 698 cm⁻¹. ¹H NMR (Benzene-d₆, 500 MHz): δ = 7.80 (dd, *J* = 17.2 and 7.8 Hz, 4H), 7.39 (t, *J* = 7.8 Hz, 2H), 7.28-7.24 (m, 6H), 7.16-7.10 (m, 3H), 5.12 (dd, *J* = 10.4 and 4.8 Hz, 1H), 5.04 (d, *J* = 8.0 Hz, 1H), 4.66 (s, 2H), 4.29 (dd, *J* = 10.9 and 8.5 Hz, 1H), 4.20 (s, 2H), 3.38 (d, *J* = 11.0 Hz, 1H), 3.27 (s, 3H), 2.52-2.46 (m, 1H), 2.42-2.37 (m, 1H), 1.81-1.79 (m, 1H), 1.61-1.56 (m, 1H), 1.47-1.37 (m, 1H), 1.20-1.15 (m, 1H). ¹³C NMR (Benzene-d₆, 125 MHz): δ = 141.1 (C_q), 139.4 (C_q), 132.7 (C_q), 129.4 (3xCH), 129.3 (3xCH), 128.8 (2xCH), 128.8 (CH), 128.0 (2xCH), 128.0 (CH), 127.8 (CH), 127.4 (CH), 127.0 (CH), 123.6 (C_q), 121.3 (C_q), 119.0 (C_q), 112.0 (C_q), 75.6 (CH), 73.2 (CH₂), 71.3 (CH), 65.7 (CH₃), 62.8 (CH), 60.6 (CH₂), 28.6 (CH₂), 21.7 (CH₂), 20.8 (CH₂). HRMS (ESI): calcd for C₃₁H₃₃N₂O₃ [M+H]⁺ 481.2491; found 481.2465.

(3*R*,8*aS*)-2-benzyl-5-methoxy-3-phenethyl-4-phenyl-3,5,6,7,8,8*a*-hexahydro-2*H*-[1,2]oxazino[4,5,6-*cd*]indole (100d)

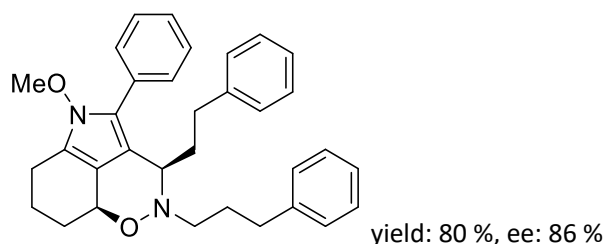


yield: 61 %, ee: 82 %

Compound **100d** was prepared according to the **general procedure 6** from 2-(phenylethynyl)cyclohex-2-en-1-one *O*-methyl oxime (**96a**, 44.7 mg, 1.5 equiv., 0.20 mmol), *N*-benzylhydroxylamine (**101b**, 16.0 mg, 1 equiv., 0.13 mmol), benzaldehyde (**102a**, 13.8 mg, 1 equiv., 0.13 mmol), 3Å-MS (130 mg), catalyst **1e** (0.41 mg, 0.3 mol%, 0.4 μmol), Ag₂CO₃ (0.06 mg, 0.15 mol%, 0.2 μmol) and DCM (2 mL). The resulting mixture was then stirred at 40 °C for 24 h, the DCM was removed under vacuum and the crude mixture was purified by flash column chromatography to give the product **100d** as a white solid (34.7 mg, 0.08 mmol, 83%).

$[\alpha]_D = +20.0$ (c 1.0, CHCl₃). ee = 82 %, determined on a Chiralpak IA column (heptane:IPA = 95:05, 1 mL/min), retention times: T_R (minor): 5.2 min, T_R (major): 4.8 min. IR (neat) ν_{max} : 2946, 1527, 1454, 1347, 1250, 1111, 1050, 939, 833, 744, 693 cm⁻¹. ¹H NMR (Acetone-d₆, 500 MHz): δ = 7.40 (m, 4H), 7.30 (t, J = 7.5 Hz, 2H), 7.22 (t, J = 7.3 Hz, 1H), 7.18 (t, J = 7.8 Hz, 2H), 7.10-7.03 (m, 6H), 5.38 (s, 1H), 4.92 (dd, J = 10.6 and 4.6 Hz, 1H), 3.79 (d, J_{AB} = 14.7 Hz, 1H), 3.65 (s, 3H), 3.31 (d, J_{AB} = 14.7 Hz, 1H), 2.80-2.71 (m, 2H), 2.16-2.11 (m, 1H), 1.96-1.92 (m, 1H), 1.88-1.79 (m, 1H), 1.32-1.24 (m, 1H). ¹³C NMR (Acetone-d₆, 125 MHz): δ = 140.4 (C_q), 140.2 (C_q), 131.8 (C_q), 131.0 (2xCH), 129.2 (2xCH), 129.0 (2xCH), 128.8 (2xCH), 128.2 (2xCH), 128.0 (2xCH), 127.9 (CH), 127.5 (CH), 126.8 (CH), 123.8 (C_q), 121.5 (C_q), 118.0 (C_q), 115.3 (C_q), 75.9 (CH), 66.4 (CH₃), 66.1 (CH), 59.7 (CH), 29.3 (CH₂), 21.8 (CH₂), 21.2 (CH₂). HRMS (ESI): calcd for C₂₉H₂₉N₂O₂ [M+H]⁺ 437.2229; found 437.2256.

(3*R*,8*aS*)-5-methoxy-3-phenethyl-4-phenyl-2-(3-phenylpropyl)-3,5,6,7,8,8*a*-hexahydro-2*H*-[1,2]oxazino[4,5,6-*cd*]indole (100e)

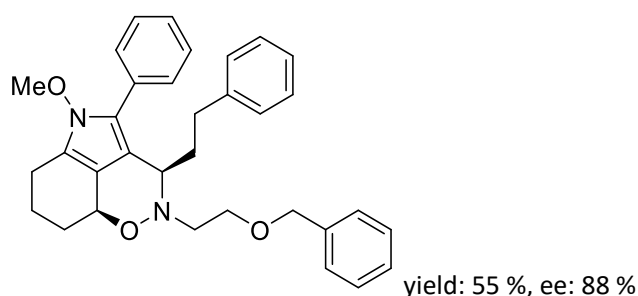


Compound **100e** was prepared according to the **general procedure 6** from 2-(phenylethynyl)cyclohex-2-en-1-one *O*-methyl oxime (**96a**, 51.8 mg, 1.5 equiv., 0.23 mmol), *N*-(3-phenylpropyl)hydroxylamine (**101c**, 22.7 mg, 1 equiv., 0.15 mmol), 3-phenylpropanal (**102b**, 20.7 mg, 1 equiv., 0.15 mmol), 3Å-MS (150 mg), catalyst **1e** (0.47 mg, 0.3 mol%, 0.45 μmol), Ag₂CO₃ (0.062 mg, 0.15 mol%, 0.23 μmol) and DCM (3 mL). The resulting mixture was then stirred at room temperature for 24 h, the DCM was removed under vacuum and the crude mixture was purified by flash column chromatography to give the product **100e** as a white solid (39.5 mg, 0.08 mmol, 80%).

$[\alpha]_D = -12.0$ (c 1.0, CHCl₃). ee = 86 %, determined on a Chiralpak IA column (heptane:IPA = 95:05, 1 mL/min), retention times: T_R (minor): 5.4 min, T_R (major): 5.0 min. IR (neat) ν_{max} : 2926, 1723, 1638, 1526, 1455, 1348, 1250, 1108, 1045, 939, 833, 760, 695 cm⁻¹. ¹H NMR (Acetone-d₆, 500 MHz): δ = 7.59 (d, J = 7.8 Hz, 2H), 7.40 (d, J = 7.8 Hz, 2H), 7.30-7.24 (m, 5H), 7.20-7.17 (m, 1H), 7.09 (t, J = 7.5 Hz, 2H), 7.03 (t, J = 7.5 Hz, 1H), 6.78 (d, J = 7.5 Hz, 2H), 4.82 (dd, J = 10.7 and 5.0 Hz, 1H), 4.29 (t, J = 4.6 Hz, 1H), 3.64 (s, 3H), 3.08-3.03 (m, 1H), 3.00-2.95 (m, 1H), 2.88-2.83 (m, 2H), 2.83-2.74 (m, 3H), 2.71-2.64 (m, 1H), 2.62-2.56 (m, 1H), 2.25-2.19 (m, 1H), 2.13-2.09 (m, 1H), 2.02-1.99 (m, 1H), 1.87-

1.78 (m, 1H), 1.73-1.63 (m, 1H), 1.17-1.10 (m, 1H). ¹³C NMR (Acetone-d₆, 125 MHz): δ = 144.0 (C_q), 143.7 (C_q), 132.4 (C_q), 129.5 (3xCH), 129.2 (2xCH), 129.0 (2xCH), 129.0 (2xCH), 128.5 (3xCH), 127.2 (CH), 126.6 (CH), 126.2 (CH), 123.9 (C_q), 121.6 (C_q), 118.1 (C_q), 113.9 (C_q), 72.3 (CH), 66.2 (CH₃), 60.8 (CH), 54.1 (CH₂), 34.6 (CH₂), 34.3 (CH₂), 33.8 (CH₂), 30.8 (CH₂), 29.1 (CH₂), 21.9 (CH₂), 21.1 (CH₂). HRMS (ESI): calcd for C₃₃H₃₇N₂O₂ [M+H]⁺ 493.2855; found 493.2818.

(3R,8aS)-2-(2-(benzyloxy)ethyl)-5-methoxy-3-phenethyl-4-phenyl-3,5,6,7,8,8a-hexahydro-2H-[1,2]oxazino[4,5,6-cd]indole (100f)



Compound **100f** was prepared according to the **general procedure B** from 2-(phenylethynyl)cyclohex-2-en-1-one *O*-methyl oxime (**96a**, 51.8 mg, 1.5 equiv., 0.23 mmol), *N*-(2-(benzyloxy)ethyl)hydroxylamine (**101d**, 25.0 mg, 1 equiv., 0.15 mmol), 3-phenylpropanal (**102b**, 20.7 mg, 1 equiv., 0.15 mmol), 3Å·MS (150 mg), catalyst **1e** (0.47 mg, 0.3 mol%, 0.45 μmol), Ag₂CO₃ (0.062 mg, 0.15 mol%, 0.23 μmol) and DCM (3 mL). The resulting mixture was then stirred at room temperature for 24 h, the DCM was removed under vacuum and the crude mixture was purified by flash column chromatography to give the product **100f** as a white solid (42.0 mg, 0.082 mmol, 55%).

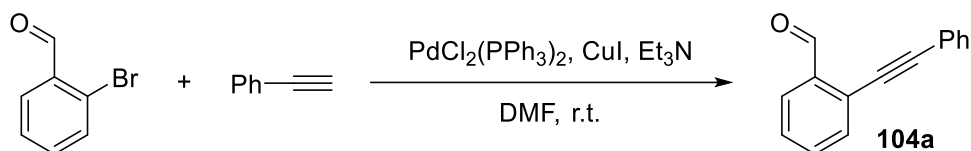
[α]_D = -17.0 (c 1.0, CHCl₃). ee = 88 %, determined on a Chiralpak IA column (heptane:IPA = 95:05, 1 mL/min), retention times: T_R (minor): 5.5 min, T_R (major): 7.0 min. IR (neat) ν_{max}: 2926, 1526, 1455, 1348, 1250, 1108, 1023, 939, 833, 760, 695 cm⁻¹. ¹H NMR (Acetone-d₆, 500 MHz): δ = 7.59 (d, *J* = 7.8 Hz, 2H), 7.42-7.34 (m, 6H), 7.30-7.24 (m, 2H), 7.10 (t, *J* = 7.5 Hz, 2H), 7.03 (t, *J* = 7.5 Hz, 1H), 6.81 (d, *J* = 7.5 Hz, 2H), 4.81 (dd, *J* = 10.7 and 5.0 Hz, 1H), 4.60 (s, 2H), 4.38 (dd, *J* = 5.1 and 3.7 Hz, 1H), 3.84-3.80 (m, 2H), 3.64 (s, 3H), 3.26-3.23 (m, 2H), 2.78-2.73 (m, 1H), 2.71-2.64 (m, 1H), 2.61-2.55 (m, 1H), 2.24-2.18 (m, 1H), 2.13-2.08 (m, 1H), 1.99-1.94 (m, 1H), 1.86-1.62 (m, 3H), 1.16-1.08 (m, 1H). ¹³C NMR (Acetone-d₆, 125 MHz): δ = 144.1 (C_q), 140.2 (C_q), 132.4 (C_q), 129.5 (3xCH), 129.1 (CH), 129.0 (2xCH), 129.0 (2xCH), 128.5 (3xCH), 128.5 (CH), 128.2 (CH), 127.2 (CH), 126.2 (CH), 123.9 (C_q), 121.6 (C_q), 117.9 (C_q), 113.8 (C_q), 73.6 (CH₂), 72.5 (CH), 69.5 (CH₂), 66.2 (CH₃), 61.0 (CH), 54.9 (CH₂), 34.5 (CH₂), 33.7 (CH₂), 29.1 (CH₂), 21.9 (CH₂), 21.1 (CH₂). HRMS (ESI): calcd for C₃₃H₃₇N₂O₃ [M+H]⁺ 509.2804; found 509.2813.

Chapter 3. Application of the TCDC strategy in reactions involving other scaffolds

Part 1. Cyclizations of imines combined with nucleophilic trapping

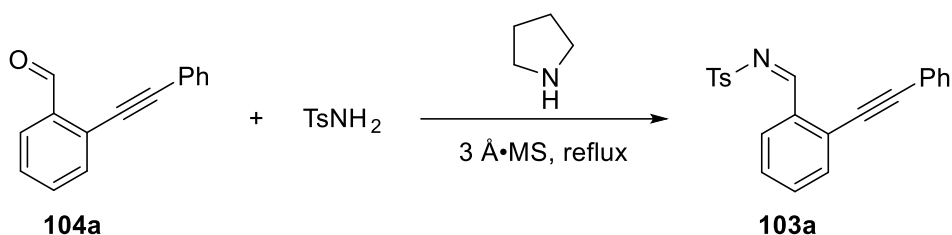
1.1. Synthesis of imines

Synthesis of 2-(phenylethynyl)benzaldehyde (**104a**)¹¹³



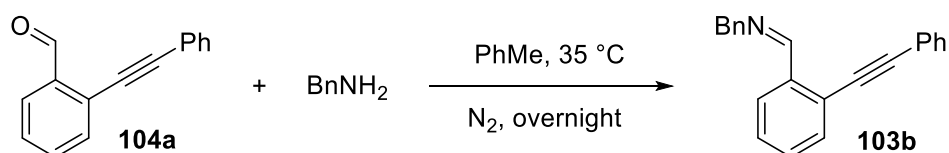
$\text{PdCl}_2(\text{PPh}_3)_2$ (1.76 g, 2.5 mmol, 5 mol%), CuI (0.24 g, 1.25 mmol), Et_3N (30 mL) and phenylacetylene (0.66 mL, 60 mmol, 1.2 equiv.) were added to a stirred solution of 2-bromobenzaldehyde (0.58 mL, 50 mmol, 1 equiv.) in dry DMF (50 mL) under N_2 . The resulting mixture was then stirred at room temperature overnight, the DMF was removed under vacuum and the crude mixture was purified by flash column chromatography to give the product **104a** (10.5 g, 50 mmol, 100%) as a yellow oil.

Synthesis of 4-methyl-*N*-(2-(phenylethynyl)benzylidene)benzenesulfonamide (**103a**)¹³⁶



To a mixture of 2-(phenylethynyl)benzaldehyde **104a** (275.5 mg, 1.2 mmol, 1.2 equiv.), TsNH_2 (171.2 mg, 1 mmol, 1 equiv.) and $3 \text{ \AA} \cdot \text{MS}$ (100 mg) in dry DCM (10 mL) was added pyrrolidine (0.01 mL, 0.1 mmol, 10 mol%). The resulting mixture was then reflux for 24 h, after cooling to room temperature, the solid was removed with celite and then concentrated under vacuum. The crude product was recrystallized ($\text{DCM}/\text{heptane}$) to obtain white crystals **103a** in quantitative yield.

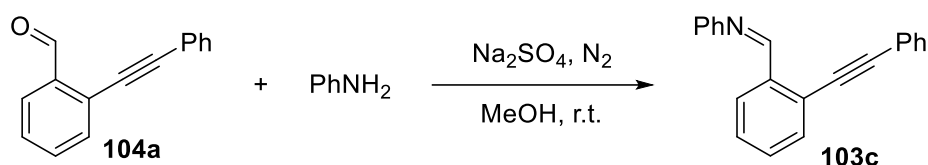
Synthesis of *N*-benzyl-1-(2-(phenylethynyl)phenyl)methanimine (**103b**)¹³⁷



The mixture of 2-(phenylethynyl)benzaldehyde **104a** (1.03 g, 5 mmol, 1 equiv.) and BnNH_2 (0.55 mL, 5 mmol, 1 equiv.) in dry toluene (7 mL) was stirred at $35 \text{ }^\circ\text{C}$ overnight. After cooling to room temperature, the

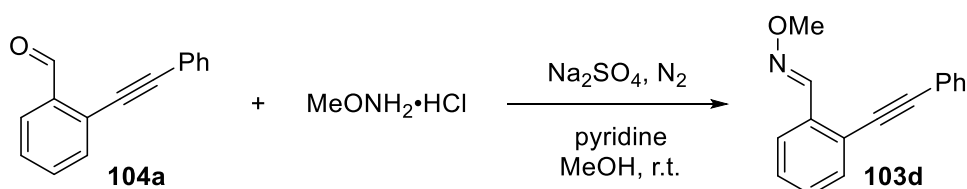
solvent was removed under vacuum, and the crude product was recrystallized (DCM/heptane) to obtain white crystals **103b** in quantitative yield.

Synthesis of *N*-phenyl-1-(2-(phenylethynyl)phenyl)methanimine (**103c**)



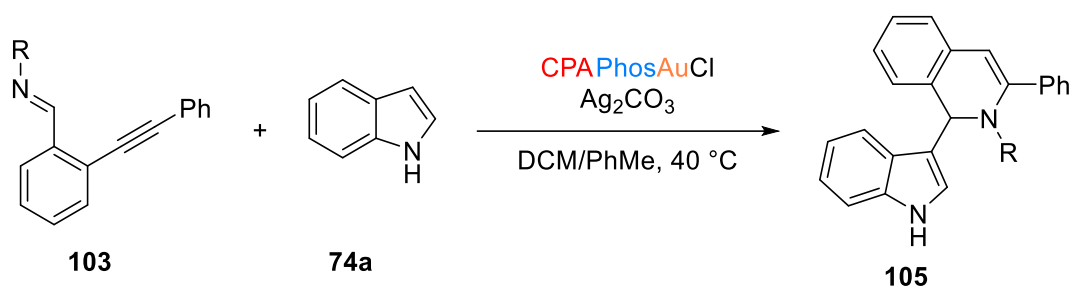
A mixture of 2-(phenylethynyl)benzaldehyde **104a** (759 mg, 3.7 mmol, 1 equiv.) and PhNH₂ (0.34 mL, 3.7 mmol, 1 equiv.) in MeOH (15 mL) was stirred at room temperature overnight. The solvent was removed under vacuum, and the crude product was recrystallized (DCM/heptane) to obtain the product **103c**.

Synthesis of 2-(phenylethynyl)benzaldehyde *O*-methyl oxime (**103d**)



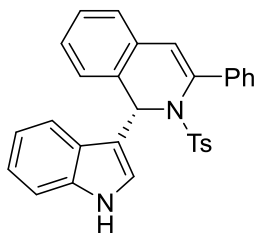
A mixture of 2-(phenylethynyl)benzaldehyde **104a** (336 mg, 1.6 mmol, 1 equiv.), MeONH₂·HCl (267 mg, 3.2 mmol, 2 equiv.), pyridine (0.28 mL, 3.5 mmol, 2.2 equiv.) in MeOH (4 mL) was stirred at room temperature. The reaction was monitored via TLC analysis, after the reaction completed, the solvent was removed under vacuum, and the crude product was purified by flash column chromatography on silica gel, yielding the product **103d** as a white solid (171 mg, 0.73 mmol) in 46% yield.

Synthesis of dihydroisoquinoline **105**



Representative procedure: The CPAPhosAuCl (2.5 μmol, 5 mol%), Ag₂CO₃ (1.25 μmol, 2.5 mol%) and indole **74a** (5.9 mg, 0.05 mmol, 1 equiv.) were stirred at room temperature in DCM (0.25 mL) for 1 h, and then the solution of imine **103** (0.055 mmol, 1.1 equiv.) in toluene (1.75 mL) was added. The resulting mixture was then stirred overnight at 40 °C. After cooling to room temperature, the solvent was removed under vacuum, the crude product was purified by flash column chromatography on silica gel to give the target product **105**.

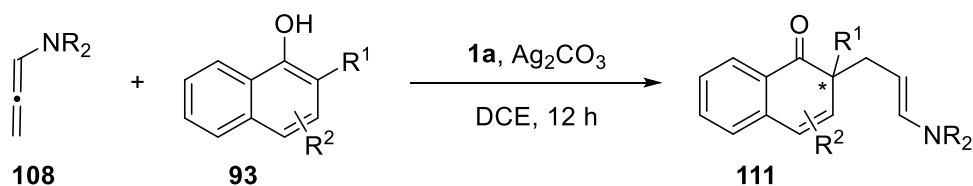
Synthesis of 1-(1*H*-indol-3-yl)-3-phenyl-2-tosyl-1,2-dihydroisoquinoline **105a**¹¹⁴



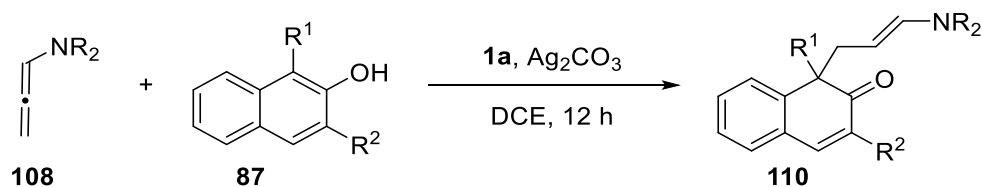
Compound **105a** was prepared according to the representative procedure: **1a** (2.1 mg, 2.5 μmol , 5 mol%), Ag_2CO_3 (0.3 mg, 1.25 μmol , 2.5 mol%) and indole **74a** (5.9 mg, 0.05 mmol, 1 equiv.) were stirred at room temperature in DCM (0.25 mL) for 1 h, and then the solution of imine **103** (0.055 mmol, 1.1 equiv.) in toluene (1.75 mL) was added. The resulting mixture was then stirred at 40 °C overnight. After cooling to room temperature, the solvent was removed under vacuum, the crude product was purified by flash column chromatography and give the product **105a** as a white solid (9 mg, 0.019 mmol, 38%).

ee = 85%, determined on a Chiralpak IC column (heptane:IPA = 70:30, 1 mL/min), retention times: T_R (minor): 11.2 min, T_R (major): 16.9 min.

Part 2. Activation of allenamides combined with naphthol dearomatization



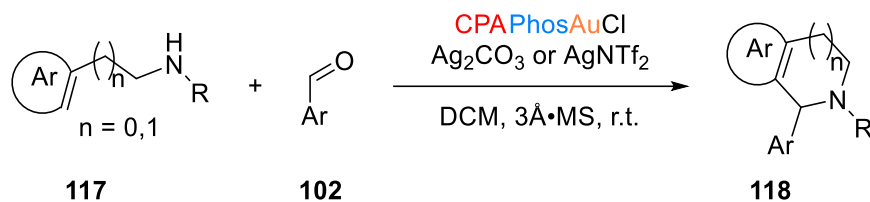
Representative procedure: The **1a** (2.1 mg, 2.5 μmol , 5 mol%) and Ag_2CO_3 (0.3 mg, 1.25 μmol , 2.5 mol%) were stirred at room temperature in DCM (1 mL) for 15 min, and then allenamide **108** (0.15 mmol, 3 equiv.) and 1-naphthols **93** (0.05 mmol, 1 equiv.) was added. The resulting mixture was then stirred at room temperature for 12 h. The solvent was removed under vacuum, and the crude product was purified by flash column chromatography on silica gel to give the target product **111**.



Representative procedure: The **1a** (2.1 mg, 2.5 μmol , 5 mol%) and Ag_2CO_3 (0.3 mg, 1.25 μmol , 2.5 mol%) were stirred at room temperature in DCM (1 mL) for 15 min, and then allenamide **108** (0.075 mmol, 1.5 equiv.) and 2-naphthols **87** (0.05 mmol, 1 equiv.) was added. The resulting mixture was then stirred at room

temperature for 12 h. The solvent was removed under vacuum, and the crude product was purified by flash column chromatography on silica gel to give the target product **110**.

Part 3. The TCDC strategy in (*iso*)-Pictet-Spengler reactions



Representative procedure: The CPA Phos AuCl (2.5 μmol , 5 mol%) and Ag_2CO_3 (0.3 mg, 1.25 μmol , 2.5 mol%) were stirred at room temperature in DCM (1 mL) for 1 h, and then (*iso*)-tryptamine **117** (0.05 mmol, 1 equiv.) and aldehyde **102** (0.1 mmol, 2 equiv.) was added. The resulting mixture was then stirred at room temperature overnight. The solvent was removed under vacuum, and the crude product was purified by flash column chromatography on silica gel to give the target product **118**.

Bibliographic section

- [1] (a) Haruta, M.; Kobayashi, T.; Sano, H.; Yamada, N., *Chem. Lett.* **1987**, *16*, 405; (b) Ito, Y.; Sawamura, M.; Hayashi, T., *J. Am. Chem. Soc.* **1986**, *108*, 6405.
- [2] (a) Hashmi, A. S. K.; Hutchings, G. J., *Angew. Chem. Int. Ed.* **2006**, *45*, 7896; (b) Hashmi, A. S. K., *Chem. Rev.* **2007**, *107*, 3180; (c) Ranieri, B.; Escofet, I.; Echavarren, A. M., *Org. Biomol. Chem.* **2015**, *13*, 7103.
- [3] (a) Gorin, D. J.; Sherry, B. D.; Toste, F. D., *Chem. Rev.* **2008**, *108*, 3351; (b) Wang, W.; Hammond, G. B.; Xu, B., *J. Am. Chem. Soc.* **2012**, *134*, 5697; (c) Ding, D.; Mou, T.; Feng, M.; Jiang, X., *J. Am. Chem. Soc.* **2016**, *138*, 5218.
- [4] Jia, M.; Bandini, M., *ACS Catalysis* **2015**, *5*, 1638.
- [5] (a) Weber, D.; Gagné, M. R., *Org. Lett.* **2009**, *11*, 4962; (b) Wang, D.; Cai, R.; Sharma, S.; Jirak, J.; Thummanapelli, S. K.; Akhmedov, N. G.; Zhang, H.; Liu, X.; Petersen, J. L.; Shi, X., *J. Am. Chem. Soc.* **2012**, *134*, 9012; (c) Zhu, Y.; Day, C. S.; Zhang, L.; Hauser, K. J.; Jones, A. C., *Chem. Eur. J.* **2013**, *19*, 12264; (d) Lu, Z.; Han, J.; Hammond, G. B.; Xu, B., *Org. Lett.* **2015**, *17*, 4534; (e) Bagle, P. N.; Mane, M. V.; Vanka, K.; Shinde, D. R.; Shaikh, S. R.; Gonnade, R. G.; Patil, N. T., *Chem. Commun.* **2016**, *52*, 14462.
- [6] (a) Teles, J. H.; Brode, S.; Chabanas, M., *Angew. Chem. Int. Ed.* **1998**, *37*, 1415; (b) Hueber, D.; Hoffmann, M.; Louis, B.; Pale, P.; Blanc, A., *Chem. Eur. J.* **2014**, *20*, 3903.
- [7] Halpern, J.; Trost, B. M., *Proc. Natl. Acad. Sci. U.S.A.* **2004**, *101*, 5347.
- [8] (a) Blaser, H. U., *Chem. Rev.* **1992**, *92*, 935; (b) Brill, Z. G.; Condakes, M. L.; Ting, C. P.; Maimone, T. J., *Chem. Rev.* **2017**, *117*, 11753.
- [9] (a) Corey, E. J.; Ensley, H. E., *J. Am. Chem. Soc.* **1975**, *97*, 6908; (b) Glorius, F.; Gnass, Y., *Synthesis* **2006**, *2006*, 1899.
- [10] (a) Pradal, A.; Toullec, P. Y.; Michelet, V., *Synthesis* **2011**, 1501; (b) Cera, G.; Bandini, M., *Isr. J. Chem.* **2013**, *53*, 848; (c) Wang, Y.-M.; Lackner, A. D.; Toste, F. D., *Acc. Chem. Res.* **2014**, *47*, 889; (d) Zi, W.; Dean Toste, F., *Chem. Soc. Rev.* **2016**, *45*, 4567; (e) Jiang, J.-J.; Wong, M.-K., *Chem. Asian J.* **2021**, *16*, 364.
- [11] (a) Cera, G.; Chiarucci, M.; Mazzanti, A.; Mancinelli, M.; Bandini, M., *Org. Lett.* **2012**, *14*, 1350; (b) Oka, J.; Okamoto, R.; Noguchi, K.; Tanaka, K., *Org. Lett.* **2015**, *17*, 676; (c) Briones, J. F.; Davies, H. M. L., *J. Am. Chem. Soc.* **2012**, *134*, 11916; (d) Guo, R.; Li, K.-N.; Liu, B.; Zhu, H.-J.; Fan, Y.-M.; Gong, L.-Z., *Chem. Commun.* **2014**, *50*, 5451; (e) Berthod, M.; Mignani, G.; Woodward, G.; Lemaire, M., *Chem. Rev.* **2005**, *105*, 1801.
- [12] (a) Zi, W.; Wu, H.; Toste, F. D., *J. Am. Chem. Soc.* **2015**, *137*, 3225; (b) Huang, L.; Yang, H.-B.; Zhang, D.-H.; Zhang, Z.; Tang, X.-Y.; Xu, Q.; Shi, M., *Angew. Chem. Int. Ed.* **2013**, *52*, 6767; (c) Jia, M.; Monari, M.; Yang, Q.-Q.; Bandini, M., *Chem. Commun.* **2015**, *51*, 2320; (d) Chiarucci, M.; Mocchi, R.; Synttrivanis, L.-D.; Cera, G.; Mazzanti, A.; Bandini, M., *Angew. Chem. Int. Ed.* **2013**, *52*, 10850.
- [13] (a) Navarro, C.; Shapiro, N. D.; Bernasconi, M.; Horibe, T.; Toste, F. D., *Tetrahedron* **2015**, *71*, 5800; (b) Zhou, G.; Liu, F.; Zhang, J., *Chem. Eur. J.* **2011**, *17*, 3101; (c) Gawade, S. A.; Bhunia, S.; Liu, R.-S., *Angew. Chem. Int. Ed.* **2012**, *51*, 7835; (d) Zi, W.; Toste, F. D., *J. Am. Chem. Soc.* **2013**, *135*, 12600; (e) Butler, K. L.; Tragni, M.; Widenhofer, R. A., *Angew. Chem. Int. Ed.* **2012**, *51*, 5175.

- [14] (a) Schmidbaur, H.; Schier, A., *Chem. Soc. Rev.* **2012**, *41*, 370; (b) Barreiro, E. M.; Boltukhina, E. V.; White, A. J. P.; Hii, K. K., *Chem. Eur. J.* **2015**, *21*, 2686; (c) Aikawa, K.; Kojima, M.; Mikami, K., *Adv. Synth. Catal.* **2010**, *352*, 3131; (d) Aikawa, K.; Kojima, M.; Mikami, K., *Angew. Chem. Int. Ed.* **2009**, *48*, 6073.
- [15] (a) Kojima, M.; Mikami, K., *Synlett* **2012**, *2012*, 57; (b) Cao, Z.-Y.; Wang, X.; Tan, C.; Zhao, X.-L.; Zhou, J.; Ding, K., *J. Am. Chem. Soc.* **2013**, *135*, 8197.
- [16] (a) Muñoz, M. P.; Adrio, J.; Carretero, J. C.; Echavarren, A. M., *Organometallics* **2005**, *24*, 1293; (b) Widenhoefer, R. A., *Chem. Eur. J.* **2008**, *14*, 5382; (c) Rudolph, M.; Hashmi, A. S., *Chem. Soc. Rev.* **2012**, *41*, 2448; (d) Wu, Z.; Leboeuf, D.; Retailleau, P.; Gandon, V.; Marinetti, A.; Voituriez, A., *Chem. Commun.* **2017**, *53*, 7026; (e) Chao, C.-M.; Vitale, M. R.; Toullec, P. Y.; Genêt, J.-P.; Michelet, V., *Chem. Eur. J.* **2009**, *15*, 1319.
- [17] de Vries, A. H. M.; Meetsma, A.; Feringa, B. L., *Angew. Chem. Int. Ed.* **1996**, *35*, 2374.
- [18] (a) Liu, F.; Wang, Y.; Ye, W.; Zhang, J., *Org. Chem. Front.* **2015**, *2*, 221; (b) Qian, D.; Hu, H.; Liu, F.; Tang, B.; Ye, W.; Wang, Y.; Zhang, J., *Angew. Chem. Int. Ed.* **2014**, *53*, 13751; (c) Teller, H.; Corbet, M.; Mantilli, L.; Gopakumar, G.; Goddard, R.; Thiel, W.; Fürstner, A., *J. Am. Chem. Soc.* **2012**, *134*, 15331; (d) Alonso, I.; Faustino, H.; López, F.; Mascareñas, J. L., *Angew. Chem. Int. Ed.* **2011**, *50*, 11496; (e) González, A. Z.; Benitez, D.; Tkatchouk, E.; Goddard, W. A.; Toste, F. D., *J. Am. Chem. Soc.* **2011**, *133*, 5500; (f) Li, G.-H.; Zhou, W.; Li, X.-X.; Bi, Q.-W.; Wang, Z.; Zhao, Z.-G.; Hu, W.-X.; Chen, Z., *Chem. Commun.* **2013**, *49*, 4770; (g) Klimczyk, S.; Misale, A.; Huang, X.; Maulide, N., *Angew. Chem. Int. Ed.* **2015**, *54*, 10365.
- [19] (a) Hahn, F. E.; Jahnke, M. C., *Angew. Chem. Int. Ed.* **2008**, *47*, 3122; (b) Hopkinson, M. N.; Richter, C.; Schedler, M.; Glorius, F., *Nature* **2014**, *510*, 485; (c) Wang, F.; Liu, L.-j.; Wang, W.; Li, S.; Shi, M., *Coord. Chem. Rev.* **2012**, *256*, 804; (d) Matsumoto, Y.; Selim, K. B.; Nakanishi, H.; Yamada, K.-i.; Yamamoto, Y.; Tomioka, K., *Tetrahedron Lett.* **2010**, *51*, 404; (e) Tang, X.-T.; Yang, F.; Zhang, T.-T.; Liu, Y.-F.; Liu, S.-Y.; Su, T.-F.; Lv, D.-C.; Shen, W.-B., *Catalysts* **2020**, *10*, 350.
- [20] (a) Yavari, K.; Aillard, P.; Zhang, Y.; Nuter, F.; Retailleau, P.; Voituriez, A.; Marinetti, A., *Angew. Chem. Int. Ed.* **2014**, *53*, 861; (b) Aillard, P.; Retailleau, P.; Voituriez, A.; Marinetti, A., *Chem. Eur. J.* **2015**, *21*, 11989; (c) Aillard, P.; Dova, D.; Magne, V.; Retailleau, P.; Cauteruccio, S.; Licandro, E.; Voituriez, A.; Marinetti, A., *Chem. Commun.* **2016**, *52*, 10984; (d) Magné, V.; Sanogo, Y.; Demmer, C. S.; Retailleau, P.; Marinetti, A.; Guinchard, X.; Voituriez, A., *ACS Catal.* **2020**, *10*, 8141.
- [21] Zuccarello, G.; Mayans, J. G.; Escofet, I.; Scharnagel, D.; Kirillova, M. S.; Perez-Jimeno, A. H.; Calleja, P.; Boothe, J. R.; Echavarren, A. M., *J. Am. Chem. Soc.* **2019**, *141*, 11858.
- [22] Wang, Y.; Wang, Z.; Li, Y.; Wu, G.; Cao, Z.; Zhang, L., *Nat. Commun.* **2014**, *5*, 3470.
- [23] Wang, Z.; Wang, Y.; Zhang, L., *J. Am. Chem. Soc.* **2014**, *136*, 8887.
- [24] Cheng, X.; Wang, Z.; Quintanilla, C. D.; Zhang, L., *J. Am. Chem. Soc.* **2019**, *141*, 3787.
- [25] Zhang, J.-Q.; Liu, Y.; Wang, X.-W.; Zhang, L., *Organometallics* **2019**, *38*, 3931.
- [26] (a) Zhang, Z. M.; Chen, P.; Li, W.; Niu, Y.; Zhao, X. L.; Zhang, J., *Angew. Chem. Int. Ed.* **2014**, *53*, 4350; (b) Liu, F.; Yu, Y.; Zhang, J., *Angew. Chem. Int. Ed.* **2009**, *48*, 5505.
- [27] Mahlau, M.; List, B., *Angew. Chem. Int. Ed.* **2013**, *52*, 518.
- [28] (a) Taylor, M. S.; Jacobsen, E. N., *Angew. Chem. Int. Ed.* **2006**, *45*, 1520; (b) Mayer, S.; List, B., *Angew. Chem. Int. Ed.* **2006**, *45*, 4193.
- [29] Lacour, J.; Hebbe-Viton, V., *Chem. Soc. Rev.* **2003**, *32*, 373.

- [30] (a) Phipps, R. J.; Hamilton, G. L.; Toste, F. D., *Nat. Chem.* **2012**, *4*, 603; (b) Mahlau, M.; List, B., *Angew. Chem. Int. Ed.* **2013**, *52*, 518; (c) Brak, K.; Jacobsen, E. N., *Angew. Chem. Int. Ed.* **2013**, *52*, 534.
- [31] (a) Jiang, G.; List, B., *Chem. Commun.* **2011**, *47*, 10022; (b) Augé, M.; Barbazanges, M.; Tran, A. T.; Simonneau, A.; Elley, P.; Amouri, H.; Aubert, C.; Fensterbank, L.; Gandon, V.; Malacria, M.; Moussa, J.; Ollivier, C., *Chem. Commun.* **2013**, *49*, 7833; (c) Augé, M.; Feraldi-Xypolia, A.; Barbazanges, M.; Aubert, C.; Fensterbank, L.; Gandon, V.; Kolodziej, E.; Ollivier, C., *Org. Lett.* **2015**, *17*, 3754; (d) Barbazanges, M.; Caytan, E.; Lesage, D.; Aubert, C.; Fensterbank, L.; Gandon, V.; Ollivier, C., *Chem. Eur. J.* **2016**, *22*, 8553; (e) Mukherjee, S.; List, B., *J. Am. Chem. Soc.* **2007**, *129*, 11336; (f) Llewellyn, D. B.; Adamson, D.; Arndtsen, B. A., *Org. Lett.* **2000**, *2*, 4165; (g) Barbazanges, M.; Augé, M.; Moussa, J.; Amouri, H.; Aubert, C.; Desmarets, C.; Fensterbank, L.; Gandon, V.; Malacria, M.; Ollivier, C., *Chem. Eur. J.* **2011**, *17*, 13789.
- [32] Parmar, D.; Sugiono, E.; Raja, S.; Rueping, M., *Chem. Rev.* **2014**, *114*, 9047.
- [33] Jiang, G.; List, B., *Chem. Commun.* **2011**, *47*, 10022.
- [34] Barbazanges, M.; Caytan, E.; Lesage, D.; Aubert, C.; Fensterbank, L.; Gandon, V.; Ollivier, C., *Chem. Eur. J.* **2016**, *22*, 8553.
- [35] Yang, L.; Melot, R.; Neuburger, M.; Baudoin, O., *Chem. Sci.* **2017**, *8*, 1344.
- [36] Hamilton, G. L.; Kang, E. J.; Mba, M.; Toste, F. D., *Science* **2007**, *317*, 496.
- [37] Raducan, M.; Moreno, M.; Bour, C.; Echavarren, A. M., *Chem. Commun.* **2012**, *48*, 52.
- [38] Handa, S.; Lippincott, D.; Aue, D.; Lipshutz, B., *Angew. Chem. Int. Ed.* **2014**, *53*, 10658.
- [39] LaLonde, R.; Wang, Z.; Mba, M.; Lackner, A.; Toste, F., *Angew. Chem. Int. Ed.* **2010**, *49*, 598.
- [40] Barreiro, E. M.; Brogini, D. F. D.; Adrio, L. A.; White, A. J. P.; Schwenk, R.; Togni, A.; Hii, K. K., *Organometallics* **2012**, *31*, 3745.
- [41] Mourad, A. K.; Leutzow, J.; Czekelius, C., *Angew. Chem. Int. Ed.* **2012**, *51*, 11149.
- [42] Miles, D. H.; Veguillas, M.; Toste, F. D., *Chem. Sci.* **2013**, *4*, 3427.
- [43] Zi, W.; Toste, F. D., *Angew. Chem. Int. Ed.* **2015**, *54*, 14447.
- [44] Spittler, M.; Lutsenko, K.; Czekelius, C., *J. Org. Chem.* **2016**, *81*, 6100.
- [45] (a) Lee, Y.-C.; Kumar, K., *Isr. J. Chem.* **2018**, *58*, 531; (b) Michelet, V.; Toullec, P. Y.; Genet, J. P., *Angew. Chem. Int. Ed.* **2008**, *47*, 4268.
- [46] Zhang, Z.; Smal, V.; Retailleau, P.; Voituriez, A.; Frison, G.; Marinetti, A.; Guinchard, X., *J. Am. Chem. Soc.* **2020**, *142*, 3797.
- [47] Parmar, D.; Sugiono, E.; Raja, S.; Rueping, M., *Chem. Rev.* **2014**, *114*, 9047.
- [48] Sasai, H.; Matsui, K.; Takizawa, S., *Synlett* **2006**, *2006*, 761.
- [49] Fouquey, J. J. a. C., *Organic Synth.* **1989**, *67*, 1.
- [50] Iwai, T.; Akiyama, Y.; Tsunoda, K.; Sawamura, M., *Tetrahedron: Asymmetry* **2015**, *26*, 1245.
- [51] (a) Iwai, T.; Akiyama, Y.; Sawamura, M., *Tetrahedron: Asymmetry* **2013**, *24*, 729; (b) Gao, L.-X.; Ma, L.; Jin, R.-Z.; Lü, G.-H.; Bian, Z.; Ding, M.-X., *Synthesis* **2007**, *2007*, 2461.
- [52] (a) Xu, Y.; Shi, D.; Wang, X.; Yu, S.; Yu, X.; Pu, L., *Eur. J. Org. Chem.* **2017**, *2017*, 4990; (b) Guo, Q. S.; Du, D. M.; Xu, J., *Angew. Chem. Int. Ed.* **2008**, *47*, 759.
- [53] (a) Damian, K.; Clarke, M. L.; Cobley, C. J., *Appl. Organomet. Chem.* **2009**, *23*, 272; (b) Nowrouzi, N.; Keshtgar, S.; Bahman Jahromi, E., *Tetrahedron Lett.* **2016**, *57*, 348.
- [54] Wang, H.-L.; Hu, R.-B.; Zhang, H.; Zhou, A.-X.; Yang, S.-D., *Org. Lett.* **2013**, *15*, 5302.
- [55] Li, P.; Wischert, R.; Metivier, P., *Angew. Chem. Int. Ed.* **2017**, *56*, 15989.

- [56] Hamdoun, G.; Bour, C.; Gandon, V.; Dumez, J.-N., *Organometallics* **2018**, *37*, 4692.
- [57] Allen, D. V.; Venkataraman, D., *J. Org. Chem.* **2003**, *68*, 4590.
- [58] Bovin, A. N.; Evreinov, V. I.; Safronova, Z. V.; Tsvetkov, E. N., *Russ. Chem. Bull.* **1993**, *42*, 912.
- [59] Tejo, C.; Pang, J. H.; Ong, D. Y.; Oi, M.; Uchiyama, M.; Takita, R.; Chiba, S., *Chem. Commun.* **2018**, *54*, 1782.
- [60] Xie, J.-H.; Zhou, Q.-L., *Acc. Chem. Res.* **2008**, *41*, 581.
- [61] Rahman, A.; Lin, X., *Org. Biomol. Chem.* **2018**, *16*, 4753.
- [62] Birman, V. B.; L. Rheingold, A.; Lam, K.-C., *Tetrahedron: Asymmetry* **1999**, *10*, 125.
- [63] Zhang, J.-H.; Liao, J.; Cui, X.; Yu, K.-B.; Zhu, J.; Deng, J.-G.; Zhu, S.-F.; Wang, L.-X.; Zhou, Q.-L.; Chung, L. W.; Ye, T., *Tetrahedron: Asymmetry* **2002**, *13*, 1363.
- [64] (a) Yang, Y.; Zhu, S.-F.; Duan, H.-F.; Zhou, C.-Y.; Wang, L.-X.; Zhou, Q.-L., *J. Am. Chem. Soc.* **2007**, *129*, 2248; (b) Čorić, I.; Müller, S.; List, B., *J. Am. Chem. Soc.* **2010**, *132*, 17370; (c) Xu, F.; Huang, D.; Han, C.; Shen, W.; Lin, X.; Wang, Y., *J. Org. Chem.* **2010**, *75*, 8677.
- [65] (a) Verrier, C.; Melchiorre, P., *Chem. Sci.* **2015**, *6*, 4242; (b) Hoydonckx, H. E., Van Rhijn, W. M., Van Rhijn, W., De Vos, D. E., Jacobs, P. A., Furfural and Derivatives. In *Ullmann's Encycl. Ind. Chem.*, 2000; Vol. 16.
- [66] (a) Qian, D.; Zhang, J., *Acc. Chem. Res.* **2020**, *53*, 2358; (b) Qian, D.; Zhang, J., *Chem. Rec.* **2014**, *14*, 280; (c) Bao, X.; Ren, J.; Yang, Y.; Ye, X.; Wang, B.; Wang, H., *Org. Biomol. Chem.* **2020**, *18*, 7977.
- [67] (a) Yao, T.; Zhang, X.; Larock, R. C., *J. Am. Chem. Soc.* **2004**, *126*, 11164; (b) Yao, T.; Zhang, X.; Larock, R. C., *J. Org. Chem.* **2005**, *70*, 7679.
- [68] (a) Patil, N. T.; Wu, H.; Yamamoto, Y., *J. Org. Chem.* **2005**, *70*, 4531; (b) Fu, W.-J.; Xu, F.-J.; Guo, W.-B.; Zhu, M.; Xu, C., *Bull. Korean Chem. Soc.* **2013**, *34*, 887.
- [69] Liang, Y.; Liu, X.; Pan, Z.; Shu, X.; Duan, X., *Synlett* **2006**, *2006*, 1962.
- [70] Oh, C. H.; Reddy, V. R.; Kim, A.; Rhim, C. Y., *Tetrahedron Lett.* **2006**, *47*, 5307.
- [71] Wang, Y.; Zhang, P.; Qian, D.; Zhang, J., *Angew. Chem. Int. Ed.* **2015**, *54*, 14849.
- [72] Siva Kumari, A. L.; Kumara Swamy, K. C., *J. Org. Chem.* **2016**, *81*, 1425.
- [73] He, T.; Gao, P.; Zhao, S.-C.; Shi, Y.-D.; Liu, X.-Y.; Liang, Y.-M., *Adv. Synth. Catal.* **2013**, *355*, 365.
- [74] Zhou, L.; Zhang, M.; Li, W.; Zhang, J., *Angew. Chem. Int. Ed.* **2014**, *53*, 6542.
- [75] (a) Zheng, Y.; Chi, Y.; Bao, M.; Qiu, L.; Xu, X., *J. Org. Chem.* **2017**, *82*, 2129; (b) Liu, S.; Yang, P.; Peng, S.; Zhu, C.; Cao, S.; Li, J.; Sun, J., *Chem. Commun.* **2017**, *53*, 1152.
- [76] (a) Gao, H.; Zhang, J., *Chem. Eur. J.* **2012**, *18*, 2777; (b) Di, X.; Wang, Y.; Wu, L.; Zhang, Z. M.; Dai, Q.; Li, W.; Zhang, J., *Org. Lett.* **2019**, *21*, 3018.
- [77] Qi, J.; Teng, Q.; Thirupathi, N.; Tung, C. H.; Xu, Z., *Org. Lett.* **2019**, *21*, 692.
- [78] (a) Xiao, Y.; Zhang, J., *Adv. Synth. Catal.* **2009**, *351*, 617; (b) Xiao, Y.; Zhang, J., *Angew. Chem. Int. Ed.* **2008**, *47*, 1903; (c) Li, W.; Zhang, J., *Chem. Commun.* **2010**, *46*, 8839; (d) Liu, R.; Zhang, J., *Chem. Eur. J.* **2009**, *15*, 9303.
- [79] Force, G.; Ki, Y. L. T.; Isaac, K.; Retaillieu, P.; Marinetti, A.; Betzer, J.-F., *Adv. Synth. Catal.* **2018**, *360*, 3356.
- [80] Huang, L.; Hu, F.; Ma, Q.; Hu, Y., *Tetrahedron Lett.* **2013**, *54*, 3410.
- [81] Rauniyar, V.; Wang, Z. J.; Burks, H. E.; Toste, F. D., *J. Am. Chem. Soc.* **2011**, *133*, 8486.
- [82] Pathipati, S. R.; van der Werf, A.; Eriksson, L.; Selander, N., *Angew. Chem. Int. Ed.* **2016**, *55*, 11863.

- [83] (a) Liu, F.; Qian, D.; Li, L.; Zhao, X.; Zhang, J., *Angew. Chem. Int. Ed.* **2010**, *49*, 6669; (b) Wang, Y.; Zhang, Z. M.; Liu, F.; He, Y.; Zhang, J., *Org. Lett.* **2018**, *20*, 6403.
- [84] Zi, W.; Toste, F. D., *Angew. Chem. Int. Ed.* **2015**, *54*, 14447.
- [85] Kampen, D.; Reisinger, C. M.; List, B., *Top. Curr. Chem.* **2010**, *291*, 395.
- [86] (a) Lu, Z.; Li, T.; Mudshinge, S. R.; Xu, B.; Hammond, G. B., *Chem. Rev.* **2021**; (b) Wang, D.; Cai, R.; Sharma, S.; Jirak, J.; Thummanapelli, S. K.; Akhmedov, N. G.; Zhang, H.; Liu, X.; Petersen, J. L.; Shi, X., *J. Am. Chem. Soc.* **2012**, *134*, 9012; (c) Homs, A.; Escofet, I.; Echavarren, A. M., *Org. Lett.* **2013**, *15*, 5782.
- [87] Rauniyar, V.; Wang, Z. J.; Burks, H. E.; Toste, F. D., *J. Am. Chem. Soc.* **2011**, *133*, 8486.
- [88] Lakhdar, S.; Westermaier, M.; Terrier, F.; Goumont, R.; Boubaker, T.; Ofial, A. R.; Mayr, H., *J. Org. Chem.* **2006**, *71*, 9088.
- [89] (a) Schmidbaur, H.; Schier, A., *Z. Naturforsch. B - J. Chem. Sci.* **2011**, *66*, 329; (b) Franchino, A.; Montesinos-Magraner, M.; Echavarren, A. M., *Bull. Chem. Soc. Jpn.* **2021**, *94*, 1099.
- [90] Gaillard, S.; Bosson, J.; Ramón, R. S.; Nun, P.; Slawin, A. M. Z.; Nolan, S. P., *Chem. Eur. J.* **2010**, *16*, 13729.
- [91] (a) Guérinot, A.; Fang, W.; Sircoglou, M.; Bour, C.; Bezzenine-Lafollée, S.; Gandon, V., *Angew. Chem. Int. Ed.* **2013**, *52*, 5848; (b) Fang, W.; Presset, M.; Guérinot, A.; Bour, C.; Bezzenine-Lafollée, S.; Gandon, V., *Chem. Eur. J.* **2014**, *20*, 5439.
- [92] Lavallo, V.; Frey, G. D.; Kousar, S.; Donnadiou, B.; Bertrand, G., *Proc. Natl. Acad. Sci. U.S.A.* **2007**, *104*, 13569.
- [93] Li, F.; Wang, N.; Lu, L.; Zhu, G., *J. Org. Chem.* **2015**, *80*, 3538.
- [94] Echavarren, A. M.; Franchino, A.; Martí, À.; Nejrótti, S., *Chem. Eur. J.* **2007**, *13*, 11989.
- [95] (a) Sen, S.; Gabbai, F. P., *Chem. Commun.* **2017**, *53*, 13356; (b) Seppanen, O.; Aikonen, S.; Muuronen, M.; Alamillo-Ferrer, C.; Bures, J.; Helaja, J., *Chem. Commun.* **2020**, *56*, 14697.
- [96] Kardile, R. D.; Chao, T. H.; Cheng, M. J.; Liu, R. S., *Angew. Chem. Int. Ed.* **2020**, *59*, 10396.
- [97] (a) Guinchard, X.; Denis, J.-N., *J. Org. Chem.* **2008**, *73*, 2028; (b) Guinchard, X.; Vallée, Y.; Denis, J.-N., *Org. Lett.* **2005**, *7*, 5147.
- [98] Yang, C.; Xue, X. S.; Jin, J. L.; Li, X.; Cheng, J. P., *J. Org. Chem.* **2013**, *78*, 7076.
- [99] Li, Z.; Peng, J.; He, C.; Xu, J.; Ren, H., *Org. Lett.* **2020**, *22*, 5768.
- [100] (a) Ilg, M. K.; Wolf, L. M.; Mantilli, L.; Farès, C.; Thiel, W.; Fürstner, A., *Chem. Eur. J.* **2015**, *21*, 12279; (b) Abadie, M.-A.; Trivelli, X.; Medina, F.; Duhal, N.; Kouach, M.; Linden, B.; Génin, E.; Vandewalle, M.; Capet, F.; Roussel, P.; Del Rosal, I.; Maron, L.; Agbossou-Niedercorn, F.; Michon, C., *Chem. Eur. J.* **2017**, *23*, 10777.
- [101] Zhang, M.; Zhang, J., *Chem. Commun.* **2012**, *48*, 6399.
- [102] Chen, M.; Zhang, Z.-M.; Yu, Z.; Qiu, H.; Ma, B.; Wu, H.-H.; Zhang, J., *ACS Catalysis* **2015**, *5*, 7488.
- [103] Zhang, M.; Di, X.; Zhang, M.; Zhang, J., *Chin. J. Chem.* **2018**, *36*, 519.
- [104] (a) Zhi, S.; Ma, X.; Zhang, W., *Org. Biomol. Chem.* **2019**, *17*, 7632; (b) Touré, B. B.; Hall, D. G., *Chem. Rev.* **2009**, *109*, 4439; (c) Ruijter, E.; Scheffelaar, R.; Orru, R. V., *Angew. Chem. Int. Ed.* **2011**, *50*, 6234; (d) Dömling, A., *Chem. Rev.* **2006**, *106*, 17; (e) Clarke, P. A.; Santos, S.; Martin, W. H. C., *Green Chem.* **2007**, *9*, 438; (f) Cioc, R. C.; Ruijter, E.; Orru, R. V. A., *Green Chem.* **2014**, *16*, 2958; (g) Bienaymé, H.; Hulme, C.; Odon, G.; Schmitt, P., *Chem. Eur. J.* **2000**, *6*, 3321.
- [105] (a) Visbal, R.; Graus, S.; Herrera, R. P.; Gimeno, M. C., *Molecules* **2018**, *23*, 2255; (b) Abbiati, G.; Rossi, E., *Beilstein J. Org. Chem.* **2014**, *10*, 481; (c) Peshkov, V. A.; Pereshivko, O. P.; Van

- der Eycken, E. V., *Chem. Soc. Rev.* **2012**, *41*, 3790; (d) Skouta, R.; Li, C.-J., Gold-Catalyzed Multi-component Reactions. In *Gold Catalysis*, pp 225.
- [106] Aliaga-Lavrijsen, M.; Herrera, R. P.; Villacampa, M. D.; Gimeno, M. C., *ACS Omega* **2018**, *3*, 9805.
- [107] Qian, D.; Zhang, J., *Acc. Chem. Res.* **2020**, *53*, 2358.
- [108] Zhang, M.; Zhang, J., *Chem. Commun.* **2012**, *48*, 6399.
- [109] (a) Yu, X.; Wu, J., *J. Comb. Chem.* **2010**, *12*, 238; (b) Ye, S.; Wu, J., *Tetrahedron Lett.* **2009**, *50*, 6273; (c) Wang, X.; Qiu, G.; Zhang, L.; Wu, J., *Tetrahedron Lett.* **2014**, *55*, 962; (d) Sun, W.; Ding, Q.; Sun, X.; Fan, R.; Wu, J., *J. Comb. Chem.* **2007**, *9*, 690; (e) Lou, H.; Ye, S.; Zhang, J.; Wu, J., *Tetrahedron* **2011**, *67*, 2060; (f) Ding, Q.; Wu, J., *Org. Lett.* **2007**, *9*, 4959.
- [110] Zhao, Y. H.; Yu, Y.; Hu, D.; Zhao, L.; Xie, W.; Zhou, Z., *Asian J. Org. Chem.* **2020**, *9*, 953.
- [111] (a) Godet, T.; Vaxelaire, C.; Michel, C.; Milet, A.; Belmont, P., *Chem. Eur. J.* **2007**, *13*, 5632; (b) Parker, E.; Leconte, N.; Godet, T.; Belmont, P., *Chem. Commun.* **2011**, *47*, 343; (c) Mariaule, G.; Newsome, G.; Toullec, P. Y.; Belmont, P.; Michelet, V., *Org. Lett.* **2014**, *16*, 4570; (d) Bontemps, A.; Mariaule, G.; Desbène-Finck, S.; Helissey, P.; Giorgi-Renault, S.; Michelet, V.; Belmont, P., *Synthesis* **2016**, *48*, 2178; (e) Bantreil, X.; Bourderioux, A.; Mateo, P.; Hagerman, C. E.; Selkti, M.; Brachet, E.; Belmont, P., *Org. Lett.* **2016**, *18*, 4814.
- [112] De Abreu, M.; Tang, Y.; Brachet, E.; Selkti, M.; Michelet, V.; Belmont, P., *Org. Biomol. Chem.* **2021**, *19*, 1037.
- [113] Zhang, J.-W.; Xu, Z.; Gu, Q.; Shi, X.-X.; Leng, X.-B.; You, S.-L., *Tetrahedron* **2012**, *68*, 5263.
- [114] Kang, Q.; Zhao, Z.-A.; You, S.-L., *J. Am. Chem. Soc.* **2007**, *129*, 1484.
- [115] (a) Campeau, D.; León Rayo, D. F.; Mansour, A.; Muratov, K.; Gagosz, F., *Chem. Rev.* **2021**, *121*, 8756; (b) Li, Y.; Li, W.; Zhang, J., *Chem. Eur. J.* **2017**, *23*, 467.
- [116] An, J.; Lombardi, L.; Grilli, S.; Bandini, M., *Org. Lett.* **2018**, *20*, 7380.
- [117] Pedrazzani, R.; An, J.; Monari, M.; Bandini, M., *Eur. J. Org. Chem.* **2021**, *2021*, 1732.
- [118] Yang, B.; Zhai, X.; Feng, S.; Hu, D.; Deng, Y.; Shao, Z., *Org. Lett.* **2019**, *21*, 330.
- [119] Pictet, A.; Spengler, T., *Ber. Dtsch. Chem. Ges.* **1911**, *44*, 2030.
- [120] (a) Zheng, C.; Xia, Z.-L.; You, S.-L., *Chem* **2018**, *4*, 1952; (b) Gholamzadeh, P., Chapter Three - The Pictet–Spengler Reaction: A Powerful Strategy for the Synthesis of Heterocycles. In *Adv. Heterocycl. Chem.*, Scriven, E. F. V.; Ramsden, C. A., Eds. Academic Press: 2019; Vol. 127, pp 153; (c) Calcaterra, A.; Mangiardi, L.; Delle Monache, G.; Quaglio, D.; Balducci, S.; Berardozi, S.; Iazzetti, A.; Franzini, R.; Botta, B.; Ghirga, F., *Molecules* **2020**, *25*, 414.
- [121] Glinsky-Olivier, N.; Guinchard, X., *Synthesis* **2017**, *49*, 2605.
- [122] Seayad, J.; Seayad, A. M.; List, B., *J. Am. Chem. Soc.* **2006**, *128*, 1086.
- [123] Gobé, V.; Retailleau, P.; Guinchard, X., *Chem. Eur. J.* **2015**, *21*, 17587.
- [124] Glinsky-Olivier, N.; Yang, S.; Retailleau, P.; Gandon, V.; Guinchard, X., *Org. Lett.* **2019**, *21*, 9446.
- [125] Milcendeau, P.; Zhang, Z.; Glinsky-Olivier, N.; van Elslande, E.; Guinchard, X., *J. Org. Chem.* **2021**, *86*, 6406.
- [126] Stankevič, M.; Włodarczyk, A., *Tetrahedron* **2013**, *69*, 73.
- [127] (a) Chowdhury, S.; Georghiou, P. E., *J. Org. Chem.* **2002**, *67*, 6808; (b) Hirose, T.; Kojima, Y.; Matsui, H.; Hanaki, H.; Iwatsuki, M.; Shiomi, K.; Omura, S.; Sunazuka, T., *J. Antibiot.* **2017**, *70*, 574.
- [128] Sundén, H.; Schäfer, A.; Scheepstra, M.; Leysen, S.; Malo, M.; Ma, J.-N.; Burstein, E. S.; Ottmann, C.; Brunsveld, L.; Olsson, R., *J. Med. Chem.* **2016**, *59*, 1232.

- [129] Cho, C.-H.; Larock, R. C., *ACS Comb. Sci.* **2011**, *13*, 272.
- [130] (a) Salacz, L.; Girard, N.; Blond, G.; Suffert, J., *Org. Lett.* **2018**, *20*, 3915; (b) Salacz, L.; Girard, N.; Suffert, J.; Blond, G., *Molecules* **2019**, *24*, 595.
- [131] Slack, E. D.; Gabriel, C. M.; Lipshutz, B. H., *Angew. Chem. Int. Ed.* **2014**, *53*, 14051.
- [132] Nemoto, K.; Tanaka, S.; Konno, M.; Onozawa, S.; Chiba, M.; Tanaka, Y.; Sasaki, Y.; Okubo, R.; Hattori, T., *Tetrahedron* **2016**, *72*, 734.
- [133] Shao, C.; Shi, G.; Zhang, Y.; Pan, S.; Guan, X., *Org. Lett.* **2015**, *17*, 2652.
- [134] Zhang, Y.; Stephens, D.; Hernandez, G.; Mendoza, R.; Larionov, O. V., *Chem. Eur. J.* **2012**, *18*, 16612.
- [135] Pedras, M. S.; Minic, Z.; Thongbam, P. D.; Bhaskar, V.; Montaut, S., *Phytochemistry* **2010**, *71*, 1952.
- [136] Morales, S.; Guijarro, F. G.; Garcia Ruano, J. L.; Cid, M. B., *J. Am. Chem. Soc.* **2014**, *136*, 1082.
- [137] Hu, Y.; Huang, H., *Org. Lett.* **2017**, *19*, 5070.

Titre : Nouvelles perspectives en catalyse énantiosélective par les complexes d'Au(I) à contre-ions phosphates

Mots clés : catalyse asymétrique, ligands et phosphates chiraux, Au(I), cyclisations énantiosélectives.

Résumé : La catalyse à l'Au(I) représente aujourd'hui un outil de choix pour la synthèse de molécules complexes, à haute valeur ajoutée. Aussi, au cours des dernières décennies, des stratégies efficaces ont été définies pour rendre énantiosélectives les réactions promues par l'Au(I). L'une d'entre elles, développée par D. Toste, fait appel à des complexes d'Au(I) à contre-ions chiraux (ACDC = Asymmetric Counteranion Directed Catalysis). Ces méthodologies, basées sur l'emploi de phosphates chiraux, ont montré d'excellentes propriétés catalytiques mais aussi des limitations importantes en termes d'étendue de leur domaine d'application. Dans ce contexte et dans l'objectif de dépasser ces limitations, ces travaux de thèse ont porté sur un nouveau design de complexes d'Au(I) dans lesquels le contre-ion phosphate serait relié au métal par un lien covalent. Selon l'hypothèse de travail initiale, le lien

entre le ligand de l'Au(I) et son propre contre-ion doit réduire la flexibilité conformationnelle et augmenter les contraintes stériques des intermédiaires clés des cycles catalytiques, favorisant ainsi l'énantiosélectivité. Nous avons donc conçu et synthétisé une série de six complexes d'Au(I) portant des ligands bifonctionnels phosphine-acide phosphorique, avec différentes chaînes entre les deux groupes. La fonction phosphine coordonne le métal tandis que la fonction acide phosphorique, dérivée des diols chiraux (*S*)-BINOL ou (*R*)-SPINOL, engendre un contre-ion phosphate dans un environnement chiral. L'efficacité de ces nouveaux complexes à de très bas taux catalytiques a été démontrée notamment dans des réactions tandem de cyclisation/addition nucléophile, où d'excellentes énantiosélectivités ont été obtenues.

Title: New Insights in Asymmetric Au(I) Catalysis with Chiral Phosphate Counterions

Keywords: asymmetric catalysis, chiral ligands, chiral phosphate counterions, Au(I), enantioselective cyclisations.

Abstract: Homogeneous asymmetric gold catalysis plays a central role in synthetic chemistry. In the past decades, chemists have unremittingly explored this field and have designed many effective strategies toward enantioselective methods. Among others, the so-called Asymmetric Counteranion-Directed Catalysis (ACDC), has become a powerful approach, leading to excellent reactivity and enantioselectivity notably in intramolecular reactions. The ACDC strategy also showed major limitations since the phosphate-gold ion pair may be too loose and flexible to shape a suitable chiral pocket around the reactive center.

In this context, we have introduced a new design for chiral gold catalysts, based on bifunctional phosphine-phosphoric acid ligands. The phosphine group is expected to coordinate the metal center, while the tethered phosphate will play the role of counteranion in the cationic gold complex. Tethering of the two functions is expected to increase the rigidity and the geometrical constraints in the key intermediates of enantioselective catalytic processes, thereby favoring the enantioselectivity. This unprecedented strategy is called 'Tethered Counterion-Directed Catalysis' (TCDC).

Based on this new catalyst design, we have synthesized a series of six Au(I) complexes bearing bifunctional phosphine-phosphoric acid ligands, with various chains connecting the two functions. The phosphoric acid units are based on either (*S*)-BINOL or (*R*)-SPINOL backbones. The new catalysts have been applied successfully in many reactions, such as a series of tandem cyclization/nucleophilic additions. The targeted reactions convert cyclic α -ethynyl-enones into bicyclic furanes functionalized by the incoming nucleophile (amines, indoles, nitrones, alcohols etc.). The newly designed Au(I) catalysts demonstrated unprecedented levels of catalytic activity, enabling the use of very low catalyst loadings (up to 0.2 mol%). Moreover, they enabled a silver-free protocol to be implemented, which is an important breakthrough in gold catalysis that is often hampered by silver side-effects. The catalysts also provided excellent enantioselectivities, with enantiomeric excesses >90% in most cases.

Overall, this PhD work allowed to validate the working hypothesis by demonstrating the relevance of the TCDC approach in enantioselective gold(I) catalysis. Meanwhile, the excellent results obtained so far offer huge synthetic perspectives.